THE UNIVERSITY *of* EDINBURGH

UNBONDED POST-TENSIONED CONCRETE STRUCTURES IN FIRE

By

John Gales

A thesis submitted to the College of Science and Engineering in conformity with the requirements for the degree of Doctor of Philosophy

University of Edinburgh

Edinburgh, Scotland, UK

July 2013

This thesis is dedicated to my grandfather, Stan Sikora

Abstract

To achieve thinner and longer floor slabs, rapid construction, and tight control of in-service deflections, modern concrete structures increasingly use high-strength, post-tensioned prestressing steel as reinforcement. The resulting structures are called post-tensioned (PT) concrete. Post-tensioned concrete slabs are widely believed to benefit from 'inherent fire endurance.' This belief is based largely on results from a series of standard fire tests performed on simply-supported specimens some five decades ago. Such tests are of debatable credibility; they do not capture the true structural behaviour of real buildings in real fires, nor do they reflect modern PT concrete construction materials or optimization methods. This thesis seeks to develop a more complete understanding of the structural and thermal response of modern prestressing steel and PT concrete slabs, particularly those with unbonded prestressing steel conditions, to high temperature, in an effort to steer current practice and future research towards the development of defensible, performance-based, safe fire designs.

An exhaustive literature review of previous experimentation and real case studies of fire exposed PT concrete structures is presented to address whether current code guidance is adequate. Both bonded and unbonded prestressing steel configurations are considered, and research needs are identified. For unbonded prestressing steel in a localised fire, the review shows that the interaction between thermal relaxation and plastic deformation could result in tendon failure and loss of tensile reinforcement to the concrete, earlier than predicted by available design guidance. Since prestressing steel runs continuously in unbonded PT slabs, local damage to prestressing steel will affect the integrity of adjacent bays in a building. In the event that no bonded steel reinforcement is provided (as permitted by some design codes) a PT slab could lose tensile reinforcement across multiple bays; even those remote from fire. Using existing literature and design guidance, preliminary simplified modelling is presented to illustrate the stress-temperature-time interactions for stressed, unbonded prestressing steel under localised heating. This exercise showed that the observed behaviour cannot be rationally described by the existing design guidance.

The high temperature mechanical properties of modern prestressing steel are subsequently considered in detail, both experimentally and analytically. Tests are presented on prestressing steel specimens under constant axial stress at high temperature using a high resolution digital image correlation (DIC) technique to accurately measure deformations. A novel, accurate analytical model of the stress-temperature-time dependent deformation of prestressing steel is developed and validated for both transient and steady-state conditions. Modern prestressing steel behaviour is then compared to its historical prestressing steel counterparts, showing significant differences at high temperature.

Attention then turns to other structural actions of a real PT concrete structure (e.g. thermal bowing, restraint, concrete stiffness loss, continuity, spalling, slab splitting etc.) all of which also play inter-related roles influencing a PT slab's response in fire. A series of three non-standard structural fire experiments on heavily instrumented, continuous, restrained PT concrete slabs under representative sustained service loads were conducted in an effort to better understand the response of PT concrete structures to localised heating. To the author's knowledge this is the first time a continuous PT slab which includes axial, vertical and rotational restraint has been studied at high temperature, particularly under localised heating. The structural response of all three tests indicates a complex deflection trend in heating and in cooling which differs considerably from the response of a simply supported slab in a standard fire test. Deflection trends in the continuous slab tests were due to a combination of thermal expansion and plastic damage. The test data will enable future efforts to validate computational models which account for the requisite complexities.

Overall, the research presented herein shows that some of the design guidance for modern PT concrete slabs is inadequate and should be updated. The high temperature deformation of prestressing steel under localised heating, as would be expected in a real fire, should be considered, since uniform heating of simply-supported elements is both unrealistic and unconservative with respect to tensile rupture of prestressing steel tendons. The most obvious impact of this finding would be to increase the minimum concrete covers required for unbonded PT construction, and to require adequate amounts of bonded steel reinforcement to allow load

shedding to the bonded steel at high temperature in the event that the prestressing steel fails or is severely damaged by fire.

Declaration

The work presented herein has been influenced by input from several colleagues and co-authors through the publication of five original research articles which have been modified and expanded to create the four central chapters of this thesis. While the thesis is written in the traditional format, large portions of various chapters have been modified from these five papers, since they were published prior to finalization of the thesis. In all cases the author of the current thesis was the primary author of the papers, the papers were written at the University of Edinburgh while the author was studying for this doctoral degree, the author wrote the first paper draft, and the author conducted all experiments described therein, unless otherwise noted. Where the author has not contributed in this central manner, or where the paper was written outside the boundaries of the current doctoral degree, the papers are referenced as secondary sources to support arguments throughout the thesis.

Chapter 2 is based on:

- Gales, J., Bisby, L., and Gillie, M. (2011). "Unbonded Post Tensioned Concrete in Fire: A Review of Data from Furnace Tests and Real Fires." *Fire Safety Journal*, 46(4):151-163.

Chapter 3 is based on:

- Gales, J., Bisby, L., and Gillie, M. (2011). "Unbonded Post Tensioned Concrete Slabs in Fire – Part I – Experimental Response of Unbonded Tendons under Transient Localized Heating." *Journal of Structural Fire Engineering*, 2(3):139-154; and

- Gales, J., Bisby, L., and Gillie, M. (2011). "Unbonded Post Tensioned Concrete Slabs in Fire – Part II – Modelling Tendon Response and the Consequences of Localized Heating." *Journal of Structural Fire Engineering*, 2(3):155-172.

Portions of Chapter 4 are modified from:

- Gales, J., Bisby, L., and Stratford, T. (2012). "New Parameters to Describe High Temperature Deformation of Prestressing Steel determined using Digital Image Correlation." *Structural Engineering International*, 22(4): 476-486.

Portions of Chapter 5 are modified from:

- Gales, J., Bisby, L., Stratford, T., and Krajcovic, M. (June 24-26th 2013). "Tests of continuous post-tensioned concrete slabs under localized fires." Interflam 2013:

13th International Conference and Exhibition on Fire Science and Engineering. Royal Holloway College, Windsor, UK. 1131-1142.*

***Note:** this is a conference paper and was written after the first draft of Chapter 5 was compiled.*

The author has also written or co-authored the following additional publications, not directly related to the current thesis, during the course of his doctoral studies. These publications are included in the thesis appendix (A-C):

(A) Gales, J., Bisby, L., and Maluk, C. (22–27 July 2012) Structural fire testing – where are we, how did we get here, and where are we going? Proceedings of the 15th International Conference on Experimental Mechanics. Porto, Portugal. 22 pp.

(B) Bisby, L., Gales, J., and Maluk, C. (2013) A contemporary review of large-scale non standard structural fire testing (circa 1980–present). Fire Science Reviews, 2(1).

(C) Roberston, L., Dudorova, Z., Gales, J., Vega, E., Stratford, T., Blackford, J., and Bisby, L. (19–20 April 2013) Micro-structural and mechanical characterization of post-tensioning tendons following elevated temperature exposure. Applications of Structural Engineering Conference. Prague, CZ. 474-479 pp.

John Gales

Edinburgh, July 2013

Acknowledgements

My time at the University of Edinburgh has introduced me to wonderful individuals. Specific thanks should be extended first and foremost to my supervisor Professor Luke Bisby for all his advice and strong support for this project and for of course allowing me to pursue side projects in addition to my core research. Additionally, my thanks extend to Dr. Tim Stratford, Dr. Guillermo Rein, and Professor José Torero who have shown keen interest in this project (and side projects) and have always been able to make time when needed. I would also like to extend thanks to Michal Krajcovic, Zafiris Triantafyllidis, Daryan Othman, and Thomas Parker. These people had no obligation to work (and for extended hours!) in the lab with me. The time and comments provided by Florian Block, Stephen Welch and Martin Gillie was greatly appreciated. I am deeply thankful for inspiring conversations with Nico, Rory, David, Mariyana, Angus, Cecillia, Adam, Joanne, Steffen, Cristian, Sam and others. Thanks also to my family who have been supportive, and understanding of my time away from home. To my friends Charles, Steph and Jose who have provided so much assistance through my studies. Thanks to the Natural Sciences and Engineering Research Council of Canada for helping to support this project financially. The organisers and participants of COST TU0904 for the Young Researchers Training School for Fire Engineers must be thanked. This training school was invaluable for finishing the final pieces of this thesis. This project would not have been possible without the many companies and individuals outside the university who have provided in kind assistance. Their help is noted throughout the text. Particular thanks extend to Bridon and Con-Force.

And finally thanks to Audrey, whose continued support and love made this possible.

Table of Contents

List of Figures

Chapter 4

Chapter 5

List of Tables

Chapter 2

Chapter 3

Chapter 4

Chapter 5

Notation

a = Z parameter equation coefficient

a_c = depth of the compressive stress block in concrete (mm)

b = Z parameter equation coefficient

b_c = width of concrete slab

c = Z parameter equation coefficient

d = Z parameter equation coefficient

A= Arrhenius function coefficient

A_s = area of mild steel reinforcement (mm^2)

A_p = area of prestressing steel (mm^2)

c_y = depth of the neutral axis assuming f_{pr} equals f_{pu} (mm)

d_s = depth of the extreme compression fibre to the centroid of the reinforcement steel (mm)

d_p = depth of the extreme compression fibre to the centroid of the prestressing steel (mm)

E = elastic modulus (MPa)

E_s = elastic modulus of steel column (MPa)

E_s = elastic modulus of concrete column (MPa)

E_T = elastic modulus at temperature T (MPa)

$E_{20°C}$ = elastic modulus at room temperature (MPa)

f'_c = compressive strength of concrete (MPa)

f_y = yield stress of mild reinforcement(MPa)

f_{pe} = tensile strength of prestressing strand/wire after losses (MPa)

f_{pr} = stress in prestressing strand/wire at factored resistance (MPa)

f_{pu} = tensile strength of prestressing strand/wire (MPa)

I_s = moment of inertia of steel column (mm^4)

I_s = moment of inertia of concrete column (mm^4)

l_o = anchor to anchor length of tendon (mm)

l_s = steel column height (mm)

l_c = concrete column height (mm)

t = time (seconds, mins or hrs)

T = temperature (°C or °K)

TC_i = thermocouple temperature (°C)

T_i = thermal region temperature (°C)

n = number of plastic hinges

Z = Zener-Hollomon Parameter (hrs^{-1})

α_1 = ratio of average stress in a rectangular compression block

β_1 = compressive stress block factor

δ = elongation (mm)

Q = activation energy of creep divided by the Universal Gas Constant (K)

ε = strain

$\dot{\varepsilon}$ = creep rate

ε_{cr} = creep strain

$\varepsilon_{cr,0}$ = dimensionless creep parameter

ε_{σ} = strain due to applied loading and prestress

ε_T = strain due to thermal elongation

σ = stress (MPa)

η = load ratio

θ = temperature compensated time (hrs)

ϕ_c = material resistance factor for concrete

ϕ_p = material resistance factor for prestressing reinforcement

ϕ_s = material resistance factor for mild reinforcement

Chapter 1

Introduction

"Today's flat-slab post-tensioned buildings, for example, with columns spaced 12 m on center and span-depth ratios of 40, are more complex and require more engineering attention than typical flat-slab buildings of 40 years ago, with columns spaced at 6 m on center and span-depth ratios of 20."

-Randall Poston,
Chair of ACI Committee 318
(Poston and Dolan, 2008)

1.1 General

Post-tensioned (PT) concrete is increasingly used in modern building construction for flat plate slab flooring systems in concrete buildings. Post-tensioned concrete uses high strength cold-drawn prestressing steel tendons which, when tensioned inside ducts in the concrete after casting, compress the concrete slab and result in excellent control of in-service deflections compared with conventional (non-prestressed) reinforced concrete slabs. This prestressing results in secondary support reactions, thereby balancing deflection on the slab. This is turn reduces use of building materials and enables large span-to-depth ratios which creates additional space and open plan compartments. Post-tensioned concrete exists in two forms: unbonded (in which the prestressing steel tendon is greased and sheathed within the concrete, preventing bond to the surrounding concrete) and bonded (in which the prestressing steel tendon is grouted within a steel or plastic duct and thus continuously bonded to the concrete after tensioning). Post-tensioned concrete structures are increasingly popular as they help to meet stringent sustainability and aesthetic objectives in modern, optimized buildings.

Post-tensioning has been used since the 1950s. In modern construction, however, aided by higher strength concretes and computer aided structural optimization in design, PT construction has become increasingly complex – with buildings of 60 storeys or more becoming common – as compared with their historical low-rise counterparts (see Figure 1.1).

Modern PT building **Modern PT building** **Older PT building**

Figure 1.1: Modern versus older PT concrete buildings.

The continual optimization of PT concrete buildings, combined with the ongoing development of stronger concretes and subtle changes in prestressing steel composition and manufacturing, has resulted in structures requiring more engineering attention to guarantee safety in the case of fire. Prescriptive building code requirements, particularly in the United States, have failed to keep up with innovation and have not changed significantly in many decades. Indeed, optimization of PT concrete buildings was a key reason motivating the re-development of the American Concrete Institute (ACI)'s 318 code which will be published in 2014; highlighted by the quote at the beginning of this chapter (Poston and Dolan, 2008).

1.2 Motivation

The above quote by Randall Poston presumably refers to the ambient temperature structural design of PT concrete buildings; however the quote can just as easily be considered to apply to issues around structural design for fire. In practice, a key benefit for designers of PT concrete slabs as compared with designers of steel-framed buildings with composite slabs (whether explicitly acknowledged or not) is

their widely claimed ‘inherent’ fire endurance (see Figure 1.2 for historical reference which has persisted within the industry until present day).

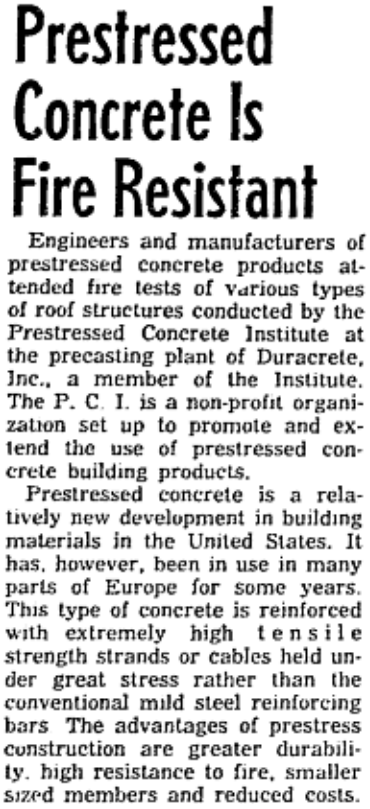

Prestressed Concrete Is Fire Resistant

Engineers and manufacturers of prestressed concrete products attended fire tests of various types of roof structures conducted by the Prestressed Concrete Institute at the precasting plant of Duracrete, Inc., a member of the Institute. The P. C. I. is a non-profit organization set up to promote and extend the use of prestressed concrete building products.

Prestressed concrete is a relatively new development in building materials in the United States. It has, however, been in use in many parts of Europe for some years. This type of concrete is reinforced with extremely high tensile strength strands or cables held under great stress rather than the conventional mild steel reinforcing bars The advantages of prestress construction are greater durability. high resistance to fire, smaller sized members and reduced costs.

Figure 1.2: Advertisement promoting prestressed concrete as a fire resistant construction material (Sarcisota Herald Tribune, 1955).

Confidence in PT concrete slabs’ ability to resist fire was ‘demonstrated’ as early as the 1950s through a series of experiments conducted under standard fire conditions in large scale testing furnaces. However, the applicability of standardized fire tests to real buildings with real fires is debatable on various grounds (Bisby et al., 2013). Standard furnace tests fail to capture many of the complexities of real structural response of PT concrete structures in real fires. For example, when unbonded and stressed prestressing steel runs continuously within a slab across several bays of a building, local damage to the tendon will affect the structural response and capacity of adjacent bays. In the event that no conventional bonded reinforcement is provided, as permitted by some codes, the PT concrete slab could lose tensile reinforcement across multiple bays, even in areas not directly exposed to the fire. A standard fire test of a simple span is thus incapable of capturing the global structural response. While this is true for virtually all structures, it is particularly

problematic for unbonded PT concrete. In addition, since most fire tests of PT concrete slabs are now more than 50 years old, the materials and construction techniques used in available tests are not representative of those used in modern PT concrete construction.

To date, no fire tests have demonstrated the degree to which restraining mechanisms in continuous PT concrete structures of realistic span-to-depth ratio can be created and sustained during a fire to prevent collapse. Because prestressing steel tendons are more sensitive to high temperature damage than mild steel reinforcement, prestressing steel requires larger concrete cover protection from fire; however this cover can be lost in a fire due to spalling, thereby directly exposing the prestressing steel tendon to severe heating. This issue has recently been the subject of debate within the UK structural engineering community with regard to the performance of PT concrete slabs in fire (e.g. Kelly and Purkiss, 2008; Bailey and Ellobody, 2009a).

It seems clear that a more complete understanding of the structural and thermal response of PT concrete slabs in fire is needed. This thesis investigates some of the above issues for realistic, modern PT concrete structures in (and after) fire so as to guide current practice and steer future research towards the development of defensible performance based and fire safe designs.

1.3 Scope of project

Previous research (Gales, 2009) identified the possibility of potential loss of strength and effects of high temperature plastic damage on the behaviour of unbonded and stressed prestressing steel tendons subjected to localised fire conditions. This prior work suggested that the mechanical properties (strength and stiffness) of prestressing steel tendons degrade under high temperatures. Under certain conditions this reduction can result in dramatic and irrecoverable loss of prestress, or even prestressing steel tendon rupture. This rupture is more likely to occur when heating is localised due to a complex interplay of plastic deformation (which causes a loss of tensioning in the prestressing steel; i.e. prestress relaxation) and strength loss (i.e. reductions in mechanical properties). However, predicting the observed responses was not possible and the consequences for the global structural response of real PT concrete structures, both during and after a fire, have never been explored in detail.

In the previous work the prestressing steel tendon behaviour could only be approximated using outdated material parameters from tests on historical materials available in the literature.

Limited information is available on the consequences of localised heating of prestressing steel tendons during fire on the global response of a PT concrete structure; this is the basis of the central problem treated herein. The research presented in this thesis explores two central themes:

(1) the thermo-physical degradation of mechanical properties of prestressing steel tendons at elevated temperature; and
(2) the structural and thermal response of realistic and modern continuous PT concrete slabs exposed locally to high temperature.

To address the first theme, numerous high temperature uniaxial tensile tests (both transient and steady-state) were performed at various stress levels to quantify the true material response and deformation behaviour of modern cold drawn prestressing steel tendons. With an accurate understanding of the prestressing steel behaviour at high temperature it was then desired to investigate the global response of a PT concrete structure in fire to address the second theme, and to develop an understanding of the full range of complexities of structural response for even very simple continuous unbonded PT elements. The structural and thermal response of several tested simplified continuous PT concrete slabs, which incorporated as many of the relevant structural behaviours as possible, to severe localised heating was then considered. This is a critical step in the development of a rational understanding of the fire performance of real PT concrete structures.

Although both the bonded and unbonded cases of PT concrete construction are considered herein, due to the progressive collapse risk potential resulting from tendon failure across multiple bays, the unbonded case is given more specific attention.

1.4 Research objectives

There are a number of load carrying mechanisms and failure modes that may be important for PT concrete structures in fire which have not yet been identified or adequately considered in literature. In particular, because PT concrete structures are

continuous across multiple bays, tests on isolated, simply-supported members with short tendon lengths cannot be considered as representative (or perhaps even conservative). Tendon continuity, deflections, and restraint can all be expected to play significant roles in real structures, particularly given UPT slabs' unusually large span-to-depth ratios. The research in this thesis thus aims to:

- study available knowledge that can be gleaned from traditional experimental fire tests of simply supported slabs and from the global behaviour of real fire-exposed PT concrete structures;
- better understand, develop input parameters for, and develop the ability to model the deformation behaviour of prestressing steel tendons at high temperatures under variable stress and heating conditions (localised, uniform, steady-state, and transient heating);
- develop an understanding of the potential influence of high temperature prestressing steel tendon stress relaxation on the structural response of a continuous multiple bay PT concrete slab;
- identify and highlight the structural actions (i.e., thermal bowing, restraint, concrete stiffness loss, continuity, spalling, slab splitting etc.) that are likely to act in continuous, multiple span (restrained) PT concrete slabs subjected to fire; and
- perform sensor rich tests on highly simplified and idealised PT concrete slabs to provide credible and detailed data which can be used in future validation of computational models to predict the response of UPT slabs during fires, thus enabling defensible performance based structural fire design of these types of structures.

1.5 Outline of thesis

This thesis has been written according to the "Traditional Format" described by the recommended format of the College of Science and Engineering at the University of Edinburgh. Portions of the thesis have previously been published in peer reviewed journals but have been modified herein to suit the traditional thesis format and to maintain flow and coherence. In these prior publications the author wrote the first draft during his doctoral studies at the University of Edinburgh and was primary

author (refer to the declaration statement on page iii for specific details). The following is a brief outline of each chapter.

Chapter 2: A Review of Experimental and Real Unbonded Post-Tensioned Concrete Structures in Fire reviews the structural fire performance of unbonded PT concrete slabs from information available in the literature. A detailed review of the available furnace test data, which have been used over the past half century to generate current fire design guidance for unbonded PT beams and slabs, is presented and discussed. A discussion of bonded post-tensioned concrete fire test behaviour follows, and considers the influence of bonded versus unbonded PT construction. Also reviewed are several case studies demonstrating the response of real unbonded PT buildings in real fires. The intent of the chapter is to highlight the current state of knowledge with respect to the fire performance of unbonded PT buildings and to suggest possible research gaps and areas which are the focus of the work presented in subsequent chapters.

Chapter 3: Experiments and Modelling of Unbonded Prestressing Steel Tendons focuses on developing a comprehensive understanding of deformation of prestressing steel in high temperature deformation that illustrating time-temperature-stress-strength interdependencies. Previous work (Gales, 2009) demonstrated experimentally that prestressing steel tendon rupture could be more likely under localised heating. This was influenced by a complex plastic deformation and mechanical property reduction interplay (causing prestress relaxation). This conclusion came from heated prestressing steel tendon tests that were performed on a 'Strongback beam' testing frame equipped with a localised furnace. The furnace was capable of subjecting a stressed prestressing tendon to localised heating and cooling. These and similar tests are reviewed in this chapter. A preliminary computational model which predicts prestress relaxation is then validated against these prior tests. A novel numerical model of an unbonded PT concrete slab continous over three bays and exposed to fire is presented. Attention is given to the deformation and potential failure of the prestressing steel tendons. A parametric analysis using the model structure is then presented which considers: (i) the uniformity of the fire (heated length ratio); (ii) real time user specified spalling scenarios (manually removing concrete cover during the heat transfer analysis); and (iii) the effect of different

specified concrete covers to the prestressing steel tendon. Modelling results are compared against current fire safety provisions in various international building codes.

Chapter 4: New Parameters to Describe High Temperature Deformation of Prestressing Steel develops new material parameters that can more accurately characterize prestressing steel behaviour in high temperature for modern prestressing steels. To develop these parameters, a series of uniaxial tensile tests at high temperature is presented and discussed. Experimental validation of a method for non contact strain measurement at high temperature, using Digital Image Correlation (DIC), is given. Digital image correlation software developed previously by White et al. (2003), is assessed and validated for this purpose. The validation exercise is performed considering prestressing steel behaviour at both ambient and high temperature conditions with comparison to conventional strain measurement instrumentation, cross-sectional area reductions to constant volume theories, and comparison to theoretical and extensometer measured thermal expansion at high temperature. The DIC technique is then used to describe the thermal, mechanical and plastic response of three different prestressing steel tendons exposed to variable stress-temperature-time regimes. More than 70 heated uniaxial tensile tests are used to develop material parameters for use in a high temperature creep/relaxation model for modern prestressing steel tendons. These parameters are then validated using stress relaxation tests.

Chapter 5: Tests of Continuous Post-Tensioned Concrete Slabs Under Localised Heating presents a series of three novel large-scale tests on locally heated, simplified, continuous PT concrete slab strips. In real multiple bay and continuous unbonded PT concrete slabs exposed to fire, other structural actions (thermal bowing, restraint, concrete stiffness loss, continuity, spalling, slab splitting etc.) may also play significant (often inter-related) roles influencing the response. To guide current design and steer future research towards the development of defensible, performance based, fire safe designs of these structures, a series of non-standard structural fire experiments on continuous, restrained PT concrete slabs tested under localised heating are presented. Both the thermal and structural response of these slabs is presented and discussed in detail. Implications for future modelling exercises are

made and a partial validation of computational modelling from Chapters 3 and 4 of prestressing tendons in PT concrete structures is given.

Chapter 6: Conclusions and Recommendations highlights the main conclusions, novelty, and practical significance arising from the research presented in the thesis, gives recommendations for use by modellers and designers, and summarizes areas for future research which is required as the structural community moves towards defining rational performance objectives for PT concrete structures in fire.

Chapter 2

A Review of Experimental and Real Unbonded Post-Tensioned Concrete Structures in Fire

"The object of all tests of building materials should be to determine facts and develop results that may be of practical value in future designing. In order that such facts and results may have real value, three conditions are necessary: First, that the materials tested shall be identical with what is commercially available in the open market; second, that the conditions, methods, and details of constructions conform exactly to those obtainable in practice; third, that the tests be conducted in a scientific manner."

-Abraham Himmelwright
On the development of a standardized fire test
(Himmelwright, 1899)

2.1 General

Unbonded post-tensioned concrete is an increasingly popular method of construction, since it allows for rapid erection of economical and sustainable buildings. While its use has been widespread in the United States since the late 1950s, it has recently seen wider use in the UK, Europe, China, and the Middle East. Unbonded post-tensioned concrete uses high strength cold-drawn prestressing steel tendons. The tendons are greased and sheathed and cast within the concrete. This prevents the tendons from bonding to the surrounding concrete. When tensioned inside ducts in the concrete after casting, the prestressing steel compresses the concrete slab and results in excellent control of in-service deflections compared with conventional (i.e. non-prestressed) reinforced concrete slabs (Khan and Williams, 1995). Unbonded post-tensioned concrete structures are increasingly popular as they help meet stringent sustainability and aesthetic objectives in modern, optimized buildings.

To help explain how optimization of PT concrete construction is achieved, it is necessary to briefly explain a design concept called load balancing (Lin, 1963; Aalami, 2007). In this concept, the prestressing tendon, which typically follows a parabolic profile within the slab, can be represented as a distributed force which is applied on the entire slab system. This distributed force may be a function of the tendon drape (the prestressing steel's eccentricity with respect to the neutral axis)

and degree of tensioning of the prestressing steel. The simulated distributed force acts to 'balance' the net loading (live and dead) which contributes to deflection. Figure 2.1 provides a visual representation. Figure 2.1 is a highly idealised schematic of loading behaviour in PT slabs; in reality the secondary loading exerted by the stressed prestressing steel is more complicated, in part due to the fixity of support conditions, compressive reactions at slab ends and the amount of tendon draped above and below the slab's neutral axis, etc. The decreased deflection in PT slabs (as can be conceived through this concept) helps minimize material usage enabling shallower, optimized slabs which enable additional space and open plan compartments.

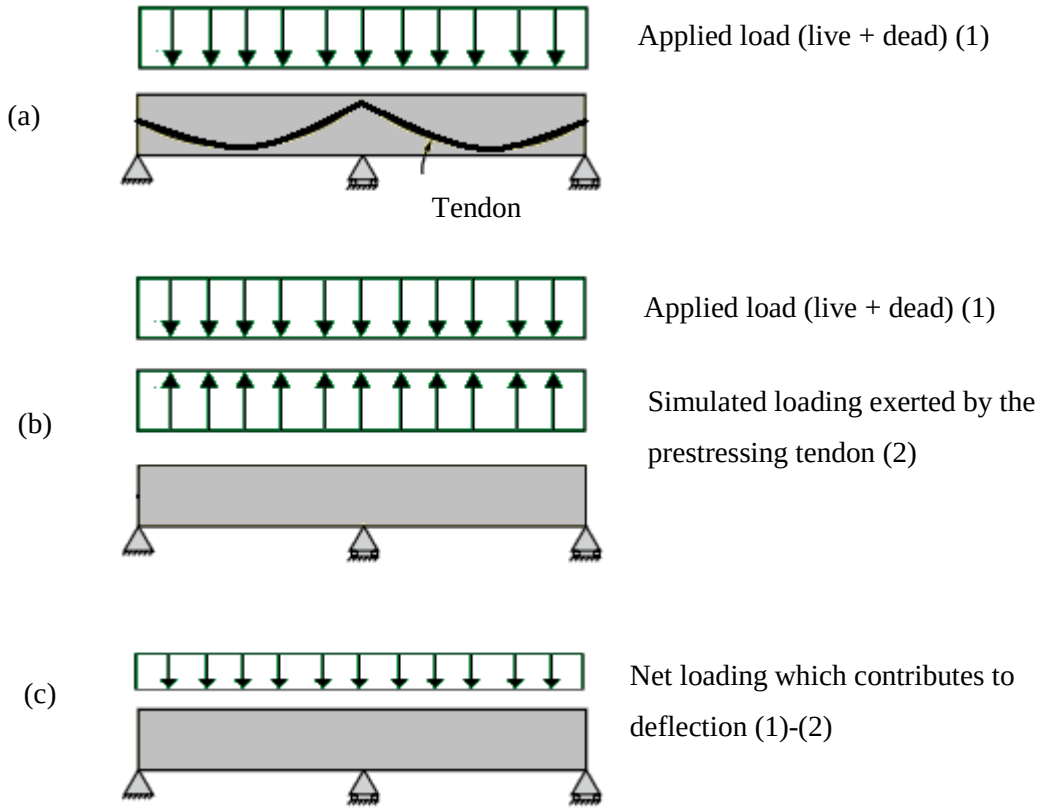

Figure 2.1: Simplified procedure of load balancing for visualizing reduced loads that contribute to deflection adapted after Lin (1963) and Aalami (2007).

However, the structural optimization and efficiency of unbonded PT elements can generate potential concerns associated with their performance during fire. Indeed, there has been some debate in recent years (Bailey and Ellobody, 2009a; Purkiss and Kelly, 2008) regarding the fire safety of PT concrete structures (flat slabs

in particular). Some of the concerns specific to unbonded PT structures in fire are openly acknowledged (and to a certain extent addressed) by available structural design codes. For instance, the fact that prestressing steel tendons are more sensitive to temperature than mild (bonded) reinforcement and suffer proportionally greater losses in strength and stiffness as temperatures increase in a fire; this is sometimes reflected by larger prescribed concrete covers to prestressed reinforcement. However, many potential credible concerns have not received sufficient research attention, and available prescriptive rules for fire-safe structural design of unbonded PT concrete beams and slabs appear somewhat outdated on the basis of available information, particularly given current trends toward performance based design for fire.

Available experimental data on the fire performance of unbonded PT structures come from relatively few unrealistic and often outdated large-scale furnace tests on unbonded PT structures (Troxell, 1959a; Troxell, 1959b; UL, 1966; Gustaferro et al., 1971; Van Herberghen and Van Damme, 1983; Falkner and Gerritzen, 2005; Bailey and Ellobody, 2009; Zheng et al., 2010; and Aimen et al., 2013). It appears that no realistic fire tests of multiple bay continuous unbonded PT concrete elements have ever been performed. While available standard furnace test data are instructive, they are neither representative nor necessarily conservative with respect to the performance of real unbonded PT buildings in real fires. Indeed, available case studies of real fires in unbonded PT buildings (Troxell, 1965; Lukkunaprasit, 1990; Barth and Aalami, 1992; Sarkkinen, 2006; Post and Korman, 2000; and Stern, 2002), discussed in detail below, suggest that when unbonded PT concrete beams or slabs fail in fire it is rarely for the reasons that would be expected on the basis of available testing or design guidance.

This chapter reviews the structural fire performance of unbonded PT concrete slabs presented within the available literature. A detailed review of the available furnace test data which have been used over the past half century to generate current fire design guidance for unbonded PT beams and slabs is provided (Sections 2.3 and 2.4). Discussion is included on bonded post-tensioned fire test behaviour so as to consider the influence of bonded versus unbonded construction (Section 2.5). Also reviewed are a number of case studies demonstrating the response of real unbonded PT buildings in real fires (Section 2.6). The intent throughout is to highlight the

current state of knowledge of the fire performance of unbonded PT buildings and to identify and prioritize research areas which will be the focus of subsequent chapters.

A less exhaustive literature review on this topic has been presented previously by Lee and Bailey (2006); however this prior work provided insufficient detail to clearly highlight the inadequacies of current knowledge.

2.2 Motivation and significance

It is acknowledged at the outset that the performance of concrete structures in real fires is generally very good. It seems clear, however, that current fire design requirements for unbonded PT buildings are based on a fundamentally limited understanding of their response to fire; the absence of widespread evidence of failures should not be construed as evidence of satisfactory response. Available fire experiments on unbonded PT elements have either been furnace tests on isolated beams or one-way slabs (Van herberghen and Van Damme, 1983; Falkner and Gerritzen, 2005; Bailey and Ellobody, 2009; Zheng et al. 2010; and Aimen et al., 2013), with their numerous, well-documented shortcomings (Iwankiw and Beyler, 2008), or are so old as to be of limited relevance to contemporary concretes and construction methods (Troxell, 1959a; Troxell, 1959b; UL, 1966; UL, 1968; Gustaferro et al., 1971). Existing prescriptive design guidelines for fire-safe structural design of unbonded PT buildings (e.g. IBC, 2012; NBCC, 2005; CEN, 2004; NZS, 2006) typically specify only minimum member dimensions and minimum concrete cover to the unbonded PT reinforcement; this approach is insufficient to guarantee safety. Many other factors which have not previously been adequately considered may also be important for unbonded PT structures in fire. These include:

- **Tendon continuity across multiple bays** – Post-tensioned buildings which contain unbonded tendons that are continuous over multiple bays may exceed 70 m in length (Nawy, 2008; Tranath, 2010). Unlike bonded PT buildings, in unbonded PT buildings the tendons are free to move longitudinally within ducts within beams and/or slabs. Localised damage to a tendon, whether due to localised heating from a fire or other factors, thus has consequences across all bays of the structure. Furthermore, research has suggested (see Chapter 3) that

the longer the total length of an unbonded tendon between anchors, the greater the likelihood of tendon rupture due to localised heating. This rupture is due to a combination of accelerating creep strains and loss of tensile strength of the tendon. The consequences of premature tendon rupture during fire have received no research attention to date outside the previous work by the author, despite the fact that tendon rupture during fire has led to progressive failure of several floors of at least one unbonded PT building (Post and Korman, 2000), and to forced demolition of several structures after real fires (Barth and Aalami, 1992; Brannigan and Corbett, 2008).

- **Higher strength concretes** – A trend in the design and construction of modern unbonded PT concrete structures is to use higher concrete compressive strengths than has traditionally been the case. Research has shown that modern, high strength concrete mixes are more likely to experience fire-induced explosive spalling than their low strength counterparts (Kodur and Phan, 2007). Thus, satisfactory performance of unbonded PT elements in fire resistance tests conducted more than 25 years ago cannot necessarily be invoked as evidence of adequate fire resistance for modern unbonded PT structures. The fact that higher concrete strengths are used in modern unbonded PT elements also results in less reserve cross-sectional cover and capacity being available should fire-induced spalling occur.
- **Pre-compression** – Unbonded PT slabs and beams are axially pre-compressed under service loads, and in general this means that a greater proportion of the soffit of an unbonded PT element will be subjected to compressive stresses in service than would be the case for a non-prestressed member. Since compressive stress is a widely acknowledged risk factor for spalling in fire (Hertz, 2003), it is reasonable to assume that that PT beams and slabs are more likely to spall than their non-prestressed counterparts (all other factors being equal). This is not explicitly considered in available unbonded PT design guidance.
- **Large span-to-depth ratios** – A primary advantage of unbonded PT structures is that they enable larger span-to-depth ratios than non-prestressed flooring systems (CPCI, 2007). There is a risk that an unbonded PT slab could experience proportionally greater deflections during fire, due to thermal bowing (caused by

uneven heating gradients in a slab) and smaller lateral restraint forces, than would occur for a non-prestressed slab. Therefore there may be less chance of developing beneficial compressive membrane action for larger unbonded PT span-to-depth ratios. The beneficial effects of compression membrane action in preventing collapse of two-way reinforced concrete flat plate slabs in fire, even when the majority of the bottom steel reinforcement is lost due to heating and/or cover spalling, was clearly shown during the concrete frame fire test performed at Cardington in the 1990s (Bailey, 2002). Bailey's (2002) post-fire assessment of the Cardington concrete frame noted that, in his words, *"during the test on the concrete building, the slab's vertical displacement was small and the static load was supported due to compressive membrane action."* However, Bailey also notes that, *"if the slab's vertical displacements were greater... then it is difficult to see how the slab could have supported the static load."* Inability to engage compressive membrane action is a credible concern for unbonded PT slabs in fire, particularly since unbonded PT tendons are reasonably likely to rupture during fire (as discussed below) and that some design guidelines allow zero mild steel reinforcement in sagging moment regions (CEN, 2004; CSA, 2005; ACI, 2008). Furthermore, slender unbonded PT slabs have larger buckling lengths and are pre-compressed. This increases the potential for global floor-plate buckling under the influence of lateral thermal restraint from surrounding bays. It can be argued that floor-plate buckling would send an unbonded PT slab into tensile membrane action in fire, which could prevent collapse, although this can only be engaged if the unbonded PT tendons are intact and/or if sufficient mild steel reinforcement is present. It is also worth noting that the span-to-depth ratios used in available furnace tests on unbonded PT members have generally been unrealistically small due to limits in available furnace sizes.

- **Fire resistance based on concrete cover** – Available structural fire resistance ratings for unbonded PT structures are based on minimum member dimensions and provision of sufficient concrete cover to the prestressed reinforcement (IBC, 2012; NBCC, 2005; CEN, 2004; NZS, 2006). The code prescribed covers are based largely on results of standard furnace tests conducted on isolated unbonded PT slabs and beams during the 1950s and 1960s (Troxell, 1959a; Troxell, 1959b;

UL, 1966; Gustaferro et al., 1971), although some codes have been revised based on more recent furnace testing (see Purkiss and Kelly (2008) for discussion pertaining to the development of EN 1992-1-2 (CEN, 2004) requirements and also Chapter 3). As described below, in some cases these tests used concrete which had been pre-conditioned before fire testing, did not define the degree of restraint adequately or used a light steel mesh within the concrete cover to prevent or arrest spalling during fire. Cover spalling was thus explicitly excluded from many of the tests, yet these important details are routinely omitted when invoking these test data to justify current prescriptive cover requirements. Clearly, use of light steel mesh in the cover and pre-drying of the concrete are non-representative of typical unbonded PT construction. Additionally, the definition of restraint of a structure can be blurred by the structure's true stiffness (which varies between building configurations). In instances where 'total' restraint is achieved, premature failure of a PT structure could be observed due to explosive spalling (see Bletzaker, 1967). This, along with the other concerns noted above, casts doubt on the wisdom of relying on prescriptive concrete cover thickness as the sole means of achieving fire resistance in unbonded PT buildings.

- **Shear-critical designs** – Because unbonded PT slabs allow shallow, flat floor-plates over large spans they can be shear-critical under ambient design loads (see Gales et al. (2009)). Such slabs have less reserve shear capacity than their non-prestressed counterparts, making them more susceptible to shear failure during fire. Furthermore, many international unbonded PT design standards (e.g. CEN, 2004; CSA, 2005; ACI, 2008) permit designers to consider the pre-compression from the unbonded and stressed prestressing steel tendons when calculating the shear capacity of the concrete at ambient. Given that tendon rupture during fire, before the prescribed fire rating is achieved, is a credible concern in unbonded PT structures, slab pre-compression may be lost during fire. Thus, there is a risk that the shear capacity of the already shear-critical structure may be compromised; this has potentially serious consequences for punching shear failure and progressive collapse during fire which are worthy of consideration.

- **Inadequacies of standard furnace tests** – As already noted, existing requirements for fire safe design of unbonded PT beams and slabs are based on a relatively small number of standard fire tests on isolated elements. It is widely recognized that standard fire exposures used in furnace tests (e.g. ASTM E119, 2001; ISO 834, 1999) are unrealistic, particularly for large compartments or open floor plates as found in many modern buildings (Stern-Gottfried and Rein, 2012). It is generally argued however that standard fires are conservative representations of credible worst-case fires for most types of construction. This rationale cannot be applied to unbonded PT concrete beams or slabs because unbonded prestressing steel tendons are, by definition, continuous over multiple bays, and localised or travelling fires are more, rather than less likely to result in premature tendon rupture (refer to tests reviewed in Chapter 3).
- **Zero bonded mild steel reinforcement** – Despite recommendations to the contrary made by researchers (e.g.Van Herberghen and Van Damme, 1983), many existing codes permit design of unbonded PT slabs with zero mild steel reinforcement in sagging moment regions (depending on the in-service concrete stress levels) (e.g. CEN, 2004; CSA, 2005; ACI, 2008). Thus, premature tendon rupture during fire could result in total loss of tensile reinforcement which would preclude engagement of tensile membrane action that may be needed to prevent collapse.

The above discussion points to numerous concerns and inadequacies of available knowledge with respect to the fire performance of unbonded PT members in real buildings. All of these are worthy of further investigation. To further highlight the apparent disconnect between existing knowledge, available guidance, and industry practice, the Sections 2.3 and 2.4 summarizes and critically appraise available data from the 41 fire tests on unbonded PT structural members that are currently available in the literature. Each section denotes the test date in the heading parenthesis. Tables 2.1-2.3 which prelude Sections 2.3 and 2.4 provide detailed summary of the assembled test data.

2.3 Legacy furnace tests (before 1980)

Current fire design guidance for unbonded PT beams and slabs is based predominantly on standard fire endurance tests performed prior to 1980. The EN 1992-1-2 (CEN, 2004) requirements for fire-safe design appear to have also been influenced by a series of furnace tests performed in 1983 (see Purkiss and Kelly (2008) for discussion). While many dozens of fire tests on reinforced and prestressed concrete slabs and beams had been performed prior to 1980, only six tests had been reported on flexural elements incorporating unbonded and stressed prestressing steel reinforcement. None of these tests can be considered as representative of current construction materials or techniques (Jimenez, 2009).

Fire Prevention Research Institute (1958-1959)

Interestingly, the earliest tests ever conducted on unbonded PT elements were among the most realistic which have ever been undertaken. In 1958, the Fire Prevention Research Institute (FPRI), California, conducted the first openly reported fire test on an unbonded PT concrete assembly, which was a single standard furnace test of a two-way unbonded PT beam and slab panel (Troxell, 1959a). Figure 2.2 shows details of the tested assembly, which consisted of a 150 mm deep siliceous aggregate concrete slab spanning 3180 mm between two 4770 mm long unbonded PT beams with different cross-sections.

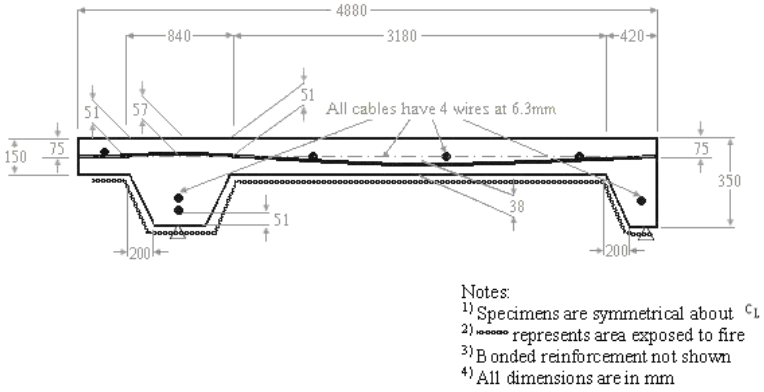

Figure 2.2: Fire Prevention Research Institute slab and beam test (after Troxell, 1959a).

The beams were prestressed longitudinally with draped unbonded prestressing steel cables. The slab was prestressed with draped unbonded prestressing steel cables in the spanning direction and with straight cables at the slab's mid-depth in the orthogonal direction. The minimum clear concrete cover to the unbonded prestressing steel cables, each of which consisted of four 6.3 mm diameter cold drawn, stress relieved wires with an ultimate tensile strength of 1760 MPa, prestressed to 1030 MPa, was 51 mm in the beams and 38 mm in the slab. There was no mild steel reinforcement within the tested spans. The assembly was pin-supported under the beams at its corners and was subjected to a uniformly distributed superimposed load corresponding to the full design live load. The assembly was exposed to the ASTM E119 (2001) fire under a "restrained" condition in both spanning directions with a heated length ratio near 100%. Restraint was accomplished by fixing the test specimen within a steel restraining frame *"to restrain it against thermal deformations and to simulate the conditions in a building."* The gap between the restraining frame and the tested assembly was filled with grout prior to testing; this very good practice appears to have been largely abandoned in many modern structural fire testing laboratories. However, neither the rotational nor lateral stiffness of the restraining frame were stated so it is difficult to gauge how closely these conditions could resemble a real building. The relative humidity (RH) in the slab at the time of testing was 62% at a depth of 38 mm (about 1.9% moisture by mass) and the concrete compressive strength was 41 MPa. It is unknown whether the slab was preconditioned, although the low moisture content suggests that this might have been the case.

Heat transmission failure criteria were exceeded at 231 minutes. No structural end-point was reached during the test, which lasted a total of 264 minutes. The maximum recorded tendon temperature was 506°C in the draped slab cables. No cable ruptures were observed. The beams experienced spalling, typically to a depth not greater than 25 mm but in some areas up to 64 mm deep, beginning at 14 minutes of fire and continuing for about one hour. The slab's soffit did not experience any spalling, although splitting cracks with a width of less than 1 mm were observed along the tendons in several locations. The unexposed surface developed large cracks as wide as 6 mm adjacent to the beams due to thermal/flexural deformations.

In 1959, FPRI conducted a second fire test of a similar two-way unbonded PT slab panel without beams (see Figure 2.3). The original testing report is not readily accessible (Troxell, 1959b), although general descriptions of the test are available elsewhere (Troxell, 1962; PCI, 1972; Gustaferro, 1973). Figure 2.3 illustrates the tested assembly, which consisted of a 152 mm deep siliceous aggregate concrete flat slab panel spanning 3910 mm by 4270 mm and supported on pins at its corners.

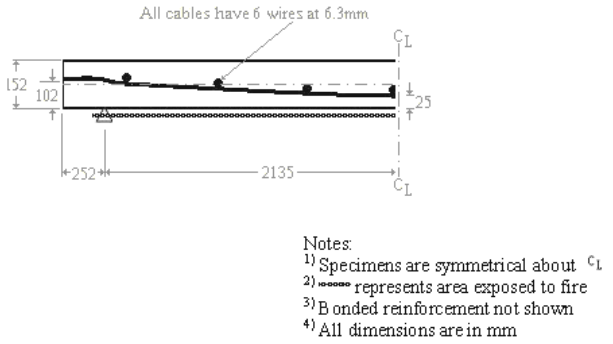

Figure 2.3: Fire Prevention Research Institute slab (after Troxell, 1959b).

The slab was prestressed with draped unbonded prestressing steel cables in both directions. The minimum clear concrete cover to the prestressing steel cables, each of which consisted of six 6.3 mm diameter wires, was 38 mm in the larger spanning direction at midspan. The tendons were stressed to 990 MPa. No mild steel reinforcement was provided within the spans. The slab was subjected to a uniformly distributed superimposed load corresponding to 1.0 times the design live load and exposed to the ASTM E119 fire, again using laterally-restrained conditions in both spanning directions. The heated length ratio was over 90%. The RH in the slab at the time of testing was 76% (about 2.3% by mass) at an unknown depth, and the concrete compressive strength was 30 MPa.

The test was halted at 190 minutes before any failures were observed, presumably because a three hour fire rating had been reached. The recorded temperatures suggest that a heat transmission failure would have occurred about five minutes after the test was stopped, if the heating had been maintained. The maximum recorded tendon temperature was 563°C. Neither cable ruptures, nor spalling or cracking are noted in the available references, although standard furnace testing

reports do not generally require disclosure of such details provided that satisfactory ratings are achieved according to load-bearing, insulation, and integrity criteria.

Portland Cement Association (1964)

In 1964, as part of a larger study on the fire performance of various types of concrete beams, the Fire Research Laboratory of the Portland Cement Association (PCA), Illinois, conducted two standard furnace tests of unbonded PT beams with T-shaped cross sections (Gustafferro, 1971; PCI, 1972; Gustafferro, 1973). The beams' cross-sections are shown in Figures 2.4 and 2.5; they were essentially rectangular, with a depth of 635 mm, a web width of 356 mm, and small flanges of 150 mm × 100 mm.

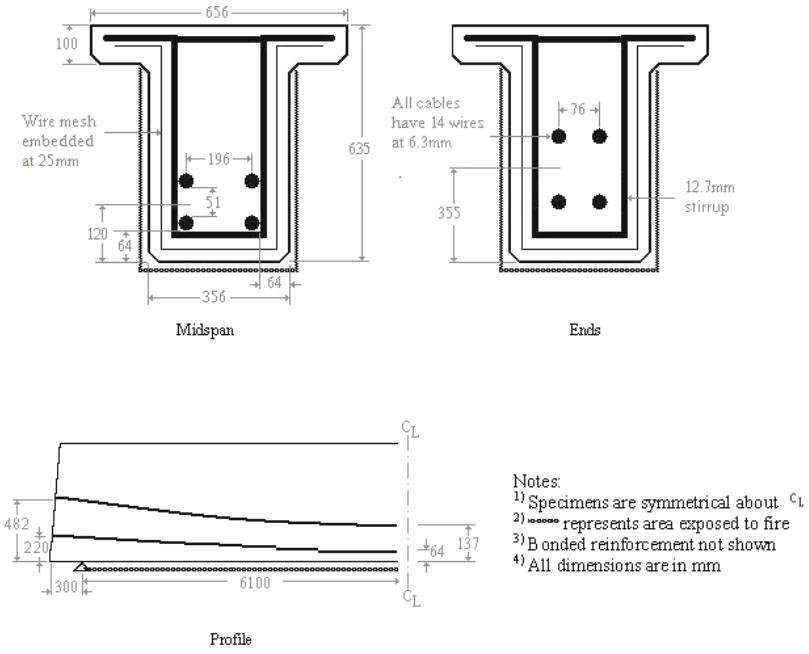

Figure 2.4: Portland Cement Association T-Beam with unbonded prestressing wire (after Gustaferro et al., 1971).

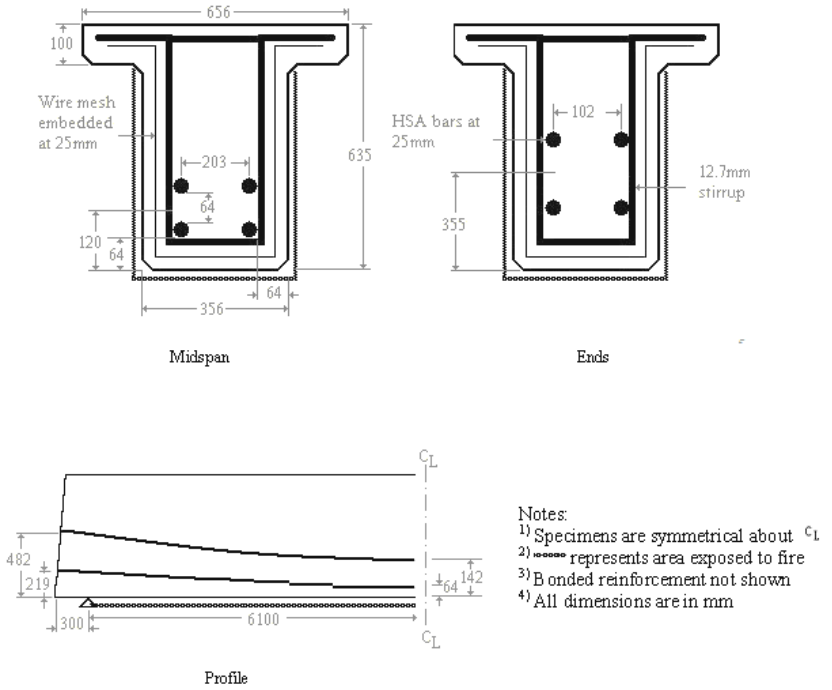

Figure 2.5: Portland Cement Association T-Beam with unbonded high strength alloy bar (after Gustaferro et al., 1971).

One beam (Beam 80) was prestressed with four draped unbonded PT high strength alloy bars, each with a diameter of 25 mm and an ultimate strength of 1168 MPa, prestressed to 770 MPa. The other beam (Beam 76) was prestressed with four draped unbonded and stressed prestressing steel cables, each consisting of fourteen 6.4 mm diameter wires with an ultimate strength of 1760 MPa, prestressed to 1168 MPa. In both cases the minimum clear cover at mid span was 64 mm on both the soffit and the sides.

It is noteworthy that while details of the mild steel reinforcement are not shown in the summaries of these tests published in PCI's Post-Tensioning Manual (PCI, 1972), the original PCA research report (Gustaferro, 1971) clearly shows that both of these beams included a light steel mesh (welded wire fabric of orthogonal 2 mm diameter wires, 51 mm on centre in both directions) placed at a depth of 25 mm (mid-depth of the concrete cover) over the entire fire-exposed perimeter of the beams. This is significant, since the presence of this mesh may have mitigated cover spalling (Khoury and Anderberg, 2000) and would have arrested it if it occurred. On the basis of similar fire endurances achieved for two pair of beams which were identical but for the fact that two had mesh in the cover and the other two did not, the original PCA test report (Gustaferro, 1971) states that, "*the use of mesh within*

concrete cover is unnecessary"; this statement appears to have been embraced in the years since these tests. It is also significant that the specimens in this study were preconditioned in a humidity-controlled environment at 30-40% relative humidity for at least two years prior to testing. The RH in Beams 80 and 76 at unknown depths at the time of testing were 75% (about 2.3% by mass) and 72% (about 2.2% by mass), and their concrete compressive strengths were 39 MPa and 41 MPa, respectively. Both beams were of normal weight concrete fabricated using carbonate aggregates, which are known to be less prone to spalling than siliceous aggregates (Kodur and McGrath, 2003).

The beams were simply-supported over a span of 12200 mm; much larger than is typical for a standard furnace test, and were subjected to uniformly distributed superimposed loads sufficient to generate load ratios (ratios of total applied midspan moment to nominal mid span moment capacity) of approximately 0.52, during exposure to the ASTM E119 fire (heated to a ratio of about 95%). Restraint was prevented using hinged-roller supports.

Both beams reached structural end points during testing, Beam 80 at 302 minutes and Beam 76 at 184 minutes. In both cases failure was evidenced by gradually accelerating mid span deflections under sustained load. No spalling was observed for Beam 80, whereas Beam 76 experienced widespread spalling, to the depth of the welded wire fabric, beginning after 10 minutes. This was a key factor contributing to the comparatively low fire resistance of Beam 76. The increased spalling for Beam 76 was despite it having only 11% higher total prestress than Beam 80. Both beams had identical applied loading. Beam 80 developed a number of longitudinal hairline cracks along the tendons during the test, but these apparently remained small. The prestressing steel in Beam 80 reached maximum recorded temperatures of 277°C, 368°C, 429°C, and 503°C after 2, 3, 4, and 5 hours of exposure, respectively. The maximum prestressing steel temperature recorded at failure was about 541°C in Beam 80 after 5 hours of exposure. Beam 76 developed two "significant flexural cracks" in the mid span region at about 150 minutes, which likely contributed, along with widespread cover spalling noted above, to failure. The prestressing steel in Beam 76 reached maximum recorded temperatures of 316°C and 416°C after 2 and 3 hours of exposure, respectively. The maximum prestressing steel

temperature recorded prior to failure was about 427°C in Beam 76 after 3 hours of exposure. No tendon ruptures were noted.

A key conclusion stated in the PCA report on these tests (Gustafferro, 1971), which is reiterated in a later summary paper by Gustaferro (1973) and which appears to have been embraced in the years since these tests, is that beams with unbonded PT reinforcement have about the same fire endurance as their counterparts with bonded prestressed reinforcement. While this conclusion is unsurprising for isolated, simply supported, non-continuous beams with uniform heating, the wider applicability of this conclusion for real unbonded PT flat plate structures is highly questionable. Indeed, recent furnace testing by Bailey and Ellobody (2009) (described later) showed that bonded PT slabs were capable of achieving their designed target fire resistance whereas otherwise identical unbonded PT slabs had fire resistances that were slightly lower than expected.

Underwriters' Laboratories (1965-1967)

In 1965, as part of a larger study involving various types of prestressed concrete members, the Underwriters' Laboratories (UL), Illinois, conducted a standard fire test of an unbonded PT inverted T-beam (UL, 1966; PCI, 1972; Gustaferro, 1973). Few details of this test have been reported in the open literature. The beam's cross-sectional details are shown in Figure 2.6.

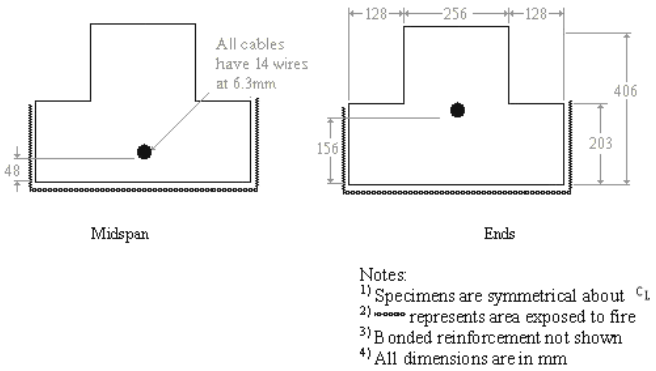

Figure 2.6 Underwriters Laboratory inverted T-beam (after UL, 1966).

The beam was fabricated from normal weight carbonate aggregate concrete of unknown strength, moisture content, and pre-test conditioning regime. It incorporated a single, draped unbonded tendon with a minimum clear concrete cover of 48 mm at mid span. No mild steel reinforcement appears to have been provided. The beam was tested under exposure to the ASTM E119 fire over its full length with a span of 5310 mm with a superimposed load corresponding to 1.0 times the design live load. The beam ends were restrained by grout fill within a restraining frame, although details of the actual restraining system and stiffness are unavailable. Neither cracking nor spalling was noted during the test. The tendon temperature at mid span was 338°C at 180 minutes and 377°C at 240 minutes. The test was stopped at 255 minutes before a structural end point was reached.

In 1967, UL conducted a single standard fire test of a two-way unbonded PT slab panel cast from lightweight concrete (UL, 1968; PCI, 1972; Gustaferro, 1973). Figure 2.7 shows the tested assembly, which consisted of a 152 mm deep, expanded shale aggregate concrete slab panel spanning 4270 mm by 5380 mm supported on steel bearing plates at its corners.

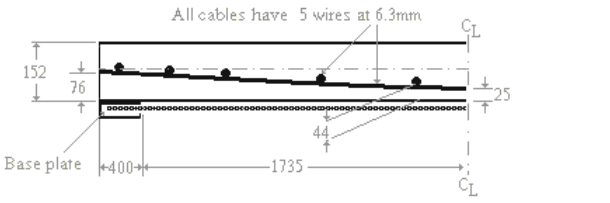

Notes:
1) Specimens are symmetrical about CL
2) ▪▪▪▪▪ represents area exposed to fire
3) Bonded reinforcement not shown
4) All dimensions are in mm

Figure 2.7: Underwriters Laboratory slab (after UL, 1968).

The slab was tensioned with draped unbonded prestressing steel cables in both directions. The minimum clear concrete cover to the unbonded prestressing steel cables, each of which consisted of five 6.3 mm diameter cold drawn, high tension stress-relieved wires, each having a minimum guaranteed ultimate tensile strength of 1655 MPa, was 25 mm in the larger spanning direction. The tendons were tensioned to achieve an in-service design stress of 992 MPa, once the superimposed load had been applied for the fire test. No mild steel reinforcement was provided within the spans. The assembly was subjected to a uniformly distributed superimposed load of 1.0 times the design live load, and was tested under an ASTM

E119 fire using a “fully restrained” condition in both directions (using similar methods as in the FPRI tests described previously). The concrete compressive strength at the time of testing is not known, although it was only 29 MPa at 28 days.

It is crucial to point out that this slab was pre-conditioned for approximately 7.5 months at an elevated temperature of 49°C and a relative humidity of approximately 20% before testing. This is not representative of a typical in-service environment. In combination with the use of expanded shale aggregates, the preconditioning makes the likelihood of cover spalling very low for this slab. The RH of the slab at the time of testing was extremely low, ranging between 42% and 47% (about 1.5% moisture by mass) at the deepest sections.

No spalling or cracking was observed on the exposed face during the fire, which lasted 225 minutes before it was stopped without a structural end point being reached. The maximum tendon temperatures recorded after 60, 120, and 180 minutes were 378°C, 516°C and 688°C, respectively. The maximum tendon temperature at the end of the test was very high, at 704°C after 3 hours. No cable ruptures are noted in the available references. At the end of fire test the slab was subjected to a hose stream for four minutes, and after cooling (overnight) to ambient temperature the slab was loaded to twice its ambient design live load “*without signs of distress.*”

2.4 Modern furnace tests (After 1980)

To the author’s knowledge no additional peer-reviewed research on the fire behaviour of unbonded PT structures was published until the early 1980s. By 1983, researchers apparently began to question the wisdom of relying on results from the pre-1980 tests to guarantee adequate fire resistance for unbonded PT buildings. In particular, a 1983 study in Belgium (Van Herbgerghen and Van Damme, 1983) (described below) recognized that both rotational restraint and tendon continuity into unheated bays could impact an unbonded PT structure’s response to fire. Recent testing in China and Germany (Falkner and Gerritzen, 2005; Zheng et al., 2010; Aimin et al., 2013) have continued in this direction; however they have failed to account for true axial, vertical and rotational restraints found in real unbonded PT structures or to use representative span-to-depth ratios typical of modern construction. More recently, tests have been performed in China (Zheng et al., 2009)

and the UK (Bailey and Ellobody, 2009a-c). Although, in these cases researchers have reverted to performing single element tests of simply-supported, one-way spanning members with unrealistically small span-to-depth ratios and without accounting for continuity or realistic restraint.

Van Herberghen and Van Damme (1983)

Van Herberghen and Van Damme (1983) report on an extensive series of non-standard structural fire tests on eight one-way continuous but unrestrained unbonded PT slab strips. These tests are particularly interesting, since they appear to be the first fire tests to ever simulate rotational restraint through continuity at internal supports – however neglecting axial restraint. These are also the first tests to rationally attempt to consider the possible influence of important parameters noted previously including: cover spalling, load ratio, and the presence and amount of "secondary" bonded mild steel reinforcement. Furthermore, they are the only tests which have ever included an unbonded PT cantilever span exposed to fire. This is significant in light of the case study by Lukkunaprasit (1990) (summarized in Section 2.6) in which an unbonded PT cantilever span in a real unbonded PT building collapsed during a fire.

Details of a typical specimen tested by Van Herberghen and Van Damme (1983) are shown in Figure 2.8. Also shown is a schematic of the test setup, support and loading conditions, and fire exposure. The eight one-way slab strips were 180 mm thick by 1900 mm wide, and approximately 9000 mm in total length. Longitudinally they all had draped 12.7 mm nominal diameter longitudinal seven-wire prestressing steel tendons, with 1150 MPa initial prestress levels, and all were continuous over two internal supports with a central span of about 6000 mm and cantilever spans at each end. Only the central span and one cantilever were exposed to fire giving a heated length ratio of approximately 80%.

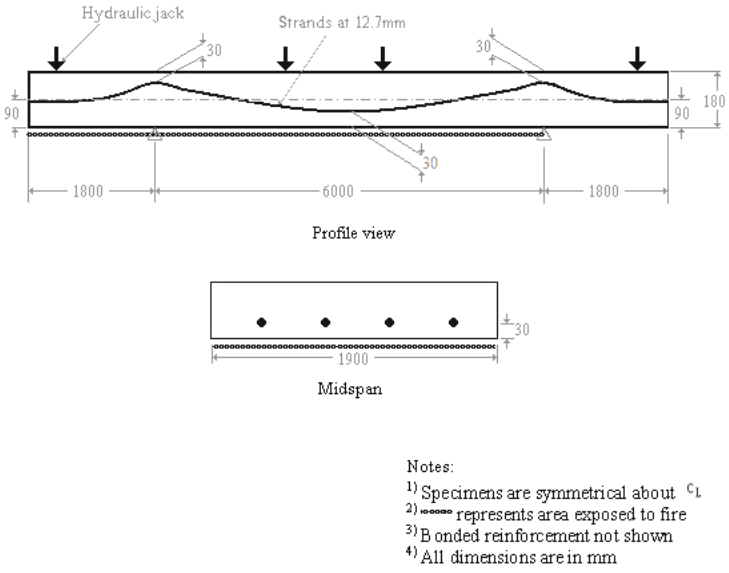

Figure 2.8: Van Herberghen and Van Damme's slab (after Van Herberghen and Van Damme, 1983).

Several parameters were varied amongst the specimens:

- **Concrete type** – Few details of the concrete mixes used in the fabrication of the slabs are available. Neither compressive strength nor moisture content is reported. Two of the slabs were fabricated with limestone aggregate concrete, whereas the other six slabs used "gravel" aggregate (assumed to mean siliceous aggregate, although this is not explicitly stated). The concrete age at the time of testing was between 98 and 273 days, making it difficult to draw meaningful correlations between concrete age, moisture content, and propensity for spalling during fire.
- **Transverse prestressing** – One of the slabs had transverse unbonded PT tendons spaced at 950 mm along its length. The applied prestress is not given, although it seems likely that it was also 1150 MPa.
- **Casting technique** – Two of the slabs were cast integrally on top of precast reinforced concrete forming planks with a thickness of 50 mm to 60 mm and differing mild steel reinforcement details. These two slabs cannot be considered as typical of unbonded PT construction and are ignored in subsequent discussion.
- **Concrete cover and tendon profile** – The remaining six slabs (not cast integrally with precast planks) had minimum clear covers to the prestressed reinforcement, at the middle of the central span, varying between 20 mm and 40 mm. The cover at the support (measured from the top surface of the slab) varied

between 20 mm and 32.5 mm. The source publication (Van Herberghen and Van Damme, 1983) should be consulted for complete details of cover combinations between slabs.

- **Passive (bonded) mild steel reinforcement** – The amount, location, and orientation of mild steel reinforcement in the slabs varied widely, as shown in Table 2.1. Two of the slabs had no passive reinforcement whatsoever, one had mild steel reinforcement in both directions only at the bottom face, and the remaining three had differing amounts of mild steel reinforcement at the top and bottom faces in both directions. The cover to the mild steel reinforcement ranged between 20 and 27.5 mm.

The slabs were loaded during testing using four hydraulic jacks (as shown in Figure 2.8) to produce "*a condition of zero rotation at the supports.*" Exactly how and why this loading condition was chosen is unclear. As a consequence of this rather unusual support condition, the applied load (and hence the bending moments at the critical sections) varied throughout the tests – it seems unlikely that this was any more representative of full-structure response in a real fire than a restrained standard fire test on an isolated structural element with constant vertical load. The initial load was chosen to simulate a comparatively high uniformly distributed superimposed live load of 4.9 kPa. In the paper describing these tests, Van Herberghen and Van Damme (1983) comment that *"the importance of the initial bending moments was of minor influence on the ultimate fire resistance."* It is not clear exactly what is meant by this, but it appears from the data presented that the evolution of bending moments during the fire exposure was far more important in governing the slabs' collapse than the initial loading condition. This is of considerable interest, since the initial load ratio is universally assumed to be of central importance to the structural fire resistance of a flexural assembly in a standard furnace test – to the extent that larger fire endurances are assigned to assemblies with lower load ratios for some types of construction (Gustaferro, 1973; Buchanan, 2001). This confirms the increasingly widespread notion that full-structure interactions in fire are likely to be more significant than the capacities of isolated members as demonstrated through standard furnace tests – this concept is further discussed in Chapter 5.

The results of these tests shed light on a number of concerns specific to unbonded PT construction which have been observed in real fires in unbonded PT buildings. Cover spalling was observed in all of Van Herberghen and Van Damme's tests. Slabs without mild steel reinforcement experienced widespread spalling, which is noted to have contributed to collapse after 40 minutes in one case (with 30 mm clear cover and a 60 minute prescriptive fire resistance rating based on EN 1992-1-2 (2004) cover requirements for a simply supported slab) and impending collapse after 59 minutes in another (with 20 mm clear cover and a 30 minute fire rating based on EN 1992-1-2 requirements for simply supported slabs). Slabs with mild steel reinforcement also experienced spalling, but in these cases it was restricted to the depth of the mild steel reinforcement, confirming that a layer of mild steel reinforcement can, in some cases, arrest cover spalling and provide a measure of additional protection to the unbonded PT tendons. In all cases spalling initiated in the most compressed region of the soffit close to the supports, confirming that pre-compression increases propensity for spalling in fire. This was particularly evident for the single slab which had both transverse and longitudinal prestressing steel (hence biaxial pre-compressive stresses) – this slab suffered severe spalling resulting in premature tendon rupture and impending structural failure in 56 minutes (despite a one hour prescriptive rating (CEN, 2004).

Slabs without mild steel reinforcement experienced transverse cracking (both over the supports and at mid span) and longitudinal ('splitting') cracking along the tendons. Van Herberghen and Van Damme noted that this was due to a combination of pre-compressive stress combined with lateral tensile stresses generated due to thermal effects during the fire; they state that transverse mild steel reinforcement is essential to address this. Slabs with increasing amounts of transverse mild steel reinforcement at the top and bottom faces displayed progressively fewer longitudinal splitting cracks. Subsequent researchers (Bailey and Ellobody, 2009a; Zheng and Hou, 2009) have also noted the importance of splitting cracks for the fire endurance of unbonded PT structures, yet design guidelines continue to essentially ignore this issue.

Very significantly for the current discussion, prestressing steel tendon rupture (of two to four of the longitudinal tendons) was observed in all eight tests. The first

prestressing steel tendon ruptures preceded overall structural collapse by between 5 and 25 minutes. Van Herberghen and Van Damme stated that these ruptures were due to localised heating of the strands resulting from a combination of cover spalling, splitting along the tendons, and transverse cracking at mid span. It is particularly interesting that tendon rupture was observed in this study, since the tendons in these experiments were long in comparison with all previous testing, they were subjected to fire only over a portion of their length, and they were locally heated as a consequence of cracking and spalling (as would occur in a real building fire). Chapter 3 will illustrate that the longer an unbonded PT tendon and the shorter the length over which it is heated, the more likely is premature tendon rupture in fire. This is confirmed by Van Herberghen and Van Damme's tests and again shows that furnace tests on short unbonded PT tendon lengths over single spans are incapable of rationally simulating the structural conditions in a real unbonded PT building; there is little doubt that traditional furnace tests are unconservative for evaluating the risk of premature tendon rupture.

Based on their results, Van Herberghen and Van Damme (1983) suggested revised minimum concrete cover depths, minimum amounts of mild steel reinforcement in unbonded PT flat plate slabs, and minimum amounts of mild steel reinforcement in support regions to prevent excessive flexural cracking. Current EN 1992-1-2 (2004) requirements appear to have been influenced by these recommendations (after adjusting from clear cover to axis distance) (Purkiss and Kelly, 2008). However, other code writing bodies (e.g. IBC, 2012), have largely ignored the recommendations emerging from this study despite additional evidence from real fires (see below) that they may be warranted. Chapter 3 will describe the historical basis behind these code cover requirements.

Litang, Aimin and Yuli (2004)

In 2004, Litang et al. reported on three one-way continuous but unrestrained unbonded PT slab strips in Chinese (Figure 2.9). These tests were translated and republished in English in 2013 (Aimin et al., 2013) making note of an additional fourth test. Each slab had three spans. The centre span was 4.2 m long and the total

slab length was 12.6 m. The slabs were heated in their edge and middle spans. A brick wall within the furnace acted as a central support.

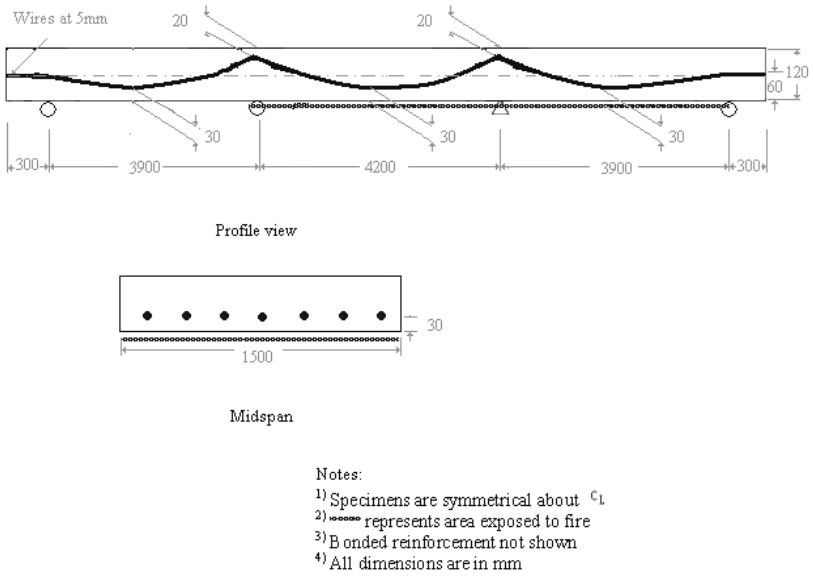

Figure 2.9: Litang et al.'s continous slab (after Litang et al., 2004).

The slabs were supported on one fixed (flat) support and three rollers. This prevented the slab from being restrained axially and vertically. Applied loading on the slabs followed Chinese code guidance of 2.0 kN/m^2, although there is no mention of the slab capacity in the English version of the paper (Aimin et al., 2013). The prestressing force is also not described in the English version. The prestressing steel strands were 15.24 mm diameter seven wire tendons measured with a tensile strength of 1860 MPa. The precompressive stresses in the concrete were less than 0.6 MPa (according to prestress values taken from the Chinese version). The Chinese paper (Litang et al., 2004) indicates initial stress levels (prior to losses) of approximately 780 MPa, which is approximately 35% below the prestress traditionally used in design (see Taranth, 2010). The slabs had 30mm of (axis distance) concrete cover at midspan.

Support reactions, relative stress loss, tendon temperature and deflection were all monitored during testing. Deflections of all spans with the exception of one test indicated thermal bowing resulting in downward deflection, tendon stress increased rather than relaxed during testing. Support reactions indicated fluctuations up to 12 kN for all supports in each test. Tendon temperatures remained below 350°C, at axis

distances of 30 mm after 90 minutes of exposure to an ISO 834 (1999) fire with a heated length ratio greater than 60%.

Of principal concern in these tests was the development of large cracks at the location of negative bonded reinforcement termination. In one test tendon rupture was confirmed at the location of localised spalling; however temperatures measured in the vicinity of the fracture were only 125°C. Tendon rupture and spalling are not described elsewhere in the paper. Longitudinal cracking was however observed in every test conducted; however, no details of transverse reinforcement are given in the reports.

Falkner and Gerritzen (2005)

Falkner and Gerritzen (2005) report briefly on the fire test of a one-way continuous but unrestrained unbonded PT concrete slab. Limited test details are provided within their report. The test was performed under a 90 minute ISO 834 (1999) fire heating two spans over a central continuous support. Both spans were 4.5 m in length, with a 200 mm thick slab designed according to DIN (German) standards. The main objectives of the test were:

(1) to compare the deflection behaviour between continous and similarly constructed reinforced concrete slab and unbonded PT concrete slabs;
(2) to provide numerical data for modelling purposes (to simplify this the researchers added 3kg/m^3 of polyproplyne fibres to the fresh concrete mix to attempt to prevent explosive concrete cover spalling; and
(3) to investigate the residual capacity of the slabs after fire exposure.

Falkner and Gerritzen (2005) found that the unbonded PT slab displayed substantially less deformation than the reinforced concrete slab during testing (20 mm compared to 50 mm at test end, respectively). No spalling was reported but some distributed cracking along the exposed soffit of the slab. The authors hypothesized that this cracking was likely due to internal restraint stresses generated during the cooling phase of the test. Finally, almost full recovery of deformation for the PT slab was observed after cooling, the final residual capacity compared to a tested ambient slab was seen to have only a 10% decrease in capacity. No repeat tests were

performed, and little if any details on tendon drape and cover are provided in the report.

Zheng and Hou (2006)

Zheng and Hou report on nine standard furnace tests on small-scale, one-way spanning unbonded PT slab strips prestressed with steel wires in a 2008 publication. Figure 2.10 provides details of a typical tested assembly.

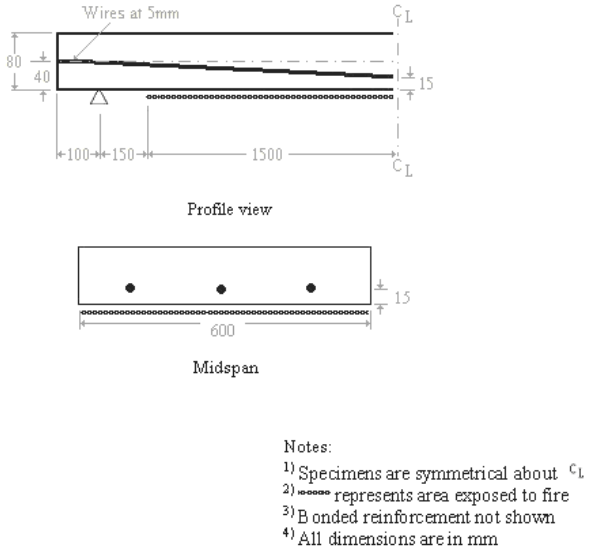

Figure 2.10: Zheng et al.'s simply supported slab (after Zheng et al., 2008).

All specimens were fabricated from carbonate aggregate concrete with a width of 600 mm and spanning 3300 mm between simple supports. The prestressing steel consisted of between two and five prestressing steel wires, each with a diameter of 5 mm and an ultimate tensile strength of 1722 MPa. The wires were prestressed to between 655 MPa and 1022 MPa prior to testing. A clear concrete cover of 15 mm, 25 mm, or 30 mm to the prestressed reinforcement was provided for the 80, 90, and 95 mm thick slabs, respectively. Varying amounts of mild steel longitudinal reinforcement were provided within each of the slabs; the mild steel longitudinal reinforcement ratio varied between 0.20% and 0.45%. All slabs had mild steel transverse reinforcement with the same clear cover as the prestressing steel reinforcement at mid span, and with a reinforcement ratio of about 0.17% to 0.20% depending on their thickness.

The slabs were subjected to uniformly distributed superimposed loads using 20 kg dead weights and were tested under exposure to the ISO 834 (1999) standard fire in an unrestrained condition. The load ratio varied between 0.41 and 0.72. The moisture content in the slabs at the time of testing varied between 1.8% and 4.0% by mass, although it is not clear how or where this was determined. The concrete compressive strength varied between 22 MPa and 57 MPa.

Unfortunately, all of Zheng and Hou's tests were halted before reaching structural failure, using a slope limit failure criterion. The resulting data are therefore not particularly useful for the current discussion. It is significant, however, that longitudinal cracking along the tendons was observed in at least two of the tests, and that spalling was observed in at least five. Spalling appears to have been most pronounced in the most compressed regions of the soffit (close to the supports), and to have been most severe for slabs with high initial total prestress levels, regardless of moisture content or concrete strength. No tendon ruptures are noted.

Zheng, Hou, Shi and Xu (2007)

Zheng and Hou continued their experimental program, publishing again in 2007 in chinese. The results of their study were republished in 2010 in english (Zheng et al., 2010). These new tests resembled those of Litang et al. (2004), and of Falkner and Gerritizen (2005) described above. Nine one-way continuous unrestrained unbonded PT concrete slabs, consisting of two spans at approximately 2.5 m each (Figure 2.11), were tested. Slabs were lifted into a modified furnace on three supports with two rollers and one flat plate support. The furnace configuration was similar to that presented by Litang et al. (2004). Both spans were heated with a target time temperature curve of ISO 834 (1999) above 85% of the slab's total length. With reference to their 2007 paper, the furnace control failed to exactly reproduce to the standard fire (ISO 834). This was apparently corrected for their 2010 paper where they indicate that the test followed the standard fire curve exactly.

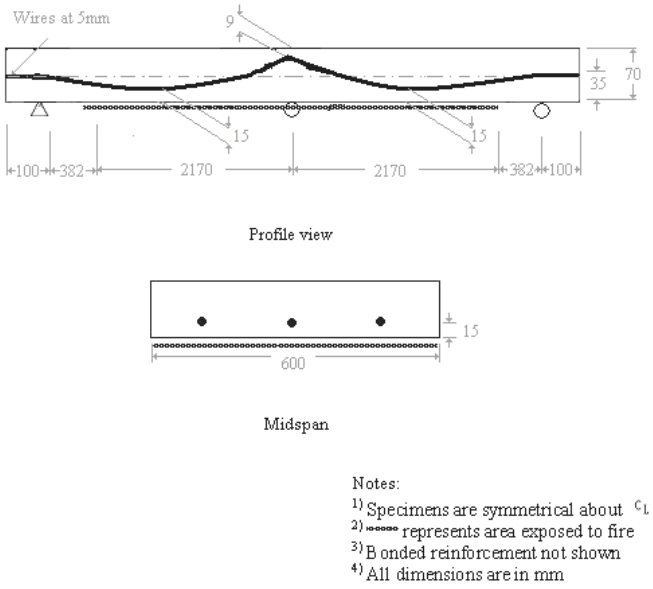

Figure 2.11: Zheng et al.'s continuous slab (after Zheng et al., 2007).

The slabs were tested in three pairs. Again unbonded prestressing steel wires (of lower than typical grade, 1722 MPa) were stressed to between 657 and 1019 MPa. A clear concrete cover of 15 mm, 25 mm, or 30 mm to the prestressed reinforcement was provided for the 70, 80, and 85 mm thick slabs, respectively. Varying amounts of mild steel reinforcement were provided longitudinally within each of the slabs with steel reinforcement ratios varying between 0.2% and 0.6%. Negative moment reinforcement ranged between 1.0% and 1.2%. All slabs had mild steel transverse reinforcement with the same clear cover as the prestressed reinforcement at mid span, and with a reinforcement ratio of about 0.17% to 0.20% depending on the slab thickness. All slabs also had negative mild steel transverse reinforcement with the same clear cover as the prestressed reinforcement at mid span, and with a reinforcement ratio of about 0.01% to 0.1%.

The slabs were subjected to uniformly superimposed loads using 20 kg dead weights. The moisture content varied between 2.4% and 4.0% by mass, although it is not clear how or where this was determined. The concrete compressive strength varied between 40 MPa and 57 MPa.

Discussion in the published reports focuses on cover spalling. The insights presented do not expand on previous work by other researchers (see for instance Hertz (2003) and Kodur (2009)); the authors concluded that spalling took place

between temperatures 200-500°C and that the strength of concrete had a significant impact related to reduced concrete permeability with higher compressive strength.

All slabs exhibited similar deflection trends as those in Litang et al.'s (2004) tests. Support reactions were measured at unexposed slab ends with load cells. The load cells showed an initial decrease in load, followed by a rapid rise in cooling, though in all cases the reactions increased by less than 1 kN. The authors hypothesized that this redistribution of force was due to changes in the deflected shape of the slab throughout the test. Tendon stress relaxation was observed of up to 400 MPa.

Although an effort was made in these tests and others (Aimin et al., 2013; Falkner and Gerritzen, 2005) to simulate a more realistic continuous slab system, it is unlikely that secondary load balancing reactions would be realistic given that the frames neglect axial, vertical and rotational restraint which would be observed in a real structure with continuity over multiple supports.

Bailey and Ellobody (2009)

Bailey and Ellobody (2009a) report results of four large-scale furnace tests on one-way spanning unbonded PT concrete floor slabs in which the lateral (longitudinal) restraint condition ("free" or "restrained") and the type of aggregate (limestone or Thames gravel) were varied. They also compare their results to the performance of a bonded PT concrete slab. Different aggregates were apparently used to investigate the effect of different amounts of thermal expansion on the structural behaviour, and perhaps also to study spalling. Details of the specimens are given in Figure 2.12. The slabs were 1600 mm wide and 160 mm deep, and spanned 4000 mm between simple supports. Each slab had three longitudinal seven-wire prestressing steel tendons, each with a nominal cross-sectional area of 150 mm^2 and an ultimate tensile strength of 1846 MPa. The tendons were prestressed to about 1120 MPa after losses. The minimum concrete cover to the centroid of the draped prestressing steel tendons was 42 mm at mid span. This corresponds to a clear cover of approximately 34 mm. No mild steel reinforcement was provided within the tested spans.

The concrete strength at the time of testing varied between 40 MPa and 48 MPa, and the moisture content varied between 1.7% and 2.5% by mass (again the

method and location of moisture measurement are not known). The applied loading was selected as 50% of the capacity of an identical slab tested at ambient temperature, resulting in a fire test load ratio of about 0.65. The slabs were exposed to the BS EN 1991-1-2 (CEN, 2002) fire until collapse (first test) or until the test was halted (three subsequent tests). The heated length was greater than 85% of the total length.

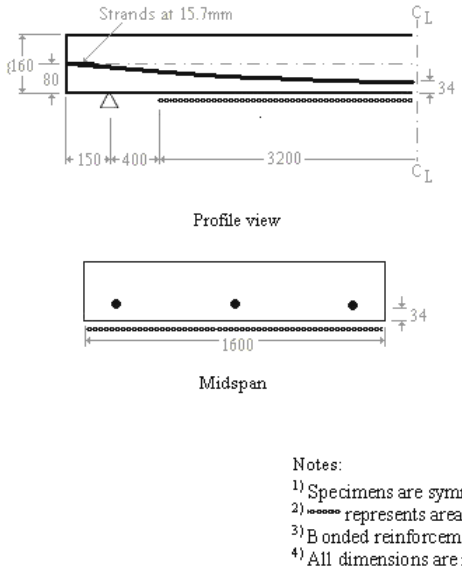

Figure 2.12: Bailey and Ellobody's slab (after Bailey and Ellobody, 2009a).

Two of the four unbonded PT slabs were "restrained" longitudinally by two steel beams, although full details of the restraining mechanism are not available. Bailey and Ellobody (2009) state that the restrained slabs were initially free to expand longitudinally during fire testing, for a total distance of 2 mm: "*until (they) came in full contact with the restraining beams and until the bolts fixing the restraining beams became intact with the edges of the holes*". The stiffness of the restraining frame, once engaged, is not known so it is difficult to draw comparisons to real structures.

None of the slabs experienced major spalling during fire testing, although some localised spalling is visible in photos published in Bailey and Ellobody's (2009) report in the Magazine of Concrete Research. The unrestrained slab with limestone aggregate developed longitudinal splitting cracks on its unexposed surface after 20 minutes of fire exposure when the maximum recorded tendon temperature was only 108°C. This slab collapsed into the furnace after 178 minutes. The collapse

was apparently due to tendon rupture at the location of a major transverse flexural crack near mid span. The maximum recorded tendon temperatures were about 200°C and 400°C after 60 and 120 minutes, respectively, and the maximum tendon temperature prior to failure was about 492°C. The restrained limestone aggregate slab performed similarly, with the exception that longitudinal cracking was observed on the unexposed face after only 15 minutes when the tendon temperature was 95°C. This test was halted after 83 minutes, when the tendon temperature reached 350°C, to avoid damaging the furnace.

The Thames gravel aggregate slabs performed similarly to the limestone aggregate slabs, with the exception that they experienced greater thermal expansion on heating. Both slabs experienced longitudinal splitting cracking on the unexposed face, at 18 minutes and a tendon temperature of 119°C or at 21 minutes and a tendon temperature of 115°C for the free and restrained cases, respectively. Both tests were halted when the tendon temperatures reached 350°C, which was at 72 minutes for the free case and 89 minutes in the restrained case.

Bailey and Ellobody (2009a) note evidence of arching (compressive membrane) action and horizontal shear cracking during their restrained tests. They reiterate Van Herberghen and Van Damme's (1983) recommendation for transverse mild steel reinforcement to prevent longitudinal splitting cracking at the location of the tendons, which they view as being the *"critical failure mode"* for their unbonded PT slabs in fire.

Table 2.1: Selected details of furnace tests available in the literature (1958-1983)

#	Year[a]	General description	Concrete precompression due to prestress (Longitudinal, MPa/ Transverse, MPa)[b]	Restraint conditions (lateral/ rotational)[c]	Specimen pre-condition[d]	Bonded steel reinf.[e] (%)	Moistu-re content at testing	Aggregate type	f_c' at testing (MPa)	Load ratio[g]	Max tendon temp. (°C)	Span/ depth ratio	Longit-udinal crack?	Trans-verse crack?	Spalling ?	Tendon rupture?	End point
1	1958	2-way beam-slab assembly	0.94/1.13	Y/P	--	0/0/0/0	62 % RH	Siliceous	41	1.0 × LL	506	21	Y	Y	Y	N	Transmission
2	1959	2-way slab panel	1.64/1.61	Y/P	--	0/0/0/0	76 % RH	Siliceous	30	1.0 × LL	563	28	--	--	--	--	None
3	1964	T-beam	6.85/0	N/N	Y	Mesh in cover	75 % RH	Carbonate	39	0.516	541	--	Y	N	N	N	Collapse
4			6.08/0				72% RH	Carbonate	41	0.520	427	--	N	Y	Y	N	Collapse
5	1965	Inverted T-beam	3.29/0	Y/P	--	0/0/0/0	--	Carbonate	--	1.0 × LL	377	--	N	N	N	N	None
6	1967	2-way slab panel	2.39/2.07	Y/P	Y	0/0/0/0	44 % RH	Expanded shale	29[f]	1.0 × LL	704	23	N	Y	N	N	None
7	1983	Continuous 1-way slab strip	0.78/0	N/Y	--	0/0/0/0	--	"Gravel"	--	Varies	--	33	Y	Y	Y	Y	Collapse or imminent collapse
8			0.78/0			0/0/0/0		"Gravel"									
9			0.78/0			0/0/0.12/ 0.12		"Gravel"									
10			0.78/1.65			0.26/0.2 6/0.1/0.1[h]		"Gravel"									
11			0.78/0			0.15/0.1 5/0.08/0. 08		Limestone									
12			0.78/0			0.2/0.2/0 .1/0.1		Limestone									
13			0.78/0			0.2/0.2/0 .1/0.1		"Gravel"									
14			0.78/0			0.2/0.2/0 .2/0.2		"Gravel"									

[a] refers to the year the tests were conducted (estimated on the basis of publication date in some cases)
[b] the precompression is the total tensioning force divided by the cross-sectional area of the slab normal to that force (Taranath, 2010)
[c] Y = yes, N = no, P = partial (assumed by current authors)
[d] "--"means that this information was not disclosed
[e] top longitudinal/top transverse/bottom longitudinal/bottom transverse
[f] 28-day compressive strength (strength at time of testing not known)
[g] in some cases the load ratio is not given, in which case the loading approach is given instead
[h] this slab was also prestressed transversely

Table 2.2: Selected details of furnace tests available in the literature (2004-2006)

#	Year [a]	General Description	Concrete precompression due to prestress (Longitudinal, MPa/ Transverse, Mpa)[b]	Restraint conditions (lateral/ rotational)[c]	Specimen pre-condition[d]	Bonded steel reinf.[e] (%)	Moisture content at testing	Aggregate type	f_c' at testing (MPa)	Load ratio[g]	Max tendon temp. (°C)	Span/ depth ratio	Longit-udinal crack?	Transverse crack?	Spalling?	Tendon rupture?	End point
15	2004	Continuous 1-way slab strip	--	N/P	Water reducer	Mesh in cover	--	Gravel	48.6	1.0x LL	200	33-35	Y	Y	--	N	None
16			0.54						58		125	33-35	Y	Y	Y	Y	
17			0.58						51.6		325	33-35	Y	Y	--	N	
18			0.59						55.8		350	33-35	Y	Y	--	N	
19	2005	Continuous 1-way slab strip	1 to .2 /0	N/P	--	--	--	--	--	--	--	23	--	Y	N	N	None
20	2006	1-way slab strip	0.77/0	N/N	--	0/0.45/0 /0.21	4.0 % by wt	Carbon-ate	57	0.41	--	41	N	Y	N	N	Slope limit
21			0.98/0			0/0.31/0 /0.21	3.5 % by wt		48	0.54		41	Y	Y	Y		
22			2.09/0			0/0.31/0 /0.21	4.0 % by wt		57	0.70		41	N	Y	Y		
23			0.88/0			0/0.46/0 /0.18	2.4 % by wt		52	0.42		37	N	N	N		
24			1.09/0			0/0.31/0 /0.18	3.3 % by wt		52	0.56		37	Y	N	N		
25			1.19/0			0/0.21/0 /0.18	2.4 % by wt		52	0.68		37	N	N	N		
26			0.7/0			0/0.25/0 /0.17	3.3 % by wt		52	0.42		35	N	Y	Y		
27			0.96/0			0/0.29/0 /0.17	3.5 % by wt		47	0.56		35	N	Y	Y		
28			1.44/0			0/0.20/0 /0.17	1.8 % by wt		23	0.72		35	N	Y	Y		

[a] refers to the year the tests were conducted (estimated on the basis of publication date in some cases)
[b] the precompression is the total tensioning force divided by the cross-sectional area of the slab normal to that force (Taranath, 2010)
[c] Y = yes, N = no, P = partial (assumed by current authors)
[d] "--"means that this information was not disclosed
[e] top longitudinal/top transverse/bottom longitudinal/bottom transverse
[f] 28-day compressive strength (strength at time of testing not known)
[g] in some cases the load ratio is not given, in which case the loading approach is given instead

Table 2.3: Selected details of furnace tests available in the literature (2006-2008)

#	Year[a]	General description	Concrete precompression due to prestress (Longitudinal, MPa/ Transverse, MPa)[b]	Restraint conditions (lateral/ rotational)[c]	Specimen pre-condition[d]	Bonded steel reinf.[e] (%)	Moisture content at testing	Aggregate type	f_c' at test (MPa)	Load ratio[g]	Max tendon temp. (°C)	Span/ depth ratio	Longit-udinal crack?	Transverse crack?	Spalling ?	Tendon rupture?	End point
29	2007	Continuous 1-way slab strip	0.92/0	N/P	--	1.2/0.18/0.61/0.10	3.98	Carbonate	56.9	0.36	--	36	--	--	N	N	None
30			1.15/0			1.2/0.18/0.39/0.10	3.98		56.9	0.5			--	--	N	N	
31			1.42/0			1.2/0.18/0.23/0.10	3.5		48.2	0.59			N	Y	Y	Y	
32			0.75/0			1.1/0.15/0.41/0.09	2.77		40.1	0.58			--	--	N	N	
33			1.19/0			1.1/0.15/0.41/0.09	2.36		52.1	0.33			--	--	N	N	
34			1.24/0			1.1/0.15/0.21/0.09	3.5		48.2	0.36			N	Y	Y	Y	
35			0.76/0			1.0/0.15/0.50/0.08	2.36		52.1	0.42			--	--	N	N	
36			0.86/0			1.0/0.15/0.29/0.08	3.29		52	0.48			--	--	N	N	
37			1.27/0			1.0/0.15/0.22/0.08	3.29		52	0.32			--	--	Y	N	
38	2008	1-way slab strip	1.97/0	N/N	N	0/0/0/0	2.5	Limestone	48	0.65	492	23	Y	N	N	Y	Collapse
39			1.97/0	Y/P			2.2		41		350[i]			Y	Y	N	None
40			1.97/0	N/N			2.3	Thames gravel	40					N	N	N	None
41			1.97/0	Y/P			1.7		40					N	N	N	None

[a] refers to the year the tests were conducted (estimated on the basis of publication date in some cases)
[b] the precompression is the total tensioning force divided by the cross-sectional area of the slab normal to that force (Taranath, 2010)
[c] Y = yes, N = no, P = partial (assumed by current authors)
[d] "--"means that this information was not disclosed
[e] top longitudinal/top transverse/bottom longitudinal/bottom transverse
[f] 28-day compressive strength (strength at time of testing not known)
[g] in some cases the load ratio is not given, in which case the loading approach is given instead

2.5 Bonded PT concrete furnace tests

Post-tensioned concrete exists in two forms: unbonded and bonded (in which the prestressing steel tendon is grouted within a steel or plastic duct and thus continuously bonded to the concrete after tensioning). While the focus of this thesis is on the unbonded PT concrete construction due to its critical failure mechanism of prestressing steel tendon rupture, it is worthwhile to comment on the influence of bonded versus unbonded construction to better understand structural mechanisms observed in unbonded PT fire tests. This can help to explain how unbonded tendon continuity might affect slab performance in fire. Three test series are of interest, including: a single slab test by Purkiss and Kelly (2008), eight slabs tested by Bailey and Ellobody (2009a), and three slabs tested by Cement Concrete and Aggregates Australia (2010).

Purkiss and Kelly (2008)

Purkiss and Kelly (2008) conducted an isolated test on a multi-strand 8.5 m long, 3.6 m long, 250 mm thick bonded PT concrete slab. The slab was designed to have a 120 minute fire rating. Their test indicated excessive spalling and premature failure at 66 minutes. This isolated test has caused significant debate in the engineering community (Bailey and Ellobody, 2009a). Bailey and Ellobody's view on these tests indicated that the moisture content was in excess at 4.6% by weight which, with the use of gravel aggregate and supplied restraint, instigated spalling. Spalling remains a poorly understood behaviour and more research is required to quantify whether this mechanism can be accounted for accurately in design. Nevertheless, these factors are all known to contribute to both bonded and unbonded PT construction.

Bailey and Ellobody (2009)

Bailey and Ellobody (2009a) conducted a series of eight bonded PT slab tests (both restrained and unrestrained) to complement their unbonded slab tests discussed previously. These tests were conducted under a standard fire and limited by tendon temperature as an end test criteria. The slabs were meant to be identical for comparison (same design geometry) as their unbonded counterparts. A particular observation of note involves longitudinal cracking.

Bailey and Ellobody (2009a) describe the formation of the longitudinal cracks due to expansion of the tendon longitudinally which relieves compressive forces in the concrete. The concrete is then subjected to tensile stresses caused by lateral expansion which causes splitting at weaker sections (close to the tendons). This failure hypothesis is supported by their numerical modelling efforts. If this scenario is compared between the bonded and unbonded cases, crack formation mechanisms may be affected. In both the bonded and unbonded cases, this cracking behaviour should arrest near the location where the prestressing steels are no longer exposed to high temperature. This would be due to the absence of tensile stresses from lateral expansion. However, since bonded tendons are cast with higher sized ducting than unbonded tendons, this further reduces the effective cross section of concrete which can carry tension thereby promoting tensile longitudinal cracking along the heated tendon length in the bonded case (assuming no transverse reinforcement).

Cement, Concrete and Aggregates Australia (2010)

A series of tests was performed in 2010 by Cement, Concrete and Aggregates Australia (CCAA) in collaboration with the Centre for Environmental Safety and Risk Engineering. Three 1000 mm × 150 mm × 6000 mm bonded unrestrained multi-strand PT slabs were tested under exposure to a real crib fire intended to simulate a standard fire for 70 minutes. The slabs were initially stressed to 1560 MPa using 12.7 mm diameter prestressing steel tendons. Significant spalling was noted during testing, and was attributed to the usage of gravel concrete. No longitudinal cracking was noted, but this could have been prevented by their use of transverse ties that were distributed through the length of the slabs. The analysis of test results confirmed only that the addition of polypropylene fibres reduced the propensity of spalling.

The above tests illustrate many structural mechanisms which can also have consequences for unbonded PT structures (spalling, cracking) and illustrate the importance on workmanship and construction for PT construction.

2.6 Real fires in PT Buildings

Case studies of real fires in unbonded PT concrete buildings are rare. A few papers assessing bonded PT concrete structures are available (Troxell, 1962; Zollman, 1960; Hamersmith, 1965; Stoddard, 2008) although these are not particularly useful for evaluating the fire performance of unbonded PT buildings for the reasons noted previously. The following is a description of six fires in real unbonded PT buildings; these confirm that the behaviour of real unbonded PT buildings in real fires merits additional study.

San Antonio (1955)

This is the earliest recorded unbonded PT building exposed to fire and is mentioned very briefly in a paper by Hammersmith in PCI (1965). The fire was caused by combustion of painting supplies during construction. The structure was made of precast channels supported by 15 m PT 'I' beams. The severity of the fire was considered weak as lead found in the plumbing area of the building was melted. Spalling was observed, but no serious structural damage was noted.

Los Angeles, California (1965)

The earliest report of a fire in a real unbonded PT building is by Troxell (1965), and describes a fire that occurred in a three year old unbonded PT school building in Los Angeles, California. The two storey building had unbonded PT flat plate lightweight aggregate concrete slabs with unbonded PT tendons running longitudinally and transversely. The prestressing steel consisted of 6.4 mm diameter stress relieved prestressing steel wires grouped into cables of 4 to 14 wires. The slab thickness was between 240 mm and 250 mm and the minimum concrete cover was 25 mm. Details of the amount and location of any mild steel reinforcement in the slabs are not given. The fire lasted about 1.5 hours and was compartmentalized within two rooms of the six room south wing of the building. Both the ceiling and floor slabs experienced spalling. The room where the fire was assumed to have originated experienced spalling over 75% of its 80 m^2 ceiling area to a maximum depth of 44 mm and exposing several of the tendons. The floor experienced an average of 10 mm of

spalling located centrally over a 900 mm diameter area. However, no tendon ruptures were observed and the structure did not collapse. The maximum temperature was estimated by noting fusion of copper wire on the ceiling, apparently indicating that the fire temperature may have peaked at about 1070°C. After the fire, tendons were tested in place using lift off tests. Troxell tested six unbonded PT strands in this manner, one unexposed control which was assumed not to have been affected by the fire and five "fire affected" tendons. No obvious prestress relaxation was observed in the fire affected tendons in comparison with the control tendon. It is noteworthy that Troxell (1965) states that severe spalling of the ceiling was due to thermal shock from a hose stream and that the tendons were not directly exposed to the peak temperatures of the fire. The building is still in service today and is shown in Figure 1.1.

Bangkok, Thailand (1987)

Partial collapse of a unbonded PT slab exposed to fire for more than five hours occurred in an 18 storey building in Bangkok, Thailand in 1987 (Lukkanprasit, 1990) Each floor of the building had 4000 m^2 of two-way prestressed unbonded PT flat plate construction, with interior bays of 80 m^2 each and 4 m long cantilevers located at the end of each floor. The concrete slab was 200 mm thick and the cover to the prestressing steel tendons was 20 to 25 mm. Minimum mild steel reinforcement was provided according to the ACI (1983) provisions at that time.

The fire started on the third floor and spread upward to the fifth floor. Widespread spalling occurred and exposed some of the tendons directly to the fire. Eventually, some of the tendons are thought to have ruptured and the cantilevers at the end of the fourth floor collapsed. This resulted in collapse of two supporting columns and caused progressive collapse of several interior bays. It was estimated that between 10 to 20 percent of the tendons in the floor plate had ruptured during the fire.

Significantly, while bays in the fire exposed region collapsed, adjacent bays did not fail even though the tendons were unbonded and continuous into the adjacent spans. Lukkunaprasit (1990) believes that tension membrane action of the slabs occurred with the tendons anchored at the edges of the collapsed bays by "kinks"

over the column lines. Large vertical displacements in the slabs are thought to have allowed a smaller tendon force to carry the slabs' weight and the imposed loads by tensile membrane action, as is widely recognized (Bailey et al., 2000) to occur in steel-concrete composite slabs in fire. On the basis of this fire, Lukkunaprasit suggested that engineers should supply unstressed bonded prestressing steel at the mid depth of unbonded PT slabs so that the additional reinforcing can act as tensile membrane reinforcement and prevent collapse during a fire. Such measures have not, however, been adopted into modern unbonded PT design codes, nor has any subsequent research seriously considered this idea.

Santa Ana, California (1988)

Tendon rupture during fire is highlighted in a report of post-fire controlled demolition of a unbonded PT two-way slab structure in Santa Ana, California in 1988 (Barth and Aalami, 1992). In this case a four storey timber frame built on top of a flat plate podium unbonded PT slab over a parking facility caught fire after completion of the slab but during construction of the timber frame. During the fire the timber frame collapsed and the podium slab was exposed to fire from above. The slab was 200 mm to 230 mm thick and 160 m × 120 m in plan. Spalling occurred at midspan at the top of the slab (i.e. in the compression zone) in locations where no passive reinforcement was present. The maximum depth of spalling was 76 mm. Three percent of the prestressing steel tendons ruptured during the fire, and based on inspection by engineers the slab was demolished. The report does not describe the severity of the fire, nor does it state the concrete cover to the prestressed reinforcement from above. However, this clearly illustrates the potential for tendon rupture during a real fire.

Portland, Oregon (1999)

A fire in a similar structure to that described in above occurred in Portland, Oregon (Sarkkinen 2006), in 1999, when a timber frame that was built on top of an unbonded PT flat plate concrete podium caught fire. In this case the unbonded PT slab was 330 mm thick and had a minimum concrete cover of 48 mm. Again the timber frame caught fire and collapsed and the slab was exposed to fire from above. Spalling was

limited to a depth of 12 mm to 19 mm and no tendon ruptures were observed. Tendons and mild steel reinforcement were manually exposed in six different locations after the fire to visually assess damage to the reinforcement. In one location the plastic sheathing of the unbonded PT tendons exhibited signs of melting, although the grease appeared to be intact. No attempts were made to assess the post-fire prestress levels in the tendons. The slab was subsequently repaired and used during rebuilding of the timber frame structure.

Florida, USA (2000)

A large uncontrolled fire occurred during construction of a 12 storey Unbonded PT condominium building in Key Biscayne, Florida in 2000 (Post and Korman, 2000). The building contained unbonded and stressed prestressing steel tendons that were continuous across seven interior bays. The construction of the building had progressed to the 12th floor when a localised fire broke out on the second floor in one interior bay next to an internal shear wall. The fire spread to an adjacent bay where a pour-strip was located (a pour strip is an area of the slab where tendons are anchored during construction and which is left void until the building is nearing completion). The fire then spread vertically, ultimately causing visible fire damage up to the seventh floor across two interior bays. The engineers who examined the structure after the fire stated *that "heat caused the tendons at the pour strips to release tension."* They further noted that release of tension *"triggered progressive failure of the post-tensioned slab well beyond the zone of visible damage."* The result of this was that *"almost half the slabs on levels three to six, and possibly seven, lost integrity"*. This represents loss of structural integrity across a total of 48 bays of the structure. The risk of progressive collapse was sufficiently high that no contractor could be found who would re-shore the floor slabs after the fire, and the entire building was demolished. This case study illustrates the potential consequences of localised tendon heating during fire and prestress loss across multiple bays.

Brannigan and Corbett (2008) have also presented a case study of an unbonded PT building which was subjected to a formwork fire during construction and which led to collapse by a progressive mechanism, although this is less worrying given the unusual nature of the fire.

Tel Aviv, Israel (2000)

A short case study presented by Stern (2002) in 2002 describes an unbonded PT slab with spans up to 16 m exposed to a severe fire in Tel Aviv, Israel. Stern indicates that spalling of the concrete cover to the tendons occurred over a 300 m^2 area. Some of the tendons apparently ruptured and the mild steel was exposed during the fire. In this case the unbonded PT slab was reinstated by re-connecting and re-tensioning the ruptured tendons. The wisdom of this approach is questionable unless considerable testing was performed to check for deterioration in post-heating residual mechanical properties of the prestressing steel (see Maclean et al., 2008 and Robertson et al., 2013).

2.7 Key issues

The above sections raise a number of issues relevant to the fire-safe design of unbonded PT concrete structures. Unbonded PT members appear to perform reasonably well in standard furnace tests, and in these scenarios they are typically able to comply with prescribed fire resistance ratings up to or exceeding three hours. However, given the large number of unbonded PT structures in service and the relatively small number of real fires which have been reported (only seven fires reported globally), this should not be construed as clear evidence of the fire safety of unbonded PT structures. The following are considered the key issues identified in the available literature:

Test data

- No realistic tests have ever been performed on multiple span continuous unbonded PT (or bonded PT) structures incorporating axial, vertical and rotational restraint.
- Most of the tests which have been used to demonstrate fire safety of unbonded PT slabs were performed prior to 1970 using construction materials which are now outdated and specimens which in some cases were pre-conditioned prior to testing (thus explicitly reducing the likelihood of cover spalling).

- Spalling was observed in at least 20 of the 41 available tests (48%). Useful correlations cannot be drawn between propensity for spalling and relevant specimen parameters such as concrete strength, pre-compression levels, aggregate type, amount and location of mild steel reinforcement, load ratio, concrete moisture content, etc. However, limiting the moisture content to less than 3.0% by mass, as is suggested in EN 1992-1-2 (CEN, 2004), is clearly not sufficient to prevent spalling during fire. The presence of non-prestressed mild steel reinforcement within the concrete cover does not prevent spalling, although in some cases it can arrest cover spalling to the depth of the mild steel reinforcement and thus provide some protection to the unbonded and stressed prestressing steel tendons.
- In unrestrained standard furnace tests with realistic load ratios, structural collapse is imminent when the tendon temperature exceeds about 400-450°C. In restrained tests, even without mild steel reinforcement, tendon temperatures as high as 700°C have been observed without collapse. Current prescriptive guidance could therefore be defensible for predicting isolated component behaviour in standard furnace tests; but not necessarily for predicting the response of real unbonded PT concrete buildings.
- Longitudinal splitting cracking along the tendons was observed in at least 20 of the 48 tests (48%). Current design guidance does not address this issue even though researchers have suggested that this is the governing mode of failure for unbonded PT structures in fire (as early as 1983).
- Transverse (flexural) cracks, in some cases as wide as 6 mm, were observed in at least 23 of the 41 tests (56%). Localised heating of tendons at these cracks (even in the absence of cover spalling) could induce localised heating and premature tendon rupture during fire. Unbonded PT members develop fewer, wider cracks than equivalent bonded PT members, both under ambient conditions and, more importantly, during fire.
- Tendon rupture during heating was observed in at least 12 of the 41 tests (30%), and was particularly evident in tests with multiple spans and localised heating. Table 2.4 provides a summary of the heated length ratios for all tests. Tendon

rupture is therefore more, rather than less, likely in a real unbonded PT building than in a furnace test of an isolated structural element or assembly.

Table 2.4 Heated length ratios of test data

Test series	Test date	Test (#)[a]	Heated length ratio (%)[b]
Fire Prevention Research Institute	1958	1	100
	1959	2	90
Portland Cement Association	1964	3-4	95
Underwriters' Laboratories	1965-1967	5-6	100
Van Herberghen and Van Damme	1983	7-14	81
Litang et al.	2004	15-18	64
Falkner and Gerritzen	2005	19	--[c]
Zheng and Hou	2006	20-28	86
Zheng et al.	2007	29-37	82
Bailey and Ellobody	2009	38-41	85

[a] refers to test numbers see Tables 2.1-3 for reference
[b] heated length ratio is exposed heated soffit divided by total length of structure
[c] discrete details available of Flakner and Gerritzen, test publication is 2005, but no details of heated length ratio, howver both spans were heated so it may be assumed that the slab was not heated locally.

Case studies

- Some degree of concrete spalling occurred in all cases. It therefore seems that without preventative measures taken to avoid spalling localised spalling should be considered as likely, rather than unlikely, in all unbonded PT buildings exposed to severe fires. It is therefore difficult to justify design for fire safety of unbonded PT systems purely on the basis of minimum concrete cover to the tendons, with an inherent assumption that the concrete cover will remain in place during fire.
- Tendon rupture or release of prestress occurred in two thirds of the case studies. This confirms that tendon rupture (or prestress loss by tendon relaxation) is likely to occur in a unbonded PT building in a real fire. Premature tendon rupture during fire has led to both partial and progressive failure of real unbonded PT buildings.
- Unbonded PT structures exposed to real fires are almost certain to experience non-uniform and localised heating, which will expose the tendons to heating over only a portion of their total length.

2.8 Summary

The goal of fire testing structural materials are to provide a practical design for life safety and property protection. The earliest set of conditions to meet these objectives was set out in the work of Abraham Himmelwright (1899) in a precursor to Ira Woolson's E119 standard fire test (see Gales et al. (2012) included within Appendix A or Babrauskas and Williamson (1978a,b) for further background in the origins of the standard fire test). The conditions Himmelwright specified are that tested materials should be identical to commercially available ones, that tested materials should be constructed as in practice, and that the fire tests should be conducted in a scientific manner. The unbonded PT concrete standard fire tests noted above raise research concerns with regards to these practical objectives. While it is widely acknowledged that standard furnace testing is unrealistic for most real structures (Bisby et al., 2013, see Appendix B), whether this raises credible concerns for meeting the goals of structural fire safety in unbonded PT concrete buildings remains under debate.

It has been shown that an awareness of the lack of realism which is inherent in standard furnace testing is particularly important for the specific case of unbonded PT concrete beams and slabs. Standard furnace testing is fundamentally incapable of rationally simulating several important (and interrelated) behaviours that can be expected (and that have been directly observed) in real unbonded PT buildings during real fires and that can lead to premature tendon rupture and progressive failure. Localised heating of unbonded and stressed prestressing steel tendons may occur due to a combination of:

(1) single bay, localised, or travelling fires in multi-bay structures;

(2) draped tendons with variable concrete cover;

(3) spalling of the concrete cover; and/or

(4) longitudinal and/or transverse cracking.

Localised heating of an unbonded and stressed prestressing steel tendon is likely to lead rapidly to tendon rupture, as has been seen in many tests and real fires. The risk and consequences of localised heating from spalling can be mitigated through the use of bonded mild steel reinforcement, although this issue is still

neglected in some design standards. Bonded mild steel reinforcement can limit the depth of spalling, promote a finer and more evenly distributed cracking pattern, and permit alternative load carrying mechanisms. Research is needed to define the appropriate minimum amount and placement of bonded reinforcement to provide the required safety against collapse during fire. The consequences of localised heating for the capacity of an unbonded PT floor plate in fire remain largely unknown and require additional investigation to ensure that unexpected failures of unbonded PT structures do not occur, both during the code-prescribed fire resistance time but also during the cooling and post-fire periods.

Because full-scale fire tests on actual or model unbonded PT buildings, however badly needed, are unlikely to occur in the foreseeable future, research is currently restricted largely to using computational analysis tools (e.g. Bailey and Ellobody, 2009) to study their response to fire. In general, these tools have not been validated against real fires in realistic unbonded PT concrete structures and their ability to accurately model various aspects of unbonded PT concrete slabs at elevated temperature can be doubtful. A detailed experimental and computational examination of the potential consequences of localised heating on unbonded PT tendons is therefore needed with a view to eventually developing a rational understanding of the performance of real unbonded PT buildings in real fires. Chapter 3 begins to address these issues.

Chapter 3

Experiments and Modelling of Unbonded Prestressing Steel Tendons

"The magic numbers embodied in regulations are accepted without question…"

Margaret Law
Former Director of Arup fire
(Law and Beever, 1995)

3.1 General

As outlined in Chapter 2, a key benefit of unbonded PT concrete structures, as is widely quoted within the concrete industry, is their 'inherent fire resistance'. This inherent fire resistance is assumed predominantly on the basis of limited (and largely outdated) standardized furnace tests on isolated unbonded PT structural members and assemblies, and is ensured during design simply by prescribing a given overall slab thickness and minimum concrete cover for thermal insulation of the prestressing steel tendons. Standardized structural fire resistance testing has many acknowledged inadequacies (Bisby et al., 2013), such as the absence of a cooling phase, the testing of isolated, often simply-supported, and non-continuous elements, and so on. Although numerous standardized tests have been performed on unbonded PT concrete structures dating back to the late 1950s, no fire experiments have yet been designed to explicitly and rationally investigate the realistic fire performance of a continuous unbonded PT slab, nor have any of the available tests rationally accounted for the critical factor that the tendons in unbonded PT structures are unbonded and continuous over multiple bays, many of which may be distant from the fire-exposed spans. Localised damage to tendons in one bay will therefore affect prestress levels, and hence structural capacity (shear and flexural for example), across several bays. This behaviour was clearly shown in a large uncontrolled fire that occurred over several floors in a 12 storey unbonded PT concrete condominium building in Key Biscayne, Florida in 2000 as reviewed in Chapter 2.

This chapter deals specifically with the issue of transient localised heating of stressed, unbonded prestressing steel tendons which are continuous over multiple bays of a structure, an important issue that was identified in Chapter 2 as never having been explicitly and rationally investigated in available research on the fire

performance of unbonded PT concrete slabs. On the basis of the review in Chapter 2 it was suggested that current prescriptive structural fire design guidance may be defensible for preventing structural collapse of isolated simply supported standard furnace test specimens, particularly in the absence of explosive cover spalling. However, multiple case studies and some of the available test data provide compelling evidence that the available tests cannot predict the response of real unbonded PT buildings in fire, particularly with respect to prestressing steel tendon rupture under localised heating. For instance, concrete spalling of some form has occurred in all known case studies of real fires in unbonded PT buildings, and in one third of these cases premature tendon rupture occurred. Spalling has also occurred in at least 20 of the 41 available standard furnace tests on unbonded PT concrete elements. Tendon rupture or release of prestress occurred in two thirds of the case studies, confirming that tendon rupture is likely to occur in a real unbonded PT concrete building in a real fire. This has led to both partial and progressive failure of real unbonded PT structures during fires. Tendon rupture has been observed in at least 12 of the 41 available furnace tests, and has been particularly evident in tests with multiple spans and local heating; tendon rupture is much more likely in a real building than in a furnace test. However, tendon rupture was reported in all eight furnace tests reported by VanHerberghen and VanDamme (1983), and these tests apparently influenced the development of the EN 1992-1-2 prescriptive requirements (CEN, 2004) but have been essentially ignored by North American design requirements (International Building Code (IBC, 2012), for example).

Under localised heating unbonded and stressed prestressing steel tendons may rupture due to a combination of high temperature creep strains (which accelerate beyond 300°C), elastic modulus reductions, and loss of ultimate strength. Localised heating may occur in a real structure due to: a single bay fire in a continuous multi-bay structure; a travelling fire (such as observed in Building 7 of the World Trade Center complex (Stern-Gottfried and Rein, 2012)); a localised ceiling jet fire (particularly in parking structures (Shipp et al., 2009)); spalling of the concrete cover (which is more likely for modern concretes and pre-compressed elements (Hertz, 2003)); and longitudinal and transverse cracking during heating (which has been observed in many fire tests and real fires with unbonded PT construction (see

Chapter 2)). With respect to current standard furnace testing procedures for unbonded PT concrete slabs, there are two fundamental inadequacies relevant to this chapter:

(1) The total anchor-to-anchor length of unbonded PT tendons in standard furnace tests is *always* much shorter than in real unbonded PT structures. An isolated component test therefore cannot capture the true behaviour in an isolated compartment fire where the tendon will be locally heated; and

(2) Standard furnace tests are, by definition and by design, intended to provide as uniform a heating as possible to the tested assembly, thus minimizing any localization of heating. In a real fire in an open plan building the heating may be spatially non-uniform, travelling, and/or localised.

Both of the above inadequacies could result in standardized testing being unconservative with respect to tendon rupture due to localised heating of a stressed and unbonded prestressing steel tendon. Whatever the cause of localised heating, it is clear that a better understanding of the potential consequences of this on tendon response is needed to ensure fire safe design and construction of unbonded PT buildings.

The current chapter reviews previously conducted experiments from Queen's University Canada by the author (Gales, 2009) and others (MacLean et al., 2008) which considered the fire performance of continuous unbonded and stressed prestressing steel tendons in an effort to establish, experimentally and for the first time computationally, the potential consequences of localised heating for a stressed prestressing steel tendon. These experiments were conducted before the author commenced his doctoral studies at the University of Edinburgh. Preliminary validation of the model is presented. The chapter then presents a novel, simplified numerical modelling exercise of a fire exposed three bay continuous unbonded PT concrete slab; with attention given to the deformation and potential failure of the prestressing steel tendon. A parametric analysis using the model structure is subsequently presented which considers: (1) the uniformity of the fire (heated length ratio); (2) the real time user specified spalling scenarios (removing concrete cover during the heat transfer analysis); and (3) the effect of different specified concrete covers to the tendon. The modelling results are compared against prescriptive design

requirements within various international building codes. This is done with a view to eventually developing the ability to rationally understand the fire performance of PT concrete structures, by first understanding the specific response of prestressing steel tendons.

3.2 Overview

The fundamental issues under consideration in the current chapter are the time (t), temperature (T), stress (σ), strength (f_{pu}) interdependencies of cold-formed prestressing steel tendons which can lead to irrecoverable prestress losses and/or premature tendon rupture during fire. The treatment herein is based on the interaction of stress relaxation from irreversible high temperature creep, $\varepsilon_{cr} = f(t, T, \sigma)$, and reversible thermal expansion, $\varepsilon_T = f(T)$ with the tendon's strength degradation, $f_{ps} = f(T)$, at high temperature.

To understand the implications of these interactions, a combination of previously performed experiments are reviewed and new numerical modelling has been conducted. Prior to consideration of the global structural response of unbonded PT buildings exposed to fire it is crucial that the transient high temperature stress relaxation behaviour of the prestressing steel tendons be accurately understood; this is the core objective of the current chapter; and a central objective of the current thesis.

To serve this goal, prior tests on nineteen isolated, prestressed unbonded prestressing steel tendons, subjected to various localised transient heating scenarios with their temperatures and stress levels continuously monitored, are reviewed. This allows the time-temperature-stress-strength interdependencies under localised heating to be more accurately modelled for any assumed tendon heating scenario (spatial or temporal). A computational high temperature mechanics model for the prediction of transient thermal creep of cold-drawn prestressing steel has been developed and partially validated by the author (see Gales et al. (2009) for further details on the functionality of this computational model, although relevant mechanics are discussed herein). This computational model is capable of treating any transient heating and cooling regime for any tendon length, heated length, tendon profile, and initial prestress level. Extension of the validation and application is presented in the

current chapter to allow assessment of high temperature tendon stress variation (or rupture) due to localised heating. The computational model is described in detail, as are its specific applications for assessing the potential implications of localised heating on a realistic unbonded PT concrete structure. The potential consequences of localised heating of unbonded PT tendons are discussed with the aid of the computational model and a simplified example structure. The model is used to study two specific issues:

(1) **Prescriptive concrete cover requirements** – The fire resistance of unbonded PT structures is typically ensured in design by prescribing minimum concrete covers to the prestressed reinforcement. The required cover is generally stated in tables which give the minimum concrete cover to the prestressed reinforcement (or minimum *axis distance*, which is the distance from the surface of the concrete to the centroid of the tendon) necessary to achieve a given fire resistance rating (IBC, 2012; CEN, 2004). These cover requirements are nominally based on an assumed critical temperature for the prestressed reinforcement required to prevent collapse in a standard furnace tests of an isolated structural element. They are often defined as the temperature causing an approximate 50% ultimate strength reduction for the tendons (see Abrams and Cruz, 1961). Such requirements are based on tests of short, uniformly heated tendons and do not account for tendon rupture due to localised heating. The computational model is used herein to compare fire resistance times and concrete covers prescribed by two widely used design codes to tendon rupture times predicted by the model assuming a number of credible fire scenarios.

(2) **Potential impacts of cover spalling** – Unbonded PT flat-plate structures are particularly susceptible to explosive concrete cover spalling during fire. This is due to a combination of high concrete compressive strength, slab pre-compression under service loads, and (typically) small amounts or (sometimes) a complete lack of bonded steel reinforcement. Explosive cover spalling in real structures is essentially impossible to predict quantitatively, and despite considerable research efforts it has not yet been accurately modelled. While spalling models are suggested in the literature (e.g. Zhang et al., 2009), it will likely be some time (if ever) before spalling can be accurately accounted for in

design. Local concrete cover spalling during a fire would obviously cause localised heating of the prestressed reinforcement in the region near a spall. The current chapter presents a preliminary qualitative modelling exercise to highlight the possible impacts of cover spalling for premature tendon ruptures during fire.

3.3 A review of experiments on locally heated unbonded prestressing steel

The response of an unbonded PT structural concrete element in fire is influenced by a host of interrelated factors. As already noted, the most important of these factors in ensuring adequate structural fire resistance are: (1) tendon rupture occurring as a consequence of localised heating, which has been widely observed both in real buildings and in standard fire tests on unbonded PT concrete elements, and (2) concrete cover spalling, which remains poorly understood and difficult to predict. The first of these issues is examined by reviewing a series of large-scale prestress relaxation tests on locally heated steel prestressing steel tendons. The second issue can then be rationally considered through simplified modelling exercises (in Section 3.4).

3.3.1 Queen's University tests (2007-2009)

To experimentally investigate the stress-strength-temperature-time interdependencies of locally heated, stressed, unbonded, and restrained prestressing steel tendons of realistic length and parabolic tendon profile, a series of transient high temperature stress relaxation tests had been previously performed using a Strongback testing frame with an integrated custom tube furnace placed at mid-span (this is shown schematically in Figure 3.1). These tests were conduceted during the author's time at Queen's University Canada as a Master's project. They are reviewed herein The Strongback testing frame was specifically designed for earlier work to simulate the conditions found within a typical unbonded PT concrete slab (MacDougall and Barrett, 2003). Cold-drawn steel prestressing steel tendons with a total length of 18.3 m were stressed against the Strongback frame, and a tube furnace with heating length of 610 mm was installed at midspan. The tendon was mounted in a guide channel which was attached to parabolic profile plates welded to the top flange of a large steel plate girder. Bearing plates were added at both ends to accommodate

anchorages, load cells and jacking of the tendon. Plastic sheathing was installed over the length of the guide channel to simulate the frictional conditions experienced by real unbonded PT tendons. Individual seven-wire No. 13 (99 mm^2 nominal cross sectional area) low relaxation prestressing steel strands of Grade 1860 MPa (ASTM 416-03 (2003)) were stressed in the Strongback frame to between 50% and 60% of their design ultimate strength. This represents a realistic in service prestress condition for a typical unbonded PT concrete structure after time dependent losses have accumulated (Martin and Purkiss, 2006). Once stressed, the tendons were locally heated, following one of a number of prescribed heating and cooling regimes, while their stress levels were continually monitored. The tendons were therefore heated over about 3.3% of their total length.

Eleven independent tests were performed using the Strongback testing frame. Selected testing details and results are given in Table 3.1. Also included in Table 3.1 are the results of eight similar tests performed previously by MacLean (2008) using the same tube furnace and stress range, but with a shorter overall tendon length (resulting in a larger heated length ratio of about 11%). The two heated length ratios allowed a comparison of the behaviour of prestressing steel tendons under different localised heating scenarios and a better experimental understanding of the effects of localised heating on stress relaxation and tendon rupture.

Each test consisted of stressing operations followed by three temperature exposure phases. For the stressing operations, the dead end of the strand was passed through a centre-hole load cell and secured within standard prestressing chucks. The live end of the specimen was stressed using a centre-hole hydraulic jack and standard chucks, also incorporating a centre-hole load cell. Once the appropriate load, approximately 100 kN in the current study, was achieved, the strand was locked off against the stressing frame using a different chuck and load cell assembly. This second assembly was equipped with a threaded expansion cylinder such that final prestress adjustments could be made manually after all seating losses had occurred. Prestress load levels were monitored for 24 hours before final adjustments were made to ensure that short term losses had occurred prior to heating and would not influence the testing results.

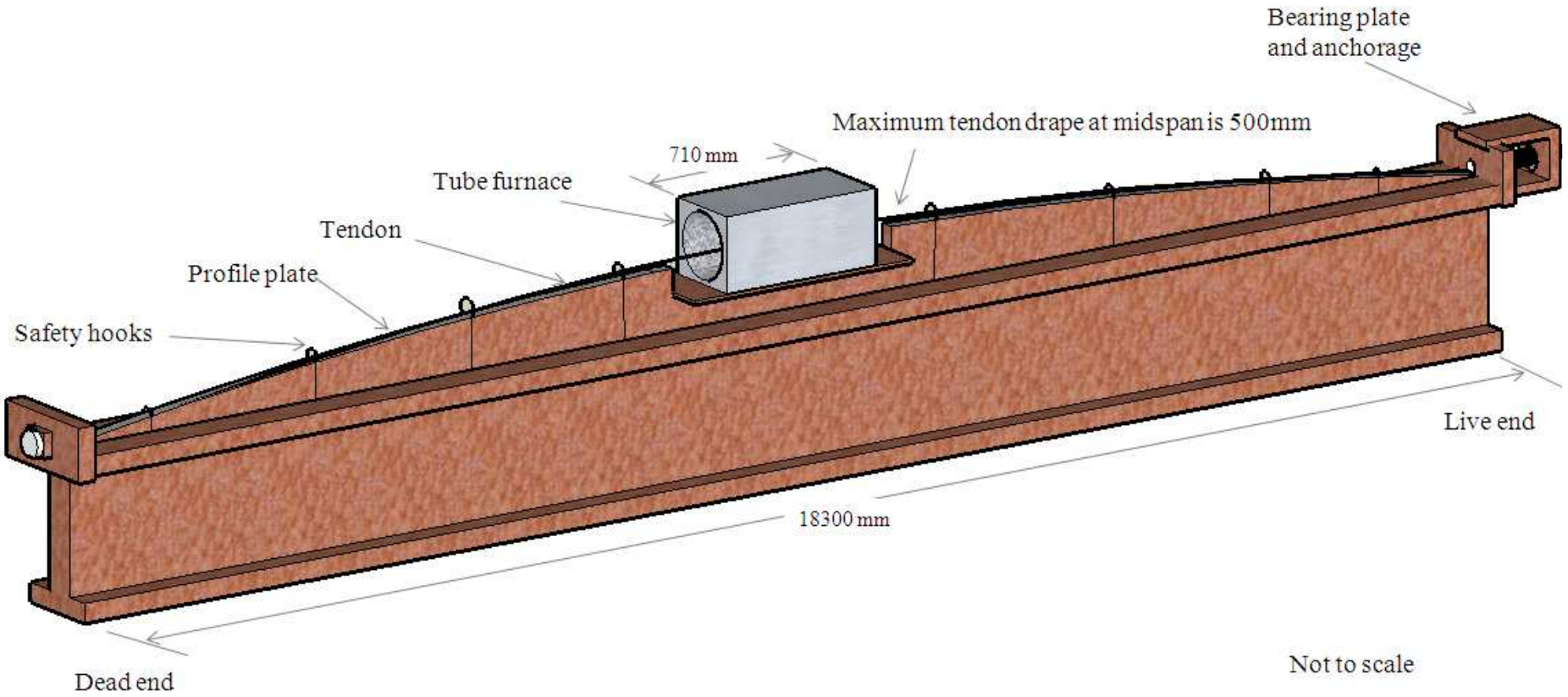

Figure 3.1: Strongback beam testing frame.

Table 3.1: Overview of experimental and computational modelling results for high temperature relaxation tests performed by Gales (2009) and MacLean et al. (2008)

		Test setup				Prestress levels			
						Experiment		Model	
Test #[a]	Heated length ratio (%)	Initial prestress [b] (MPa)	Target soak temp[c] (°C)	Soak time (min)	Ramp rate (°C/min)	End of soak (MPa)	Residual stress (MPa)	End of soak (MPa)	Residual stress (MPa)
Gales tests									
1	3	974	200	90	10	961	972	959	972
2	3	971	300	90	10	941	953	935	948
3	3	973	400	90	10	808	831	669	688
4	3	1009	400	90	10	807	831	664	686
5	3	599	400	90	10	549	569	533	556
6	3	997	400	5	10	882	897	808	829
7	3	1015	400	45	10	815	824	702	713
8	3	1007	400	90	2	805	814	645	668
9	3	1015	400	90	30	769	786	631	657
10	3	997	500	2	10	--[d]	--[d]	--[d]	--[d]
11	3	983	700	--	10	--[d]	--[d]	--[d]	--[d]
MacLean et al. tests									
12	11	1002	200	90	10	947	993	939	993
13	11	1006	300	90	10	896	972	882	975
14	11	1001	400	90	10	648	762	576	680
15	11	1014	400	90	10	663	775	567	670
16	11	1022	400	45	10	697	812	622	754
17	11	1036	400	5	10	771	875	727	855
18	11	1003	500	90	10	245	388	175	313
19	11	975	700	90	10	3	140	32	136

[a] Tests 12-19 details can be found in MacLean et al. (2008)
[b] The target initial prestress was 1000MPa with exception of Test 5 in which it was 600MPa
[c] The maximum overshoot for tests 1-11 was 1.5 ± 2.0°C and tests 12-19 was 5.6 ± 3.6°C
[d] Tendon rupture

The prestress prior to heat treatment for all specimens varied between 971 MPa (52% of ultimate strength) and 1036 MPa (55% of ultimate strength), except for a single test intentionally performed with a target initial prestress level of only 600 MPa to investigate differences in response under lower stress levels.

Once the prestressing steel tendons were stressed in the Strongback frame, the temperature was increased at a constant rate of 10°C/min (with two exceptions noted below) to a predefined temperature set-point between 200°C and 700°C. This ramp rate was chosen to be approximately representative of a heating rate to be expected for an unbonded PT tendon within a concrete structure subjected to a standard fire (assuming no cover spalling), and is also consistent with prior high temperature material testing available in the literature. The second phase consisted of a soak period of 90 minutes at the set-point temperature. This was selected to be approximately representative of typical prescriptive North American fire resistance ratings for restrained unbonded PT floor systems with 19 mm or more of clear concrete cover to the prestressed reinforcement (Gales, 2009). The soak phase allowed for the direct observation of the (approximately) steady-state temperature dependency of creep deformation. Finally, the third phase consisted of slow (passive) cooling (in air) to ambient temperature; this enabled the investigation of the residual/recoverable prestress after transient localised heating.

Figure 3.2 shows the instrumentation used during the Strongback testing. Temperatures on the tendon were monitored by nine K-type thermocouples placed along its length. Strains on the tendon were monitored using bonded electrical resistance foil gauges at two locations: one adjacent to the live end load cell, which was used to verify prestress readings; and the other outside the furnace near mid span, which was used to provide an indication of the importance of frictional effects along the length of the parabolically draped tendon. While some tests used additional bonded strain gauges to monitor frictional effects across the entire tendon length, it was found that frictional effects were negligible in all cases (see Gales, 2009).

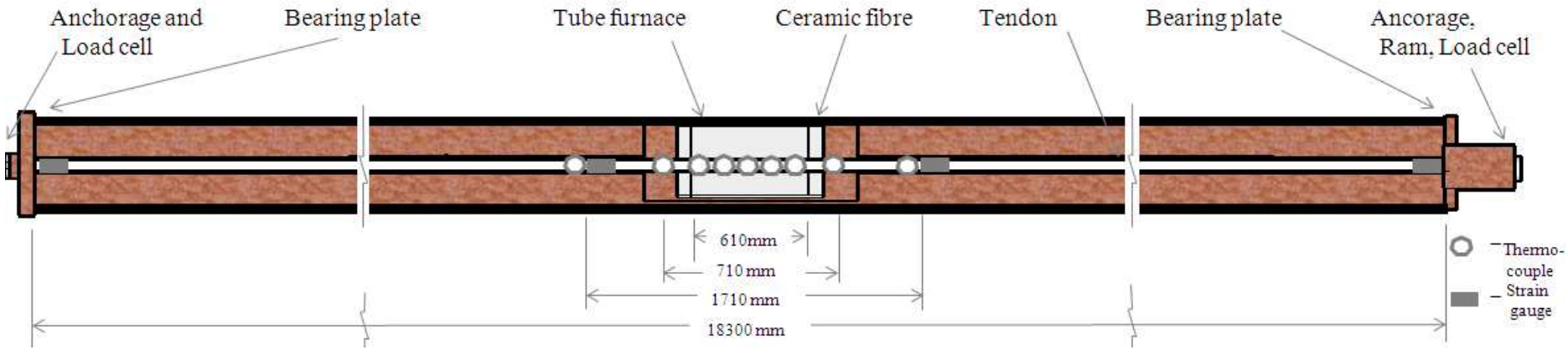

Figure 3.2: Schematic of Strongback beam and instrumentation.

It must be emphasized that these experiments considered the response of only the restrained prestressing steel tendon. Neither the potential impacts of the response of the surrounding structure nor of the imposed loads on tendon stress levels during fire were directly considered. In real unbonded PT structures, applied loads, self weight, thermal deformations (elongation of the structure, thermal bowing), continuity, restraint, membrane actions (both compressive and tensile), discrete cracking, and shear failure modes may all influence the response of continuous multiple-bay PT concrete structures in fire. The aim in the current chapter is to understand the behaviour of cold-drawn steel prestressing steel tendons under transient localised heating; this is a prerequisite to understanding the fire performance of real unbonded PT structures in real fires, as is discussed further in Chapters 4 and 5.

3.3.2 Results of Queen's University tests

The results of the 11 high temperature transient prestress relaxation tests performed using the Strongback frame (denoted tests 1 to 11 in Table 3.1 and not to be confused with other test numbers denoted in other chapters in the current thesis) are briefly reviewed in this section. Gales et al. (2009) have previously used the results of tests 12 to 19 (from MacLean et al., 2008) to verify the predictions of the aforementioned computational prestressing steel deformation algorithm which explicitly accounts for creep deformations and have shown reasonable agreement in terms of trends and overall behaviour (Section 3.4 of the current thesis provides an overview). These tests are also included in Table 3.1 for comparison. Various parameters were varied amongst the tests shown in Table 3.1, including the:

(1) heated length ratio, 3.3% or 11.4%;

(2) initial targeted prestress level, 600 MPa or 1000 MPa (default);

(3) soak temperature, between 200°C and 700°C at 100°C intervals;

(4) soak duration, 5 min, 45 min, or 90 min (default); and

(5) heating ramp rate, 2°C/min, 10°C/min (default), or 30°C/min.

It was found for all testing configurations that stress relaxation was time, temperature, and stress dependent – indicating a clear influence of irrecoverable

creep deformation at temperatures above about 300ºC. The effects of the respective experimental variables are summarized below.

Heated length ratio

Figure 3.3 shows the effect of the heated length ratio on the variation of tendon stress with heating by comparing tests performed by MacLean at 11.4% heated length and Gales at 3.3% heated length for a 10°C/min ramp, a hold of 90 minutes at 400°C, and passive (air) cooling to ambient.

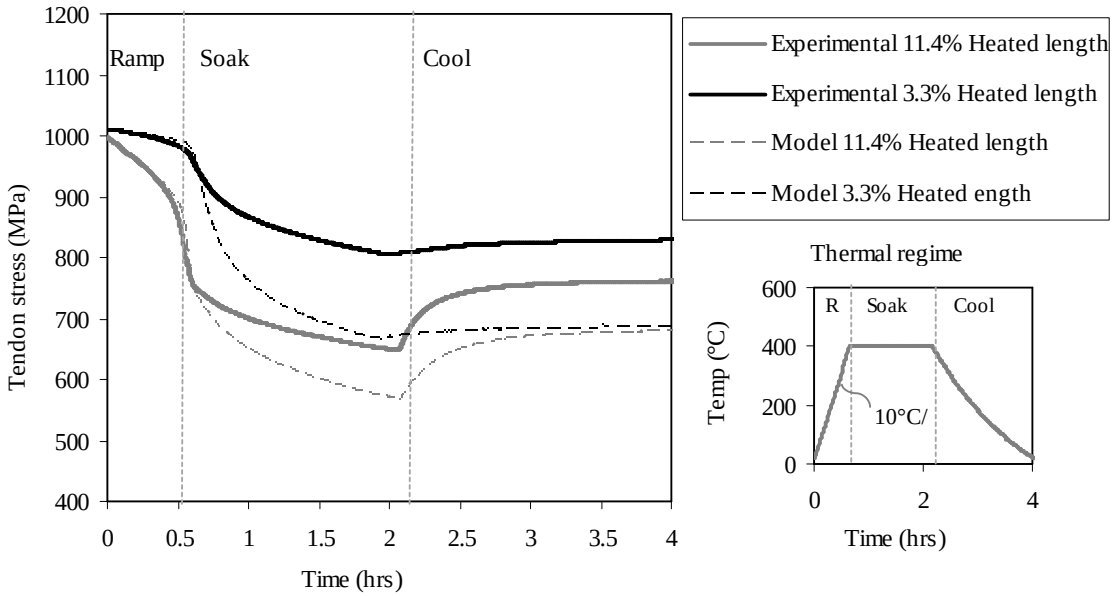

Figure 3.3: Measured and predicted variation of tendon stress for tendons with different heated length ratios heated to 400ºC for 90 minutes and subsequently passively cooled to room temperature.

Figure 3.3 shows that the longer heated length ratio results in greater overall prestress relaxation, but also shows that more prestress is recovered on cooling. These differences in behaviour are due to the fact that the longer heated length ratio experiences proportionally more thermal expansion, which means that the stress reduced more quickly during heating. A longer heated length ratio is thus less likely to experience a situation in which the tendon stress would exceed its strength (i.e. less likely to experience premature tendon rupture). An important consequence of this is that the critical temperature for rupture of an unbonded prestressing steel tendon depends to some extent on its heated length ratio, rather than being a single temperature as is assumed in all currently available design documents (e.g. CEN,

2004; PTI, 2006). Figure 3.3 also shows considerable irrecoverable reductions in prestress which persist after cooling; this is important for post-fire evaluation of unbonded PT concrete structures.

Initial prestress

Only a single test (Test 5 in Table 3.1) was performed with a target initial prestress level other than 1000 MPa. This test had an initial prestress 600 MPa, a heated length ratio of 3.3%, and a soak phase of 90 minutes at 400°C. In comparison with tests 3 and 4, Test 5 shows the strong stress dependency of creep at elevated temperature, as it demonstrates only about 30 MPa (Table 3.1) of irrecoverable prestress after cooling as compared with about 142 MPa and 178 MPa for tests 3 and 4 with higher initial prestress levels. This also demonstrates that creep is less important for mild steel reinforcement than for prestressed reinforcement during fire, assuming comparable creep response, since the stress in mild steel reinforcing bars is likely to be less than 200 MPa under service loads.

Soak temperature

Figure 3.4 shows the effect of soak temperature for tests with heated length ratios of 3.3% and 11.4%, a ramp rate of 10°C/min, a soak temperature of 400°C, and a soak time of 90 minutes. Included in Figure 3.4 are lines showing the tendon stress at the start of the soak period, the end of the soak period, and after cooling to ambient temperature. Figure 3.4(a) shows the effect of soak temperature for strands tested at a heated length ratio of 3.3%. Test 10, with a soak temperature of 500°C, ruptured shortly after reaching the soak temperature, and Test 11, with a soak temperature of 700°C, never reached its soak temperature and ruptured at a temperature of 524°C. Figure 3.4(b) shows the effect of soak temperature for strands tested at a heated length ratio of 11.4%; in this case all tendons survived all phases of heating and cooling without experiencing rupture.

It is clear from Figure 3.4 that reductions in tendon stress are apparent at temperatures above 300°C, and that the effect of creep deformation becomes important between 300°C and 400°C.

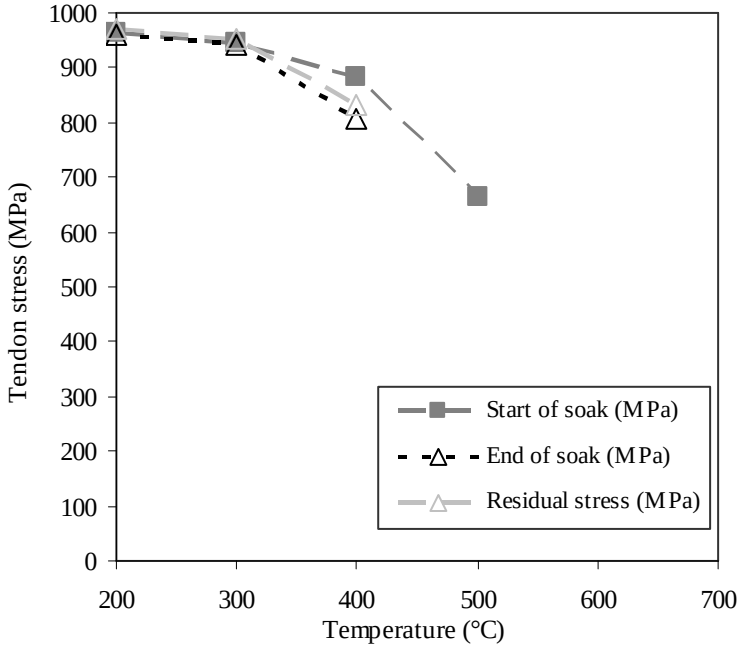

(a)

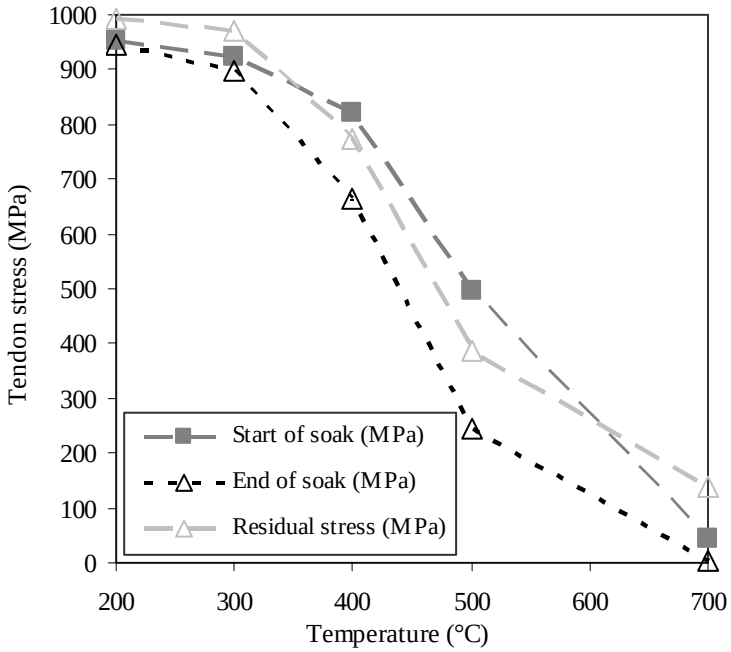

(b)

Figure 3.4: Comparison of experimentally observed variation in tendon stress for different soak temperatures: (a) 3.3% heated length ratio (b) 11.4% heated length ratio.

Figure 3.5 shows the irrecoverable prestress loss exhibited for tendons with different soak temperatures and heated length ratios. The acceleration of irrecoverable prestress loss at temperatures above 300°C is clear.

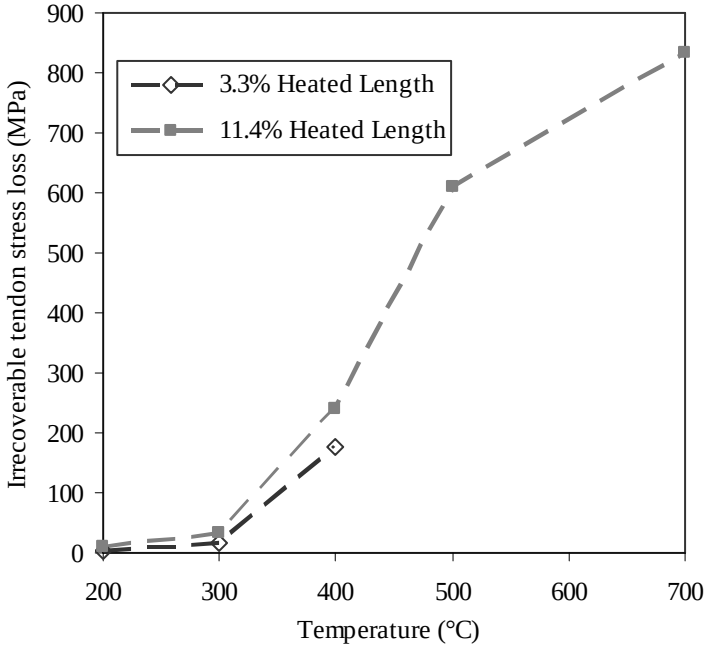

Figure 3.5: Experimentally measured irrecoverable tendon stress loss for different heated length.

Soak duration

Figure 3.6 shows the effect of soak duration for tendons with 3.3% and 11.4% heated length ratios, again by comparing tendon stress levels at the start and end of the soak period and after cooling to room temperature. This figure shows the time dependency of creep strains, since longer soak times tend to cause lower residual prestress values and larger prestress changes during the soak period (which can be considered a steady-state "secondary" creep phase at elevated temperature). This is particularly evident by comparing the "start of soak" and "end of soak" trends. Figure 3.6 demonstrates that the time dependency of creep strain is significant within minutes and occurs at temperatures well below those considered the critical temperature of prestressing steel in North American guidance; i.e. 426°C (PTI, 2006; CPCI, 2007).

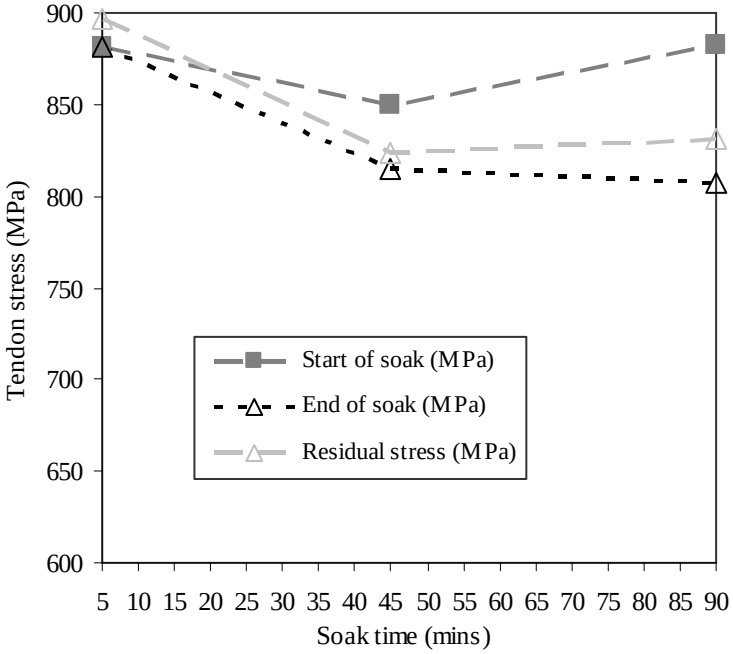

(a)

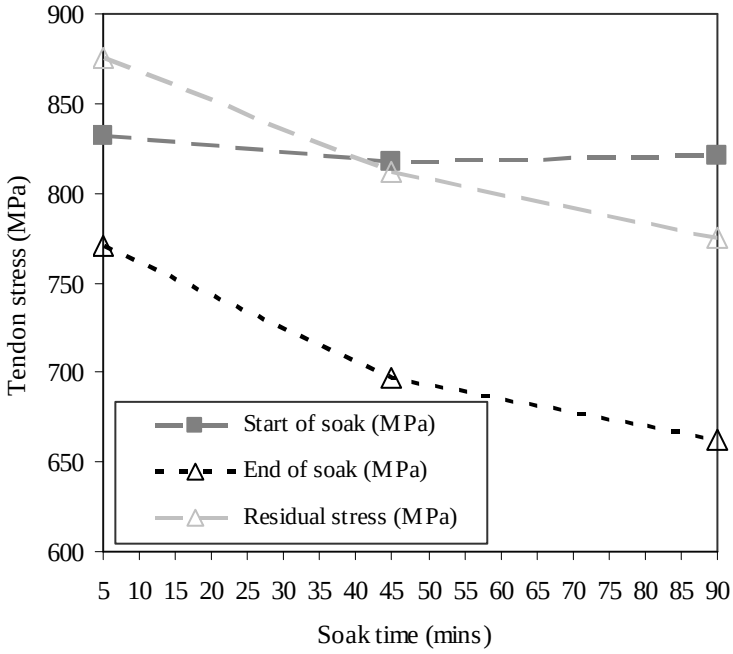

(b)

Figure 3.6: Experimentally observed variation of tendon stress for different soak durations: (a) 3.3% heated length ratio and (b) 11.4 % heated length ratio.

Heating ramp rate

Tests 4, 8, and 9 were identical but for the fact that they used heating ramp rates of 2°C/min, 10°C/min, and 30°C/min, respectively. On the basis of these tests the heating ramp rate appears not to play a critical role within the range tested and up to a soak temperature of 400°C; the prestress reductions during the ramp phase showed no obvious trend and were similar to each other within 4%. It is expected, however, that ramp rate would play a more important role at temperatures between 400°C and 500°C, where creep strains accelerate rapidly. It is worth noting that the observation that the ramp rate do appears not to be significant up to 400°C lends credence to EN 1992-1-2's (Eurocode 2 background notes, 2004) implicit inclusion of creep in defining the stress-strain characteristics of prestressing steel at elevated temperature, but only if tendon temperatures are limited to less than 400°C. Actually the stated limit is 350°C for unbonded PT tendons in EN 1992-1-2 (2004), however in North American guidance it is 426°C (2012), which seems hard to justify on the basis of the data reviewed herein.

Repeatability

Acceptable repeatability was shown at both heated length ratios (i.e. tests 3 and 4 at 3.3% heated length and tests 14 and 15 at 11.4% heated length). In both cases, identical tests with a 90 minute soak at 400°C showed negligible differences (<10 MPa) in tendon stress during all heating phases.

Tendon rupture

Sudden and violent tendon rupture was observed in two tests (10 and 11), both of which were performed in the Strongback frame with a heated length ratio of 3.3%. While at first glance 3.3% seems an unrealistically small heated length ratio, the fact that that unbonded PT tendons in real structures have parabolic profiles and may be continuous over multiple bays with a total length of more than 70 m between anchorages (Taranath, 2010) means that 3.3% could be a credible (even likely) heating scenario in a real building fire. Tendon rupture will cause immediate reductions in both the flexural and shear capacity of a floor plate across multiple bays of a structure, and would also prevent the mobilization of tensile membrane

mechanisms in cases where no additional bonded reinforcement is provided; as permitted by some design codes (e.g. CEN, 2004; ACI 318, 2011; CSA, 2004). This is particularly troubling for structures using banded multi-strand unbonded PT tendons, where four or more tendons could be lost in rapid succession and with little warning.

Figure 3.7 compares observed tendon stress variations versus heated region temperature profiles for tests 10 and 11 (3.3% heated length ratio) and Test 18 (11.4% heated length ratio). The Eurocode's (EN 1992-1-2 (CEN, 2004)) recommended tensile strength reduction curve for prestressing steel at elevated temperature is also shown (taken from Table 3.3 of EN 1992-1-2 (CEN, 2004)) along with a less conservative tendon strength reduction curve suggested independently by Abrams and Cruz (1961). It is worth noting that tendon strength reduction factors presented by Abrams and Cruz (1961), show 50% loss of ultimate tensile strength at 426ºC (800ºF) these curves are therefore responsible for the 426ºC critical temperature currently assumed for prestressing steel in North American design guidance, and thus also for the prescriptive concrete covers imposed in North America for fire resistance ratings for unrestrained unbonded PT concrete slabs (PTI, 2006).

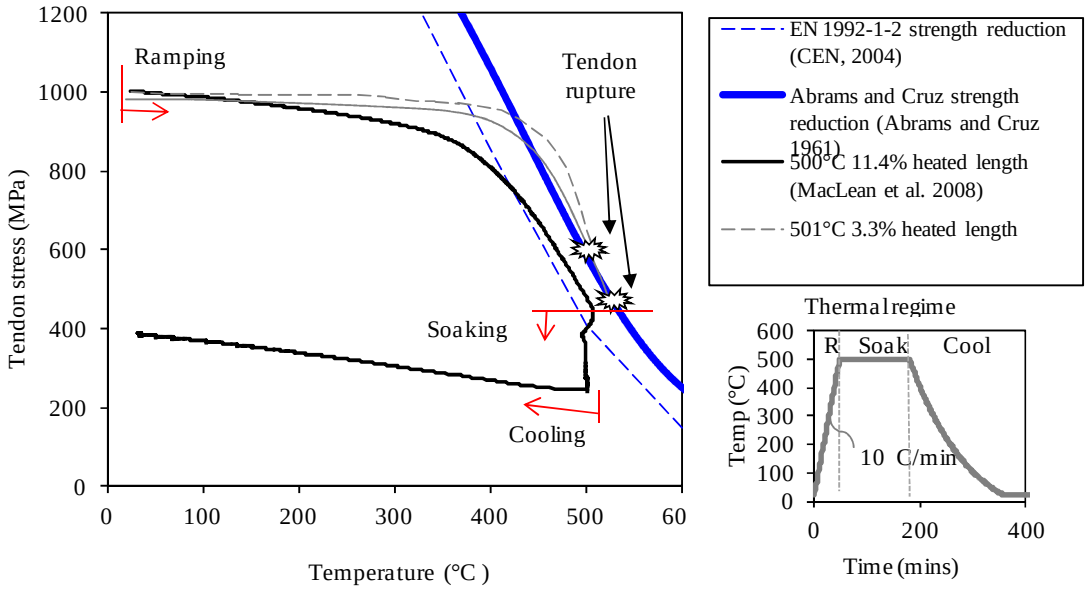

Figure 3.7: Strength-stress-temperature-time dependency of tendon stress levels during transient high temperature relaxation tests of various configurations.

Test 10 experienced tendon rupture at 501°C (two minutes into the targeted 500°C soak phase) and Test 11 ruptured at 524°C (during the ramp phase). MacLean et al.'s (2008) experiments, with an 11.4% heated length ratio, did not experience tendon rupture for the same temperature exposures (tests 18 and 19 in Table 1). This is because the larger heated length used in MacLean's test had larger recoverable prestress relaxation due to thermal expansion. This reduced the stress in the tendon so that the instantaneous tendon stress did not exceed the tendon strength, and therefore failure was avoided. Whether this would occur in a real building would depend on the ability of the tendons to shed gravity loads and differential thermal stresses to the bonded reinforcement (if present), and on the deformations of the structure during heating. However, it is clear that tendons with shorter heated length ratios experience less thermal expansion in proportion to the total unbonded length, and that tendon rupture is therefore considerably more likely in these cases.

The EN 1992-1-2 (CEN, 2004) temperature strength reduction formulae are thought to represent a conservative lower bound for predicting the tensile strength of prestressing steel at elevated temperature (EC2 Background, (CEN, 2004)), and this is evident as being the case for the tests shown in Figure 3.7, for which the experimental stress profiles cross the EN 1992-1-2 strength curve at temperature as much as 100ºC below the point where rupture was observed. In the case of MacLean's test, where rupture was not observed, the EN 1992-1-2's curve predicts failure at a temperature about 120°C less than was actually experienced by the tendon (prior to or without rupture). EN 1992-1-2's strength reductions predict tendon rupture for an additional six of the 11 Strongback tests (excluding tests 1, 2 and 5) and six of MacLean's eight tests (excluding tests 12 and 13) where none was observed. This confirms the conservative nature of the EN 1992-1-2 recommendations, as previously noted by Ellobody and Bailey (2009), although it also shows that this conservatism is reduced as the heated length ratio decreases and tendon rupture becomes more likely. The Abrams and Cruz (1961) strength reduction curve shows a small degree of conservatism in predicting tendon rupture. Figure 3.7 also shows the cooling phase of MacLean's 500°C test (in which rupture did not occur); the irrecoverability of tendon stress on cooling is clear.

The above discussion raises a number of issues related to the colloquial distinction between creep straining and mechanical plastic straining (yielding), particularly at elevated temperature. As the temperature of a stressed tendon increases and its yield strength and elastic modulus decrease, the distinction between yielding and creep deformation becomes blurred and the classical definitions of these strains lose meaning. What is therefore necessary for defensible computational modelling, at temperatures and stress levels where creep and yielding are so closely intertwined, is an ability to rationally account for all the relevant physical processes, rather than trying to inherently account for creep by introducing blanket conservatisms which may not actually be universally conservative, as discussed in Section 3.4, below.

3.3.3 Summary of Queen's University tests

The experiments reviewed in this section have clearly illustrated the time-temperature-stress-strength interdependencies affecting unbonded and stressed prestressing steel tendons subjected to transient and steady localised heating. They have demonstrated that the effects of creep deformation become important at temperatures between 300°C and 400°C, and that creep accelerates rapidly at temperatures above about 350°C. Explicit consideration of creep strains is thus important for structural fire modelling at temperatures well below the 426°C critical temperature of prestressing steel currently assumed in North American codes (IBC, 2012), and in some cases at temperature below the 350°C critical temperature imposed by EN 1992-1-2 (CEN, 2004). The tests additionally show that:

- longer heated length ratios result in greater overall prestress relaxation, but also in greater prestress recovery on cooling; and
- tendons with shorter heated length ratios experience less thermal expansion in proportion to their total unbonded length, so that tendon rupture is considerably more likely under localised heating.

The above observations compellingly suggest that the critical temperature for unbonded PT tendons depends on their heated length ratios, with smaller heated lengths having lower critical temperatures with respect to tendon rupture.

3.4 Preliminary computational modelling

An analytical algorithim defined and coded as a computational model by Gales et al. (2009) can be used to predict stress relaxation at high temperature in locally heated unbonded PT tendons. With suitable input parameters this model is able to capture the transient time-stress behaviour of an unbonded tendon exposed to any spatial and/or temporal heating regime, initial loading level, and time-temperature history. The model assumes the unbonded prestressing steel tendon to be discretized into finite thermal regions of constant uniform temperature within a given time step. This implies that during a specific time interval the tendon physically moves through the heated regions when it locally expands; the thermal regions remain spatially stationary with time.

The temperature of the tendon within each thermal region is input into the computational model via a one-dimensional finite difference heat transfer model coded previously by Bisby (2005) for semi-infinite concrete slabs exposed to fires from below. Alternatively, the model can accept tendon temperatures measured from tests (as is necessary in validating the model against the experiments reviewed in Section 3.3).

The computational model assumes that the longitudinally discretised tendon is considered to be restrained, with fixed total length such that any deformation along the tendon, whether due to mechanical, thermal, or creep deformation (described below) during heating sums to zero over the entire tendon length. Any increase in mechanical, creep and/or thermal deformation is proportionally followed by a decrease in stress, which in turn causes stress relaxation of the tendon (and vice versa in the event of thermal contraction during cooling). Figure 3.8 presents a simplified schematic of the calculation procedure and mechanics involved in the computational model. The equations and parameters used within the computational model to describe relevant deformations are highlighted below.

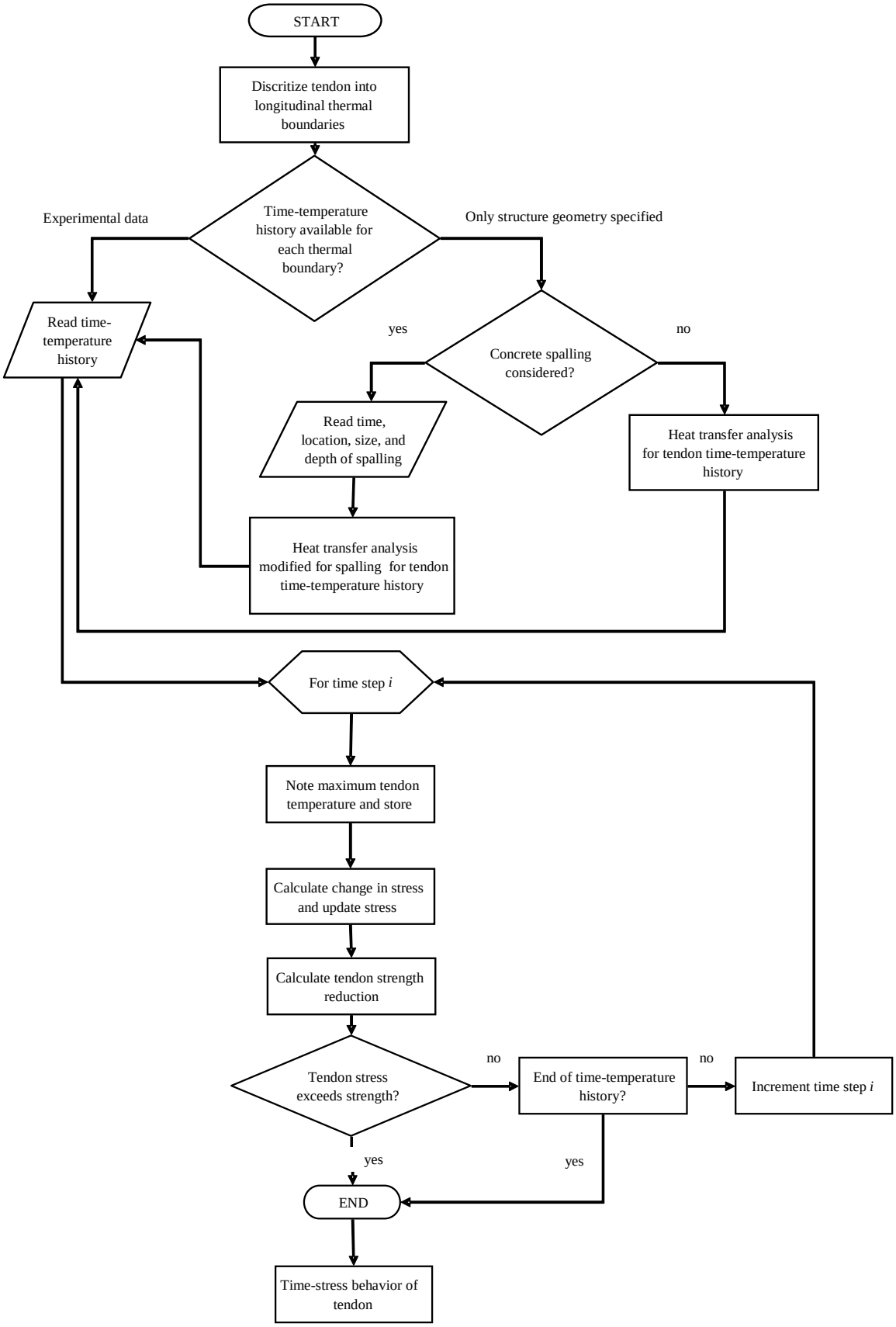

Figure 3.8: Flowchart of main computational model for high temperature stress relaxation.

The computational model assumes that the thermal strain for each thermal region is computed using EN 1992-1-2 guidance (CEN, 2004). Equation 3.1 represents the thermal strain:

$$\varepsilon_{\mathrm{T}} = -2.016\times10^{-4} + 1.0\times10^{-5}T + 0.4\times10^{-8}T^{2} \quad [3.1]$$

$$\text{for } \; 20°C < T < 1200°C$$

where T is the tendon's temperature in degrees Celsius. The model considers the current and previous temperatures of the thermal region to calculate the change in thermal strain, $\Delta\varepsilon_{\mathrm{T}}$, during the current time step. This component of strain is reversible upon cooling. The above thermal strain equation can be used to treat both heating (expansion) and cooling (contraction).

The irrecoverable creep strain of prestressing steel is determined using Equation 3.2 (Harmathy, 1967) during a finite time interval in the analysis:

$$\varepsilon_{cr} = \frac{\varepsilon_{cr,0}}{\ln 2}\cosh^{-1}(2^{Z\theta/\varepsilon_{cr,0}}) \;\text{ for } \sigma = \text{constant} \quad [3.2]$$

Equation 3.2 is a function of temperature and time at a given stress level, and is used to describe primary and secondary creep effects (under which no change in cross-sectional occurs). Creep strains at high temperature can be approximated using Harmathy's (1967) research on steel at high temperature, along with guidance from additional sources (Hill and Ashton, 1957; Abrams and Cruz, 1961; Harmathy and Stanzak, 1970). Harmathy (1967) also reports that Equation 3.2 can be extended for use in cases where stress changes slowly with time. Equation 3.2 is dependent on the Zener-Hollomon parameter, Z (described below), and a dimensionless creep parameter, $\varepsilon_{cr,0}$, which was originally derived by plotting experimental creep strain data versus so-called temperature-compensated time, θ. Temperature compensated time is described using an Arrhenius equation (Dorn, 1955):

$$\theta = te^{\frac{-Q}{T}} \qquad [3.3]$$

where temperature, *T*, is in Kelvin, the length of the current time interval, *t*, is in hours, and the constant, *Q*, which represents the activation energy required to cause molecular motion, is taken as 30550 Kelvin for prestressing steel (Harmathy and Stanzak, 1970; Purkiss, 2008). This is based on an approach outlined by Dorn (1955) that assumes that the steel behaves like a Newtonian liquid with high viscosity; as temperatures increase the average oscillations of atoms also increase, thus promoting creep by more frequent stress-driven molecular rearrangements. Haramthy and Stanzak (1970) found, by creep testing Grade 1720 prestressing steel up to 690 MPa stress level at various temperatures, that the *Z* parameter and the dimensionless creep parameter could be described using Equations 3.4a, 3.4b and 3.5, respectively based on the current stress level, σ (in MPa), in a given thermal region.

$$Z = 195.27 \times 10^{6} \sigma^{3} \quad \text{for } \sigma \leq 172 \text{ MPa} \qquad [3.4a]$$

$$Z = 8.21 \times 10^{13} e^{0.0145\sigma} \text{ for } 172 < \sigma \leq 690 \text{ MPa} \qquad [3.4b]$$

$$\varepsilon_{cr,0} = 9.262 \times 10^{-5} \sigma^{0.67} \qquad [3.5]$$

The *Z* parameter must be invoked with caution since it has only previously been determined experimentally up to stress levels of 690 MPa for Grade 1720 prestressing steel, whereas the tests and simulations presented herein assume Grade 1860 prestressing steel under higher service stresses in the range of 1000 MPa. This chapter extrapolates the equations beyond 690 MPa. This has specific consequences as discussed herein and remedied in Chapter 4.

The *Z* and $\varepsilon_{cr,0}$ parameters for transient creep calculations are determined based on the tendon's current stress level (Equations 3.4 and 3.5). This, combined with the current temperature compensated time, θ, (Equation 3.3) allows computation of the creep strain as shown above (Equation 3.2) for a given thermal region at the start of a time step.

To calculate the change in creep, the process is repeated using the projected creep parameters based on the tendon stress and given thermal region temperature at

the end of the given time step. By using the values of θ in Equation 3.3 at the start and end of the current time step, the difference in creep strain during the time step can be calculated for the given thermal region.

Following the computation of transient thermal creep for the individual thermal regions of the tendon during any given time step, the total strain change for each region can be computed by summing strain increments. Strain changes for each thermal region are converted to an overall elongation (deformation) by their thermal region length. To consider mechanical degradation and to relate overall deformation to stress for each thermal region, a temperature-dependent modulus of elasticity is used for the prestressing steel (based on a regression analysis of data presented by Ruge and Winklemann in Anderberg,1983):

$$\frac{E_T}{E_{20°C}} = -2\times10^{-6}T^2 + 0.2\times10^{-6}T + 0.987 \qquad [3.6]$$

where E_T is the modulus of elasticity at a given temperature, *T*, is in degrees Celsius, and $E_{20°C}$ is the modulus of elasticity of the tendon at 20°C (the assumed ambient temperature).

Stress change over the length of the tendon is then determined. The resulting overall change in tendon stress (stress relaxation or prestress loss) is taken as the initial stress at the beginning of the next time step. Time is then incremented forward and the stress relaxation calculation process is repeated, using the same thermal regions but with updated initial stress levels and temperatures. Full model details are provided by Gales et al. (2009).

3.4.1 Model validation

Table 3.1 presents selected predictions from the computational modelling as compared against the results of the 19 restrained, unbonded, locally heated tendon stress relaxation tests reviewed in Section 3.3. In comparing the tests at different heated length ratios at a soak temperature of 400ºC (tests 4 and 14), the computational model tends to show proportionally greater recoverable prestress for larger heated length ratios, where the shorter heated length ratios maintained a higher

overall stress level but experienced greater irrecoverable losses. The predicted and experimental stress-time histories for selected cases are illustrated in Figure 3.3. The resulting predictions are generally consistent with the observed trend response; however the model tends to over-estimate the prestress loss for both heated length ratios due to an over-prediction of creep during all heating phases. To address this problem additional creep tests are needed to provide the necessary model inputs at stress levels above 600 MPa (see Purkiss (2008) and Gales et al. (2009)). This point is highlighted by examining tests 4 and 5, which had different initial prestress levels. Test 5 used an initial prestress of 600 MPa, in comparison to approximately 1000 MPa used in Test 3. Modelling inaccuracy was a maximum of 3% for Test 5 and 18% for Test 4. Figure 3.9 illustrates the results of both tests in comparison with the predicted results.

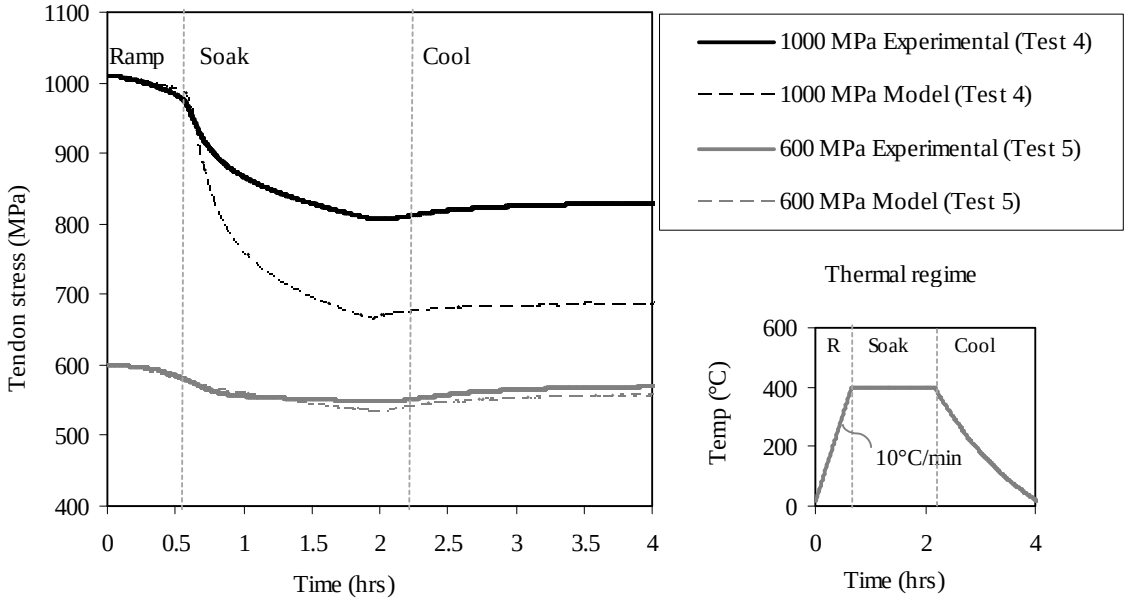

Figure 3.9: Measured and predicted stress versus time for varying initial stress levels.

This figure suggests that creep is modelled more accurately at lower tendon stress levels using the available creep parameters but is in need of refinement for higher stress levels. The high accuracy at low stress levels may be a product of the lower amount of load dependent creep accrued.

Table 3.1 provides modelling data for other tests. Interestingly, while all being of the same target stress (1000MPa) and temperature (400ºC), Tests 3, 6, and 7 which describe different soak times of 5, 45, and 90 minutes indicate decreasing

modelling accuracy. This is indicative of the creep model being time dependendent. Any modelling errors will therefore increase as the duration of heating at high load also increases.

Since the parameters used in the stress relaxation model were developed for prestressing steel specimens in the late 1960s (see above discussion); subtle differences in modern metallurgy will produce a different creep response. These observations suggest that the parameters used for calculation in the stress relaxation model should be investigated at all relevant stress levels. Chapter 4 considers this subject in detail.

In a real building during a real fire, deformations (e.g. thermal expansion and thermal bowing) of the concrete in an unbonded PT concrete slab and the effects of gravity loads may actually cause stress in the tendon to increase rather than decrease (see Franssen and Bruls, 1997). Such potential effects have been conservatively neglected in the current analysis and in subsequent computational studies of tendon response in a flat plate unbonded PT structure. The focus in this chapter is on the strain and deformation behaviour of the tendon reacting to high temperature alone, and potential interactions with the rest of the structure are ignored for the time being. Further research is necessary to account for the full suite of interactions in a continuous concrete slab and to eventually develop a rational understanding of the fire performance which can account for all relevant factors. This issue is considered experimentally in Chapter 5. In the meantime the model as described is considered suitable for an illustrative investigation of premature tendon rupture due to localised heating.

3.4.2 Modelling the behaviour of tendons in flat plate structures during fire

To study the potential implications of localised heating of an isolated unbonded PT tendon of realistic length and parabolic profile within a concrete structure during a standard fire, with particular emphasis on the likelihood of premature tendon rupture during heating in light of the summary of tests in Section 3.3 above, illustrative calculations were performed using the coupled heat transfer analysis-tendon relaxation computational model for a typical multiple bay unbonded PT concrete slab. The example structure is a flat plate continuous unbonded PT concrete slab that

spans three bays. The default slab dimensions and tendon profile used in the analyses are shown in Figure 3.10 and are based on a design example taken directly from the Portland Cement Association (PCA) (PCA, 2005). The example structure represents a typical design which might be applied in North America for a multi-storey residential occupancy building.

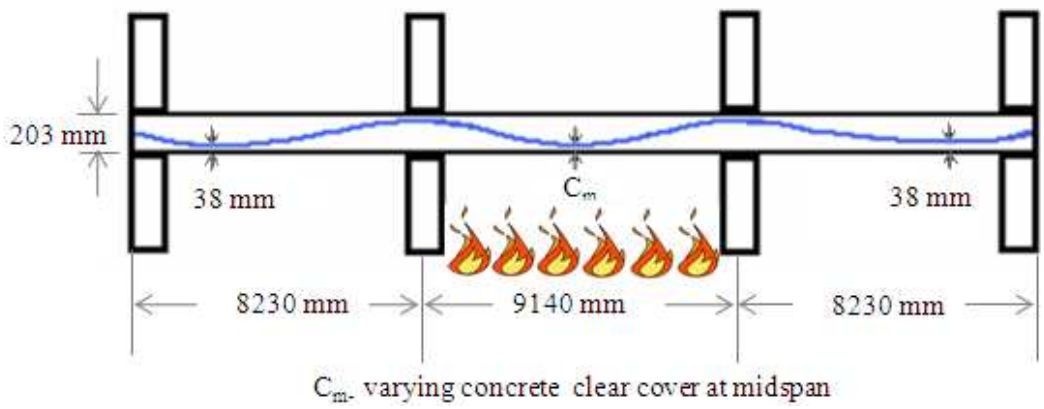

Figure 3.10: Schematic of the default example unbonded PT slab configuration used in the current chapter for computational studies (based on design example slab taken from PCA (2005)).

The example slab is assumed to be cast from carbonate aggregate concrete. The slab thickness is 203 mm and the tendon prestress is 1200 MPa after losses for a No. 13 (99 mm^2 nominal cross sectional area) unbonded prestressing steel strand. The default minimum concrete clear cover at midspan of the central (restrained) bay is assumed as C_m = 19 mm, and in the edge (unrestrained) spans it is taken as 38 mm. This configuration gives a prescribed restrained fire resistance rating of 120 minutes according to the International Building Code (2012), but only 60 mins according to EN 1992-1-2 (2004) (for reasons discussed below). The default total length of unbonded tendon is 25.6 m.

Using the coupled computational model described earlier, the tendon stress variation was predicted for exposure of the slab to an ASTM E119 (2001) fire restricted to the central bay. This represents heating over about 36% of the total length of the structure, notwithstanding variable heating of the tendon within the central bay resulting from its parabolic profile within the slab (hence variable concrete cover). The moisture content of the concrete was conservatively assumed as 2% by mass for the purposes of the heat transfer analysis, and the tendon temperature

was assumed to be uniformly the same as the surrounding concrete (i.e. on the basis of axis distance).

Tendon rupture was assumed to occur in the coupled computational model if, at any instant during the analysis, the 'current' tendon stress level and temperature combination fell above the ultimate tendon strength limits given in Cl. 5.2(6) of EN 1992-1-2 (CEN, 2004). EN 1992-1-2's tendon strength reduction curve is known to be conservative as far as tendon rupture is concerned, as discussed earlier. The EN 1992-1-2 strength reduction factors are considerably more conservative than those proposed by Abrams and Cruz (1961), and the Eurocode explicitly states (in Cl. 5.2(5) of EN 1992-1-2 (CEN, 2004)) a critical temperature of 350ºC for prestressing steel. This is apparently based on a 45% reduction of the characteristic 0.1% proof-stress due to temperature. While allowance is made in EN 1992-1-2 (CEN, 2004) to increase the critical temperature of prestressing steel based on its load ratio, Cl. 5.2(9) of EN 1992-1-2 (CEN, 2004) states an objective critical temperature for unbonded tendons of 350ºC, and warns that higher temperatures should not be used unless accurate methods of determining the effects of slab deflection, and more specifically prevention of tendon rupture (Cl. 4.1-3), are accounted for in design (see Section 3.5). This suggests that a performance based design for an unbonded PT slab should be taken by modelling the behaviour of prestressing steel in fire and accounting for the effects on the entire structure's response, although no obvious method of accurately doing this is given (or currently available).

To illustrate typical outputs from the computational model for the example structure, Figure 3.11 shows the predicted variation in tendon stress levels for the default analysis with the central bay exposed to an ASTM E119 fire (ASTM, 2001) from below. Also included in this figure are the tendon strength reduction curves suggested by Abrams and Cruz (1961) and EN 1992-1-2 (CEN, 2004), as well as the predicted temporal variation in temperature of the tendon at its smallest axis distance (i.e. midspan of the central bay). This figure clearly demonstrates the complex interplay between stress, creep, and strength at elevated temperature, and also shows the importance of what otherwise appear to be subtle differences in strength reduction equations suggested in different sources (CEN, 2004; Abrams and Cruz, 1961). As mentioned above, EN-1992-1-2 (CEN, 2004) shows a smaller strength

reduction than Abrams and Cruz (1961). The difference may be explained by the fact that the equations for strength reduction were developed on the basis of different transient heating rates (approximately 5.6ºC/min for Abrams and Cruz and ranging from 2.5 to 10 ºC/min for EN 1992-1-2 (as described in the background documents (CEN, 2004).Differences in steel composition and fabrication method may also account for differences in the equations (see Chapter 4). As already noted with reference to the test data given in Section 3.3 and tabulated in Table 3.1, prestress relaxation is predicted to accelerate rapidly at temperatures above about 300°C. For the default analysis case the tendon is predicted not to rupture according to the Abrams and Cruz (1961) strength reduction curve up to maximum temperatures exceeding 500°C (beyond two hours), whereas the EN 1992-1-2 (CEN, 2004) curve conservatively predicts tendon rupture at 323°C after only 42 minutes of exposure to fire. These differences and their significance are highlighted below in Section 3.5.

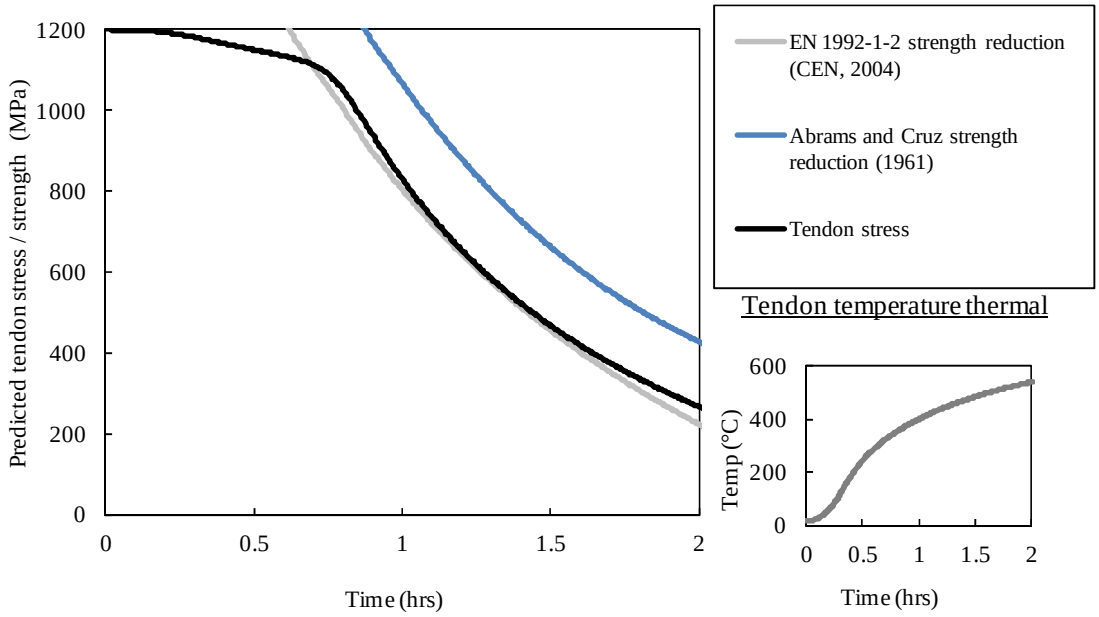

Figure 3.11: Predicted tendon stress variation with time for the default analysis of the two hour fire-rated example slab with 19 mm concrete clear cover (28 mm axis distance) in the central bay (refer to Figure 3.10).

3.5. Potential consequences

Cold drawn prestressing steel is more sensitive than mild steel to deterioration of mechanical properties at elevated temperature, and it therefore requires larger concrete cover for fire protection (CEN, 2004; IBC, 2012). The Eurocodes (EN 1992-1-2 (CEN, 2004)) recognize this and explicitly require that an additional 15

mm of concrete cover axis distance be provided for prestressed steel reinforcement in comparison with mild steel reinforcement, both for continuous (including flat plate) and for simply supported slabs (IStructE, 2006).

In general, concrete cover requirements for achieving a given fire resistance are given in international design codes for restrained and unrestrained flexural members (sometimes distinguished as continuous and simply-supported). However, none of the available codes explicitly distinguishes between bonded and unbonded construction. EN 1992-1-2 (CEN, 2004) appears to be aware of some of the hazards specific to unbonded PT construction but provides no direct design guidance to account for this. For instance, EN 1992-1-2 (Cl. 4.1(3)) states that "*sudden failure caused by excessive steel elongation from heating for prestressed members with unbonded tendons should be avoided*," but it provides no guidance on how this can be achieved in practice. EN 1992-1-2 (CEN, 2004) also states (Cl. 5.2(9)) that "*for unbonded tendons critical temperatures greater than 350°C should only be used where more accurate methods are used to determine the effects of deflections*," although again no practical guidance is given and the reasons for focusing on deflection rather than tendon rupture are not clear. In the absence of specific design guidance it is reasonable to assume that designers will simply adhere to the minimum prescriptive (tabulated) concrete cover requirements given for prestressed flexural elements; it is shown below that these may be insufficient to prevent tendon rupture.

3.5.1 Prescriptive concrete cover requirements for UPT construction

To investigate the implications of currently prescribed concrete cover requirements for unbonded PT slabs, the typical example slab shown in Figure 3.10 was used to perform a number of computational simulations assuming different axis distances at mid span (C_m) for the unbonded PT tendon based on covers required to achieve prescribed fire resistance ratings (from 30 minutes to 240 minutes). Both EN 1992 1-2 (CEN, 2004) and IBC (2012) requirements were considered. The IBC clear cover requirements have been adjusted to axis distance to allow a fair comparison. This has been achieved by adding 3 mm for the tendons' sheathing and half of the strand diameter (6.5 mm) (CS, 2005).

The tendon temperatures used in the model trials (including the default analysis) were assumed as the temperature of concrete at the level of the tendon's centroid, rather than at the bottom of the tendon or at the centroid of the single wire closest to the heated face. This approach is consistent with the axis distance definition used by EN 1992-1-2 (CEN, 2004).

EN 1992-1-2 Cover Requirements

The axis distance concrete cover requirements in EN 1992-1-2 (CEN, 2004) are based on validated computational heat transfer calculations that nominally assume a critical temperature of 350ºC for the tendon. The heat transfer analysis used in the author's stress relaxation model was used to verify that the EN 1992-1-2 axis distances are representative of the 350ºC isotherm for the respective fire ratings quoted in the code for simply supported members. For continuous, two-way, or flat plate unbonded PT slabs, prescribed axis distances are reduced in EN 1992-1-2 to account for fire resistance enhancements arising from other actions (i.e. restraint, continuity, membrane actions, etc.) although the magnitudes of these axis distance reductions are not rationalized in any obvious way. It appears that they are based on observed load-bearing capacities of isolated elements in standard furnace tests on reinforced concrete slabs (from the background documents to EN 1992-1-2 (CEN, 2004)), and subsequently increased by 15 mm to account for the lower assumed critical temperature of prestressing steel as compared with reinforcing steel (IStructE, 2006). It has also been stated in the literature (Purkiss and Kelly, 2008) that the concrete covers suggested in EN 1992-1-2 have been influenced by a series of tests on continuous one-way unbonded PT concrete slabs performed by Van Herberghen and Van Damme (1983) (described in detail in Chapter 2).

IBC Cover Requirements

The IBC (2012) concrete cover requirements are based on an assumed critical temperature of 426ºC rather than 350ºC. In general, the IBC therefore requires considerably less cover than EN 1992-1-2 (CEN, 2004), even when the clear covers are adjusted to axis distance (refer to Table 3.2, pg 91). The IBC covers are apparently based on measured reinforcement temperatures observed in standard

furnace tests on isolated structural elements. The required covers in the IBC appear also to have been influenced by a 1973 report by Gustaferro (1973) in which measured tendon temperatures in standard furnace tests were used to argue for reduced required cover requirements. Gustaferro used data collected from six standard fire tests on prestressed concrete slabs to compare the temperatures of tendons at a given cover depth to the temperature of the concrete at the same depth, and found that the tendons were cooler than the surrounding concrete by amounts corresponding to between 3/8" (10 mm) and 9/8" (29 mm). On this basis, Gustaferro successfully argued at committee level for a reduction of "at least 3/8" (10 mm)" in the required concrete cover for post-tensioned slabs. This concept was subsequently adopted in some North American standards (e.g. PCI, 1972) resulting in concrete cover requirements which are unlikely to ensure that tendon temperatures will be maintained below 426ºC even for the simply supported (unrestrained) case. It should also be noted that in making the comparisons between measured tendon temperatures and temperatures in the concrete at the same level, Gustaferro used the *average* recorded tendon temperature even for parabolic tendons with variable concrete cover. This approach is hard to defend, particularly in light of the discussion in the following section.

The IBC makes no distinction between one-way and two-way slabs, nor does it refer to continuous slabs. Rather, it uses the terminology 'restrained' to refer to these situations. Required concrete covers are further reduced for restrained cases, but again it is difficult to rationalize these reductions since they appear to be based on observations from standard furnace tests of isolated structural elements. For unrestrained slabs the IBC covers have remained essentially unchanged since at least 1959 (Ashton, 1961) (note that IBC was called UBC at that time). For restrained slabs the covers have not changed since at least 1973 (Gustafferro et al., 1973) despite tests by Van Herberghen and Van Damme (1983) which provided compelling evidence that cover requirements should be increased for unbonded PT slabs.

Finally, it is noteworthy that mild steel reinforcing bars are a single, homogeneous structural component, whereas prestressing steel is fabricated from a helix of seven individual wires, plus grease and sheathing. A conservative assumption in defining concrete cover for fire protection of unbonded PT tendons

would be to assume the tendon temperature based on the clear cover alone (i.e. the tendon temperature is equal to the temperature at the bottom of the tendon); this is essentially the approach used by the IBC (2012), albeit with considerably smaller required covers than EN 1992-1-2. In the case of an axis distance definition for cover it could reasonably be argued that, for prestressing steel tendons consisting of multiple wires, the temperature should be taken as that of the most heated wire rather than the tendon's centroid temperature. Thus, the axis distance of the most heated wire would be used, resulting in a 4 mm increase in the required cover for a 13 mm nominal diameter tendon. Nevertheless, the correct, conservative definition of cover depth for prestressing steel tendons warrants further study, particularly in light of the importance of cover for preventing premature tendon rupture during fire, as demonstrated below.

3.5.2 Concrete cover and tendon rupture

To study the effectiveness of current prescribed concrete covers for preventing premature tendon rupture during a localised fire, code-prescribed concrete cover requirements for both restrained and unrestrained cases were assessed using the computational model applied to the example structure with the central bay subjected to a standard fire (i.e. the time to tendon rupture was predicted by the model for an assumed midspan tendon axis distance (C_m) in the central bay). Tendon strength reductions were assumed according to EN 1992-1-2 (CEN, 2004).

Figure 3.12 plots the predicted time to tendon rupture versus mid span axis distance for three heated length ratios. Smaller heated length ratios were simulated by 'adding' additional bays to both sides of the default structure while still considering only the central bay exposed to fire (i.e. by effectively elongating the total length of unbonded tendon while maintaining the same single bay fire exposure). The heated length ratios were 36% (9.1 m heated out of a total tendon length of 25.6 m for the default case in Figure 3.12), 21% (a total tendon length equal to 43.7 m), and 13% (a total tendon length equal to 71.1 m). The curves are truncated in cases where the concrete cover was to prevent tendon rupture (i.e. for 21% and 36% at times greater than 120 minutes of fire exposure).

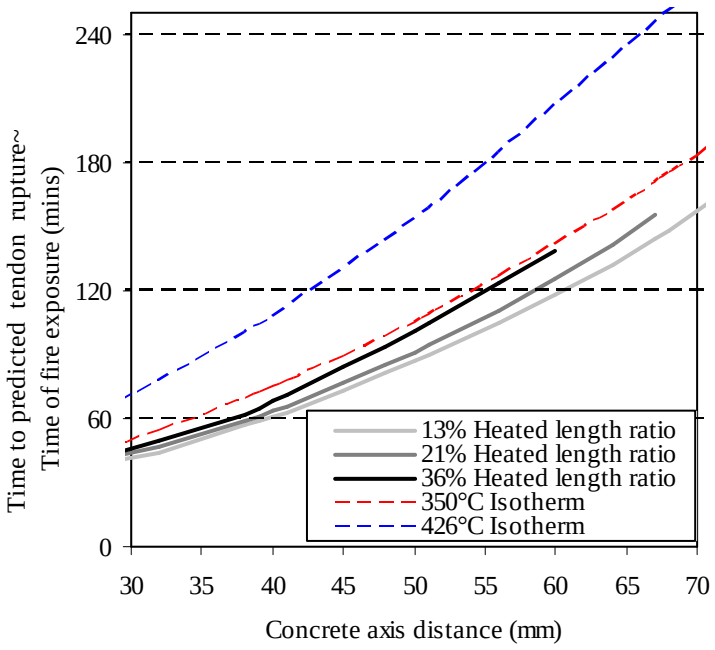

Figure 3.12: Calculated axis distance to prevent tendon rupture versus fire resistance time.

Also shown in Figure 3.12 are the 350ºC and 426ºC isotherms predicted by the heat transfer model at the tendons' axis distance; these are significant because they nominally represent the tendon critical temperatures assumed by EN 1992-1-2 (2004) and the IBC (2012), respectively, for simply supported unbonded PT concrete flexural elements.

Comparison of the predicted tendon rupture times versus these isotherms indicates that the IBC's critical temperature of 426ºC is difficult to justify and requires revision, since premature tendon rupture will occur well before a temperature of 426ºC is reached in real unbonded PT structures. Of course, this assumes that it is essential to avoid tendon rupture to achieve adequate fire resistance, which might not be the case provided that sufficient bonded steel reinforcement is present or if moment redistribution or membrane actions can be relied upon to prevent collapse. However, given the unknowns associated with these secondary behaviours, it would seem prudent at present to design unbonded PT concrete slabs for fire with prevention of tendon rupture taken as an explicit design objective.

The EN 1992-1-2 (CEN, 2004) critical temperature of 350ºC is far more defensible, although for shorter heated length ratios even this may not be sufficiently

conservative to prevent tendon rupture due to localised heating before the code-prescribed fire resistance is achieved. For example, for 120 minutes fire resistance and a 13% heated length ratio, about 54 mm of axis distance is needed to keep the tendon below 350ºC, whereas about 61 mm is needed to prevent tendon rupture. While the prescriptive requirements of EN 1992-1-2 closely reflect the 350ºC isotherm, they do not account for the stress-strength-temperature-interaction that develops under smaller heated lengths as are likely to be experienced in a modern unbonded PT structure.

The IBC prescriptive cover requirements (IBC, 2012) for simply supported unbonded PT slabs are slightly conservative with respect to the 426ºC isotherm (compare the data in Table 3.2 on Pg 91 against the 426ºC isotherm in Figure 3.12). However, a limiting temperature of 426ºC is inadequate to prevent tendon rupture within the prescribed fire resistance time. For example, at 120 mins an additional 12 mm of concrete cover is required simply to equal the 350ºC isotherm equivalent of the EN 1992-1-2 (CEN, 2004) requirements, and an additional 18 mm is required to prevent tendon rupture for smaller heated length ratios.

Table 3.2 provides a tabular summary of the analysis results and code requirements, comparing prescribed concrete cover axis distances against covers required to prevent tendon rupture for the example structure at 36% and 13% heated length ratios. This table confirms that the EN 1992-1-2 covers for the simply supported case essentially represent the 350ºC isotherm, but that they are unconservative with respect to tendon rupture for shorter heated lengths. The table also confirms that the IBC covers are considerably less than are required to prevent tendon rupture on the basis of the model's predictions.

In both codes the required covers for restrained slabs are somewhat reduced, since collapse prevention is assumed to be aided by restraint and continuity and is not wholly dependant on the tendon temperature. While this approach may be defensible on the basis of available standard furnace test data, it means that tendon rupture, is likely well before the prescribed fire resistance time is met, inmultiple span continuous or flat plate unbonded PT concrete structure during a standard fire exposure.

Table 3.2: Summary of analysis results for prediction of tendon rupture times with varying prescribed axis distances (concrete covers) assuming carbonate aggregate concrete

Fire resistance rating (mins)	Depth of 350ºC contour (mm)[a]	Required fire resistance axis distance (mm)						
		For stress > strength at 36% heated length[b]	For stress > strength at 13% heated length[b]	Prescribed by EN 1992-1-2 (2004)			Prescribed by the IBC (2012)	
				For simply supported slabs	For continuous slabs	For flat plate slabs[c]	For simply supported slabs[d]	For continuous slabs[d]
30	20	21	22	25	25	25	--[f]	--[f]
60	34	36	39	35	25	30	--[f]	--[f]
90	45	46	51	45	30	40	--[f]	28
120	54	55	61	55	35	50	47	28
180	69	--[e]	75	70	45	60	59	34
240	81	--[e]	87	80	55	65	--[f]	41

[a] Based on HTA using Bisby (2005) which compares satisfactorily with those performed by EN 1992-1-2 (2004) and in experimentation (CEN. 2004, and Section 5.8)

[b] Based computational model stress reduction compared to EN 1992-1-2 strength reduction (2004). This time may be higher or lower depending on possible modelling improvements suggested within the chapter

[c] 15mm additional axis distance was added (IStructE, 2006) to tabulated data from (CEN, 2004)

[d] Clear cover adjusted to axis distance, by adding 3mm sheathing and ½ bar diameter of 12.7mm

[e] In this simulation an axis distance greater than 58mm does not predict failure by tendon rupture

[f] The IBC (2012) does not tabulate values for these fire resistances

It is important to reiterate that the tendon rupture predictions in Figure 3.12 and Table 3.2 were made using the conservative ultimate strength reductions suggested in EN 1992-1-2 (2004). Using the less conservative strength reductions suggested by Abrams and Cruz (1961) would mean that no tendon ruptures are predicted for any of the above cases. It should also be noted, however, that the stress relaxation model employed has previously been shown to predict stress relaxation in a conservative matter (i.e. it overestimates the amount of creep/relaxation), such that the tendon stress is expected to be higher than predicted by the model, making tendon rupture more likely in a real structure.

Furthermore, thermal bowing, vertical deflections due to gravity loads, and lateral thermal expansion during heating will all act to increase tendon stress during the early stages of a fire; also making tendon rupture more likely. It is therefore plausible that the tendon stress reductions predicted by the current model would be less than in a real structure, and that tendon rupture may occur even earlier than predicted in these simulations.

Additional experimentation and modelling presented in chapters 4 and 5 further investigates the above issues. Nonetheless, the current analysis provides compelling evidence that the IBC's (2012) prescriptive concrete cover requirements are insufficient to prevent tendon rupture during fire.

In light of the above discussion it is interesting to consider what effect tendon rupture and full loss of prestress might have on the structural capacity of a real flat plate unbonded PT concrete slab; relevant experimental data are available in the literature. Total loss of prestress in a continuous two-way unbonded PT flat slab at ambient temperature has previously been investigated experimentally at the University of Texas (Burns and Hemakom, 1977). In 1975, a nine bay (3 span × 3 span) scaled two-way unbonded PT concrete flat slab structure was damaged by manually de-stressing all of the tendons passing through its central bay. The slab remained stable under its self weight. It was then loaded with an imposed design live load, and again remained stable. However, the imposed live load was applied only over the exterior spans; the central bay was subjected to self-weight effects only. While this test shows that a two-way continuous unbonded PT concrete flat slab can withstand total loss of prestress without collapsing at ambient temperature under uniform self weight only, in a fire scenario it is typical to assume loads of at least self weight plus 50-100% of the live load. Furthermore, the test at ambient temperature would not include damage due to thermal bowing, thermal stress cracking, and material property degradation (both steel and concrete) at elevated temperature. Additional research to study these issues is clearly warranted.

3.5.3 Effects of cover spalling on localised heating and tendon rupture

All of the prescriptive code requirements discussed in the previous section assume that no cover spalling occurs. The literature review in Chapter 2 provided clear evidence that the assumption of zero cover spalling is hard to defend, either on the basis of standard furnace tests performed on unbonded PT concrete structural elements or based on evidence from real fires in unbonded PT buildings. It was therefore desired to use the prestress relaxation and tendon rupture model to investigate the potential consequences of different amounts of cover spalling on the likelihood of tendon rupture during fire.

To simulate the effect of spalling on the example slab, the computational heat transfer algorithm coded by Bisby (2005) was modified to simulate any desired location, time, length and depth of concrete cover spalling with resolution to within 1 mm. The analysis assumes one-dimensional heat transfer analysis based on a finite

difference algorithm essentially identical to that proposed by Lie (1992). Spalling is manually imposed in the model by 'killing' elements in the model to the desired depth. Once the spalled elements are 'killed' in the analysis the heat transfer equations assumed at the new exposed surface are changed to reflect a radiative/convective boundary defined by gas temperature in accordance with the standard fire (ASTM E119 (2001)) rather than a conductive boundary. The time, location, length, and depth of spalling are thus prescribed by the user. It must be noted that this is in no way an attempt to model when and how cover spalling will occur; this would be premature given current understanding of the factors influencing spalling despite published attempts to do this by others (Dwaikat and Kodur, 2009). The current analysis is merely intended to illustrate the possible effects of spalling on tendon rupture for unbonded PT slabs, should it occur.

The default spalling analysis considered spalling to occur between minutes 10 and 11 of a standard fire, to a depth of 10 mm over a length of 1000 mm centred on midspan in the central bay of the example structure, as shown in Figure 3.10. This is the time when the concrete at a depth of 10 mm reaches 350 to 375ºC according to the heat transfer analysis; this temperature is roughly the value used by Hertz (2003) for the critical point of steam beyond which pressures increase, as does the risk of spalling. Spalling at mid span is the most damaging location in terms of tendon rupture since the concrete cover is smallest at this location. Again, the analysis assumes that only the central bay is exposed to fire. The initial concrete cover axis distance (C_m) for the central bay was taken as 28 mm (19 mm clear cover). The depth (10 mm to 28 mm), time (5 minutes to 20 minutes), length (100 mm to 9140 mm), and location (centred on mid span or adjacent to the left hand column) of assumed spalling were varied and the time to tendon rupture predicted.

The results are summarized in Table 3.3. For spalling at mid span, using the EN 1992-1-2 (CEN, 2004) tendon strength reduction factors tendon rupture is predicted within 14 minutes of the imposed spalling event. If, however, the Abrams and Cruz (1961) tendon strength reductions are used tendon rupture is predicted not to occur in several cases (because the prestress is predicted to relax faster than the tendon's strength reduces). In the case that spalling removes the entire clear cover, tendon rupture occurs essentially instantaneously using either the Abrams and Cruz

(1961) or EN 1992-1-2 (CEN, 2004) tendon strength reduction factors. Spalling adjacent to the left hand column was found not to cause tendon rupture providing the spalling length was less than 2 m and the depth was less than 20 mm. Clearly, this is because larger covers are provided near supports due to the parabolic tendon profile. This suggests that any amount of cover spalling in sagging moment regions of unbonded PT structures is likely to lead rapidly to tensile rupture of any unbonded PT tendons in proximity to the spall and is consistent with observations from furnace tests and real fires.

Table 3.3: Predicted time to tendon rupture for different assumed spalling configurations

Simulation #	1	2	3	4	5	6	7	8	9	10	11	12
Time of spalling (min)	n/a	10			5	20	10					
Spalling depth (mm)	0	10	20	28	10					20		
Spalling length (mm)	0	1000					9140	100	1000	2000	3000	4000
Location	Mid span								Adjacent to support			
EN 1992-1-2 strength	42	22	10	10	19	28	23	21	42	42	18	10
Abrams and Cruz	--	--	11	10	--	--	--	--	--	--	36	11
Time to reach 350ºC	47	26	10	10	24	32	26	26	47	47	21	10
Time to reach 426ºC	67	37	11	11	34	42	37	37	67	67	28	11

* Note: Default configuration (Simulation 2) of sample slab assumes spalling centred at mid span over 1000mm to a depth of 10mm, with an initial concrete axis distance of 28mm. Tendon strength reduction is based on EN 1992-1-2 (2004). Note that "--" denotes no tendon rupture calculated by direct stress exceeding strength

ACI/ASCE Committee 423 (ACI, 2005) recommends a fully developed system of non-prestressed bonded reinforcing in all one-way slabs and beams such that total loss of prestress will not cause collapse under full dead load plus 25% of the specified live load. This criterion is not applied to two-way slabs since they are thought to possess increased and 'inherent redundancy' (PTI, 2006), mainly as demonstrated through the University of Texas tests mentioned previously (Burns and Hemakon, 1977). However, the Texas tests are not representative of the loading or structural conditions that would be found in a building during a fire. Van Damme and Van Herberghen (1983) have suggested that bonded reinforcement should be provided over the entire soffit of unbonded PT slabs for increased fire resistance. A steel reinforcing percentage of 0.2% in both directions was deemed as sufficient, and the research presented in this chapter supports this assertion. Additional research is needed to more accurately define the minimum bonded reinforcement levels that should be provided in all unbonded PT slabs, such that sufficient amounts tensile stress can be shed to the bonded steel reinforcement to prevent collapse

3.6 Summary

The preliminary modelling and a review of locally heated experiments presented in this chapter have illustrated the time-temperature-stress-strength interdependencies affecting unbonded and stressed prestressing steel tendons. Localised heating of unbonded PT tendons in real flat plate concrete slabs could induce tendon rupture during a fire before prescribed code procedures would indicate, as shown by the preliminary modelling exercises presented in Section 3.4.

Modelliing presented within this chapter suggests as far as the prescriptive axis distance requirements stated by EN 1992-1-2 (CEN, 2004) are concerned, the assumed critical temperature of 350ºC appears to be defensible for simply supported slabs, although for shorter heated length ratios it appears to be questionable to prevent tendon rupture before the fire resistance period is achieved. Preliminary modelling suggests an increase in the EN 1992-1-2 prescribed covers by about 5 mm could address the issue of tendon rupture under localised heating for the simply supported case.

For North American design guidance in particular (IBC, 2012) the assumed critical temperature of 426℃ is difficult to rationalise and may be in need of revision. In all modelling cases the IBC (2012) covers were considerably less than required to prevent tendon rupture before the prescribed fire resistance time was achieved. For example, for 120 minutes fire resistance preliminary modelling suggests an additional 18 mm of concrete cover is required to prevent tendon rupture for smaller heated length ratios for the simply supported case.

In both EN 1992-1-2 (CEN, 2004) and the IBC (2012) the required concrete covers (or axis distances) for restrained slabs are further reduced even from the unrestrained case, since collapse prevention during fire is assumed to be aided by restraint and continuity (redistribution of moments). Additional research is needed to determine whether this increases the risk of structural collapse of unbonded PT structures during fire in the event of tendon rupture.

Performance based structural fire design codes are currently in the process of being developed and refined around the world. With this in mind a fundamental understanding of various aspects of the real behaviour of continuous unbonded PT concrete slab structures (both flat plates and other types of unbonded PT structures),

when subjected to elevated temperatures, is needed. Available mechanical property reduction models for prestressing steel, which ‘implicitly’ account for high temperature creep, cannot possibly capture the time-dependency of creep deformation under transient heating conditions as would occur in a real fire. The ability to quantify the true material behaviour at high temperature of prestressing steel will be therefore be explored in more detail, supported by a new set of tests on prestressing steel at elevated temperature, in Chapter 4.

Chapter 4

New Parameters to Describe High Temperature Deformation of Prestressing Steel

> *"Even the most sophisticated treatise on the behaviour of buildings or building elements in fire remains mere speculation if it is not based on a thorough knowledge of the behaviour of the component materials…"*
>
> -Tibor Harmathy
> Former head of fire research at NRC, Canada
> (Harmathy and Lie, 1970)

4.1 General

A computational stress relaxation model describing the behaviour of isolated unbonded prestressing steel tendons in any fire was presented and discussed in Chapter 3. The model was used to illustrate the potential dangers of localised heating of a PT concrete building with regards to premature unbonded prestressing steel tendon rupture and to increase our understanding of the time-temperature-stress-strength interdependencies that may affect unbonded and stressed prestressing steel tendons in real building fires. While accurately describing the unbonded prestressing steel tendon deformation trends under various high temperature exposures, the stress relaxation model, with input parameters based on testing available in the literature, consistently overestimated the degree of thermal deformation and thereby potentially underestimated the risk of tendon rupture during fire. This error was hypothesized to be due to two possible factors:

(1) the fact that modern metallurgy of prestressing steel tendons may have advanced since the available parameters were derived and therefore that model does not properly describe modern prestressing steel; and/or

(2) that the parameter range for which the model was used was extrapolated beyond the boundaries under which they were developed (stress level in particular).

Accurate knowledge of how the prestressing steel tendons deform in fire is essential; otherwise any performance based analysis which attempts to describe the full-structure response of a PT building in fire will be largely speculative (see Harmathy and Lie, 1970). Thus, new experiments are needed to properly characterize

modern prestressing steel tendon behaviour at high temperature, and this is the central objective of the current chapter.

The thermal deformation response of isolated prestressing steel tendons exposed to a wide range of transient and steady state loading and heating conditions is presented in this chapter. Specific attention is given to high temperature plastic (creep) behaviour, allowing better understanding of the mechanisms which control premature tendon rupture and tendon stress relaxation during fire. The thermal deformation model reviewed in Chapter 3 for prestressing steel tendons is improved by the development of new material input parameters. Validation exercises, as well as discussion pertaining to the creep resistance of various modern prestressing steel tendons used internationally, are given. The work is needed to enable consideration of the global structural response of a PT concrete structure when prestressing steel tendon damage in a fire occurs, as is experimentally considered in Chapter 5.

4.2 Overview

The propensity for rupture of unbonded and stressed prestressing steel tendons at elevated temperature within a concrete structure depends on a complex interaction between thermally induced loss of strength and tendon stress variations which are due to time, stress, and temperature dependent irrecoverable creep as illustrated in Chapter 3. An accurate, robust and explicit method for predicting creep deformation for any possible transient heating regime is therefore necessary to computationally assess the performance of unbonded PT buildings both during and after fire.

A computational model for predicting high temperature stress variation of locally-heated unbonded and stressed prestressing steel strands has previously been developed and shown to predict deformation trends was given in Chapter 3. However, this modelling was forced to make use of dated input parameters from the early 1970s (Harmathy and Stanzak, 1970) which may not reflect the metallurgy and processing of modern prestressing steels. When applied here to predict the response of modern prestressing steel exposed to localised heating, the model significantly overestimated prestress relaxation.

The high temperature creep response of modern prestressing steel is investigated in this chapter. The focus is on the high temperature behaviour of

modern prestressing steel sourced from a British steel supplier (fabricated according to BS-5896-12 (BSi, 2012) by Bridon Steel, UK). A testing regime using uniaxial both steady-state and transient thermal regime tensile tests has been employed (Section 4.4).

Unfortunately conventional contact strain instrumentation does not easily allow for accurate derivation of high temperature material properties. Therefore a non-contact strain and deformation measurement technique using high resolution Digital Image Correlation (DIC) is used and validated herein at elevated temperature (Section 4.5). The technique is then applied to accurately characterize the creep and mechanical parameters for the entire service stress range of the BS 5896-12 steel (Section 4.6).

The results of the new tests using DIC challenge classical assumptions used in creep theory and provide novel insights into modelling the true nature of runaway creep failure (so-called 'Tertiary' creep). A validation exercise for the newly developed creep parameters is presented while discussing and addressing the model's limitations. The chapter concludes with discussion of creep resistance of various available prestressing steels (Section 4.7).

Available creep parameters for any steel are widely assumed to apply equally to all grades sourced from different mills. However, fabrication and microstructural differences from mill to mill may influence respective steels' creep resistance, particularly at high temperature. This chapter therefore considers the creep behaviour of "equivalent" grades of prestressing steel sourced from three separate mills in the UK (BS 5896-12 (BSI, 2012)), the North America (ASTM 416 (ASTM, 2003)), and Australasia (AS/NZS 4672 (AS/NZS, 2007)). The creep behaviour of these modern prestressing steels is also compared to available results for tests of older prestressing steel from the 1970s; fabricated according to ASTM 421-65 (ASTM, 1965) and presented previously by Harmathy and Stanzak (1970), and previously used in the modelling presented in Chapter 3. The consequences of an engineer/designer using the wrong creep parameters for equivalent grades of prestressing steel are explored with a simple modelling exercise to emphasize the importance of using the correct material input parameters.

4.3 Creep theory background

To improve prestressing steel creep calculations it is necessary to review the background creep theory employed in the prestressing steel computational mechanics model for stress relaxation given in Chapter 3. This section provides and reviews the necessary background information needed to define new material parameters and to test the suitability of these for describing prestressing steel high temperature response. The section finishes by stating cautions when using this theory.

4.3.1 Creep equation

Creep strain (ε_{cr}) is deformation, largely irrecoverable, which for prestressing steel depends on manufacturing, metallurgy, stress, temperature, and time. For either transient (i.e. load-then-heat) and steady state (i.e. heat-then-load) uniaxial heating test conditions, by plotting the measured ε_{cr} , after careful removal of strains due to thermal expansion and mechanical strains due to elastic modulus reduction, for a constant sustained uniaxial tensile load level a sigmoidal (S-shaped) curve can be plotted with respect to a lumped time-temperature parameter. This is commonly called 'Temperature Compensated Time', θ. Invoking an empirical coefficient Q, the 'activation energy' for creep, which is measured in Kelvin, θ can be described using an Arrhenius equation as follows:

$$\theta = \int_0^t e^{-Q/T} dt \qquad [4.1]$$

where t is the duration, measured in hours, for a given analysis time step (see Purkiss (2008) and Gales (2009)), T is temperature in degrees Kelvin, and Q is described in Section 4.3.2. A typical example of an ε_{cr} versus θ curve for representative prestressing steel is illustrated in Figure 4.1(a). The trends shown in Figure 4.1 come from real test data; however the magnitudes in Figure 4.1 have been omitted for clarity and illustrative purposes.

The classical ε_{cr} versus θ creep curve (derived using constant uniaxial tensile load) has three distinct phases. The Primary phase is characterised by a decreasing deformation rate and is dominated by strain hardening. The strain rate progressively decreases as the hardening process increases due to counteraction from dislocations within the grain structure of the steel. The secondary phase can be described as a

'steady' minimum straining rate. The formation and growth of voids (in the form of cavities, pores, and/or cracking) along the grain microstructure takes over which then causes the straining rate under constant load to accelerate (see Figure 4.1(b)) as 'run away' strain during a final Tertiary phase. The voids are theorized to form along grain boundaries and may be influenced by material impurities, dislocation breakthrough or distortion of the grains (Yao et al., 2007). The final Tertiary creep phase leads eventually to tensile failure (Smith, 1996).

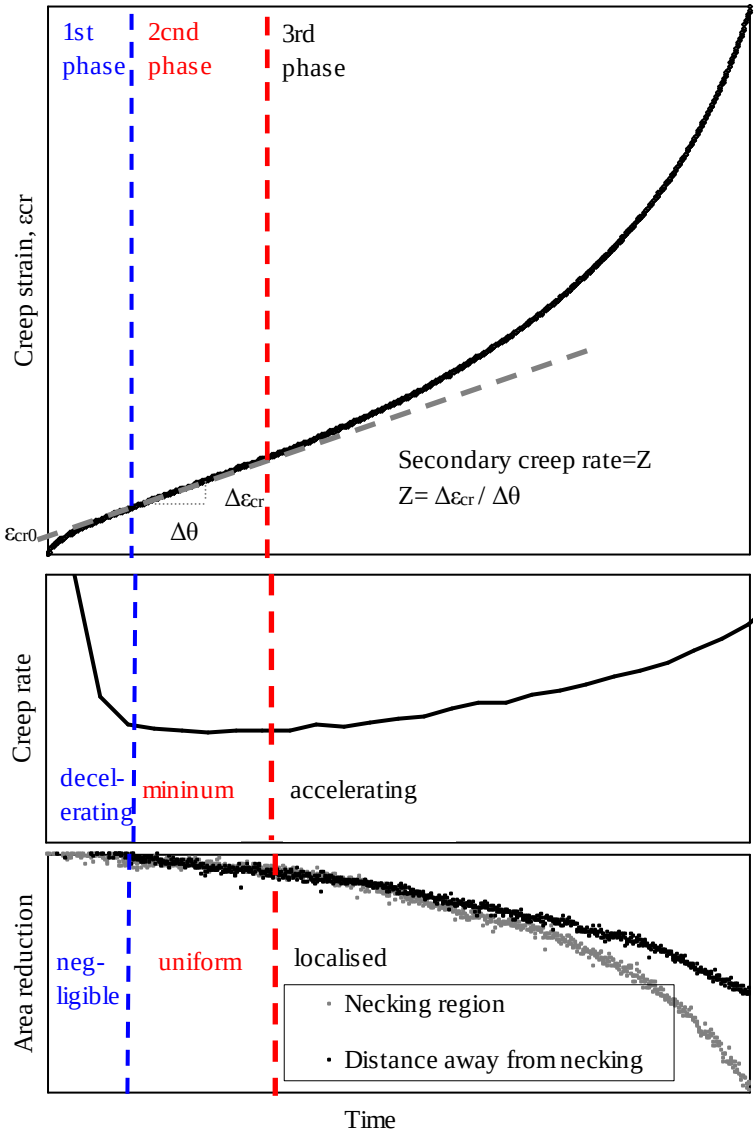

Figure 4.1: Creep theory applied to prestressing steel.

Defining the initiation point of the Tertiary phase is difficult. The classical theoretical definition of the beginning of the Tertiary phase is the moment at which

the minimum creep rate is observed (see Wilshire, 2009). By determining the minimum creep straining rate for a ε_{cr} versus θ plot, a Zener-Holloman parameter, Z, can be derived (in hrs^{-1}). This may be approximated by determining the slope of the approximately linear Secondary creep phase. A linear tangent to the Secondary phase will intercept the vertical-axis at the primary creep value, $\varepsilon_{cr,o}$. The extraction of Z and $\varepsilon_{cr,o}$ from a sustained stress uniaxial creep test is illustrated in Figure 4.1(a). In fire engineering design (Purkiss, 2008; Harmathy, 1986) these parameters can be used to predict the amount of creep during the Primary and Secondary creep phases. Equation 4.2 is often used to predict ε_{cr} for steel:

$$\varepsilon_{cr} = \frac{\varepsilon_{cr,0}}{\ln 2} \cosh^{-1}\left(2^{\frac{Z\theta}{\varepsilon_{cr,0}}}\right) \quad [4.2]$$

Harmathy (1967) also provides an alternative equation to approximate creep based on the same parameters:

$$\varepsilon_{cr} \approx \left(3Z\varepsilon_{cr,o}^{\ 2}\right)^{0.33}\theta^{0.33} + Z\theta \quad [4.3]$$

Equation 4.2 is suggested for use in design, both by Purkiss (2008) and by Harmathy himself (1986).

4.3.2 Creep activation energy

The advantage of Equation 4.2 is that two steady state creep curves at different temperatures and same loading should overlap with respect to θ (see Harmathy, 1967). Thus, transient and steady state creep tests at the same loading level should also overlap. This can be used to advantage if the temperature compensated time reasoning suggested by Equation 4.1 is valid, since a steady state test can take many hours to complete whereas a shorter transient test may yield the necessary parameters. Test equivalency should be achieved through a proper derivation of the activation energy for creep, Q, which is an essential parameter for defining θ. This section describes two techniques (see Lewinsohn et al., 1996; Smith 1996) which may be used to derive a value of Q for a given prestressing steel. In both cases Q is measured in degrees Kelvin.

Several creep tests performed at the same load but at different temperatures can be used to derive a value of *Q*. Using this technique, creep strain is plotted against θ rather than against time for each test at the same load level. An arbitrary value of *Q* is first chosen for use in Equation 4.1 to relate time and temperature. This value is then iterated by trial and error until all creep curves at the same loading coincide with respect to θ. The *Q* at which coincidence appears is the approximate correct value.

A traditional and more conventional technique can be used to calculate an exact value for *Q* by a minimum of two tests. This technique considers several steady state temperature creep tests at the same loading. Two parameters from each test are needed: (1) the value of the constant creep rate, $\dot{\varepsilon}$, (taken as strain/strain to time) and (2) the respective temperature, *T*, that the test was performed at, measured in Kelvin. For each test, the natural logarithm of $\dot{\varepsilon}$ and the inverse temperature of the test, *T* is plotted. Figure 4.2 shows three steady state creep tests plotted using this method; a single value of *Q* is represented by the slope of the line in this plot.

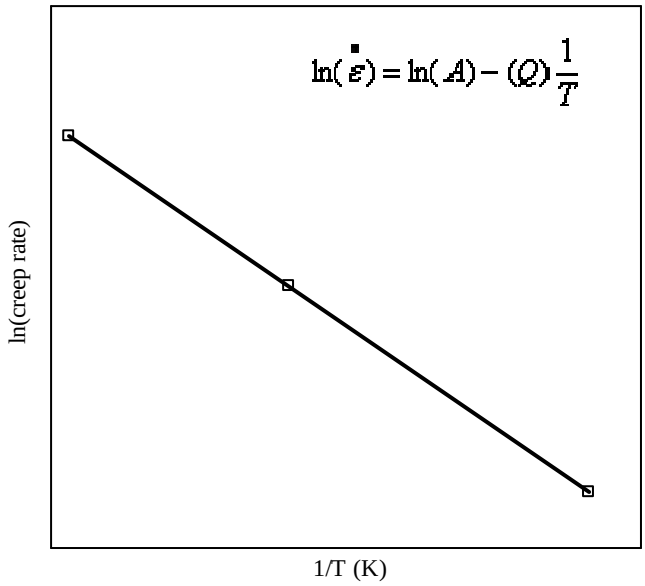

Figure 4.2: Calculating activation energy from a series of steady state creep data sets.

Equation 4.4 describes this empirical relationship:

$$\ln(\dot{\varepsilon}) = \ln(A) - (Q)\frac{1}{T} \qquad [4.4]$$

Where *A* is a constant and the intercept of the creep rate axis but is not needed for the creep modelling performed herein. This method is akin to viewing the deformation characteristics in steel at high temperature as a chemical reaction which takes place at an increasing rate with increasing temperature.

Both of these techniques assume that the defined value of *Q* is independent of temperature, which may or may not be a valid assumption (checks on this are discussed later). It is noteworthy that *Q* depends on metallurgy meaning that if the microstructure of a metal changes, the instantaneous activation energy for creep may also be influenced (Smith, 1996).

4.3.3 Creep theory caveats

It is prudent to re-emphasize some cautions of the above creep theory for prestressing steel, all of which were considered herein when developing new material input parameters for creep:

- **Dated material parameters may not be applicable to modern materials** – Steel from older tests may not be representative of current materials. The metallurgical characteristics used in modern steels may differ considerably from those used in the past since small changes chemical composition and in the fabrication processmay influence the creep response of a material.
- **The full creep curve must be considered** – It is not acceptable to terminate a creep test before entering the Tertiary phase (e.g. Morovat et al., 2012). The Zener-Holloman Parameter, *Z*, represents the minimum creep rate and can only be determined from a full creep curve. This is particularly important when defining the activation energy for creep *Q*.
- **Only one set of parameters should be derived from one test** – During a creep test the cross-sectional area of a specimen will decrease, due to the Poisson effect and then to necking. If the load is increased during a test so that multiple creep parameters are determined at different stresses, *Z* may be overestimated since the engineering stress will be less than the true stress. For example, Harmathy and

Stanzak (1970) attempted to derive multiple creep parameters from a single specimen by adjusting loading mid test, and thus the creep parameters obtained may overestimate the creep response even for the older specimens they tested.

- **Creep equations have traditionally been applied only to Primary and Secondary creep** – Equation 4.2 has historically only been assumed valid until the transition between Secondary and Tertiary creep phases; it does not account for cross-sectional area reduction which is likely to occur during Tertiary creep. Equation 4.2 was intended for use where 'true' stress changes slowly with time. It is noteworthy that it may not be possible to extract Z from creep data sets for all metal alloys, since ε_{cr} may never exhibit linearity with respect to θ in some cases. For prestressing steel, however, Equation 4.2 has been shown to satisfactorily represent creep behaviour trends (see Chapter 3), and it is therefore applied herein to derive new creep parameters for use in high temperature creep modelling (i.e., Z, $\varepsilon_{cr,o}$) based on a new series of creep tests on modern steel at elevated temperature.
- **Creep is influenced by metallurgy which may change with temperature** – The activation energy, Q may change since a specimen may experience metallurgical changes with increases in temperature. Caution is therefore needed if a creep model for steel is to be used in a transient heating condition. This behaviour could be given some consideration either in performance of the model in variable heating conditions or by consideration of the steel's microstructure at different elevated temperatures.

4.4 Creep test methodology

Both ambient and high temperature uniaxial tensile tests were performed to define new creep parameters for three equivalent grades of modern Grade 1860 MPa prestressing steel. Core wires were taken from 7-wire spiral strand tendons originating from the UK (BS 5896-12 (BSi, 2012)), USA (ASTM 416-03 (ASTM, 2003)), and Australasia (AS/NZS 4672-07 (AS/NZS, 2007)). These specimens were 4.15, 4.40, and 4.40 mm in diameter, respectively, and cut to 660 mm in total length.

Materials

Each of the specific steel strands tested herein allowed for quantification of high temperature creep parameters; however each also played additional roles. This chapter focuses on the BS-5896-12 (BSi, 2012) strand. This prestressing steel was used also for large scale experiments presented in Chapter 5. The ASTM 416-03 (ASTM, 2003) strand was taken from the same coil as was used for the Strongback beam tests discussed in Chapter 3. This was used to verify the creep model and to compare against other modern prestressing steel. To help describe the creep resistance of steel from different mills, AS/NZS 4672-07 (AS/NZS, 2007) strand was obtained from colleagues from the University of Canterbury, New Zealand. This allowed an international comparison of creep behaviour, metallurgy, and strength for these modern prestressing steels. High temperature uniaxial tensile test results for a historical steel, in accordance with ASTM 421-65 (ASTM, 1965) were referenced from the paper of Harmathy and Stanzak (1970), and these results are also used for comparison to illustrate differing creep responses.

Testing apparatus

All uniaxial tensile tests were performed using an Instron 600LX materials testing frame equipped with an environmental chamber for heating specimens up to 625°C under load. The environmental chamber was equipped with a quartz glass viewing window so that strains could be measured optically using DIC. Test specimens were gripped outside the environmental chamber, as shown in Figure 4.3 and Figure 4.4. K-type thermocouples (with an accuracy of ± 0.0075T, where T is measured in ºC) were used to monitor the temperature of the specimens during the tests. Five thermocouples were attached to the specimens at 50 mm spacings (T1 through T5 in Figure 4.4). It should be noted that most strain measurements were made between T1 and T2; readings from these two thermocouples were then averaged to define the specimen temperature at the location of strain measurement which is needed for high temperature tests. Thus, in some tests only three thermocouples were used and placed at locations T1, T2, and T5. A non-contact DIC technique was applied herein for measuring strain and deformation using the GeoPIV8 algorithm (White et al., 2003)

through post-test image processing of high resolution digital images captured during tests.

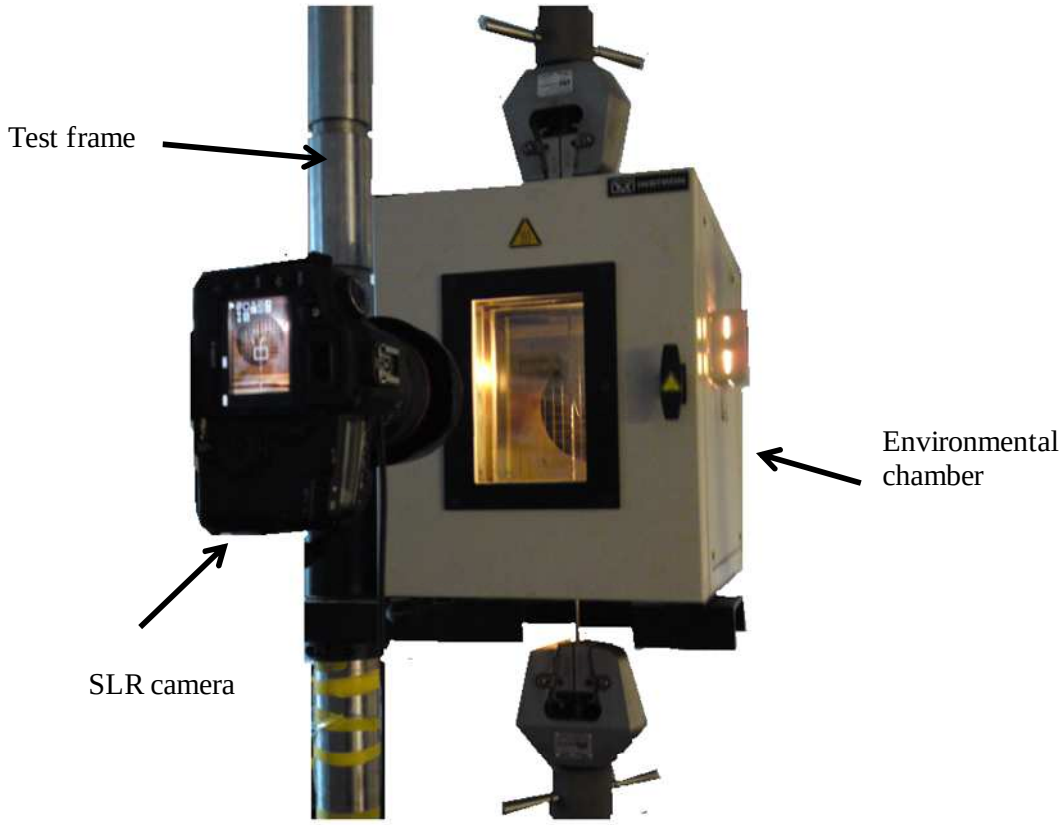

Figure 4.3: Test setup and digital SLR camera used for DIC analysis.

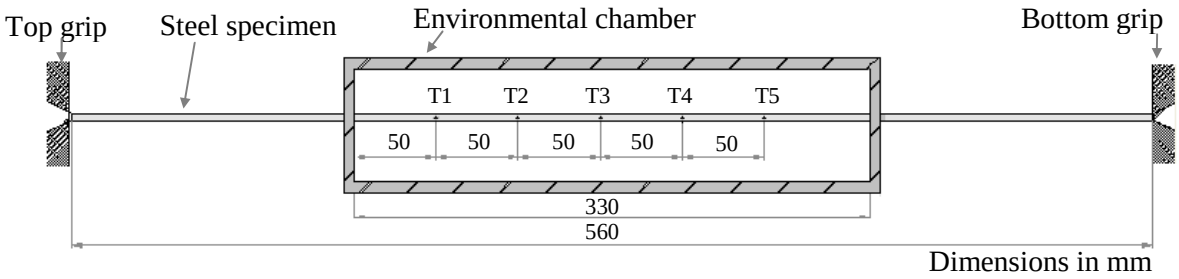

Figure 4.4: Instrumentation location schematic for tensile tests.

Testing regimes

A variety of different uniaxial tensile testing regimes were used to study various aspects of the creep response and mechanical behaviour of prestressing steel at elevated temperature. These included:

(1) **Steady state creep tests –** wherein the sample was heated to a predefined constant temperature and strain was measured while load was increased up to a sustained target stress or until failure.

(2) **Transient creep tests –** in which the specimens were loaded initially to a target load (stress) at ambient temperature, and strain was then measured while the specimens were heated at a uniform heating rate until failure.

(3) **Thermal expansion tests** – following the same procedure as for transient creep tests, however with zero loading.

(4) **Stress relaxation tests** – in which specimens were loaded initially to a target stress at ambient temperature and then fully restrained and heated using a pre-defined heating curve for a fixed duration.

(5) **Tensile strength tests -** heated without applied load up to a fixed temperature and then tested to failure under crosshead displacement control. It should be noted that different straining rates and heating rates will implicitly accrue different amounts of creep strain during tensile strength testing; thus the effect of varying straining and heating rates has also been studied.

Figure 4.5 and Figure 4.6 provide procedural references for the above tests. All tests which required pre-heating for steady state conditions were soaked at the target temperature for 15 minutes once reached to ensure uniform temperature throughout the specimens' cross-sections. Fifteen minutes was chosen as the soak time on the basis of tests in which a prestressing steel strand was heated to 500ºC while monitoring thermal expansion, and noting when all thermal expansion had ceased. Post test analysis using the digital image correlation processing algorithm allowed the total strain to be determined. Mechanical and thermal strains were then isolated and removed to estimate creep strain, ε_{cr}. Table 4.1(a-c) provides an overview of the more than 70 individual tests that were performed.

Prior to describing the results of the creep and mechanical response tests (Section 4.6) it is first necessary to validate the utilised non-contact DIC system used for measurement at high temperature (Section 4.5); This specific DIC technique using GeoPIV8 has never been used in this high temperature materials testing and therefore requires validation before application.

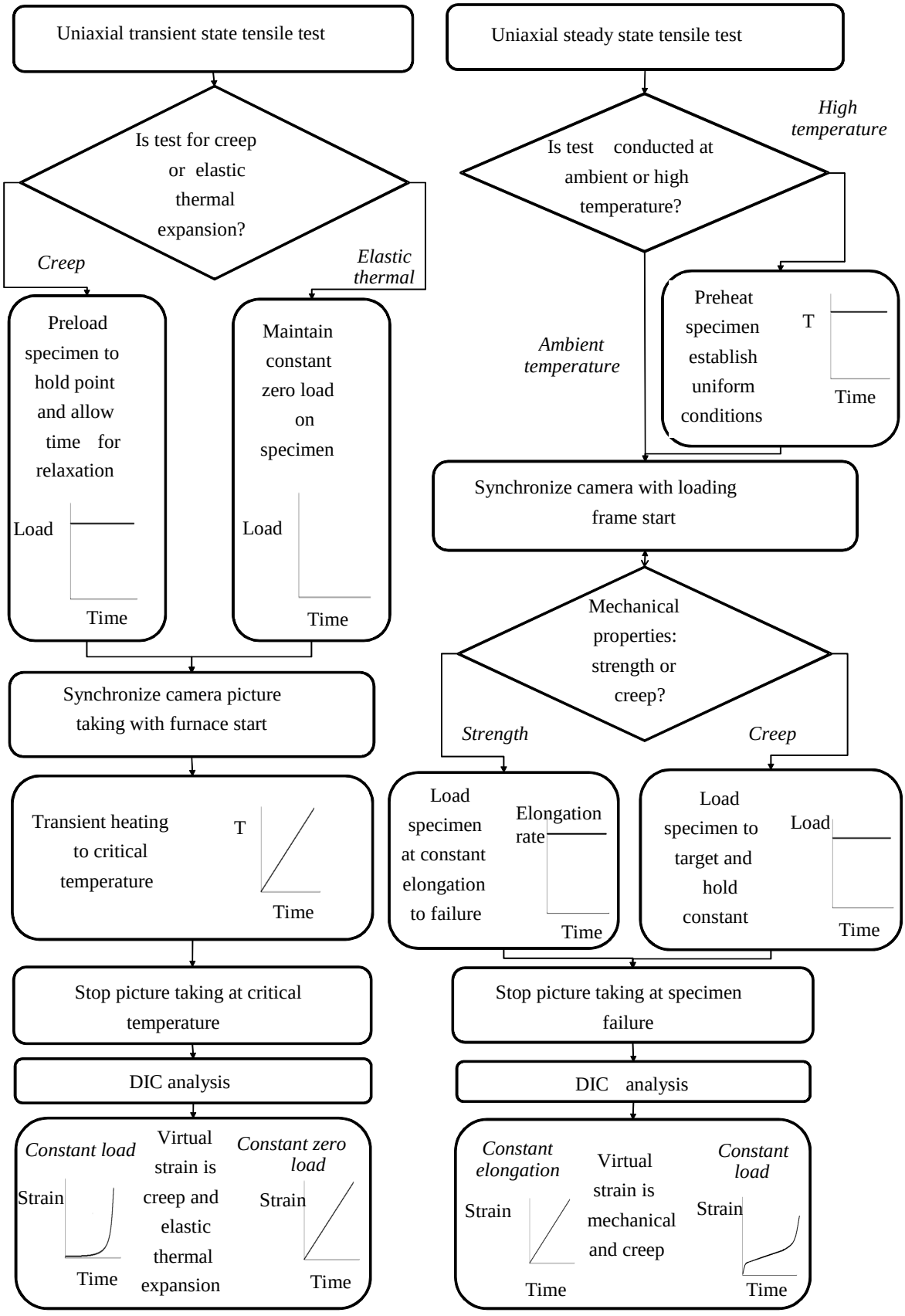

Figure 4.5: Experimental procedure for creep, strength, and thermal expansion tests.

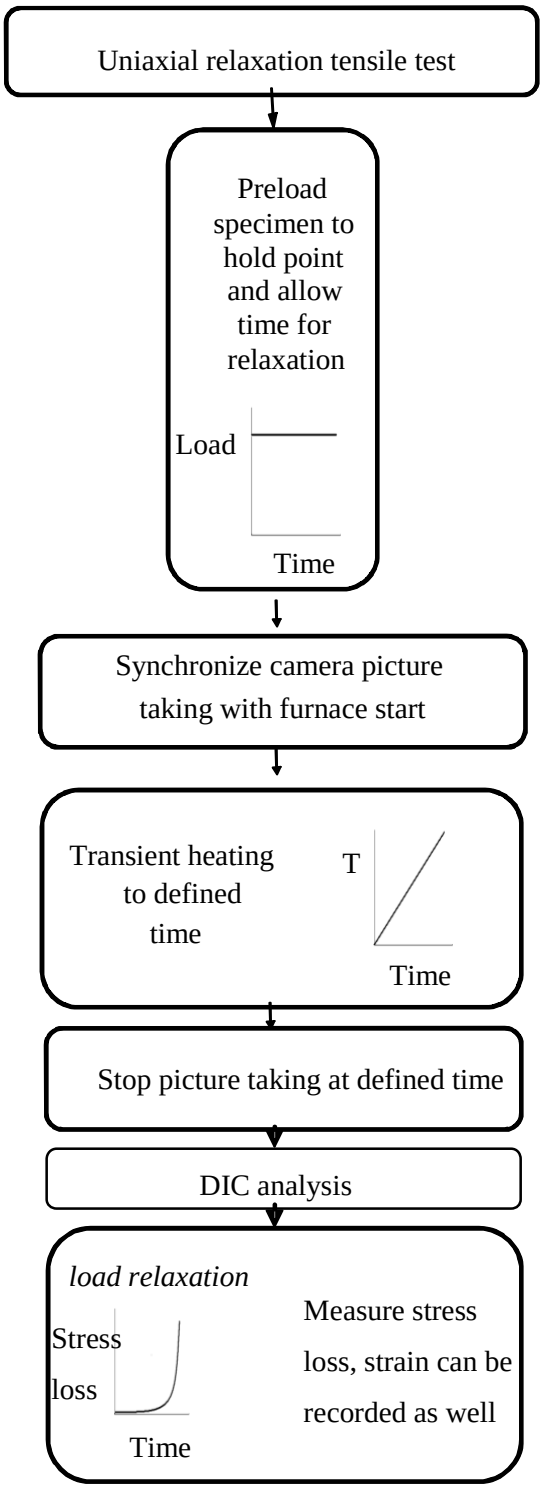

Figure 4.6: Experimental procedure for stress relaxation tests.

Table 4.1: Summary of test series

a) BS 5896-12

Test series	Test type	Target stress (MPa)	Target temperature (°C)	Loading (mm/min or °C/min)	# Tests
1a	SC	200	480	-	3
2a	SC	647	440	-	3
3a	SC	700	410	-	1
4a	SC	700	427	-	2
5a	SC	700	440	-	1
6a	SC	927	365	-	1
7a	SC	1115	365	-	1
8a	SC	1200	365	-	1
9a	TC	462	-	2	1
10a	TC	647	-	2	1
11a	TC	700	-	2	1
12a	TC	927	-	1	1
13a	TC	927	-	2	4
14a	TC	927	-	10	1
15a	TC	1020	-	2	1
16a	TC	1110	-	2	1
17a	TC	1294	-	2	1
18a	TC	1480	-	2	1
19a	TC	1664	-	2	1
20a	TE	0	500	10	3
21a	S	-	22-500	1, 2	17
22a	SR	1200	-	variable	2

b) ASTM 416-03

Test series	Test type	Target stress (MPa)	Target temperature (°C)	Loading (mm/min or °C/min)	# Tests
1b	SC	690	427	-	1
2b	TC	690	-	2	1
3b	TC	800	-	2	1
4b	TC	1000	-	2	2
5b	TC	1000	-	10	1
6b	CL	1000	-	-	1
7b	TE	0	500	10	2
8b	S	-	22,500	2	2

c) AS/NZS 4672 -07

Test series	Test type	Target stress (MPa)	Target temperature (°C)	Loading (mm/min or °C/min)	# Tests
1c	SC	700	427		2
2c	SC	700	440		1
3c	TC	700	-	2	1
4c	TC	1000	-	2	1
5c	TC	1200	-	2	1
6c	TE	0	500	10	1
7c	S	-	22-500	2	7

SC- Steady state creep, TC- Transient state creep, CL- Constant load, TE-thermal expansion, S- Strength, SR- Stress Relaxation

4.5 Digital image correlation for high temperature deformation measurement

A substantial challenge during high temperature materials testing is accurately measuring strains; however this is critical to determine the creep parameters described in Section 4.3. Strain in a uniaxial tensile test has traditionally been measured by either adhesively bonded foil gauges or by contact extensometers. Both of these types of instrumentation have limitations at ambient and particularly at high temperature. In an ambient uniaxial tensile test with prestressing steel rupture strain can be as high as 7% (CPCI, 2007) and at high temperature these strains can be even greater (Harmathy and Stanzak, 1970). At ambient temperature most conventional foil strain gauges can reliably measure strains only up to about 2% before debonding (Bisby and Take, 2009) plastic strain measurement with this technique is thus notoriously unreliable. Furthermore, strain gauging (especially for high temperature testing) is costly, since specialist gauges, wiring and adhesives are required for reliable measurement. High temperature ceramic arm extensometers are also available and have the advantage of being re-useable; however, it is difficult to accurately measure strains during both the elastic and plastic phases using a single device. Furthermore, contact extensometers can only measure strain along a predetermined gauge length, and hence the true rupture strain cannot be determined due to random occurrences of necking locations. Finally, contact extensometers are extremely delicate and can be badly damaged if they are not removed prior to failure, thus making Tertiary creep measurements risky or impossible.

The experiments described herein used DIC to measure deformation and strains of specimens at high temperature. Digital image correlation compares a sequence of high-resolution digital photographs using an image-processing (pixel tracking) algorithm, to determine the deformations of a specimen during a test. It is an economical, robust, and non-contact measurement method that can be used to measure strains up to and including failure. Furthermore, the technique allows the deformation and strain of any region of interest to be examined after the test; consequently the true rupture strain can be determined so long as the region of necking/failure is within the field of view of the camera. It must be noted that image processing techniques have been used prior to the results of these tests for describing deformation of materials. For example, Spyrou and Davison presented image

processing results of steel T-stub connections at high temperature using commercial hardware (2001).

The DIC technique applied for the current tests used an off-the-shelf high-resolution digital single lens reflex (SLR) camera. The test specimens were painted black with white speckle patter to give a random high contrast image texture (note that this is not the same technique as speckle pattern interferometry). The images were processed using GeoPIV8, a custom-coded image-processing algorithm that was previously developed by White et al (2003). The algorithm was used to track patches of pixels from one image to the next, by correlation of each image in the sequence with an image taken at the start of the test. It could thus be used to determine the deformation of any region of interest to be determined after testing; strains could then be determined by comparing the relative motion of two pixel patches. A typical painted sample and patch movement during subsequent photos is illustrated in Figure 4.7.

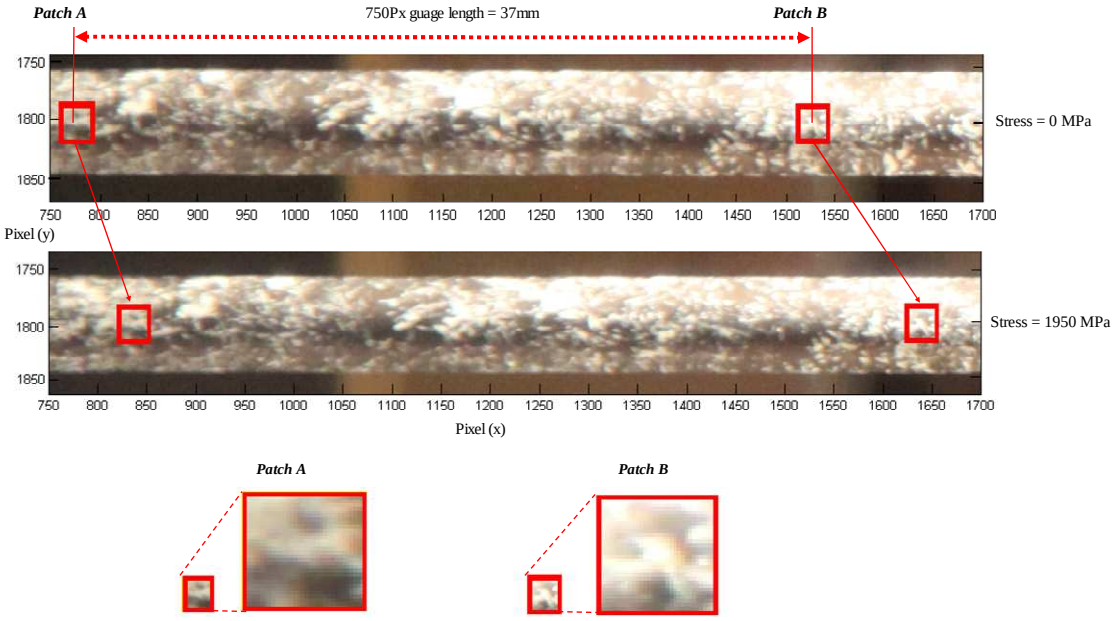

Figure 4.7: Contrast pattern used for strain calculation in DIC.

The GeoPIV8 image-processing algorithm has previously been validated for various civil engineering deformation and strain measurement applications at ambient temperature (Bisby and Take, 2009; White et al. 2003). The measurement accuracy is related to the image size, frame of view, camera resolution, user experience, and the gauge length that is chosen for strain calculations (Bisby and

Take, 2009). Previous validation of the image processing algorithm at ambient temperature has shown sub pixel accuracy better than 0.1 pixels (Px) (Bisby and Take, 2009; White et al., 2003).

The DIC method has not yet been comprehensively evaluated for high temperature strain measurement. At high temperature, DIC techniques may encounter errors due to emission of radiation from the surface of highly heated samples, specimen corrosion/oxidation, and convective heat hazes, etc (Grant et al., 2009). This section presents a validation of the DIC technique for high temperature measurement.

4.5.1 Method

The uniaxial tensile tests presented in this chapter were intended first to validate the use of DIC strain measurement at ambient and high temperatures for prestressing steel, and then to extract high temperature material properties for modern prestressing steel to improve the modelling of creep and stress relaxation (in Section 4.6). The validation tests were conducted on ASTM 416-03 (ASTM, 2003) Grade 1860 MPa prestressing steel.

A Canon EOS 5D Mark II (21 mega pixel image resolution) digital SLR camera was used to acquire images of the test specimens at a predefined rate of 0.2 Hz. This frequency means that failure was not precisely captured, with a temporal error of up to 5 seconds. This has no significant impact on the data presented in the current chapter. Images were taken for DIC strain measurement through a quartz window in the environmental chamber built within the testing space of the Instron 600LX materials testing frame (see Figure 4.3). The samples were lit from inside the environmental chamber to minimise glare on the window which would likely corrupt the strain measurement. The design of the environmental chamber, which re-circulating internal fans, helped to minimise optical effects due to convective hazes. Since the accuracy of the DIC algorithm can be dependent on image contrast, the specimens were painted with high temperature matt black paint and speckled with matt white paint. Conventional bonded electrical resistance foil strain gauges and a ceramic arm contact extensometer were also used to compare against and validate the DIC technique at both ambient and elevated temperatures.

4.5.2 Validation at ambient temperature

The deformations measured by the DIC technique in this chapter have a small and unavoidable numerical scatter of about 0.1 pixels (see White et al. (2003) for further details). Strain is measured from the relative movement of two pixel patches (see Figure 4.7) divided by the initial distance between the patches, and consequently the scatter in the calculated strain increases as the gauge length between the pixel patches is reduced. Thus, longer gauge lengths are preferred. However, longer gauge lengths do not allow variations in strain along the specimen to be measured. Two tests were conducted at ambient temperature to establish the optimal position of pixel patches for robust, repeatable tensile strain measurements.

An ambient strength test was performed at a constant crosshead displacement rate of 2 mm/min. The sample was tested in the environmental chamber even though the test was not heated to check that images could be acquired through the chamber's window. Standard 120 Ω foil strain gauges were bonded to the specimen at locations T3 and T5 (Figure 4.4), for comparison with conventional strain measurements.

The dimensions of the patch of pixels used by the image processing algorithm was set to 32 × 32 pixels, which has previously been demonstrated to achieve optimal tracking resolution while minimizing processing time (White et al., 2003); this represents a 'real' patch size of about 1.75 mm × 1.75 mm for the current tests. The DIC algorithm was used to calculate strains using various gauge lengths, which were always centred about pixel location 1150 (in Figure 4.7). Figure 4.8 shows the calculated strain versus time for gauge lengths of 30, 200, 500 and 1500 Px (1.5, 10, 25, and 75 mm respectively). The strains calculated using all of the gauge lengths follow the same linear trend, as expected for a constant crosshead displacement rate. Scatter was considerable for smaller gauge lengths, and good convergence to the expected linear trend ($R^2 > 0.99$) was achieved for gauge lengths larger than 200 Px. A gauge length of 750 Px was used for all subsequent analysis.

Figure 4.9 compares the DIC results obtained using a gauge length of 750 Px (37.5 mm) to those measured using the bonded foil strain gauges. It is clear that:

(1) there is negligible difference (<0.0008 strain) between the foil gauge and DIC measurements; and

(2) the foil gauges debonded below 2% strain and consequently failed to capture the full plastic range of the response, whereas the DIC technique was able to capture the plastic strains up to and including until failure.

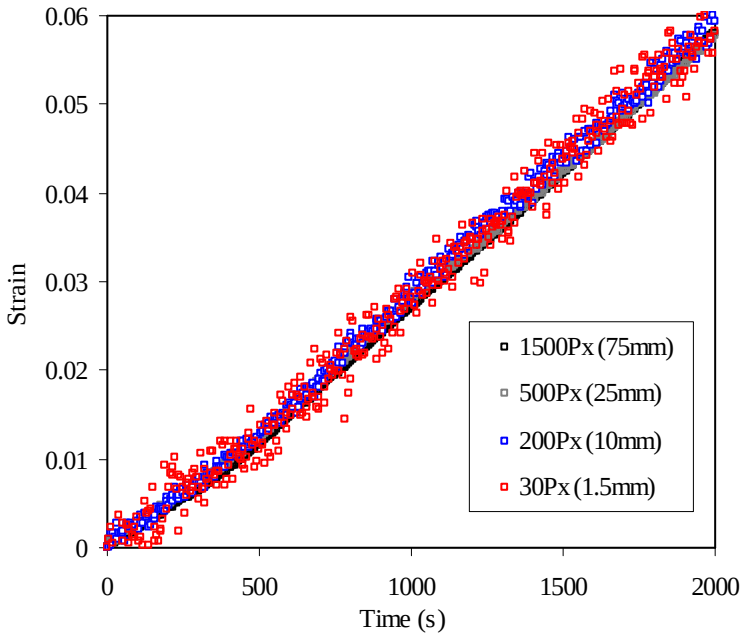

Figure 4.8: Gauge length convergence for ambient strength test of prestressing steel with DIC strain measurement.

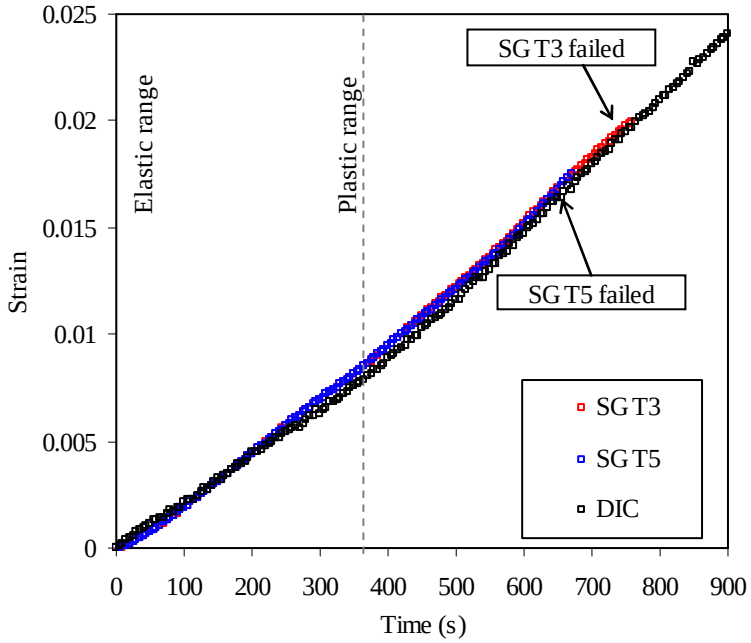

Figure 4.9: Comparison of the strain measured using bonded strain gauges and DIC for ambient strength test of prestressing steel.

The DIC technique thus has good measurement accuracy, and is able to record much higher strains than conventional strain instrumentation.

Creep tests involve measuring strain under sustained stress (more precisely under sustained load) and hence the second ambient temperature test was performed under a constant sustained stress of 1000 MPa to observe the static scatter in strain readings from DIC. The load was held for 3 hours, and strains were determined using DIC with a 200 Px gauge length. Despite being influenced by negligible (and expected) time-dependent relaxation effects on the strand, the scatter in strain measurement was negligible at approximately 0.0002 (or 0.02% strain). For all subsequent tensile tests in the current chapter, a gauge length of 750 Px (37.5 mm) minimum has been used, such that the strain measurements are expected to have a scatter of less than about 0.007% strain.

4.5.3 Validation at high temperature

Previous researchers have used unrestrained thermal expansion tests on steel alloys to evaluate the strains measured using DIC at high temperature as compared to the values due to unrestrained thermal expansion. Grant et al. (2009) conducted thermal expansion tests on a nickel-based alloy, primarily to study how high temperature surface emission interferes with DIC (generally of concern only for temperatures greater than about 500ºC). Results were recorded at 100ºC intervals, and (neglecting one isolated large error at 100ºC), the DIC technique was stated as being accurate to within 2% of the conventionally measured thermal expansion for their alloy using seven DIC measurements. Pan et al. (2001) conducted thermal expansion tests on a chromium-nickel austenite stainless steel alloy up to 1200ºC, with results presented at 50ºC intervals. Their results showed some differences compared to tabulated handbook values, which were attributed to using the new technique and to small differences in the alloy material used in their testing. Both sets of tests study high temperatures; however, very few DIC images were analysed, which can lead to errors, as observed in the tests by Grant et al. (2009). The work presented herein uses a much more rapid image acquisition rate, giving a larger pool of data that allow scatter to be evaluated and minimized.

The second part of the DIC validation testing involved two unrestrained thermal expansion tests on the ASTM 416-03 (ASTM, 2003) prestressing steel. The theoretical thermal expansion of prestressing steel is given by EN 1992-1-2 (CEN, 2004) as:

$$\varepsilon_t = -2.016\times10^{-4} + 10^{-5}\,T + 0.4\times10^{-8}\,T^2 \quad \text{for } 20^{o}\text{C} < T < 1200^{o}\text{C} \qquad [4.5]$$

Figure 4.10 and Figure 4.11 plot the strains measured using DIC during two unrestrained thermal expansion tests. The values predicted by Equation 4.5 are also included; these were calculated using the average of temperatures T1 and T2 measured during tests since these bounded in the strain measurement gauge length (Figure 4.4). The thermal strains measured using DIC matched the predicted values very closely (with less than 0.0003 strain difference).

A ceramic arm contact extensometer was also used, centred on Section T3 and with a gauge length of 25 mm. The extensometer results are also plotted in Figure 4.11, and also show good agreement with the DIC measurements (again with less than 0.0003 strain difference).

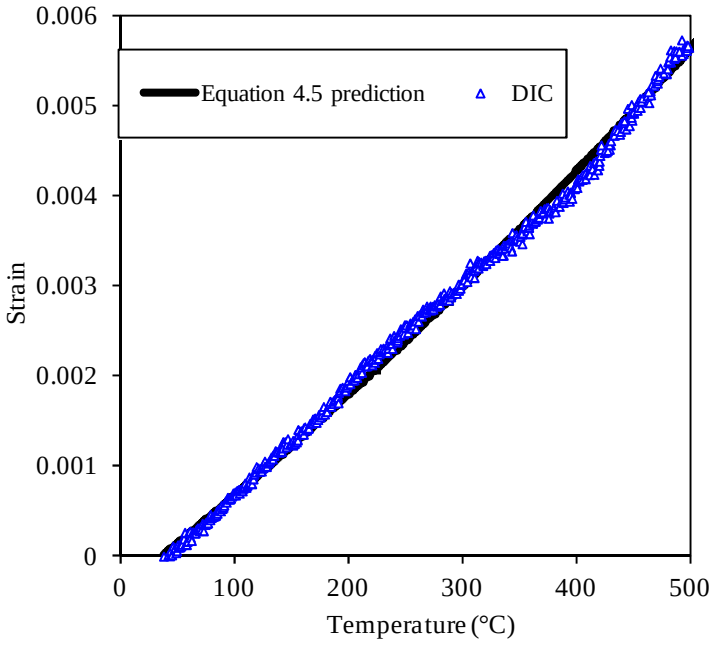

Figure 4.10: Validation of DIC strain measurement technique by comparison to EN 1992-1-2 (CEN, 2004) for thermal expansion of prestressing steel.

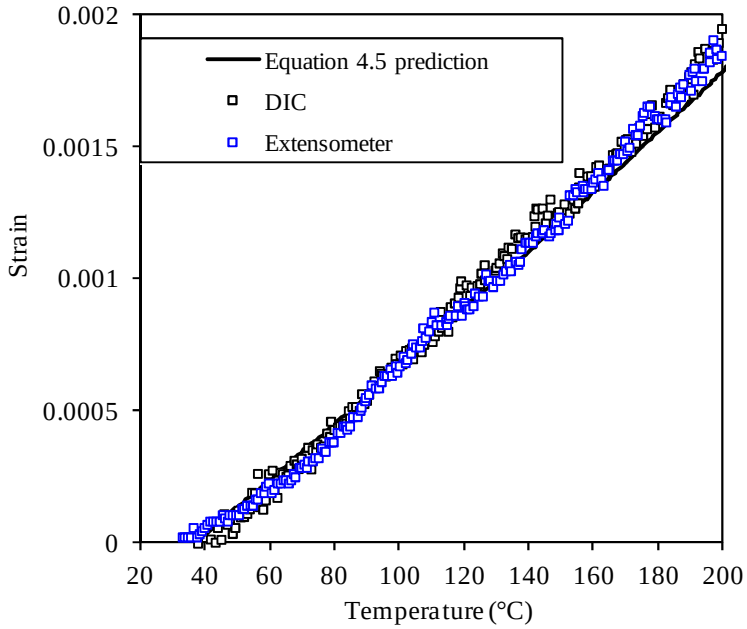

Figure 4.11: Validation of DIC strain measurement technique by comparison to extensometer and EN 1992-1-2 (CEN, 2004) for thermal expansion of prestressing steel.

4.5.4 Validation for cross-sectional area reduction measurements

Previous researchers have attempted to show that DIC techniques can be used to evaluate reductions in cross-sectional area that occur during necking, when deformation localises within the specimen before rupture (Zhao, 2009; Scheider et al., 2004). Indeed, Tertiary creep may be influenced by necking since straining rate increases exponentially under sustained load in a creep test, and hence reduction trends in cross-sectional area are important for understanding creep failure in prestressing steel tendons at both ambient and elevated temperature. The final evaluation test aimed to establish whether DIC can be used to determine the reduction in cross-sectional area that occurs during necking, and hence to measure true stress versus strain (rather than simply engineering stress versus strain).

DIC was used to examine the reductions in tendon diameter (and thus the cross-sectional area) during the ambient strength test and an additional strength test conducted at a steady-state temperature of 500ºC. Both tests used the same extension rate (i.e. 2 mm/min). Two pixel patches were defined in the initial reference image, on opposite sides of the specimen. The relative deformation of these patches perpendicular to the tendon was used to find the reduction in cross-sectional area of the tendon (assuming axisymmetric necking). The initial diameter of the core

prestressing wire used in these tests was 4.40 mm, so the gauge length was limited to less than 88 Px and significant scatter in the DIC strain results was unavoidable.

Figure 4.12 plots the cross-sectional area measured during the ambient strength test, compared to the theoretical reduction in cross-sectional area of the prestressing steel wire, calculated from the longitudinal strain assuming a Poisson's ratio of 0.3. Necking occurred outside the field of view of the images recorded during the ambient strength of the ASTM A416-03 (2003) prestressing steel and therefore it is not captured in Figure 4.12 which relates to a position between points T1 and T2. There is considerable scatter in the DIC data; however, the method compares well with the theoretical prediction during the elastic phase. The larger reduction in measured cross-sectional area compared to the prediction based on a constant Poisson's ratio is also expected, since Poisson's ratio is known to change at strains above yield (Davis, 2004).

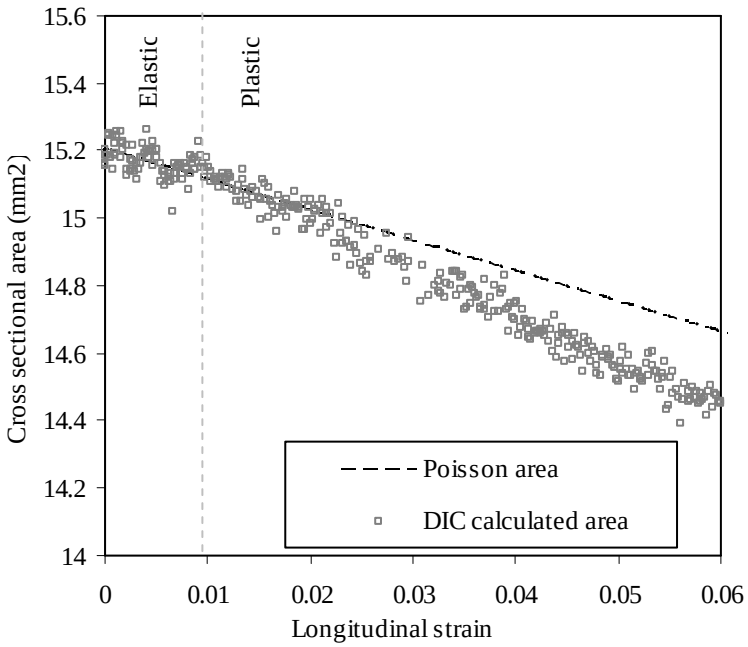

Figure 4.12: Cross-sectional area reduction measured using DIC during for ambient strength test of prestressing steel.

Figure 4.13 compares stress-strain curves using engineering stress (calculated using the original cross-sectional area) and true stress (calculated using the actual measured cross-sectional area). For the ambient strength test, the curve is terminated just beyond the peak stress point, because necking was not captured and hence the true stress cannot be estimated. Necking did, however, occur within the field of view

of the images during the high temperature test, between locations T1 and T2 in Figure 4.4. The true stress-strain curve shows runaway necking behaviour just prior to failure (as can be visually observed during most tensile tests of steel bars).

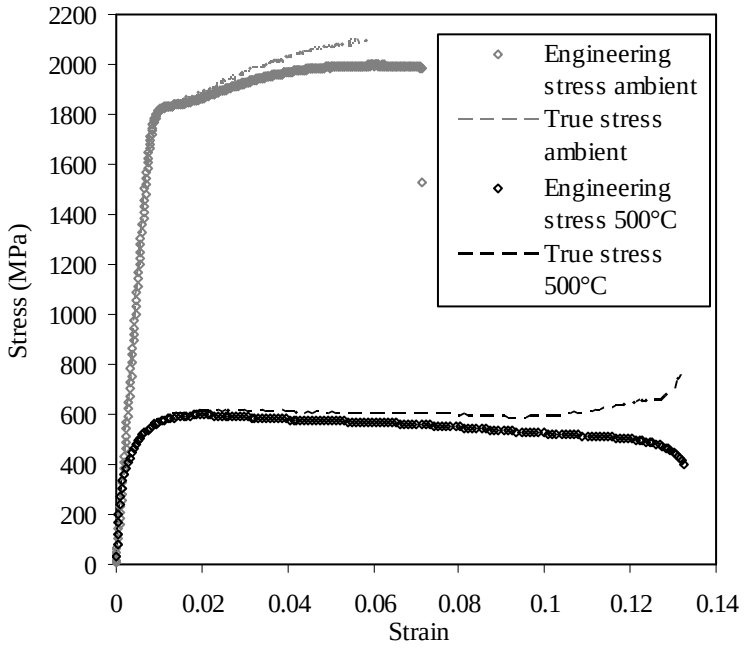

Figure 4.13 Stress strain curves from strength tests on ASTM 416-03 (ASTM, 2003) prestressing steel.

These results suggest that the DIC measurement technique descried herein is capable of capturing the area reduction trends experienced during high temperature uniaxial tests, without any test interruption as would occur with traditional area reduction test observations (such as laser photogrammetry, or the engraving/drawing of local grids) (Zhao et al., 2009; Jeschke et al., 2011). These observations are significant because the DIC technique allows true numerical validation of theoretical area reduction models at high temperature (Ling, 1996; Giroux, 2010). Specifically for the current chapter, it allows the onset of necking trends and their relationship to Tertiary creep strains to be investigated at high temperature, as shown in Section 4.6.

4.5.5 Validation of DIC for rupture strain measurement

As already mentioned, a steady-state high temperature strength test (uniformly heated at 500ºC) was performed for validation purposes. Harmathy and Stanzak (1970) have shown that the rupture strain of prestressing steel during a steady-state strength test increases with temperature. Figure 4.13 plots the stress versus strain

responses for both the aforementioned ambient and high temperature strength tests. Approximately, 13% rupture strain was recorded at high temperature, while for ambient temperature the value was 7%, in agreement with Harmathy and Stanzak's observations. Also already noted, in the ambient strength test the actual region of localised necking occurred outside the field of view of the camera; however, the strain observed outside the region of necking corresponded to the expected value for prestressing steel and indicated the expected trends (CPCI, 2007). Being able to measure strains up until failure is crucial, since the full creep curve must be analyzed to identify the Primary and Secondary creep variables discussed in Section 4.3 and to be able to rationally predict tendon rupture, particularly under localised heating at elevated temperature.

4.6 High temperature strain characterization for prestressing steel

The calibration and validation tests described for DIC in the previous section demonstrate that this approach can be used to accurately measure deformation at high temperature. Using the creep theory described in Section 4.3, DIC is used in the following sections to determine high temperature creep deformation trends and material input parameters (Q, Z, $\varepsilon_{cr,o}$) for modelling modern (BS 5896-12 (BSi, 2012)) prestressing steel. Other prestressing steels are considered for comparative purposes in Section 4.7.

4.6.1 Separating creep strain from total strain

A steady-state creep test can take many hours (or days) to complete and is difficult to repeat. The specimen is first heated to the chosen steady temperature, after which the specimen is loaded to the required constant load (stress). Both temperature and load are then held constant for the remainder of the test. This test sequence makes it difficult to accurately separate the mechanical from the creep strains (Purkiss, 2008; Holdsworth, 2010). Because creep strain can occur during the loading process, the true amount of creep that occurs might be poorly estimated.

A transient creep test is loaded prior to heating and hence the mechanical strain can be approximately determined. The load is then held constant whilst the temperature is increased, so that the creep strain can be determined by subtracting the

strain that occurs due to thermal expansion as well as the additional mechanical strains which occur due to reductions in elastic modulus of the steel on heating.

The distinction between creep strain and mechanical plastic strain (i.e. yielding) breaks down at elevated temperature. As the temperature of the steel increases and its yield strength and elastic modulus decrease, yielding and creep deformation become intertwined and the classical definitions of these strains lose meaning.

In the current work creep strain was approximated by separation of thermal and mechanical (elastic and plastic) strains. The thermal strain is relatively easily predicted by an unloaded transient test (see Figure 4.5). When comparing an unloaded thermal relaxation test of BS 5896-12 (BSi, 2012) prestressing steel against the predictions of BS EN 1992-1-2 (CEN, 2004) (Equation 4.5), it was found that negligible 0.13% strain difference was observed at 500ºC. Therefore it is assumed that Equation 4.5 can be used to isolate creep strains. Plastic strains can be approximately accounted for by calculating the additional mechanical strain occurring due to reductions in elastic modulus during each five second interval during heating, based on the measured increase in temperature during each interval, and then subtracting this strain value from the overall observed strain which occurred during that same interval (i.e. accumulating these plastic strains during the heating exposure). EN 1992-1-2's (CEN, 2004) equations for reduction in elastic modulus were used to perform these adjustments. It should be noted that these equations implicitly include the creep effects observed during the tests upon which they were developed. These equations were used due to a limited data pool available to justifiably propose a new model for this behaviour which would be temperature rate independent. Additional research is clearly needed to understand the interrelationships between yielding and creep as temperature increases (Section 4.6.4 begins to consider this behaviour).

4.6.2 Steady state and transient creep tests

The concept of temperature-compensated time, θ, and associated creep theory was introduced in Section 4.3. Harmathy (1967) suggests that the same creep curve (ε_{cr}

versus θ) can be obtained using either a transient or a steady-state thermal regime uniaxial creep test at constant load.

As described in sections 4.3 and 4.4, creep parameters can be extracted from the ε_{cr} versus θ curve produced from a creep test. Transient creep tests can better represent the conditions in a real fire and, given that these tests can be performed relatively quickly, creep parameters at constant loads for structural steels can be produced using a limited number of such tests. To the author's knowledge, parameters from transient state creep tests have not previously been derived for prestressing steel.

Activation energy for creep

To plot ε_{cr} versus θ correctly, Q in Equation 4.4 must first be determined. This requires careful measurement of creep strains under various stress and temperature conditions. Activation energy for creep, Q, is physically the energy needed to provoke movement of atoms (dislocation and/or slip of the grain structure of the steel) from one stable state to a new one. The value of Q has real physical meaning although it can easily be mistaken as simply an empirical correction factor; treating it in this way will produce erroneous ε_{cr} versus θ plots which may appear to be correct, exhibiting all three phases of creep, but which are fundamentally flawed as illustrated below. Section 4.3.2 described how tests can be performed to calculate Q. Both methods described were used to calculate Q for the BS 5896-12 (BSi, 2012) prestressing steel tested herein, and all methods yielded similar results.

Four creep tests at steady state temperatures were performed at 410ºC, 427ºC (repeated for verification), and 440ºC, all at the same load (equivalent to a stress of 700 MPa). Figure 4.14 illustrates the creep strain with respect to time data taken from three of these tests. Immediately it can be observed that the slope of the Secondary phase appears to increase with increasing temperature, showing that the minimum creep rate (Z) increases with increasing temperature. Taking the minimum creep rate with respect to time for temperatures 410ºC, 427ºC and 440ºC and applying Equation 4.4, gives Q as 37200K with an R^2 = 1.00. Figure 4.15 is constructed using a Q of 37200K, and shows that the three creep tests converge to a single curve. If an arbitrary Q is used (say 20000K as an example) the creep tests

diverge as shown in Figure 4.16. The above comparison illustrates that caution must be taken to develop the appropriate Q for plotting creep strain with θ; otherwise when using an inappropriate Q the creep data for different creep tests at the same load will not coincide with each other.

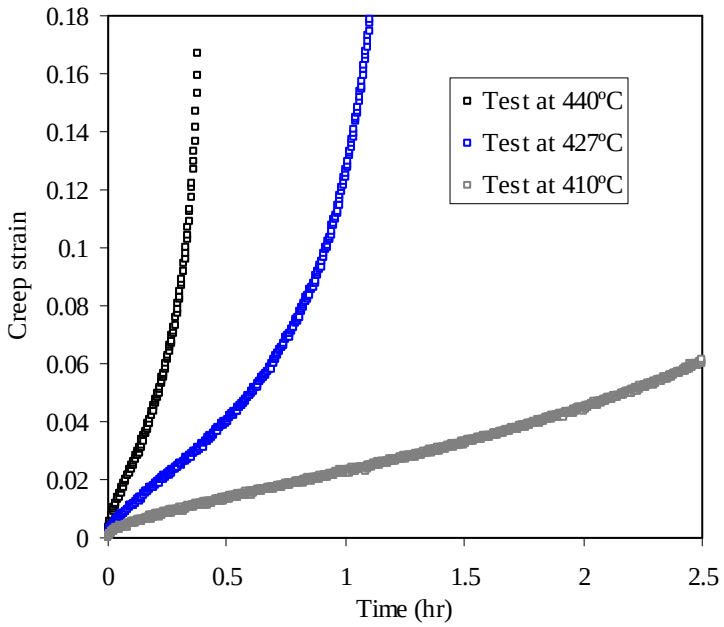

Figure 4.14: Steady state creep tests with respect to time at a stress level of 700 MPa for BS 5896-12 (BSi, 2012) prestressing steel.

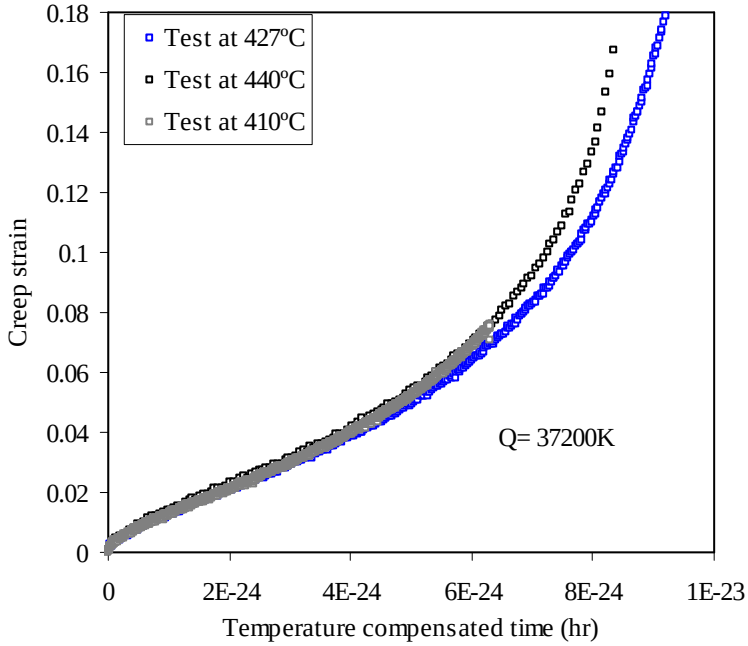

Figure 4.15: Steady state creep tests with respect to temperature compensated time at 700 MPa for BS 5896-12 (BSi, 2012) prestressing steel.

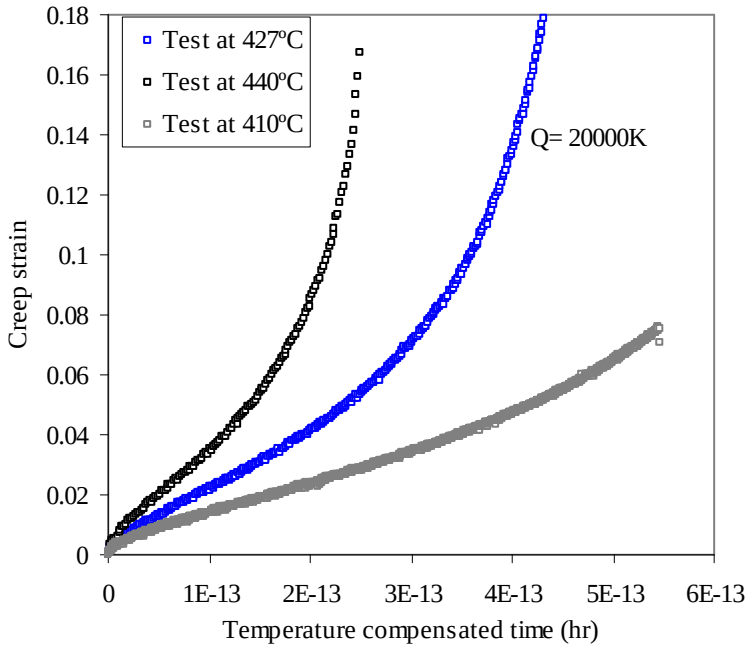

Figure 4.16: Steady state creep tests with respect to temperature compensated time at 700 MPa for BS 5896-12 (BSi, 2012) prestressing steel using an arbitrary activation energy.

A verification exercise was also performed using a series of transient creep tests, each using a different heating rate (1ºC/min to 10ºC/min) and a load level of 927 MPa. Figure 4.17 illustrates the time versus creep strain plots, showing that as the heating rate increases the time to failure decreases.

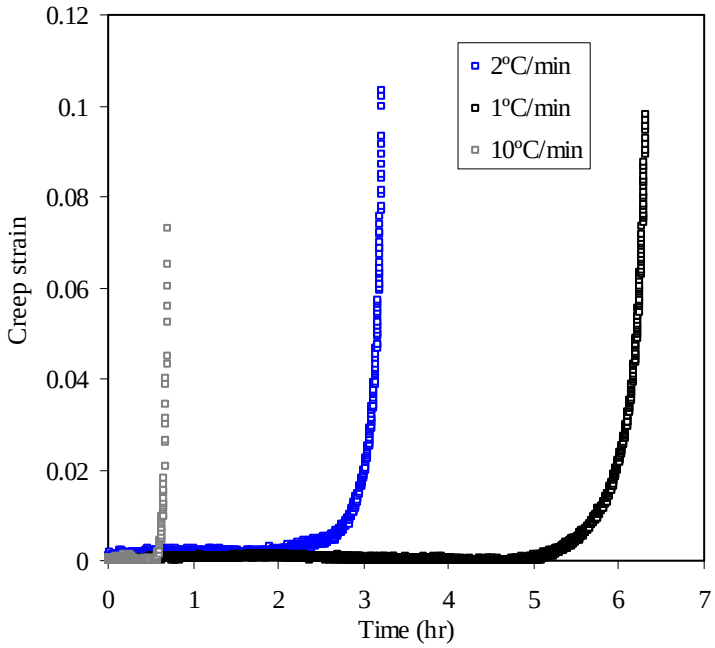

Figure 4.17: Transient creep tests plotted with respect to time for BS 5896-12 (BSi, 2012) prestressing steel at 927 MPa at different heating rates.

The trends observed in Figure 4.17 do not resemble the trends observed in the steady state test (Figure 4.14). However, when plotted versus θ (calculated using Q = 37200K) the curves coincide (Figure 4.18). If one uses an arbitrary Q (again say 20000K) to plot the creep curves they again diverge (Figure 4.19). Therefore, providing Q is estimated correctly, a lumped temperature-time coefficient (θ) will yield similar creep test results at the same loading level for either steady state or transient tests, regardless of the temperatures or the heating rate used.

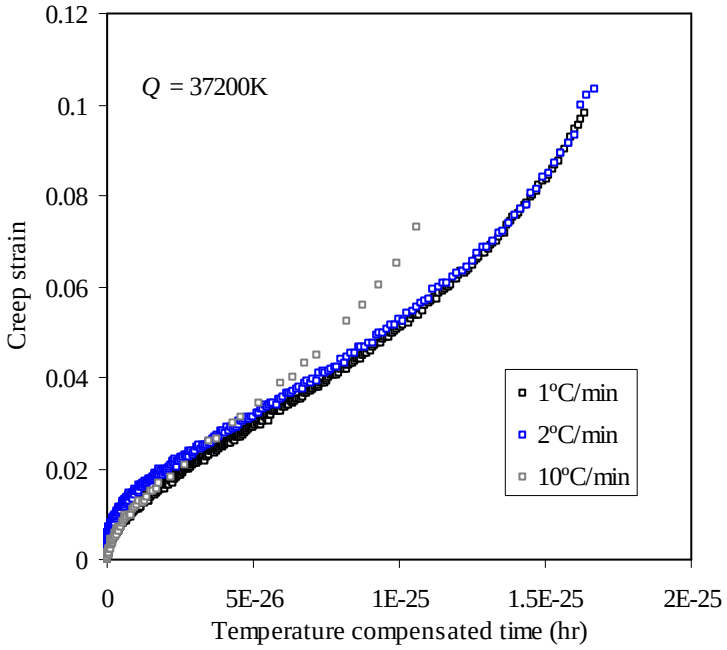

Figure 4.18: Transient creep tests plotted with respect to temperature compensated time for BS 5896-12 (BSi, 2012) prestressing steel at 927 MPa at different heating rates.

It is noteworthy that since Q is highly dependent on the microstructure of steel it can presumably also change with temperature. However, the author has found that within the tested stress and temperature ranges used herein the derived creep parameters appear to satisfy modelling efforts used for validation. Furthermore, since the available codes restrict the stress ranges in which prestressing steels can be used in service, only creep tests within this range (<500ºC and <1300 MPa stress) are considered in further detail.

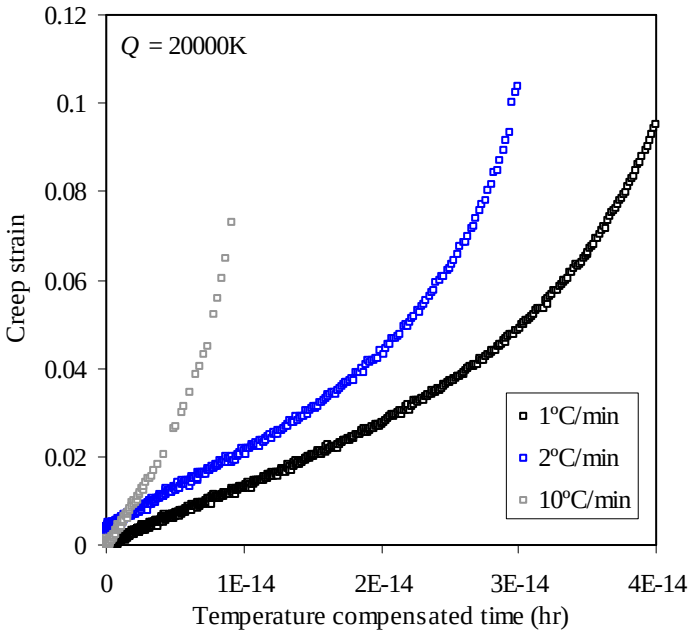

Figure 4.19: Transient state creep tests plotted with respect to temperature compensated time at 927 MPa for BS 5896-12 (BSi, 2012) prestressing steel using an arbitrary activation energy for creep.

It is the author's opinion that the data set used to define Q should be expanded to determine the sensitivity of the values extrapolated from tests. Considering the inherent error in DIC; however, the above estimation of Q appears satisfactory for the purposes of further discussion herein.

Equivalency

A comparison between transient and steady state creep tests at two different load levels is given in Figure 4.20. The temperature for the steady state tests was 440ºC whereas in the transient test the heating rate was 2ºC/min. The creep curves at the same loading level exhibit all three characteristics of Primary, Secondary and Tertiary creep, as well as having similar magnitudes with respect to time. These tests also illustrate that the slope of the creep curve naturally increases with load for both steady and transient test conditions, which reinforces the hypothesis that transient and steady state creep tests can both be used to give similar creep deformation results for prestressing steel.

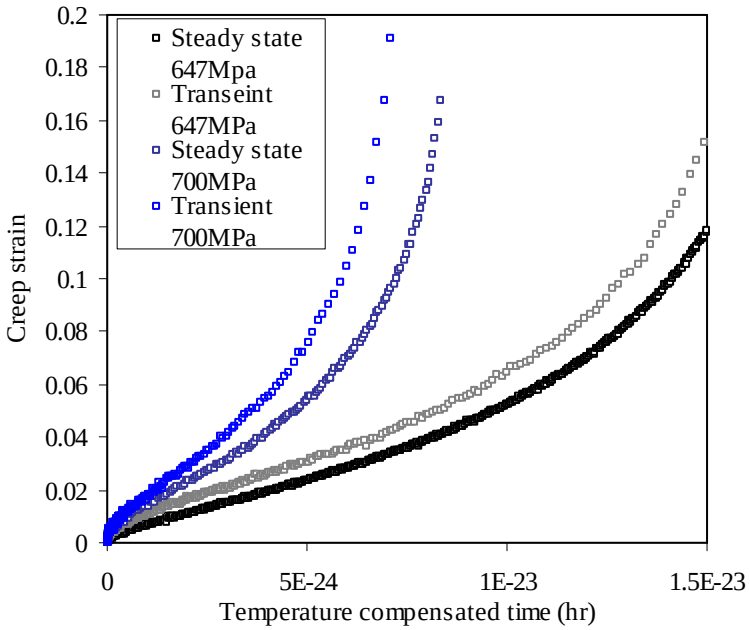

Figure 4.20: Equivalent steady state and transient creep tests at different loading conditions for BS 5896-12 (BSi, 2012) prestressing steel.

Repeatability

Two sets of creep tests were performed to investigate the repeatability of both the steady and transient creep tests. To examine repeatability of testing, four transient creep tests were performed at a sustained stress level of 927 MPa and heating at 2ºC/min. Results are given in Figure 4.21. Although the individual tests exhibit some variability (a derived Z of 4.62 ± 0.54 × 10^{23} hrs^{-1}) from one to another, and the computed Z parameters were different to a small degree, all curves lie within an envelope which is defined by the stated accuracy of the K-Type thermocouples used for specimen temperature measurements (i.e. the greater of ±2.2ºC or ±0.0075T, where T is measured in ºC). This envelope was created using the measured creep strain from Test 1 (Figure 4.21), and offsetting the temperature used for Equation 4.1 from the measured data by the amount of the potential temperature measurement error. The same procedure was performed for a set of steady state creep tests. Three tests were repeated at a constant stress of 647 MPa and a temperature of 440ºC. The results are presented in Figure 4.22. For steady state tests the thermocouple error no longer increases as the temperature increases, rather it remains constant throughout the tests. As expected, the steady state tests exhibited some variability (Z = 4.75 ± 0.75 × 10^{21} hrs^{-1}) but in general they also appeared to be reasonably repeatable.

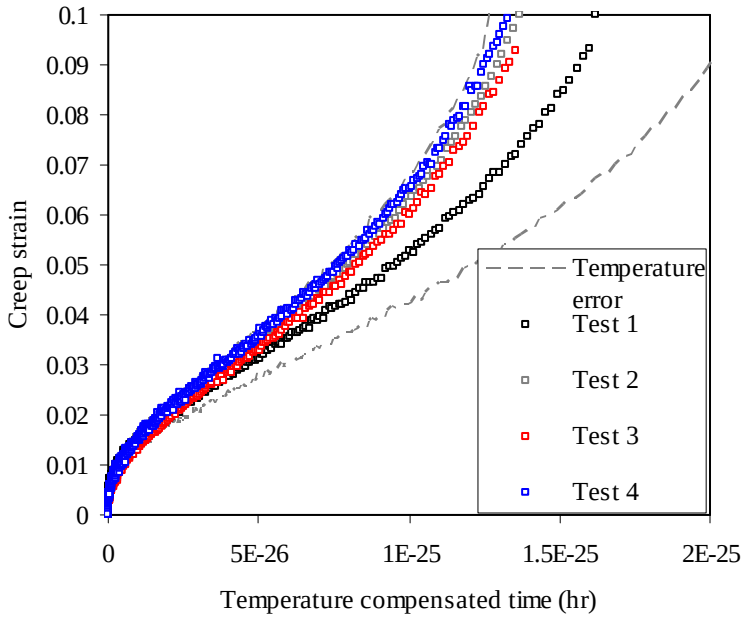

Figure 4.21 Transient creep tests repeated at 927 MPa at 2ºC/min for BS 5896-12 (BSi, 2012) prestressing steel.

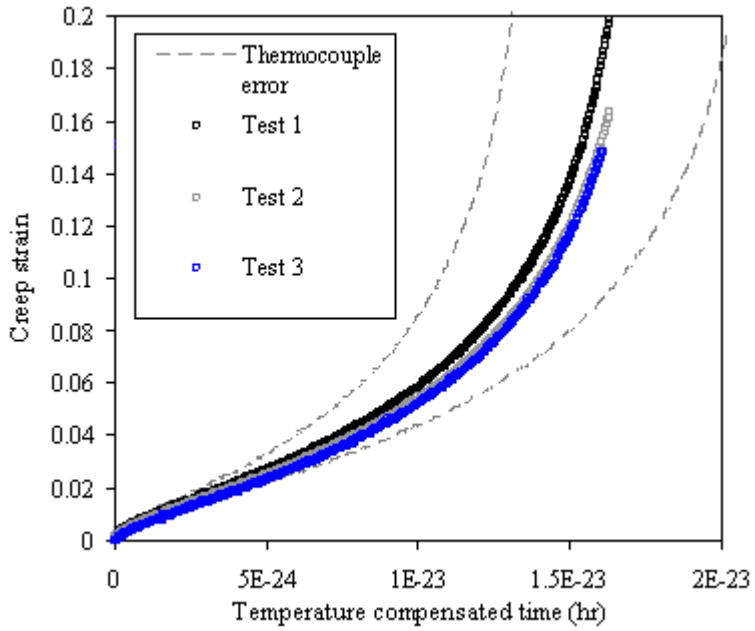

Figure 4.22 Steady state creep tests at 647 MPa at 400ºC for BS 5896-12 (BSi, 2012) prestressing steel.

The two repeat series demonstrate that the variability in creep tests can potentially be due to the error accuracy of temperature measurement. They also demonstrate that both transient and steady-state creep tests should be repeatable. Future tests could use thermocouples with better accuracy to confirm this. As a consequence of the results illustrated in this and previous sections, and considering

the time savings that result from using transient tests, this thesis makes more use of transient tests rather than steady state.

4.6.3 Creep parameters

Table 4.1(a) summarizes all test conditions used to characterize BS-5896-12 (BSi, 2012) prestressing steel's high temperature material response. As already noted some test series' purposes were to develop *Q* parameters (while considering the effect of different transient heating results), to compare steady and transient test results, and, in the case of this section, to characterize the prestressing steel over a range of credible in-service stresses. Creep tests were performed at stress levels between 200 MPa and 1664 MPa at temperatures below 500ºC. It would be unlikely that this steel would be used at stress levels above 1300 MPa in practice. Expressions were then fitted to the data to describe the variation in the creep parameters with applied stress, σ. The new expressions for the creep parameters for BS 5896-12 (BSi, 2012) prestressing steel are:

$$Z = ae^{b\sigma} = 1.02x10^{16} e^{0.019\sigma} \qquad 687 \text{ MPa} < \sigma < 1300 \text{ MPa} \qquad [4.6a]$$

$$Z = 0.7x10^{8}\sigma^{5} \qquad 200 \text{ MPa} < \sigma < 687 \text{ MPa} \qquad [4.6b]$$

$$\varepsilon_{cr,0} = c\sigma^{d} = 1.072x10^{-7}\sigma^{1.645} \qquad [4.6c]$$

where the units of σ are MPa and Z are in hrs^{-1}. Equations 4.6(a-c) take the same form as suggested for Z, and $\varepsilon_{cr,o}$ by Harmathy and Stanzak (1970), but with different values for the empirical constants (*a*, *b*, *c*, and *d*). The coefficients were defined based on non-linear least-squares best fits to the data. These equations are strictly only valid with Q = 37200K and for the stated stress ranges for this particular batch of prestressing steel. The equations illustrate that as the stress level increases so too does the Secondary creep rate, as should be expected. The primary creep variable was derived from very poorly reproducible (but small) values. Both steady state and transient tests were used to construct these equations. Figures 4.23(a) and 4.23(b) illustrate the raw data used for Equation 4.6, with the corresponding equations overlaid.

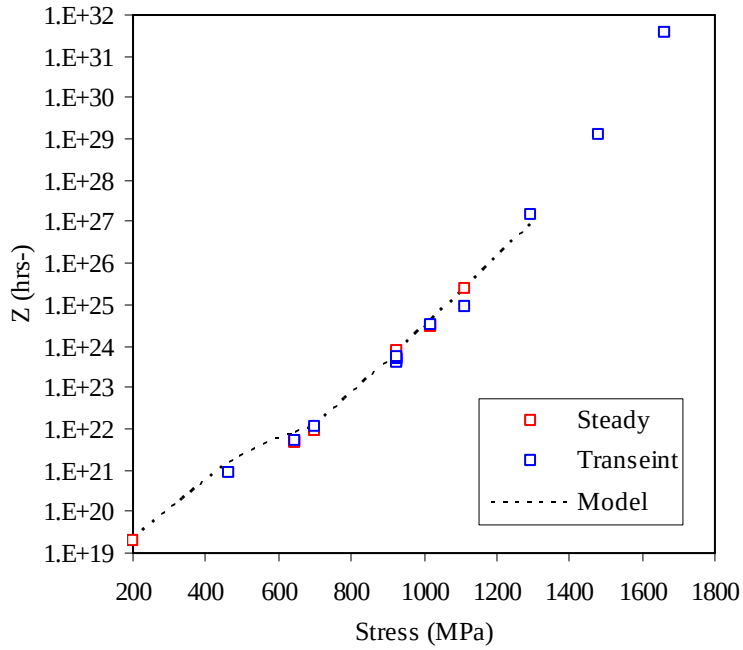

(a)

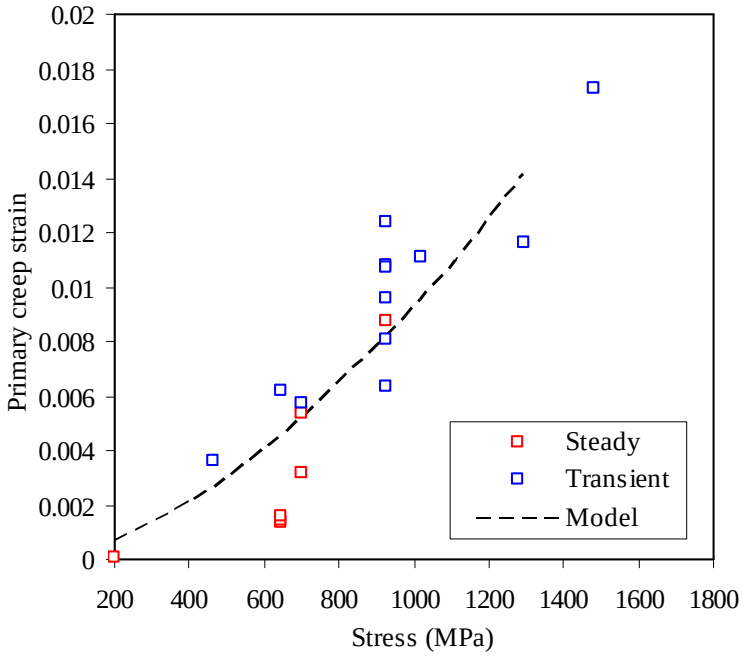

(b)

Figure 4.23: Creep parameters values and Equation 4.6 predictions for BS 5896-12 (BSi, 2012) prestressing steel (a) Z (b) $\varepsilon_{cr,o.}$.

4.6.4 Creep equation validity

Harmathy (1967) presents two (largely) empirically based equations in his work on creep of prestressing steel. Initially, Harmathy promoted the use of Equation 4.2 over Equation 4.3 in his early creep modelling work. However in his later work

(Harmathy, 1986), he returned to Equation 4.2, stating that "*(creep at high temperature) can be satisfactorily described by (it).*" Furthermore this equation has been used for modelling of other structural steels (see Purkiss, 2008).

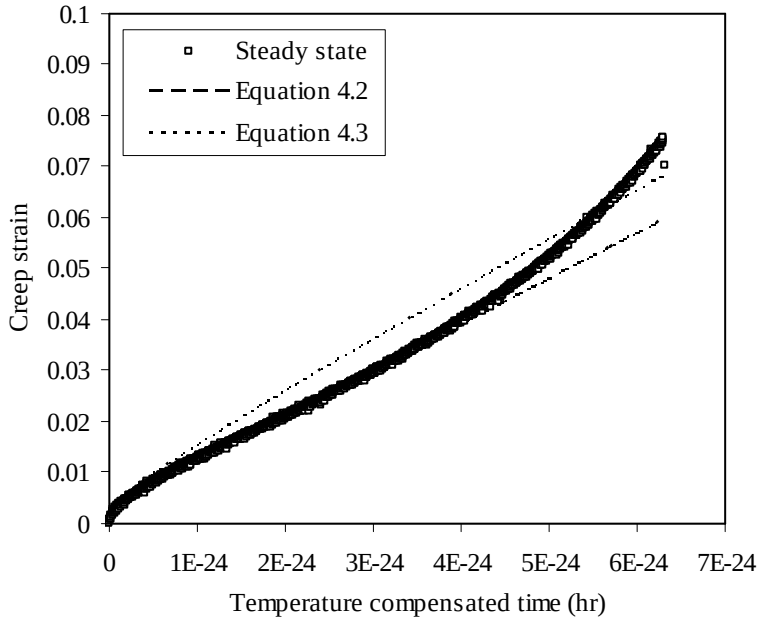

(a)

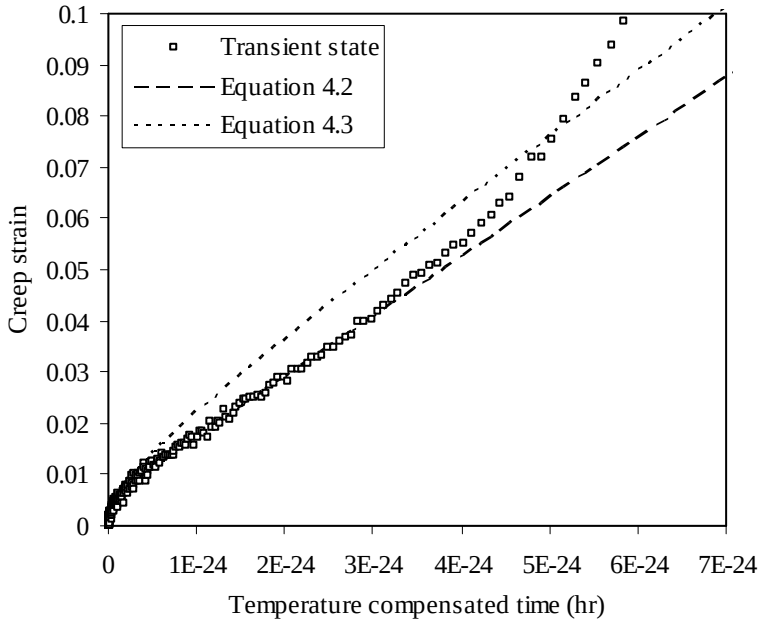

(b)

Figure 4.24: Choice of creep equation for creep prediction for BS 5896-12 (BSi, 2012) prestressing steel.

However, it is necessary to compare the estimations provided by both of these equations to settle any dispute in choosing the appropriate form of creep equation.

Figures 4.24(a) and 4.24(b) give comparisons of both transient and steady state tests at a stress level of 700 MPa.

Equations 4.2 and 4.3 are both used in conjunction with the material parameters provided in Section 4.6.3 to estimate the creep behaviour. Creep is overestimated significantly by Equation 4.3, whereas Equation 4.2 shows a good correlation with the test data for both tests types. In all cases in the current work Equation 4.2 has provided better estimation of creep as compared with Equation 4.3 which consistently overpredicts the amount of creep in the modern prestressing steels tested.

4.6.5 Specimen failure at high temperature

Figure 4.24 illustrates that Harmathy's creep equations (4.2 and 4.3) do not predict the Tertiary phase, as expected. This section investigates both the creep and mechanical failures observed in the author's tests at high temperature.

Tertiary creep behaviour

Equation 4.2 only predicts the Primary and Secondary creep phases; it does not consider the Tertiary creep phase that ultimately leads to failure. This equation assumes that knowledge of the creep developed during the secondary phase is sufficient to define failure, and neglects the Tertiary phase (Harmathy, 1970; Williams-Leir, 1983). Tertiary creep is commonly defined as starting when a specimen begins to 'rapidly' deform, leading to runaway failure. Revisiting Figure 4.1, which is based on a real creep test of prestressing steel but with magnitudes removed, the cross-sectional area reduction can be calculated using the DIC technique, since necking appears within the gauge length in the camera's field of view. The reduction in cross-sectional area for this figure was determined (as described in Section 4.4) at the precise position of necking and at a point arbitrarily chosen away from the position of necking.

Figure 4.1 shows both the creep strain curve (ε_{cr} versus θ) and the cross-sectional area reduction at these two positions. This figure demonstrates that Tertiary creep is closely associated with necking of the specimen; the cross-sectional area responses are coincident at the two positions along the specimen during the Primary

and Secondary creep phases, but they diverge during the Tertiary phase, where the creep curve cannot be modelled by Equation 4.2. At this stage the creep rate reaches its minimum value and then steadily accelerates during the Tertiary phase in tandem with evidence of necking. The Tertiary creep curve is consequently dependent not only on material properties, but also upon geometry changes. Indeed, it may be that Tertiary creep in prestressing steel (and possibly in other materials) is simply the engineering strain manifestation of necking. Figure 4.1 demonstrates that the DIC technique can capture the boundary between the Secondary and Tertiary creep phases; however, there is considerable scatter in the data due to the short gauge lengths which were necessarily used, which prevents necking in the tertiary phase from being measured accurately.

It is hypothesized however that by using the reduced cross-sectional area, Equation 4.2 could compensate to account for measured area reduction; and therefore true stress. Two BS 5896-12 (BSi, 2012) prestressing steel creep test examples are used for comparison. The first test is a steady state test performed at 647 MPa and 440ºC. Equation 4.2 was extrapolated with the appropriate Z, and $\varepsilon_{cr,o}$ parameters (which would be applicable for true stress). Figure 4.25 shows both the area reduction measured in the test and the true stress compensated creep curve, as well as the prediction without compensation. It can be observed that Equation 4.2 can subsequently predict close to the correct strain providing the true stress is estimated correctly, *a posteriori*.

A second more complicated transient test can also be considered. This presents additional complexity, as in this case thermal dilation effects are present which should also be separated. Since significant scatter was present in the DIC technique for measuring small gauge lengths the dilation is difficult to quantify with current DIC tools. For the time being the dilation is ignored. Figure 4.26 illustrates the predicted responses; again the model matches the trends, however with some scatter.

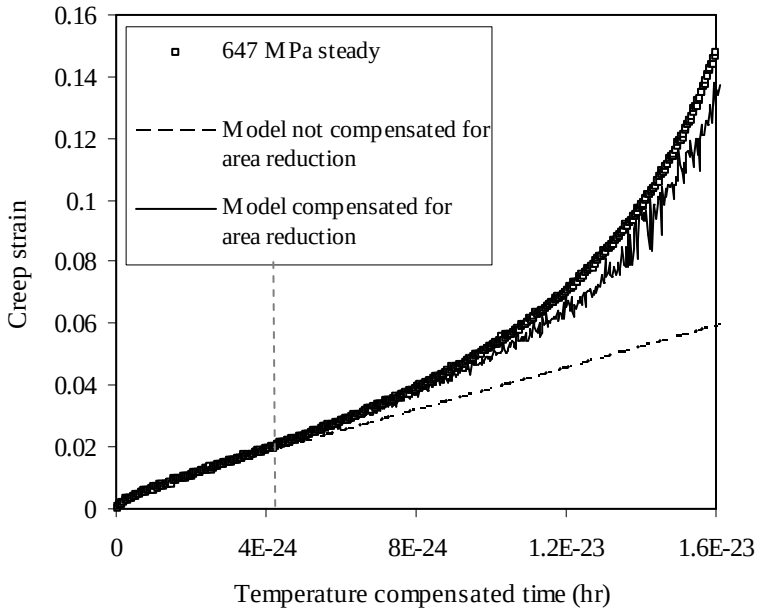

(a)

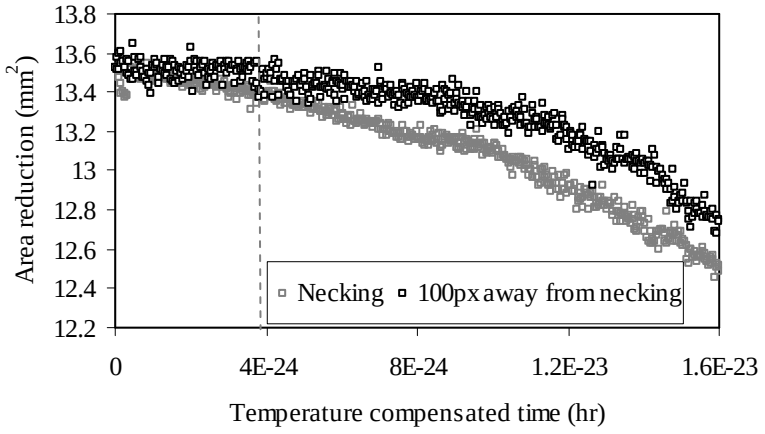

(b)

Figure 4.25: Steady state creep test of for BS 5896-12 (BSi, 2012) prestressing steel with (a) *a posteriori* tertiary modelling prediction and (b) quantified area reduction included.

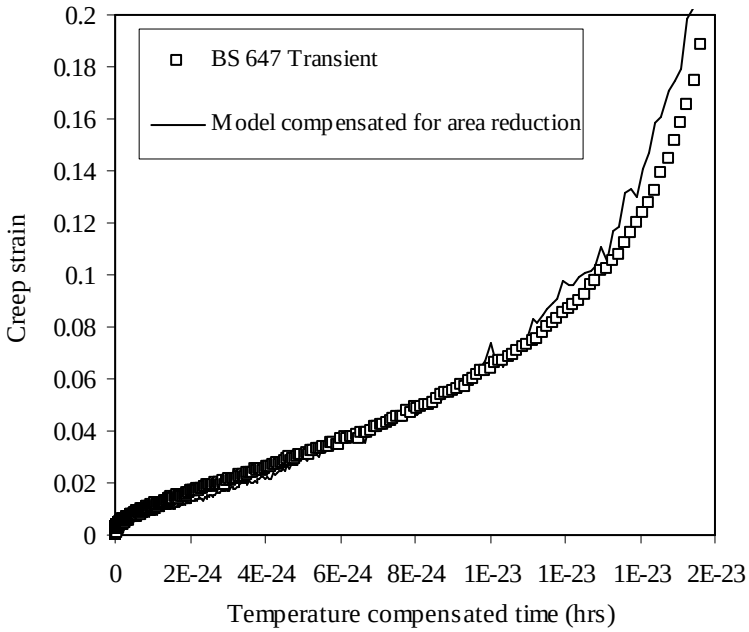

Figure 4.26: Transient state creep test with *a posteriori* tertiary modelling prediction for BS 5896-12 (BSi, 2012) prestressing steel.

Additional issues will require future scrutiny prior to defensible Tertiary creep (failure) modelling:

- A more thorough investigation into the sensitivity of the creep equations to model Tertiary creep is required since stress increases exponentially during this phase. The creep model was only intended for use when true stress changes were relatively slow with time. Previously for the Primary and Secondary creep phases a sensitivity analysis has been performed giving satisfactory results (Gales, 2009).
- The above comparison relies on knowing the true stress *a posteriori*; this itself requires confident prediction *a priori*.

To address either of the above issues will require a more accurate DIC technique to define the true necking behaviour during Tertiary creep.

Mechanical Behaviour

Tensile failure at high temperature of BS 5896-12 (BSi, 2012) prestressing steel is discussed in this section by comparison of the test data against the models provided by EN 1992-1-2 (CEN, 2004) temperature-based strength reduction factors. The strength reduction results obtained during testing for the BS 5896-12 (BSi, 2012)

steel are shown in Figure 4.27 (these data are based on steady state testing at a crosshead displacement rate of 2 mm/min). An average ultimate strength at ambient temperature of 2033 MPa ±11 MPa (standard deviation based on six tests) was obtained for the BS 5896-12 (BSi, 2012) strand's core wire, with subsequent strength reductions determined at 100ºC intervals up to 500ºC. High temperature strength tests were repeated twice. These strength reductions are based on an engineering definition of stress, wherein the cross-sectional area of the specimens is assumed to be constant up to failure and the Poisson and necking effects are ignored. Also shown in Figure 4.27 is a curve showing the reductions in strength with temperature if a true stress definition is used. True stress is based on the DIC measured reduction of cross-sectional area (i.e. necking) which was measured using DIC at elevated temperature.

The true versus engineering stress versus strain responses for tests up to 500ºC with different loading rates are shown in Figure 4.28. It is clear that true stress actually increases drastically approaching failure, in much the same way it does during Tertiary creep. These values should be considered with caution since DIC struggles for small gauge lengths as already noted. Temperatures greater than 500ºC were not considered, as the high temperature paints used for DIC were not rated above this temperature and prestressing steel would rarely be relied on at such high temperatures in any case.

Figure 4.27 shows that the strength reduction of the BS 5896-12 (BSi, 2012) steel followed the expected behaviour based on EN 1992-1-2 (CEN, 2004) guidance, which indicates nearly 50% stress loss at temperatures below 400ºC. Figure 4.27 also shows that the true strength retention of prestressing steel at elevated temperature is actually better than assumed on the basis of an engineering stress definition, at least up to about 300°C where the engineering stress versus strain response experiences post-peak softening (Figure 4.28) and the distinction between true and engineering stress becomes blurred. Interestingly, this post-peak softening is not captured by the EN 1992-1-2 (CEN, 2004) models for stress-strain response at elevated temperature, however it may be important for modelling the response of structures in fire.

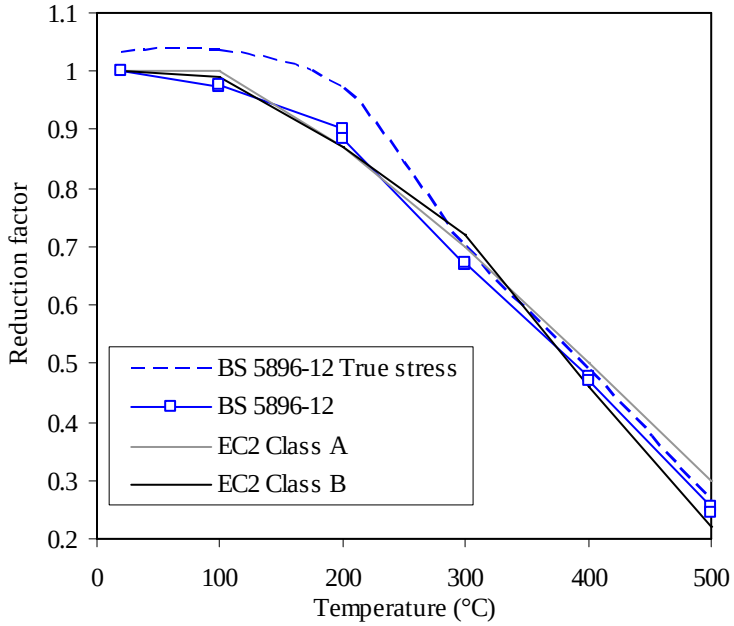

Figure 4.27: Strength reduction relationships for BS 5896-12 (BSi, 2012) prestressing steel in comparison to EN 1992-1-2 (CEN, 2004).

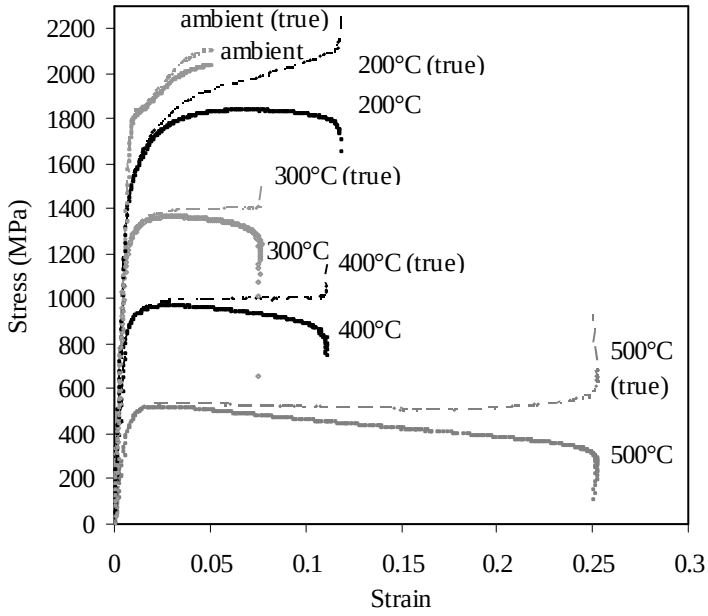

Figure 4.28: Engineering and true stress versus strain curves for strength tests of BS-5896-12 (BSi, 2012) prestressing steel.

Failure

Design code guidance is universally vague regarding the rates that were used in testing (loading/heating rate) to develop material property models for use at high

temperature. These rates are typically not provided in documentation but will influence the results obtained as failure is influenced by time-dependent creep. In the steady state strength tests for the current project a crosshead speed of 2 mm/min was chosen. Had a different displacement rate been used, say 1 mm/min, the ultimate strength values might have been different (lower) with failure earlier resulting in a smaller reduction factor (this was seen when a second 500ºC test was performed at 1mm/min and the corresponding ultimate stress was 12% lower than in two tests performed at 2 mm/min). It is therefore important that time based controls are noted when high temperature strength tests are reported.

Two observations can be made from Figure 4.29, which plots rupture from both creep and tensile strength tests: first, the predominant heating rate used for transient creep tests (2ºC/min) appears to agree with reduction factors given in BS EN 1992-1-2 (CEN, 2004), as does the displacement rate of 2 mm/min; and second, depending on the heating scenario it is possible to fail the steel below the code provided definition of failure depending on the time-temperature conditions.

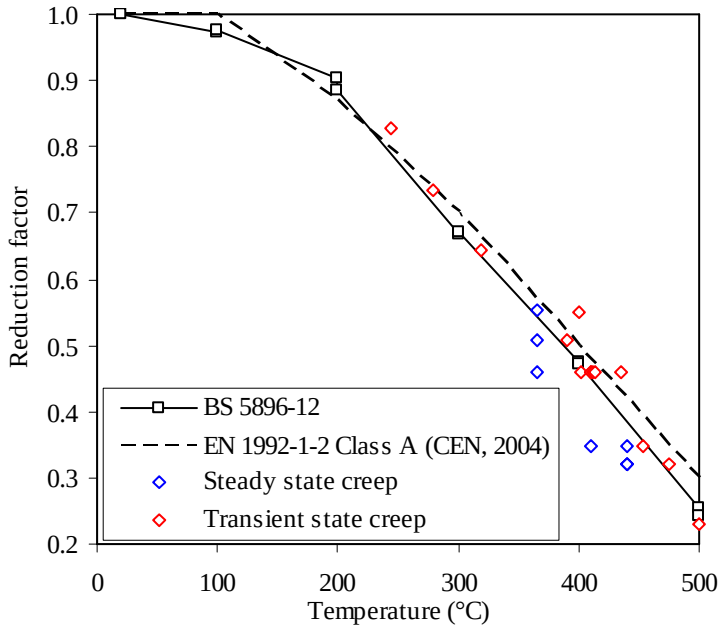

Figure 4.29: Steady state and transient creep rupture strengths plotted with temperature for BS 5896-12 (BSi, 2012) prestressing steel.

This is further complicated by the maintenance of mechanical loading on the prestressing steel tendon as would be present in a real structure, and the degree of relaxation that a prestressing tendon might experience, as considered in Chapter 3. It

would appear that additional investigations into the failure of prestressing steel are warranted for future research before Tertiary creep and mechanical failures can be accurately distinguished and predicted (see Section 4.6.1).

4.6.6 Validation

A validation exercise was performed to confirm that the BS 5896-12 (BSi, 2012) prestressing steel creep parameters developed herein could be used satisfactorily for predicting Primary and Secondary creep response. The new parameters, given in Equation 4.6, were used in conjunction with the stress relaxation computational model described in Chapter 3, which uses Equation 4.2 for predicting creep (see Gales (2009) for background information). The stress relaxation model had previously used parameters developed by Harmathy and Stanzak (1970) based on tests of older steels; these parameters resulted in overestimation of creep in Chapter 3 as already noted.

Since the Strongback tests discussed in Chapter 3 used ASTM 416-03 (ASTM, 2003) prestressing steel and not BS 5896-12 (BSi, 2012) prestressing steel, a validation of the computational model with new creep parameters against those tests is immediately impractical. Instead, new test series using BS 5896-12 (BSi, 2012) prestressing steel was performed for validation purposes. The aforementioned Instron 600LX materials testing frame and environmental chamber were used to conduct two stress relaxation tests of BS 5896-12 (BSi, 2012) prestressing steel using a more complicated transient heating regime than was employed in the Strongback tests. The validation exercise took advantage of the environmental chamber's capability to program multiple predefined transient heating rates. Using the heat transfer model described in Chapter 3 and developed by Bisby (2005), the environmental chamber was programmed to simulate the heating exposure for prestressing steel strand embedded in a concrete slab and exposed to an ASTM E119 standard fire (ASTM, 2001). Two heating rates were used, representing predicted heat transfer behaviour of two concrete axis distances of 28 mm and 35 mm. These axis distances are representative to those needed to achieve standard fire ratings of 120 minutes in IBC (2012) and EN 1992-1-2 (CEN, 2004), with respect to continuous construction (refer to Table 3.2). Five thermocouples were used to

characterize the temperature of the strand for modelling purposes. One thermocouple was placed on the bottom on the environmental chamber on the tendon (T1), three thermocouples placed inside the chamber on the tendon (T2-T4) equally spaced, and one was placed on the strand outside the top of the chamber (T5). Since the test did not involve mechanical extension, it was deemed satisfactory that the thermocouple positions would remain stationary during the test. The heated length ratio was high, at 80%. The test began at an initial stress level of 1200 MPa (as would be typical for prestressing tendons in a building in practice). The grips were locked in place and the strand was allowed to relax through thermal expansion, mechanical degradation, and creep. The temperature distribution for each test is noted in Figure 4.30 and Figure 4.31.

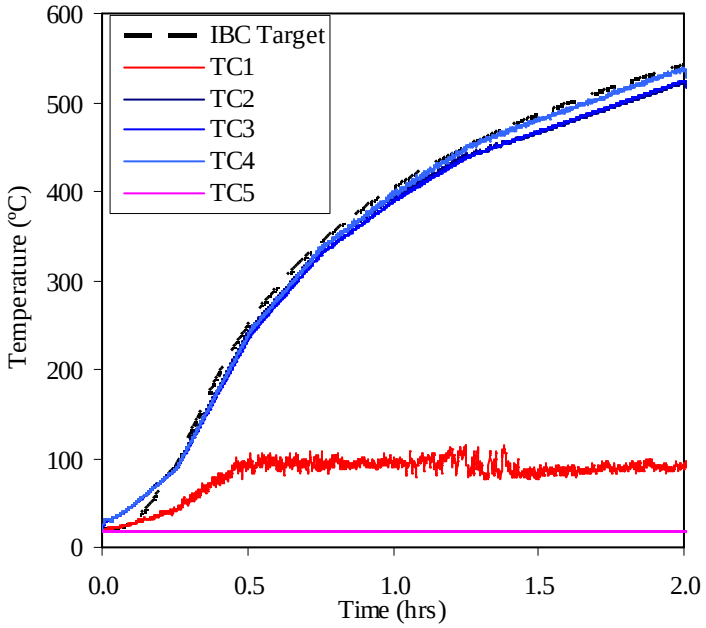

Figure 4.30: Temperature profile for various thermocouples during stress relaxation test for a standard fire simulated at 28 mm axis distance.

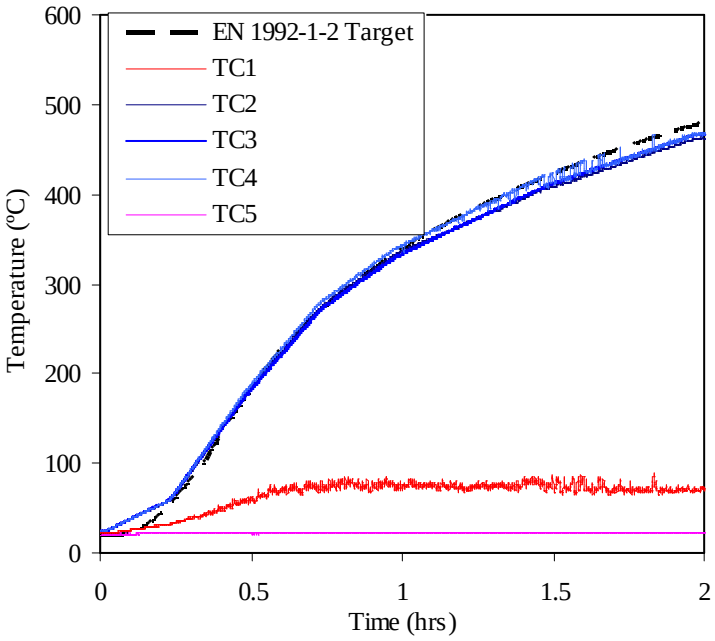

Figure 4.31 Temperature profile for various thermocouples during stress relaxation test for a standard fire simulated at 35 mm axis distance.

The stress relaxation model from Chapter 3 was used; however with the new creep parameters developed in the current chapter. This allowed both the thermal expansion and the creep to be quantified and separated in the tests. Figure 4.32 illustrates the results for both tests (the IBC cover and the EN 1992-1-2 cover).

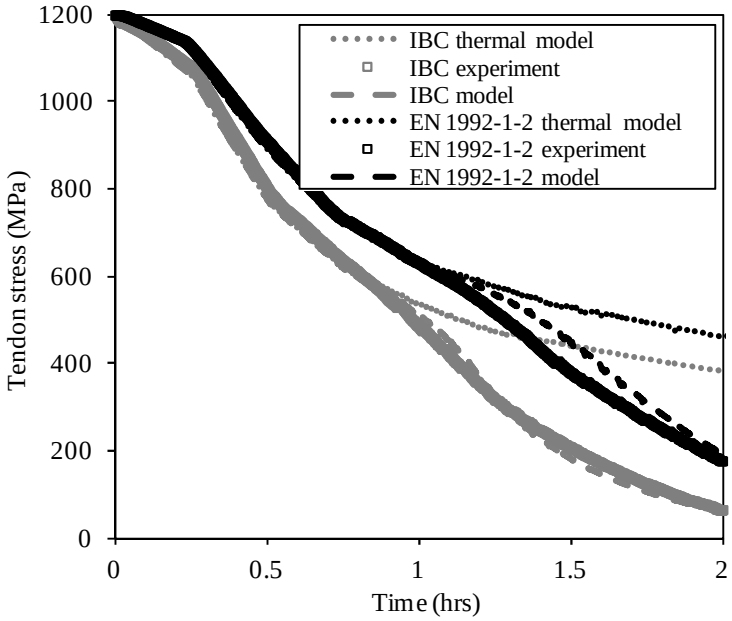

Figure 4.32: Stress relaxation with simulated standard fire and axis distance for BS 5896-12 (BSi, 2012) prestressing steel.

Less than 50 MPa error was observed for both tests, indicating a satisfactory validation of use of the new creep parameters within Equation 4.6.

4.7 Creep response

Available deformation parameters for prestressing steel could be assumed to apply to all equivalent grades sourced from different mills. Equivalence is not assured and should be tested. Fabrication and microstructure differences (from mill to mill, or from metallurgical improvements with time) influence creep resistance and deformation of steel at high temperature. This section studies creep response for "equivalent" grades of prestressing steel sourced from three separate geographic regions; their respective creep behaviour is also compared to prestressing steel from the 1970s.

4.7.1 Materials

Section 4.6 focused on steel manufactured in accordance with BS 5896-12 (BSi, 2012). The supplied stock was used for testing in Chapter 5, and therefore the material was completely characterized over a wide stress-temperature range. A second steel manufactured in accordance with ASTM 416-03 (ASTM, 2003) was characterized for the same reasons, allowing comparison to the Strongback tests discussed in Chapter 3. This steel was also used for the DIC validation exercises discussed previously in this chapter. Only a limited stock of the North American prestressing steel remained after the Strongback tests, and therefore only a few creep tests could be performed on this material and only parameters which fell within the Strongback stress range were derived. A third batch of prestressing steel that was manufactured according to AS/NZS 4672-07 (AS/NZS, 2007) was also sourced (provided by the University of Canterbury, New Zealand).

4.7.2 Creep parameters for AS/NZS (2007) and ASTM (2003) prestressing steels

Table 4.1(b) and Table 4.1(c) describe the tests performed for each of the aforementioned prestressing steels. Where possible the testing regime followed the same as was performed for the BS 5896-12 (BSi, 2012) prestressing steel, and the general conclusions made for test repeatability, steady state versus transient testing

equivalency, and increases in Z with increases in load (stress) level all agreed with those previously made.

The activation energies for creep, Q, however for each prestressing steel were significantly different. As only a limited supply of each batch of steel existed, the Q for the ASTM 416-03 (ASTM, 2003) steel was derived as 23000K on the basis of equating two transient creep tests at the same load level but different heating rate. The AS/NZS 4672-07 (AS/NZS, 2007) steel value was derived from Equation 4.4 using two steady state tests, giving Q of 34350K. These values are viewed with caution due to the limited data used in their derivation.

Equations 4.7 and 4.8 were derived based on a $R^2 > 0.99$ fit with respect to minimum creep rate, Z. The primary creep rate variable had significant scatter and relatively poor repeatability. These equations should only be used with the activation energies noted above.

NZS 4672-07 (AS/NZS, 2007) prestressing steel

$$Z = ae^{b\sigma} = 4.37x10^{14} e^{0.015\sigma} \qquad 700 \text{ MPa} < \sigma < 1200 \text{ MPa} \qquad [4.7a]$$

$$\varepsilon_{cr,0} = c\sigma^{d} = 1.15x10^{-11}\sigma^{2.72} \qquad [4.7b]$$

ASTM 416-03 (ASTM, 2003) prestressing steel

$$Z = ae^{b\sigma} = 2.5x10^{8} e^{0.0145\sigma} \qquad 690 \text{ MPa} < \sigma < 1000 \text{ MPa} \qquad [4.8a]$$

$$\varepsilon_{cr,0} = c\sigma^{d} = 4.1x10^{-7}\sigma^{1.2} \qquad [4.8b]$$

The previous equations derived by Harmathy for an activation energy of 30550K and ASTM 421-65 (ASTM, 1965) prestressing steel are as follows:

$$Z = ae^{b\sigma} = 8.21x10^{13} e^{0.0145\sigma} \qquad 172 < \sigma < 690 \text{ MPa} \qquad [4.9a]$$

$$\varepsilon_{cr,0} = c\sigma^{d} = 9.26x10^{-5}\sigma^{0.67} \qquad [4.9b]$$

As can be immediately observed from Equations 4.6 through 4.9, each of these nominally identical prestressing steels has significantly different derived creep parameters.

4.7.3 Prestressing steel comparison

Three additional exercises were conducted to compare the prestressing steels studied in the current work. These included:

(1) **Experiments** – a creep test was performed for each steel at 427ºC at approximately 700 MPa, this allowed the creep response of all three modern prestressing steel to be compared experimentally, at least for a single load case. Both the full creep curve and the creep rate are considered for these tests. Strength tests were performed for the AS/NZS 4672-07 (AS/NZS, 2007) steel for comparison with the BS 5896-12 (BSi, 2012) steel. Both strength and modulus of elasticity were considered.

(2) **Microstructural analysis** – all three modern steels were compared at the microstructural level (at 100X magnification). Grain structure at ambient and after exposure to steady state heating at 500 and 700ºC were compared for each of the three modern prestressing steels.

(3) **Numerical comparisons** – a numerical modelling exercise was performed to construct predicted creep response curves for each of the modern prestressing steels for a simulated creep test, to predict (*a priori*) the creep response for each of them in comparison to that proposed by Harmathy and Stanzak (1970) and currently advocated in the literature (e.g. Purkiss, 2008).

Experiments

Five creep tests were performed to compare each of the prestressing steels. Each creep test was steady state conducted at a temperature of 427ºC at an initial stress (constant load) of 700 MPa (approximately 35% of ultimate strength). A repeat test for the BS 5896-12 (BSi, 2012) and AS/NZS 4672-07 (AS/NZS, 2007) steels were also performed. It was not possible to perform a repeat test for the ASTM 416 (ASTM, 2003) steel as only a limited of supply was available. The full creep curve and the normalized creep rate were compared.

Figure 4.33 illustrates the strain versus time results for one creep test for each type of steel. Note that the ASTM 416-03 (ASTM, 2003) steel was tested at a stress of 690MPa rather than 700 MPa, for simplicity this result is used for comparison. The results indicate that the AS/NZS (AS/NZS, 2007) steel exhibits the least creep, whereas the BS 5896-12 (BSi, 2012) steel exhibits the most. Interestingly, the ASTM 416-03 (ASTM, 2003) steel also exhibited more creep than its AS/NZS (AS/NZS, 2007) counterpart, despite the lower applied stress level. This comparison suggests that nominally identical steels can display significantly different creep behaviour.

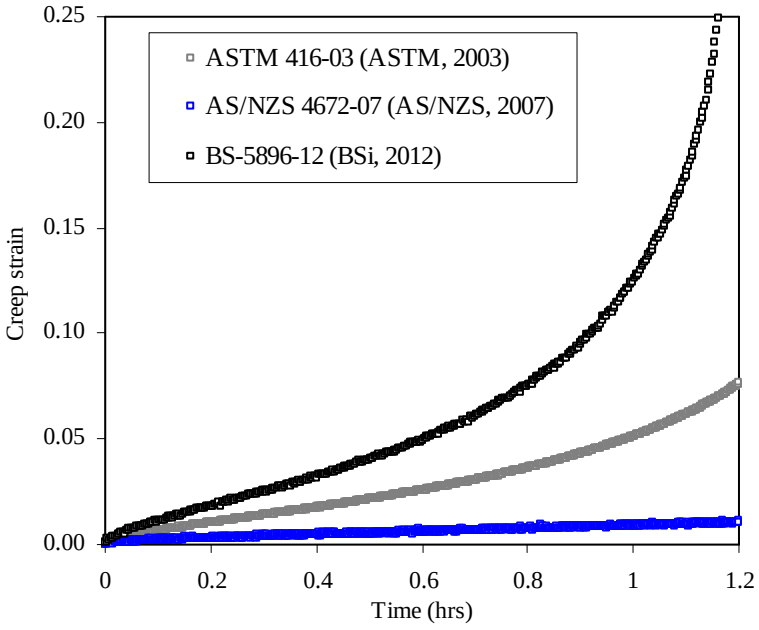

Figure 4.33: Experimental creep curves at 427ºC near 700 MPa.

Figure 4.34 illustrates the normalized time (the total test time divided by its duration) with respect to creep rate (with the creep rate determined with respect to each 0.1 normalized time interval) for both the BS 5896-12 (BSi, 2012) and AS/NZS 4672-07 (AS/NZS, 2007) steels. Repeat tests are also shown in this figure. The AS/NZS (AS/NZS, 2007) steel exhibits a much smaller creep rate than its BS 5896-12 (BSi, 2012) counterpart. In fact, both AS/NZS (AS/NZS, 2007) steel tests lasted over five hours in duration prior to failure whereas both BS 5896-12 (BSi, 2012) steel tests lasted less than 1.2 hours until failure. The ASTM 416-03 (2003) counterpart, of same cross-sectional area as the AS/NZS (AS/NZS, 2007) specimen lasted 1.4 hours until failure. By a relative comparison, the tests suggest that AS/NZS (AS/NZS, 2007) steel exhibits higher creep resistance than its prestressing steel

counterparts. Since the testing pool was small in this comparison and the results are only for one stress level, these results should be treated with caution; additional loading levels and repeat tests would have been useful for comparison.

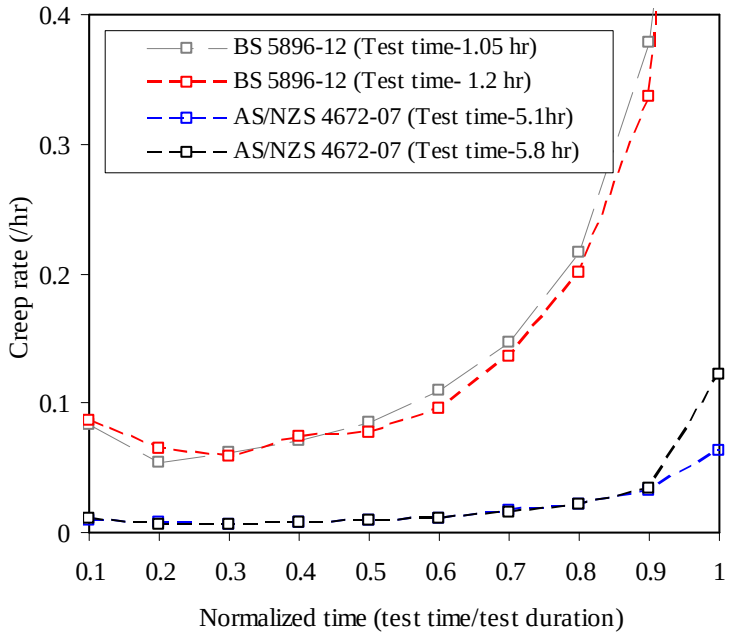

Figure 4.34: Creep rate with normalized time for BS 5896-12 (BSi, 2012) and AS/NZS 4672-07 (AS/NZS, 2007) prestressing steels.

Figure 4.35 and Figure 4.36 give a comparison of the strength and normalised modulus of elasticity of both the BS 5896-12 (BSi, 2012) and AS/NZS 4672-07 (AS/NZS, 2007) prestressing steel, respectively. The ASTM 416-03 (ASTM, 2003) steel could not be included due to limited supply. The AS/NZS 4672-07 (AS/NZS, 2007) steel shows significantly greater strength at elevated temperature as compared to the BS 5896-12 (BSi, 2012) steel. For example, at 400ºC the BS 5896-12 specimen has an ultimate strength of 965 MPa, whereas the AS/NZS 4672-07 (AS/NZS, 2007) specimen has a strength of 1079 MPa; more than 100 MPa higher. The results for the AS/NZS 4672-07 (AS/NZS, 2007) steel suggest lower ultimate strain values at higher temperature compared to their BS 5896-12 (BSi, 2012) counterparts.

A comparison of calculated normalised modulus of elasticity for both BS 5896-12 (BSi, 2012) and AS/NZS 4672-07 (AS/NZS, 2007) prestressing steels suggests a higher retention of stiffness at elevated temperature for the AS/NZ 4672-07 (AS/NZS, 2007) steel than for BS 5896-12 (BSi, 2012). This suggests that at

elevated temperatures the AS/NZS 4672-07 (AS/NZS, 2007) samples have higher resistance to thermal and creep effects.

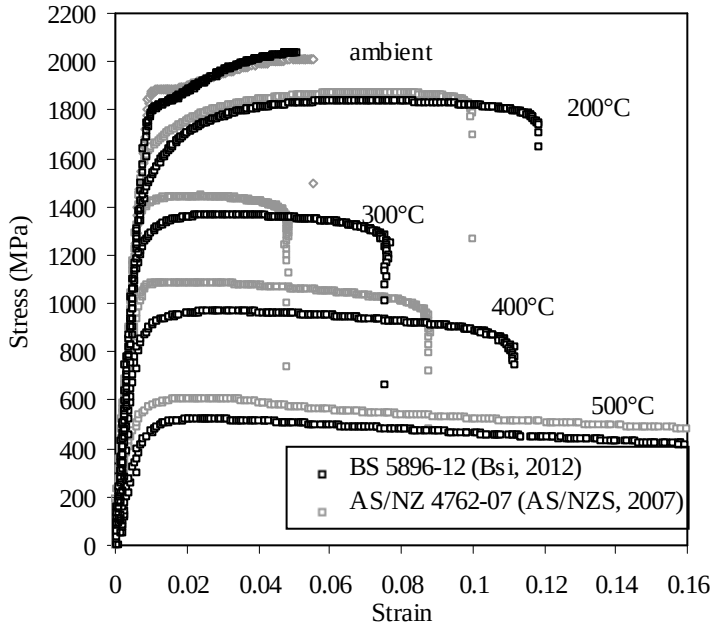

Figure 4.35: Ultimate strength comparison between BS 5896-12 (BSi, 2012) and AS/NZS 4672-07 (AS/NZS, 2007) prestressing steels.

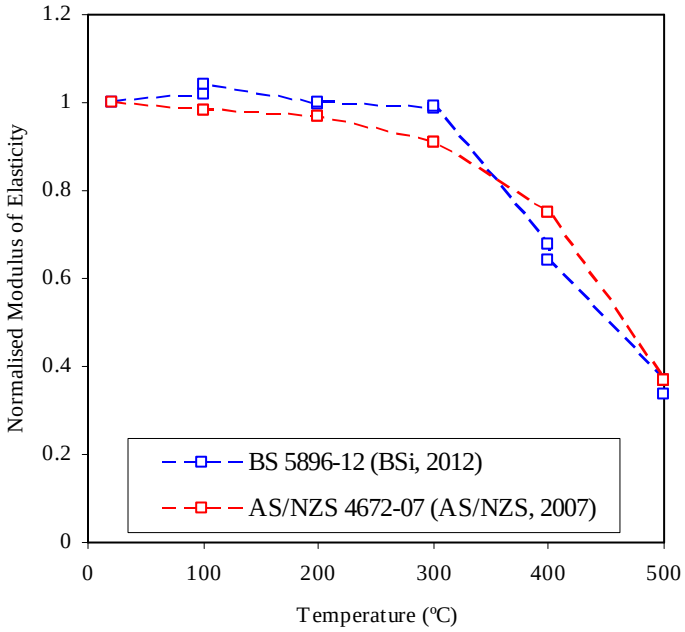

Figure 4.36: Normalised modulus of elasticity with temperature for a loading rate of 2 mm/min for two different prestressing steels.

The superior high temperature performance of the AS/NZS (AS/NZS, 2007) prestressing steel may be explained by the history of the manufacture of each prestressing steel – which is not indicated in documentation which accompanied the commercially available prestressing steel in this thesis. Table 4.2 indicates the material composition the prestressing steels used in this thesis showing all to be slightly different in material composition.

Table 4.2. Chemical composition of the three different prestressing steel studied herein.

Element	BS 5896 (BSi, 2012)	ASTM 416 (ASTM, 2003)	AS/NZS 4672 (AS/NZS, 2007)	ASTM 421 (ASTM, 1965)
C	0.90	0.80	0.82	0.79
Cr	0.011	0.04	-	-
Mn	0.66	0.87	0.64	0.78
P	0.0070	0.023	0.012	0.012
Si	0.25	0.45	0.22	0.19
S	0.014	0.12	0.006	0.031
Ni	0.021	-	-	-
Cu	0.011	-	-	-

Note: Trace elements are not considered in this table

This may suggest that the manufacturing history is also different. Indeed all strands were sourced from different mill owners and fabricated in different countries. The manufacture of prestressing steel is well known to affect the creep response at ambient temperature (Clark and Walley, 1953), and since creep accelerates in elevated temperature, the manufacture history may explain high temperature creep behaviour differences. During the manufacturing process to obtain high strength and low relaxation, the steel is plastically drawn into smaller diameter and heat treated to treat material defects induced during the drawing. The heat-treatment also helps achieve low relaxation characteristics (Collins and Mitchell, 1987). Since creep is highly dependent on the microstructure of steel, any differences in manufacturing between mills might impact the high temperature performance of the steel. For this thesis an attempt was made to relate the behaviour of different but seemingly equivalent prestressing steels which are commercially available. The experimental results suggest that the prestressing steels considered all behaved uniquely and various factors during the manufacture process may likely be impacting their creep behaviour. These manufacture differences between mills which make prestressing steel could be an interesting topic for future research to confirm differences in behaviours.

Microstructural analysis

The microstructure and grain characteristics of the AS/NZS 4672-07 (AS/NZS, 2007) and BS 5896-12 (BSi, 2012) steels before and after high temperature exposure were considered. This characterization is described in detail by Robertson et al. (2013), which represents the output from a MEng thesis project that was co-supervised by the author during the completion of the current thesis. This output is attached as an appendix (C) to this thesis. Additional micro-structural analysis of prestressing steel wires (ASTM 416-03 steel (ASTM, 2003)) was conducted previously by MacLean (2007), and where relevant the results of his analysis are provided for comparison. This analysis is also of particular importance with respect to the stability of the prestressing steel's microstructure – an assumption which can give some credence to the use of a constant Q for the test range used in this thesis.

For the BS 5896-12 (BSi, 2012) and AS/NZS 4672-07 (AS/NZS, 2007) prestressing steels, unrestrained and unloaded wires were heated to temperatures of 200, 400, 500, 600, 700 and 800ºC, respectively. The wires were placed in an annealing oven and heated to the respective target temperatures at a rate of 10°C/min. Four thermocouples were used to monitor the furnace and sample temperatures. The steel wires were then held at the target temperature for 1.5 hours, before being cooled in air. The micro-structure of the samples was examined using a Zeiss Axioscope light microscope. A section was cut from each prestressing steel wire and mounted in EpoxiCure resin. Samples were then ground using gradually finer grit paper and then polished with cloths and diamond paste, to obtain a flat, scratch-free surface. The samples were etched with 2% Nital solution to expose the grain structure. Figures 4.37 to 4.39 show the microstructural images for wires at ambient temperature and after exposure to 500 and 700ºC, respectively, for longitudinal sections.

Examination of sections from both unheated prestressing wires and those which were heated (below 500ºC) exhibited long, well defined grains running parallel to one another across the field of view. These grains are a result of the cold drawing manufacturing process. Pearlitic banding can also be observed.

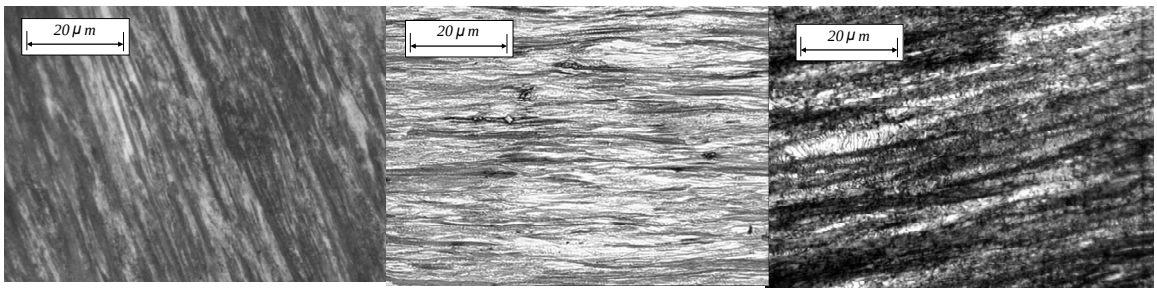

(a) (b) (c)

Figure 4.37: Prestressing steel microstructure for (a) AS/NZ 4672-07 (AS/NZS, 2007) (b) ASTM 416-03 (ASTM, 2003) (Maclean, 2007) (c) BS 5896-12 (BSi, 2012) prestressing steels.

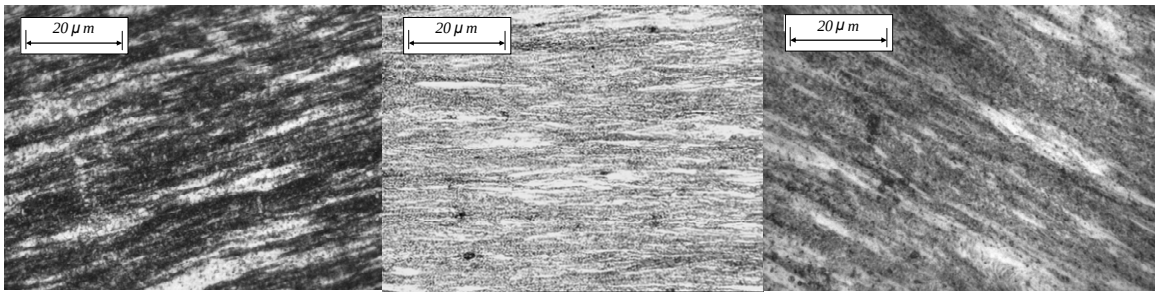

(a) (b) (c)

Figure 4.38: Prestressing steel microstructure after heating at 500ºC for 1.5 hours for (a) AS/NZ 4672-07 (AS/NZS, 2007) (b) ASTM 416-03 (ASTM, 2003) (Maclean, 2007) (c) BS 5896-12 (BSi, 2012) prestressing steels.

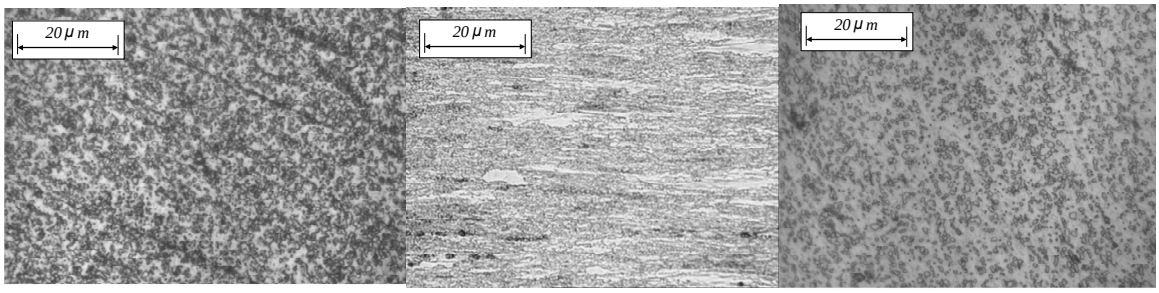

(a) (b) (c)

Figure 4.39: Prestressing steel microstructure after heating at 700ºC for 1.5 hours for (a) AS/NZ 4672-07 (AS/NZS, 2007) (b) ASTM 416-03 (ASTM, 2003) (Maclean, 2007) (c) BS 5896-12 (BSi, 2012) prestressing steels.

This pearlitic banding disappears after exposure to temperatures above 500ºC. The wires heated to 500°C and 600°C began to exhibit a finer grain structure, having less well defined longitudinal grains. Pearlitic bands in this temperature region begin to dissociate into ferrite and globular iron carbide. This new grain structure is a mixture of pearlite and the new globular structure, and becomes evident at exposure temperatures beyond 600ºC. By 700ºC the directionality of the grain structure is lost. Each prestressing steel wire exhibited similar trends at each temperature. Each structure appeared stable below temperatures of 500ºC. The microstuructural

characterization lends credence to the creep parameters used in this thesis such as *Q* which may have sensitivity to changes in temperature since all testing was performed below 500ºC. Beyond this temperature significant microstructure changes were occurring and parameters (such as *Q* which is treated as a constant assuming little to no microstructure change) will be influenced significantly affecting the validity of the creep theory utilised herein.

Numerical modelling

Two numerical modelling predictions were made to compare the modelling results between the modern and older models (for Primary and Secondary creep only). The modelling results are a compilation of preceding creep parameter equations (Equations 4.6-4.9) used in conjunction with the creep equations 4.1 and 4.2. The first comparison (Figure 4.40) considers a steady state temperature of 350ºC and loads of 700 and 1000 MPa.

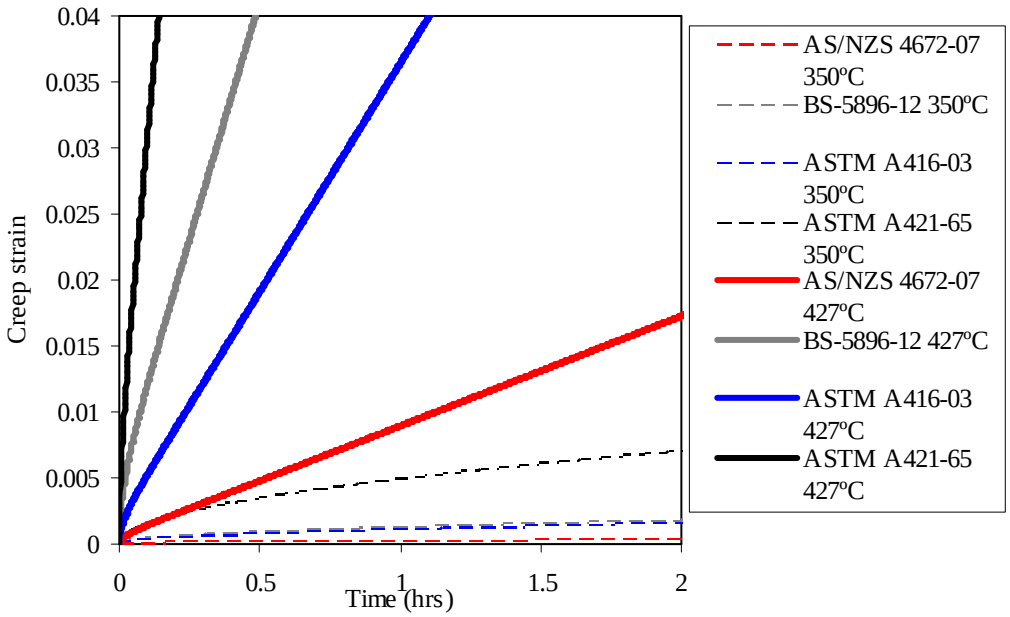

Figure 4.40: Steady state modelled creep deformation at 700 MPa for ASTM 421-65 (ASTM, 1965), ASTM 416-03 (ASTM, 2003), AS/NZS 4672-07 (AS/NZS, 2007) and BS 5896-12 (BSi, 2012).

The predicted results for each model illustrate that the older prestressing steel would experience more creep losses, whereas the AS/NZS ((AS/NZS, 2007)) steel would exhibit the least. Both ASTM (ASTM, 2003) and BS (BSi, 2012) prestressing steel

exhibited similar creep responses. In all cases modern prestressing steel specimens exhibited the least creep.

A second predictive comparison (Figure 4.41) with a loading of 700 MPa and two steady state temperatures of 350 ºC and 427ºC was also made. These results indicated that the model predicted the same creep resistance ranking between the respective steels.

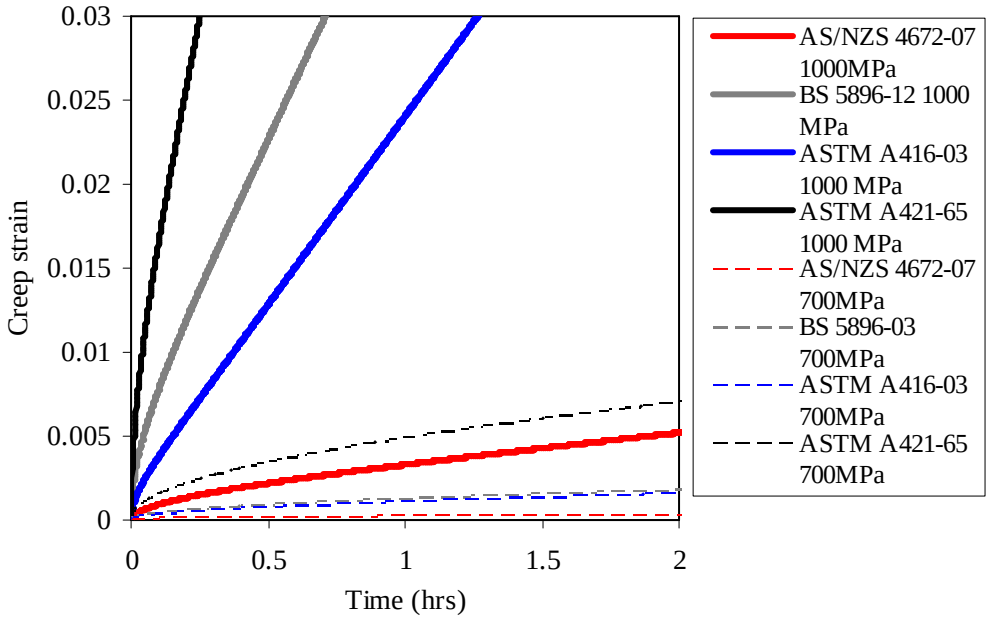

Figure 4.41: Steady state modelled creep deformation at 350ºC ASTM 421-65 (ASTM, 1965), ASTM 416-03 (ASTM, 2003), AS/NZS 4672-07 (AS/NZS, 2007) and BS 5896-12 (BSi, 2012).

4.7.4 Modelling errors

The fundamental motivation behind the work presented in this chapter stemmed from the fact that the computational model reviewed in Chapter 3 to predict stress relaxation of locally-heated unbonded and stressed prestressing steel tendons considerably over-predicted stress relaxation when compared against test results. This was believed to be due to the use of creep parameters formulated by Harmathy and Stanzak in 1970, which were not thought to be appropriate for modern prestressing steels given advances in steel processing during the decades since this early work, as well as the limited stress and temperature ranges which necessitated excessive extrapolation of the available data. Sections 4.7.2 and 4.7.3 have demonstrated that the high temperature material parameters for modern prestressing steels are indeed different. This section checks whether the new creep parameters

(i.e. Z, Q, $\varepsilon_{cr,0}$) allow better prediction of the stress relaxation that occurred during previously performed tests on locally-heated unbonded and stressed prestressing steel tendons described in Chapter 3.

It must be re-iterated that the tendons used for each of the tests described in Chapter 3 were seven-wire Grade 1860 MPa steel prestressing steel strands, precisely the same as the tendons studied in the current section for ASTM 416 (ASTM, 2003).

Three locally-heated tests from the test series are of interest for this section. These tests involved transient heating at rates of 2, 10 and 30ºC/min up to a steady-state temperature of 400ºC which was held for approximately 90 minutes. The tendons were then allowed to cool to ambient temperature. Further details of methodology are given in Chapter 3. The numerical model is for pratical application of prestressing steel embedded with varied concrete cover, which would experience varied transient heating rates in a fire. The tests for validation were chosen as those with heating rates repreasent slow (2ºC/min) to more rapid heating (30ºC/min). This would allow the creep prediction, which is time dependednt to be assessed appropriately. Figures 4.42 through 4.44 show the stress versus time response recorded during the Strongback tests for each of the aforementioned tests respectively. The figures also show the stress relaxation curves predicted using the stress relaxation computational model with the new creep parameters that were developed herein (Equations 4.6-4.9). In all of these figures, model predictions which use Harmathy and Stanzak's (1970) creep parameters overestimate stress relaxation by up to 18%. The stress range recorded during the tests falls within the stress range for which the parameters of ASTM 416-03 (ASTM, 2003) were previously defined. The new creep parameters clearly model stress relaxation more accurately, with percentage errors ranging between 3 and 6% maximum as compared to 18% for the older model parameters.

The improvement in model predictions for stress relaxation provides an independent check upon the creep parameters derived earlier in this chapter. Figure 4.43 repreasents the same experimental data used to build Figure 3.3 for reference, The 11% heated length ratio is omitted from this figure as its experimental data falls outside the domain of applicability for the new creep parameters developed. The strongback beam tests indicate a substantial three fold modelling accuracy

improvement. The use of the new creep parameters gives more precise predictions of tendon stress, and hence can be used to predict potential strength failure of modern unbonded and stressed prestressing steel tendons during fire.

Additionally, Figures 4.42-4.44 illustrate stress relaxation predictions for using AS/NZS (AS/NZS, 2007) and BS (BSi, 2012) creep paramters. In all cases AS/NZS (AS/NZS, 2007) creep paramters underestimate the stress relaxation by approximately 8%. In all cases where BS (BSi, 2012) creep paramters were used to predict stress relaxation, the error was at maximum 14%. These results suggest greater inaccuracies than would be observed if the creep paramteres developed for ASTM 416 (ASTM 416) prestressing steel were used. This emphasizes that creep parameters should only be used for the steel which they were develop to minimize error.

In closing, it should be noted that in a real, full-scale unbonded PT concrete building subjected to a real fire, the tendon stress will be dependent upon the complex interaction between tendon creep and relaxation, loads shed to the bonded steel reinforcement, the redistribution of load through the structure, and the potential offset of tendon de-stressing due to thermal expansion of the floor plate; some of these influences are experimentally studied and discussed in Chapter 5.

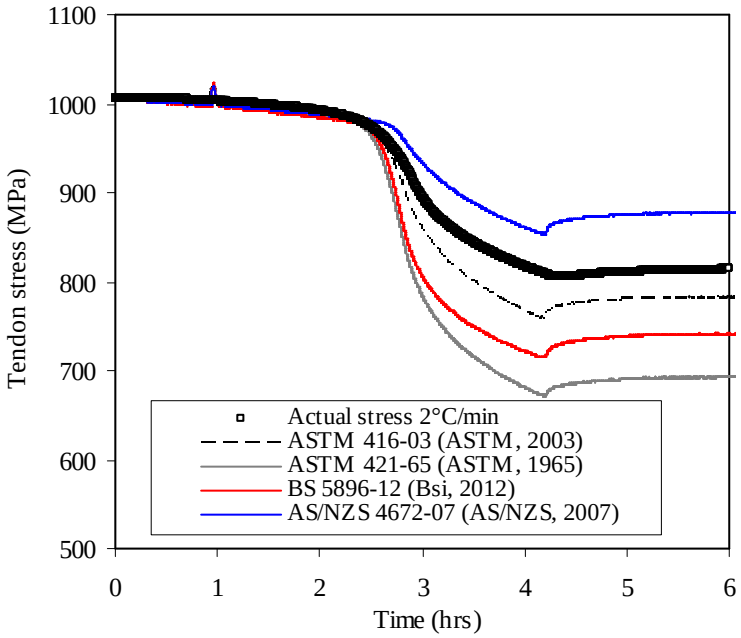

Figure 4.42: Strongback test with model comparison and a transient heating rate of 2ºC/min.

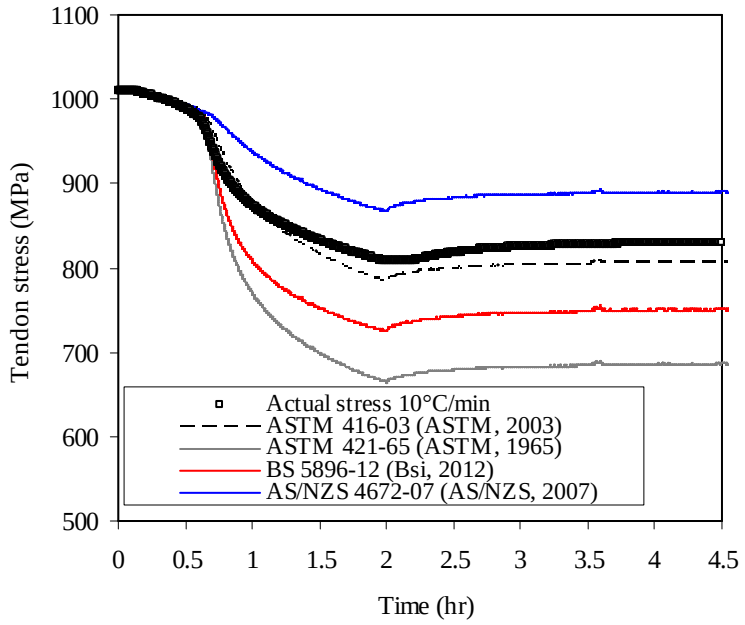

Figure 4.43: Strongback test with model comparison and transient heating rate of 10ºC/min.

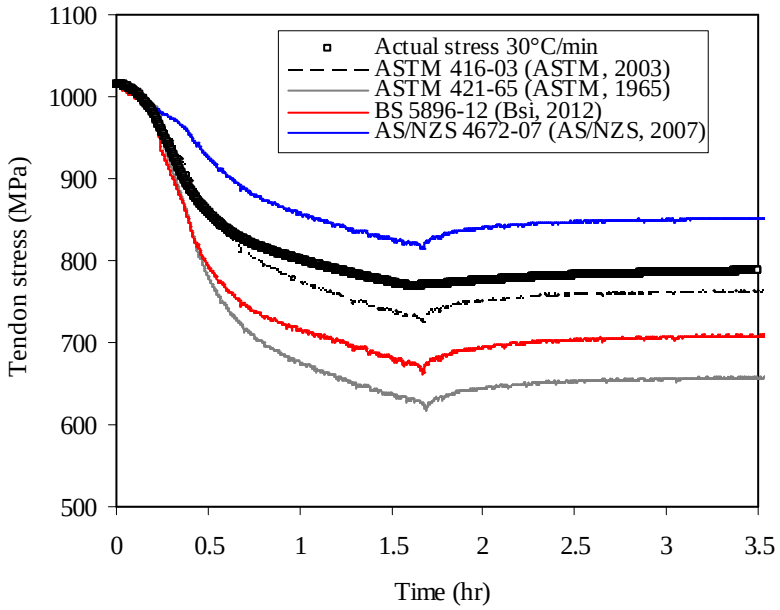

Figure 4.44: Strongback test with model comparison and a transient heating rate of 30ºC/min.

4.8 Summary

This chapter has described the results of a series of uniaxial tensile tests on prestressing steel wires at high temperatures under sustained load. Creep tests were conducted under both steady-state and transient conditions, and has demonstrated the importance of accurate and current creep parameters for modelling stress relaxation

in heated steel prestressing tendons. The creep parameters available in the literature were developed decades ago, and both the uniaxial tests presented in this chapter, and locally-heated tests on unbonded and stressed steel tendons have demonstrated that modern prestressing steels can have very different creep behaviour. This comparison emphasized the necessity for an engineer/designer to use the correct material properties in numerical structural fire engineering modelling. This clearly presents a level of additional modelling complexity which requires future research attention. Key insights from this chapter include:

- Digital image correlation was used to measure tendon deformation during the uniaxial tests conducted in the current work. A series of validation tests were first conducted to establish that this DIC technique using GeoPIV8 could accurately measure the required deformations at high temperature. These tests demonstrated that this DIC technique is a reliable method for measuring strain at high temperatures, and that it is not hampered by some of the limitations that prevent traditional strain measurement techniques being used at high temperatures and for high strains.
- Using DIC for cross-sectional area reduction analysis during elevated temperature tensile testing has allowed initial assessment of high temperature creep behaviour in the Tertiary phase, indicating that this appears as merely a manifestation of localised necking in prestressing steel – it has also been shown that Primary and Secondary creep parameters can be useful for predicting the behaviour of steel within the runaway Tertiary creep phase. Further refinement of the image processing algorithm, GeoPIV8 would improve the accuracy of the cross-section reductions.
- The new creep parameters developed in this chapter greatly improve the accuracy of stress-relaxation modelling of the Strongback tests presented in Chapter 3. The accuracy in modelling the behaviour of unbonded post-tensioning subjected to local heating was improved from 18% error (using previously available creep parameters) to less than 6% using the new parameters derived herein.

Chapter 5

Tests of Continuous Post-Tensioned Concrete Slabs under Localised Heating

> *"If we attempt to develop the fire endurance of a construction system in actual buildings under fire conditions we would not obtain a single-valued answer, but rather we would have to measure a range of performance levels depending upon methods of structural framing existing in a single building as well as the methods of structural framing of any and all buildings into which the construction system under consideration could be incorporated…"*
>
> - RW Bletzaker
>
> On sponsored composite slab tests presented at ASTM-E119 meeting, 1966
> (Bletzaker, 1967)

5.1 General

The specific behaviour of unbonded prestressing steel tendons in fire has been accurately defined and predicted in Chapter 4. However, in real multi-bay continuous unbonded PT concrete structures exposed to fire, thermal deformations, restraint, reductions in concrete stiffness, continuity, spalling, slab splitting, etc, will all also play roles influencing the structural response. To date, relatively little experimental investigation has been conducted which has attempted to understand these structural interactions in fire using realistic PT concrete slab construction configurations. To steer the structural and fire engineering community towards the development of defensible, performance based, fire-safe designs for these structures, a series of non-standard structural fire experiments were performed on continuous and restrained PT concrete slabs; these are presented in this chapter with a view to better understanding their response under localised high temperature exposure.

5.2 Overview

Chapters 3 and 4 sought to understand and predict the effects of high temperature stress relaxation and rupture of unbonded prestressing steel tendons from different sized (i.e., localised) fires. The results indicated that localised heating, as would be experienced in a real fire (due to travelling fires, ceiling jets, etc), is in fact the more severe heating exposure with respect to rupture of unbonded prestressing steel tendons. However, the global response to fire of a continuous unbonded PT concrete

slab system has not yet been considered. Little experimental data exist which can help designers understand the fire performance of realistically constructed and continuous (restrained) unbonded PT concrete slabs, despite the industry's rapid optimization trends for ambient design. The experiments presented in this chapter were designed to study the structural and thermal response of simplified continuous unbonded PT concrete slabs, incorporating as many of the relevant structural behaviours as possible, under severe localised heating. Such tests represent a critical step in the development of a rational understanding of, and ability to model, the fire performance of unbonded PT concrete structures.

Three one-way continuous, restrained, monostrand PT concrete slabs were constructed and tested under localised heating. Two slabs were designed with unbonded tendons, while a third slab incorporated a bonded tendon. All slabs were precast and then connected to steel column restraints/supports prior to testing. These columns were designed to be representative of the axial-flexural restraining stiffness that would be present in a real PT building. This resulted in three spans on four fixed partially rigid connections. After installation, the slabs' prestressing tendons were post-tensioned and anchored. This allowed possible restraining mechanisms during heating to be investigated. All previous testing presented in literature has been unable to represent this condition as it has used either roller connections or flat plate frictional bearings at support locations (see Chapter 2). The columns used for this experimental series were instrumented with strain gauges (as described below) which made it possible to monitor the restraining forces developed during testing. Deformations were monitored during testing with displacement transducers, and tendon stress levels with load cells. Each slab was statically loaded with lead weights during testing to simulate a representative in-service condition. Localised heating was applied using an array of radiant heaters placed underneath the central span. Temperatures were monitored using thermocouples embedded in each slab as well as a thermal imaging camera to measure the soffit temperatures. The slabs were monitored for structural and thermal responses in both heating and cooling phases.

All slabs had the same overall dimensions, thickness, axis distance to the prestressing tendon, concrete type, bonded steel reinforcement, age, and moisture condition at the time of testing. They were constructed to investigate the influence of

unbonded tendon length (and thus heated length ratio) on the performance of the tendons in a real structure, as well as to directly interrogate possible differences between bonded and unbonded construction. The three slabs were as follows:

- **Slab A:** This was the base case. The prestressing tendon was installed as unbonded (greased and sheathed) and subjected to heating over its central span, at 17% of its total length.
- **Slab B:** This slab was included to investigate the influence of bonded versus unbonded construction, and the only difference from Slab A was that the prestressing tendon was installed as bonded (i.e. grouted within a plastic post-tensioning duct).
- **Slab C:** This slab was identical to Slab A with the exception that a custom-built disc spring was installed at its dead end anchorage. This decreased the stiffness of the unbonded tendon thereby simulating a longer unbonded tendon length and a shorter heated length ratio (less than about 10% in this case).

Temperatures, tendon stress levels (and stress relaxation), restraining forces, and deflections were all monitored during testing. Since very little data exist for the cooling phase response of concrete structures, all three slabs were monitored during cooling. Slabs A and B were heated twice, for interest's sake and to study their response under secondary heating to help develop a better understanding of concrete behaviour in high temperature. Slab C was heated only once. The test series were:

- Test A, first heating of Slab A; A.1 denotes the second heating of Slab A;
- Test B, first heating of Slab B; B.1, denotes the second heating of Slab B; and
- Test C, first and only heating of Slab C.

Selected details of the test specimens are provided in Table 5.1. Figure 5.1 gives a schematic of the slab, support, and heating systems, whereas Figure 5.2 gives a schematic view of the slab and its instrumentation.

Table 5.1: Selected details of test specimens.

Test	General Description	Concrete precompr-ession due to prestress at start of test (Mpa)[a]	Restraint conditions (lateral/ rotational) [b]	Bonded steel reinf.[c] (%)	$f'c_{cube}$ at testing (MPa)	Moisture content at testing (% by weight)	Aggreg-ate type	Load ratio[d]	Max. tendon temp. (°C)	Span/ depth ratio	Longitudinal cracking?	Transverse cracking?	Spalling?	Tendon rupture ?	End Point
A	Unbonded tendon	2.37	Y/Y	0.22/0 0.22/0	41	4.0	10mm mixed gravel	0.42	361	43	N	Y	N	N	Critical temp-erature
A.1		1.85[e]			-	-		-	426		N	Y	N	N	
B	Bonded tendon	2.42			42	3.9		0.32	376		Y	Y	Y[f]	N	
B.1		2.42[e]			-	-		-	435		-[g]	Y	N	N	
C	Unbonded tendon with stiffness spring	2.39			43	3.8		0.42	432		?[h]	Y	N	N	

[a] Precompression is the stress level divided by the slab cross section
[b] Y = yes, N = no, P = partial
[c] Top longitudinal/top transverse/bottom longitudinal/bottom transverse
[d] Load ratio is applied moment reaction to theoretical moment capacity at mid span
[e] Test A.1 and B.1 are a repeat heating, so in service stress at time of test is used to calculate precompression
[f] Spalling is defined in this case as any concrete which debonds (sloughs) from the slab and falls off
[g] Longitudinal crack appeared in Test B and was present in Test B.1; the size of the crack was <1mm and did not grow in Test B.1.
[h] Longitudinal crack not measurable on surface of slab, but flaming parallel with the tendon was observed during the test

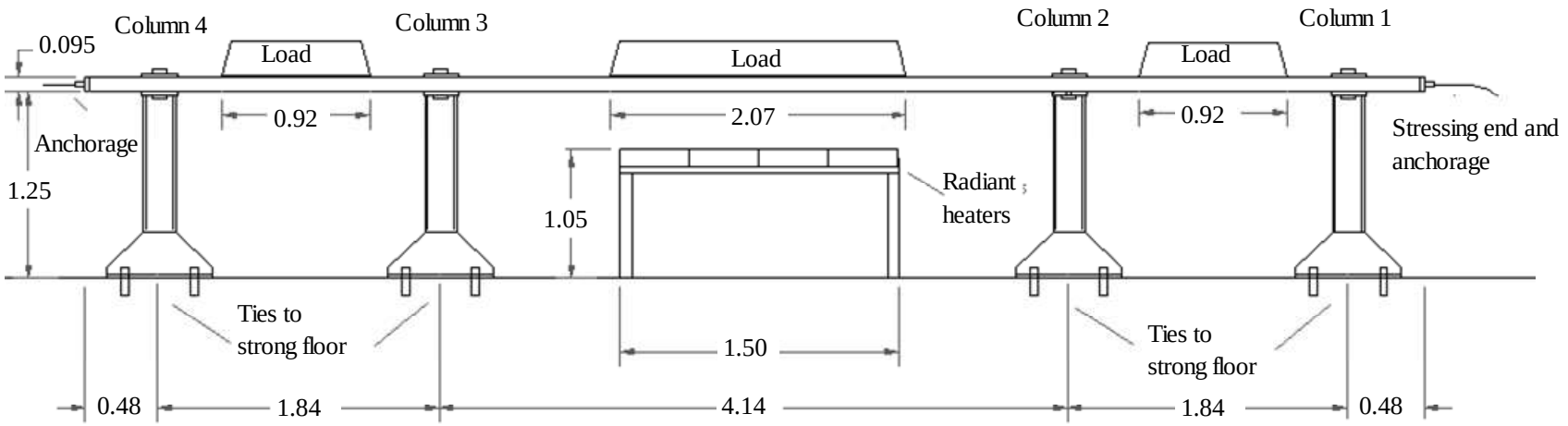

Figure 5.1: Schematic showing the test set up and selected geometry (dimensions in m, instrumentation and insulation boards not shown).

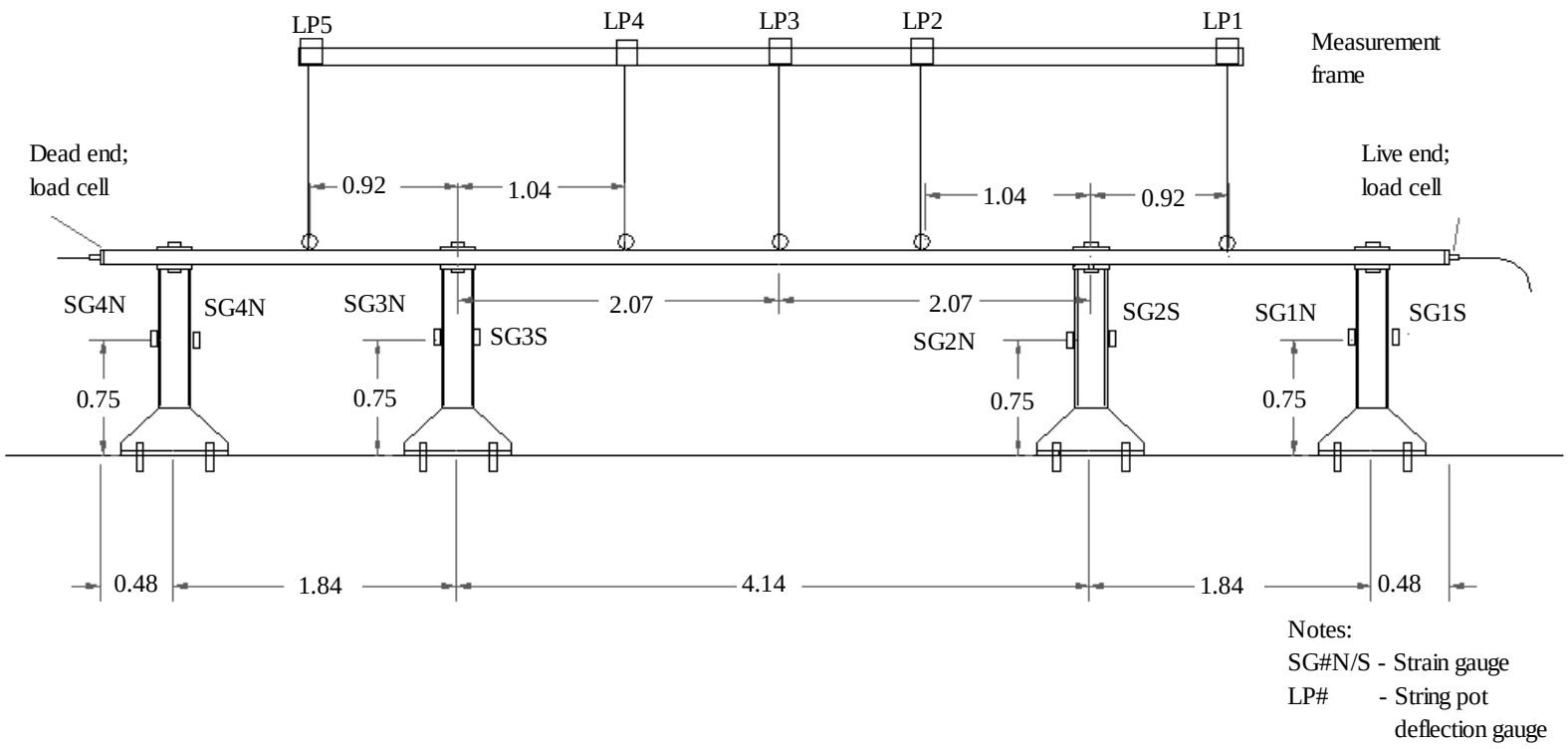

Figure 5.2: Schematic showing the instrumentation set up and selected geometry (dimensions in m, insulation boards not shown, thermocouples in Figure 5.13).

5.3 Test apparatus

In Chapter 2 it was demonstrated that most prior testing of PT concrete slabs has used materials and techniques that are too old to be representative, dimensions which cannot be considered typical of modern construction, and/or support conditions which do not resemble reality. The tests performed herein begin, for the first time, to explore these potentially important issues. The test apparatus used was shown in Figures 5.1 and 5.2.

5.3.1 Design assumptions and test limitations

Each of the slabs was precast with eight bolt hole connection points and four lift hooks. After casting and curing (for a minimum of six months) they were lifted into place on top of four semi-rigid steel columns. A rigid connection was made between the slabs and the columns, and the slabs were then post-tensioned to representative in-service prestressing levels. An imposed service loading was then applied prior to heating.

Slab dimensions

The principal goal in designing the slabs was to develop a representative, scaled, one-way spanning restrained continuous monostrand PT concrete slab. The slab spans therefore needed to be restrained vertically, axially, and rotationally at all connections. This is representative of the conditions for an interior span in a real building. It was decided to design three bays with two short cantilevers at either end. The minimum slab width-to-depth ratio was chosen as five, in accordance with CL 5.3.1 (4) of EN 1992-1-2 (CEN, 2004) so as to be classified as a slab rather than a beam. Additionally, a minimum one hour fire resistance rating was sought with respect to the slab overall thickness. The thickness and width of the slab were chosen accordingly, which resulted in a slab width of 475 mm and a total depth of 95 mm.

A minimum span-to-depth ratio of about 40 was necessary for the centre span to be representative of modern PT concrete construction. The length of the centre span was therefore taken as 4140 mm. The total length of the slab (8770 mm) was restricted by the maximum dimensions of the strong floor in the Large Structures

Test Hall at the University of Edinburgh. Cantilevers outside the end supports accommodated bursting reinforcement in the prestressing anchorage zones.

The slab dimensions are illustrated in Figure 5.3. Concrete cover was chosen to maintain a nominal one-hour fire resistance rating according to EN 1992-1-2 (CEN, 2004), with bonded mild steel reinforcing bars at 25 mm cover and tendon axis distances at 35 mm at midspan (and 35 mm to the top surface at supports). The specified drape of the monostrand seven-wire 12.5 mm diameter Grade 1860 prestressing tendon followed a parabolic profile to provide balancing of the applied service load (as would be the case in design of a real PT concrete building). The drape is illustrated in Figure 5.3. The tendons used are from the same coil as was used for the BS 5896-12 (BSi, 2012) creep and strength testing described in Chapter 4. To ensure that Slab B would have the same axis distance after tensioning as Slabs A and C, the prestressing duct for this slab was positioned before casting to account for alignment changes during tensioning. The prestressing duct was supplied by *GT Technologies*^{TM} (with 23 mm inner diameter); this prestressing duct is not shown in Figure 5.3.

The slabs were required to have sufficient positive moment reinforcement running the length of the slab to satisfy the expected lifting stresses without cracking. A custom lifting rig was constructed so as to minimize stresses during lifting and is shown in Figure 5.4. All non-prestressed steel reinforcement was 8 mm diameter deformed Grade 500 reinforcement. Negative moment reinforcement was provided over all supports, as indicated in Figure 5.3.

The final slab configuration was verified for in-service stresses, flexural, shear and final expected camber. The design is representative of a strip of a one-way PT slab that would be expected in a real building, with load balancing effects typical of real PT slabs.

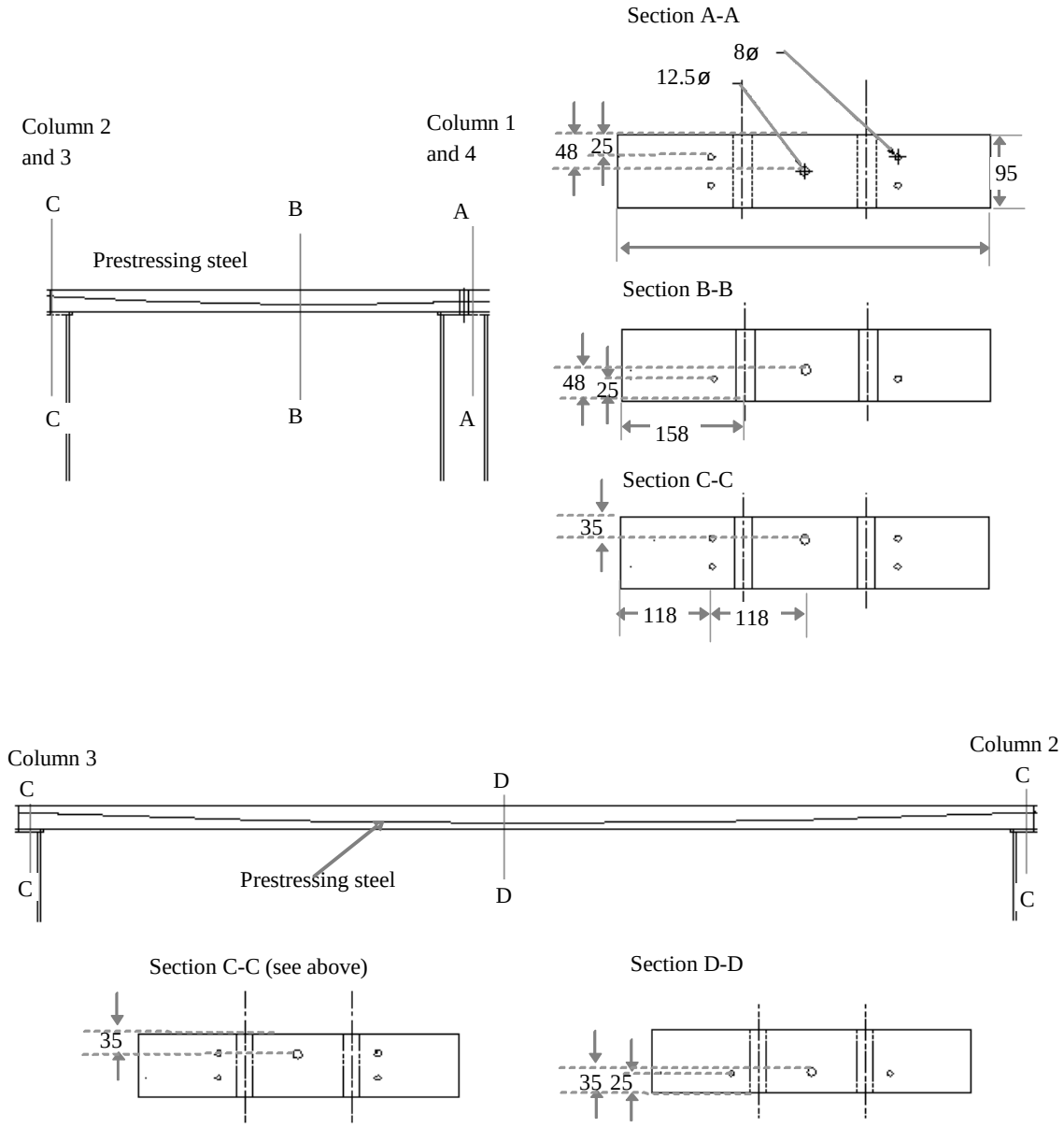

Figure 5.3: Slab dimensions including axis distance covers (to scale, dimensions in mm).

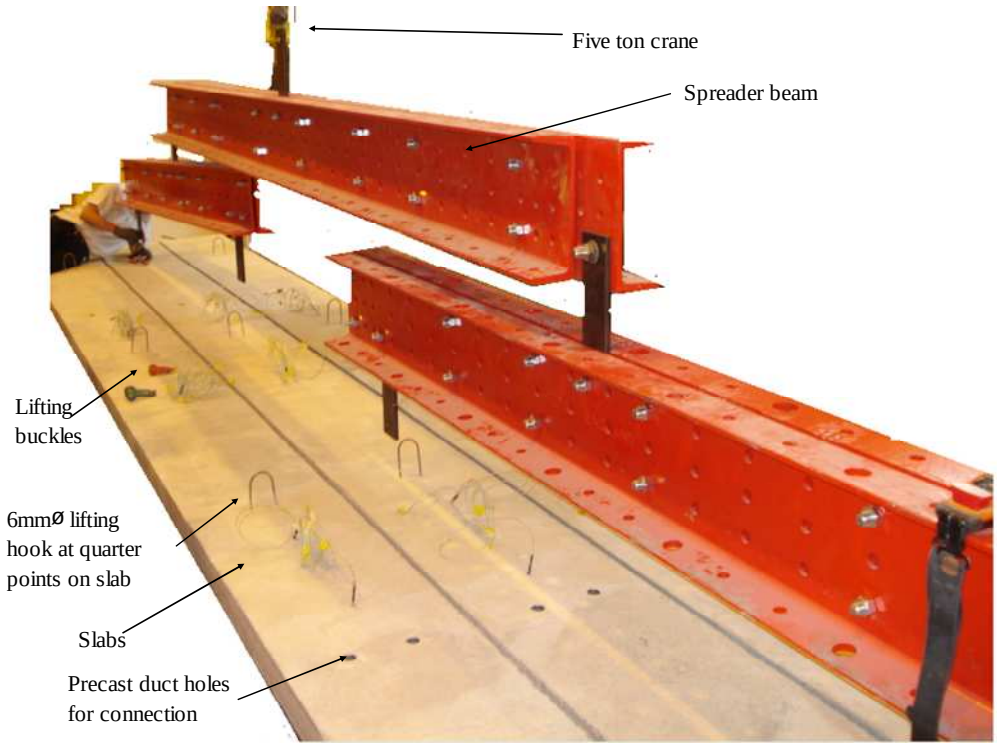

Figure 5.4: Four point spreader beam lifting rig.

Supporting column design

A set of elastic steel column supports were used to support and restrain the slabs during testing. These were designed on the basis of their axial and flexural stiffness at ambient temperature. The columns were selected based on restraining deflection compatibility described by:

$$\frac{E_c I_c}{l_c^3} = \frac{E_s I_s}{l_s^3} \qquad [5.1]$$

where E is the modulus of elasticity (compensated for reinforcement ratio in concrete), I is the columns' moment of inertia, and l represents the length of the column. Subscript s is for steel (the test columns) and subscript c represents concrete (columns to be expected in a real UPT building). A representative concrete column in a real PT building might have dimensions of 450 × 450 mm, an internal steel reinforcement ratio of 0.05%, a specified concrete compressive strength of 50 MPa, and a storey height of 2.6 m (see CPCI, 2007; CSA, 2005; CSTR, 2005). An appropriate commercially available steel section was selected to nominally match

these properties, giving a 203 × 203 × 60 I-section made from Grade 275 steel. The column height was taken as 1.25 m for convenience during testing.

Whilst care was taken to select a representative column size for the testing rig, clearly not all buildings are constructed according to the above dimensions. Real column designs will depend on the expected applied loading, floor configurations, and architectural demands, etc. This comment is especially important when considering the restraining forces induced during the tests, and is discussed in detail in Section 5.6.3.

The concrete slab-to-steel column connection was made in accordance to EC3-1-8 (CEN, 2005). A steel top plate of dimensions 475 mm × 203 mm × 25 mm, with two bolt holes cored at 20 mm diameter to allow a seat for the slab. The top plates were welded completely to the tops of the steel columns. This would minimize the flexibility of this connection. Column base plates of dimensions 700 mm × 600 mm × 25 mm, each with four bolt holes cored for 36 mm diameter anchor bolts, were added to the bases of the columns. Two plates were added to increase the rigidity of the base plate detail. Figure 5.5 gives schematics for the columns.

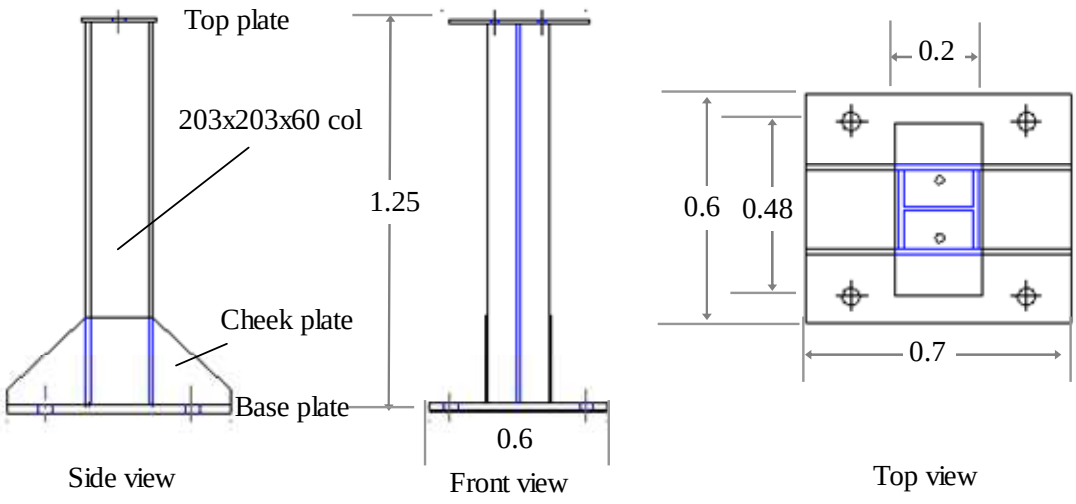

Figure 5.5: Column support schematics (dimensions in m).

Each column was bolted and tied into a strong floor using four (Grade 275) 36 mm diameter bolts through two 610 mm steel channel sections (size 150 × 75 × 18). Prior to installation of the columns on the strong floor a detailed survey of the strong floor was necessary to ensure that the column tops would be level. This was necessary to ensure that the slab would not be exposed to settling moments when placed on top of

the columns. A calibration exercise to gauge the stiffness of the column was conducted through a load unload exercise. This procedure is explained in Section 5.4.3. The columns are shown in Figure 5.6.

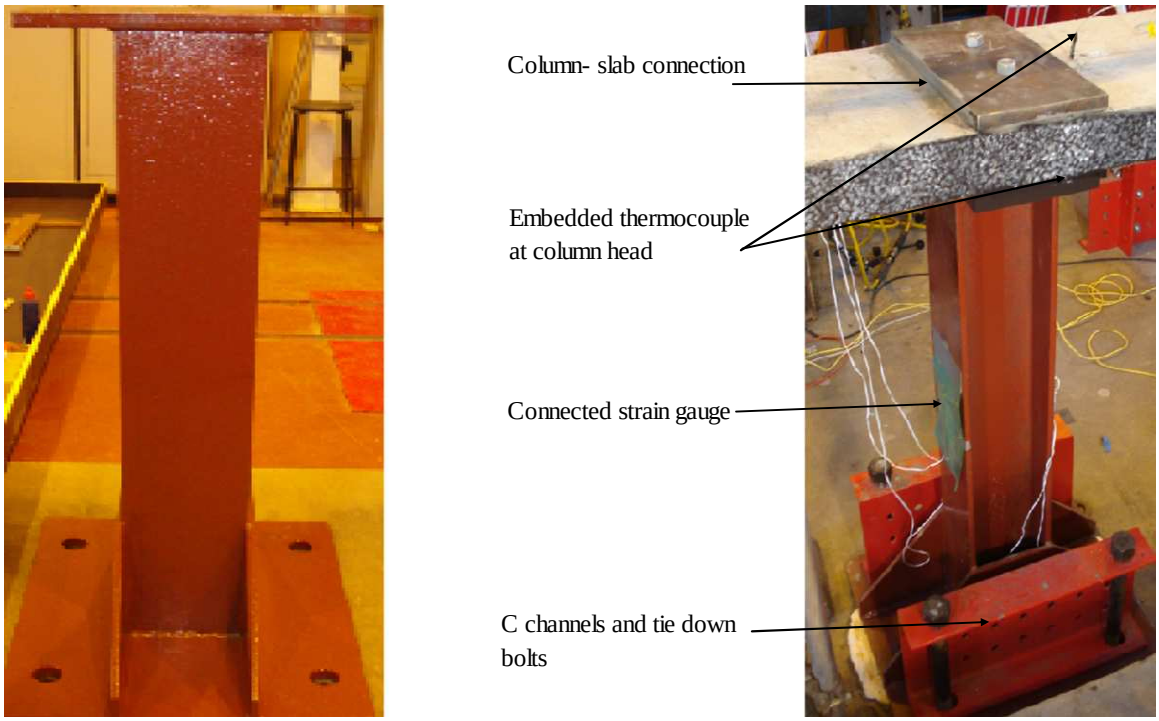

Figure 5.6: Column support (a) pre-assembly and (b) after connection to strong floor and slab.

Post-tensioning anchorage zone design

The anchorage zone reinforcement design followed guidance from BS 8110-1 (BS, 1997) and the CPCI design manual (CPCI, 2007). Bursting stresses were determined based on a 95 × 95 mm bearing plate (with prestressing anchors resting against the bearing plate). The design included reinforcement for spalling, bearing, and end stress accumulation at transfer during jacking. This design was meant to accommodate a 130 kN applied load on the surface of the concrete, whereas in the tests the prestressing steel in the slabs was tensioned to approximately 125 kN before losses. All reinforcement links in the bursting zone were made of 6 mm diameter mild steel reinforcement (tensile strength 610 ± 5 MPa). Coiled reinforcement with 3 mm diameter and tensile strength of 355 MPa was used for confinement of the bursting zone. The assembled anchorages for both live and dead ends are illustrated

in Figure 5.7, including the load cell and barrel wedge anchors. An adjusting screw was also installed in the dead end anchorage (Figure 5.7); this was used to help de-tensioning the unbonded prestressing steel after testing.

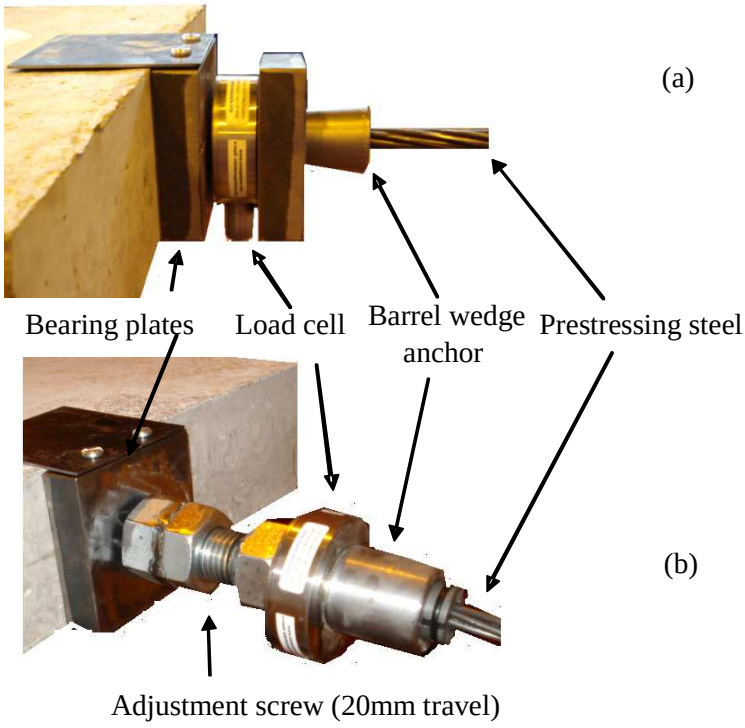

Figure 5.7: (a) Stressing (live) end and (b) dead end.

To simulate a smaller heated length ratio without exceeding the dimensions of the strong floor an industrial spring mechanism was built and installed at the dead end anchorage for Slab C. The anchorage system (shown in Figure 5.8) was constructed with 36 disk springs (200 mm outer diameter, 102 mm inner diameter, and thickness 5.5 mm with an uncompressed height of 12.5 mm) stacked in series and enclosed within a cylindrical steel shaft. The spring assembly was connected to a fixed bearing plate which rested against the end of the slab. A second ‘free’ plate acted on the top of the spring stack inside the sheath. A hole through the spring assembly allowed the tendon to pass through its centre. Thus, when the prestressing tendon was tensioned the free bearing plate compressed the spring stack.

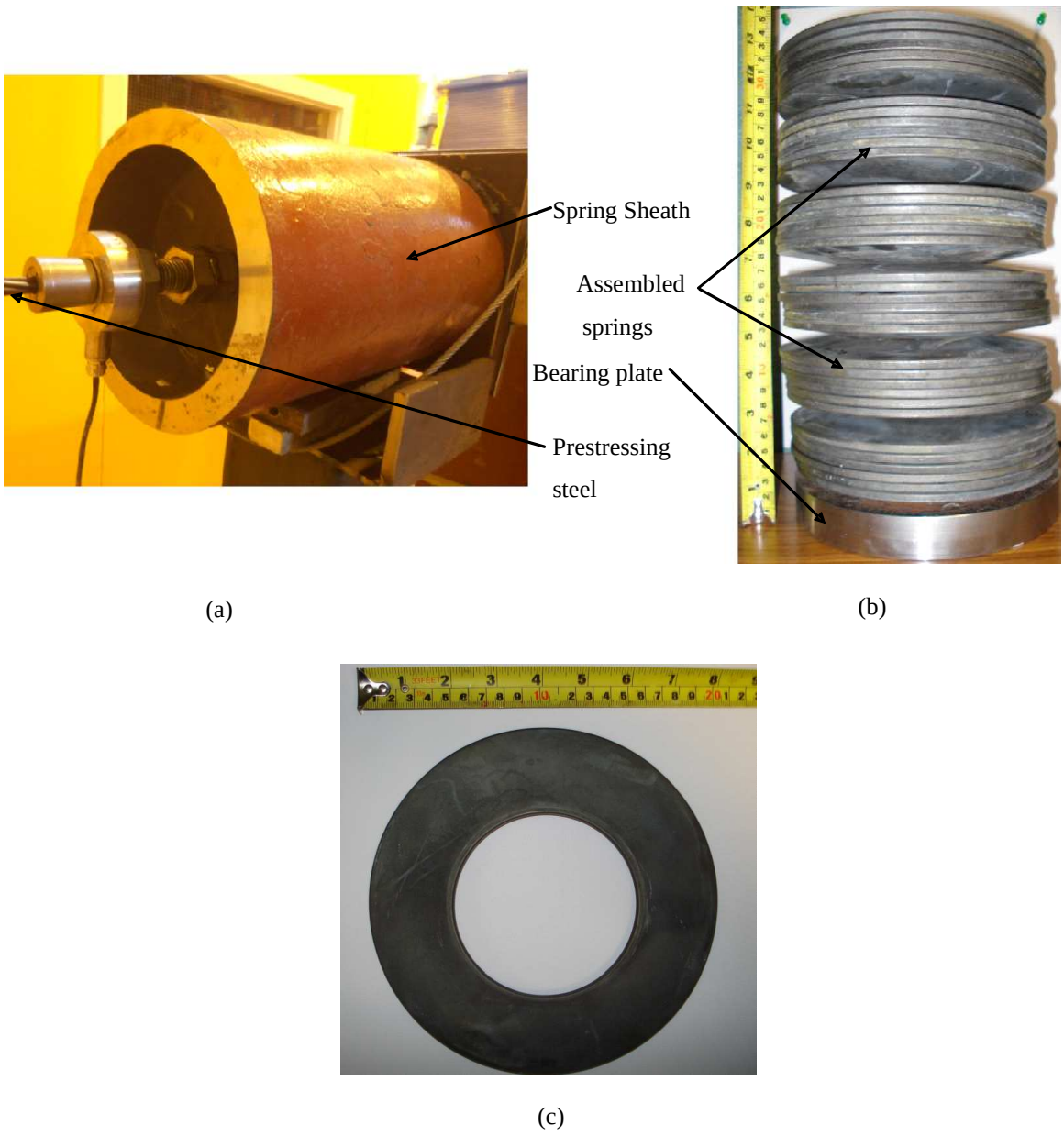

Figure 5.8: (a) Full spring assembly bearing on slab end, (b) spring stack, and (c) individual spring disk.

The compression of the spring stack is representative of a decreased effective stiffness of the unbonded tendon, thereby simulating the structural effects of a longer unbonded tendon length. A calibration exercise on the disc-spring anchorage (compressed under load using the Instron 600LX testing frame described in Chapter 4) confirmed the added simulated tendon length as an additional 8.5 m, simulating a total tendon length of approximately 17.3 m as opposed to the true length of 8.8 m. The spring stack calibration results are given in Figure 5.9.

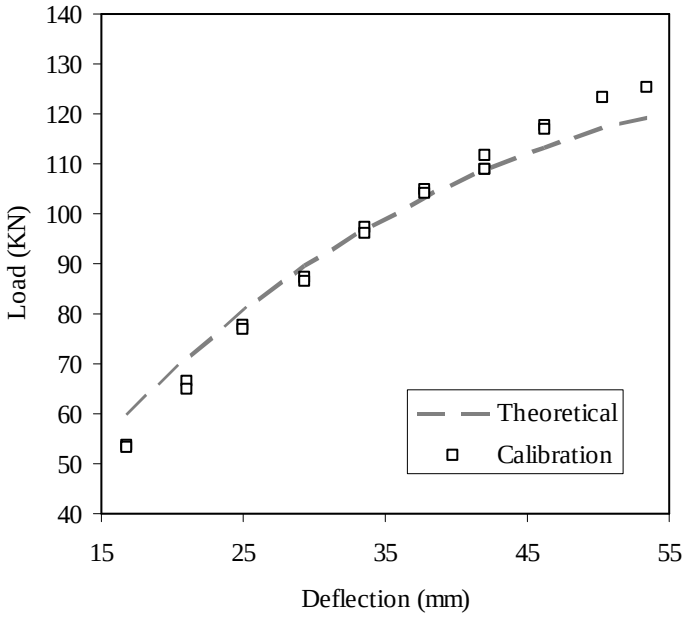

Figure 5.9: Disc spring calibration versus theoretical calibration.

5.3.2 Applied loading

The fire test load ratio, η, represents the applied loads (self weight plus partitions and imposed loads) divided by the predicted capacity of the slab at ambient temperature. From a practical perspective, owing to the small number of slabs which could be cast and tested due to time and space limitations, no slabs were tested to failure at ambient temperature. This necessitated a theoretical analysis of the ambient temperature strength. This analysis is included in Appendix D.

The capacity of a PT slab will be influenced by the loading configuration, span to depth ratio, unbonded tendon length, etc (Allouche et al., 1998; 1999). When prestressing steel is unbonded, simple flexural strain compatibility cannot be relied on as is the case bonded tendons. The theoretical capacity for the base case (Slab A) was approximated as 7.3 kN·m using guidance from CSA (2005) and Ghallab (2013); the latter reference giving a review of available load capacity calculation methodologies. Applied distributed loading for each span was provided using 70 individually weighed lead weights, applied over the central half of each span (see Figure 5.1). This was maintained constant throughout heating and gave η equal to 0.42 with respect to the theoretical capacity of Slab A at ambient temperature (assuming all material safety factors taken as unity). A load ratio of below 0.5 can be considered a likely service condition in the event of a fire (Buchanan, 2001).

5.3.3 Heating array

An array of four radiant heaters, each constructed of cast-iron bodies with ceramic combustion surfaces, was mounted on a horizontal steel frame in order to heat the slab. Figure 5.10 shows the heating assembly. Figure 5.11 shows the heating array in-situ underneath a slab during testing, with attached ceramic fibre boards to prevent direct heating of adjacent portions of the slab and the supporting columns.

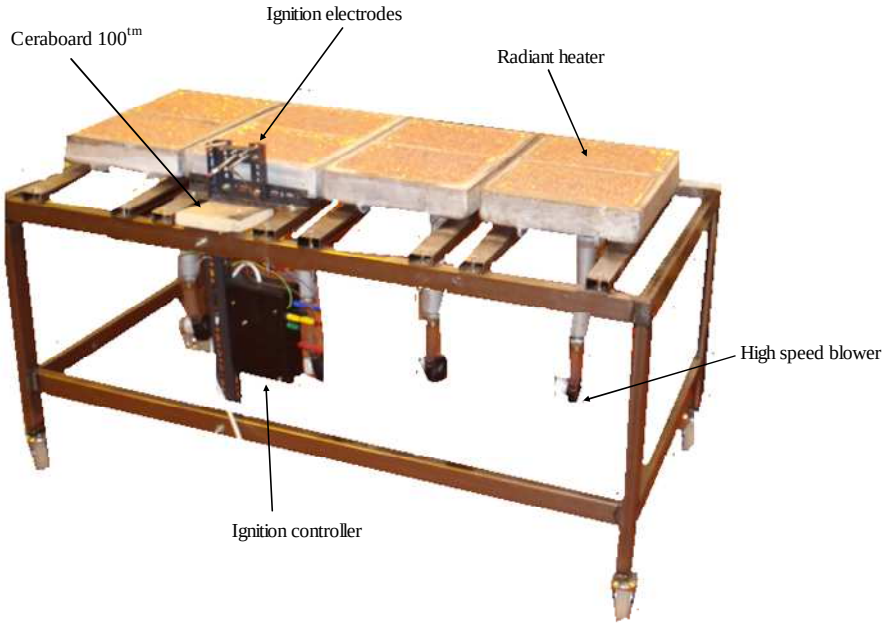

Figure 5.10: Radiant panels and heater assembly (debris cage installed for spalling protection not shown).

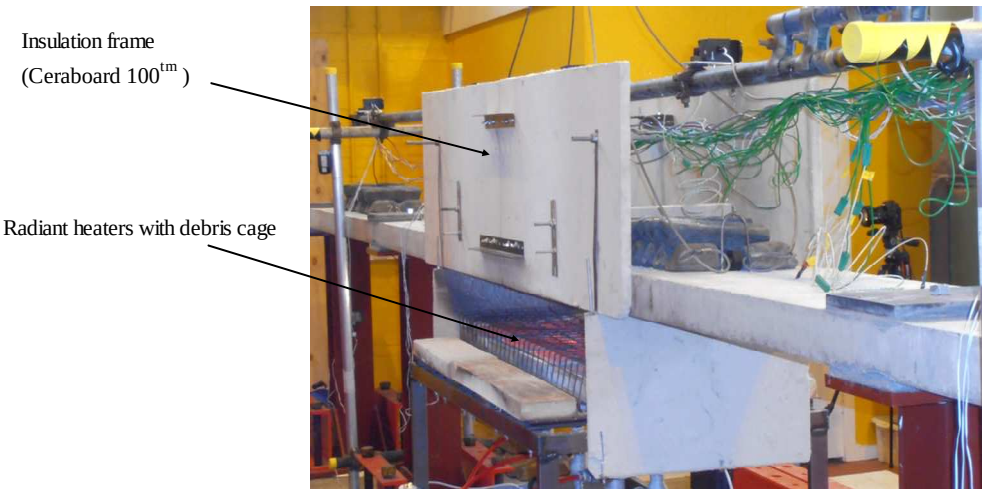

Figure 5.11: Radiant heater assembly in use during test.

Propane and air were fed into mixer valves mounted on the back or each panel. Air was supplied by four electric blowers. A mass flow controller was used to

regulate the gas flow upstream of the gas manifold, and the flow of propane was maintained at 1.4 g/s during all tests. The burners were lit with automatic sparkers. The radiant panel heater array had a total length of 1500 mm and width of 480 mm, with an intention to subject the slabs to uniform heating over their central spans; or about 17% of their total tendon length. It is noteworthy that Slab C, with additional spring-simulated tendon length, had a simulated heated length ratio intended to be 9~10%.

Due to heat losses, the heating system used cannot apply heating as severely as would occur during a 'standard' ASTM E119 (ASTM, 2001) or ISO 834 (ISO, 1999) time-temperature curve; however the intent of the current experimental programme is to investigate possible structural performance of PT structures under well defined heating and to generate thermal data for future numerical modelling techniques and design, rather than to develop certification with standard fire resistance ratings which may have little bearing on reality. The temperatures achieved during testing are discussed in Section 5.6.1.

5.4 Instrumentation

An instrumentation schematic is provided in Figure 5.2. Four main types of measurements were of interest during the experiments: (1) temperatures, (2) tendon load (stress) levels, (3) column strains, and (4) slab deflections. A Vishay Measurements Group™ System 7000 data acquisition system was used to record all sensor data from the instrumentation during testing.

5.4.1 Slab temperatures

Slab temperatures are crucial for predicting unbonded prestressing steel tendon stress relaxation and the thermal/structural response of the slabs. Type K thermocouples were cast into each slab to provide thermal data during testing. As designed, thermocouples were placed at mid span, with three thermocouples installed across the exposed soffit of the slab, two thermocouples within the concrete at the axis distance of the prestressing steel tendon, one thermocouple at the depth of the flexural reinforcing steel, and two thermocouples along the unexposed (top) surface. One supporting column adjacent to the heated central span was monitored for

temperature changes, with thermocouples placed along the head of the column. Additional thermocouples were installed at the quarter points of the central span.

Unexposed surface temperatures of the slab were measured with thermocouples consisting of ceramic fibre wool and aluminium tape padding (see Figure 5.12). All thermocouple locations are shown in Figure 5.13. While care was taken to ensure instrumentation was functional for testing, some thermocouples could not be used due to the unavailability of sufficient data channels. The location of thermocouple instrumentation at mid span was verified after testing for all slabs and found to be within ± 2 mm (see Section 5.7).

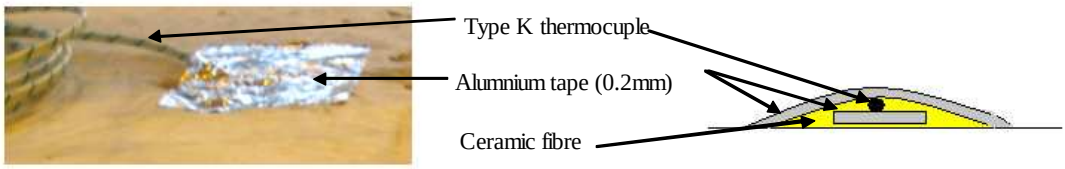

Figure 5.12: Surface thermocouple treatment and placement.

A thermal imaging camera (FLIR A320A) was also used to record the spatial and temporal distribution of slab exposed soffit temperatures during heating. This system was used to gauge the uniformity of heating of the slab's exposed soffit, to identify pockets of high temperature, observe possible cracking, and indicate the time(s) at which any spalling occurred. The thermal imaging camera data were compared against the exposed soffit thermocouples (as discussed in Section 5.6). It is noteworthy that in a traditional standard fire furnace test it would be impossible to measure soffit temperatures in this manner, since furnace construction prohibits a full view of the heated region. The data from this camera will be invaluable for future computational modelling efforts and validation.

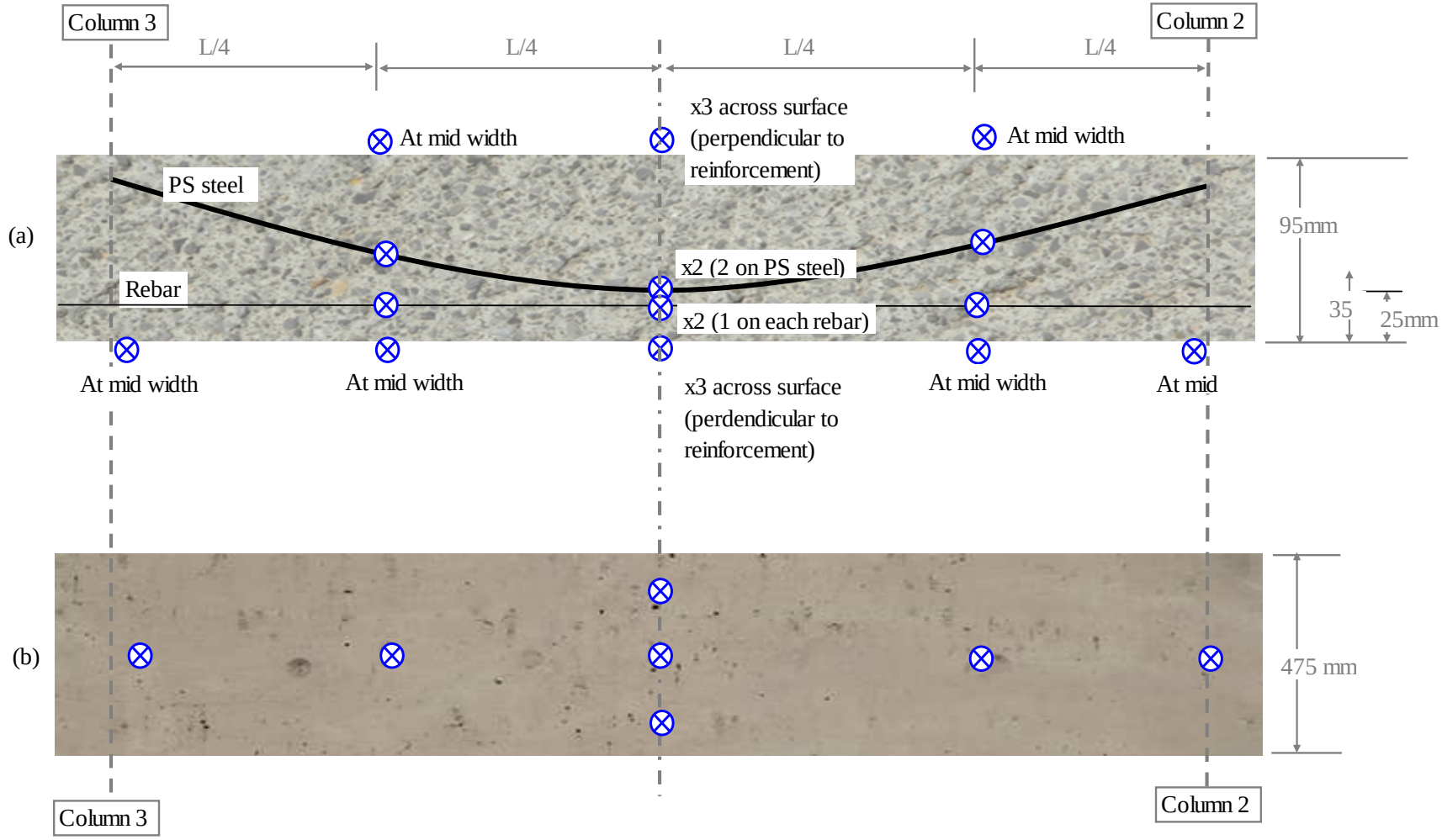

Notes: *L= length of slab, 4140mm* *= Thermocouple (surface thermocouples embedded at 1mm)*

Figure 5.13: Thermocouple locations shown for mid span of slab.

5.4.2 Tendon stress levels

Two through-hole load cells were installed at both the 'live' (jacked and anchored) and 'dead' (anchored) ends of the prestressing tendon in each slab to measure tendon stress levels before, during, and after fire testing (see Figure 5.7). These were calibrated prior to and after the heating experiments and no significant differences were observed. Tendon stress in this chapter is indicated by dividing the average value of the load cells by the nominal tendon area of 93 mm^2.

5.4.3 Column strains

Column strains were measured to give an indication of the resulting longitudinal restraint forces generated during testing. Column strains were measured by two FLA-3-23 TML^{TM} (3 mm gauge length) unidirectional bonded electrical resistance foil strain gauges mounted on each column face. The gauges were mounted 750 mm from the base of the columns; this being half the distance between the top of the column cheek plates and the top plate (see Figure 5.2). To verify the calibration of the gauges against temperature changes during the course of testing, temperatures were monitored adjacent to the strain gauge at Column 3 during every test. The strain gauges were compensated for temperature changes using manufacturer specifications, however it should be noted that the steel temperature actually changed during testing and thus experienced thermal expansion which was also recorded by the gauges, thus complicating data analysis significantly. Every ºC change in temperature of the steel columns induced approximately 12 με in the steel (Ghosh, 2009). This is discussed further in Section 5.6.3.

The strain gauges installed on the supporting columns were calibrated by applying known loads to the columns with hydraulic jacks and measuring the resulting column strains at various locations (see Figure 5.14a). A load/unload exercise was performed on each column, such that recorded microstrains could be converted to restraining force (kN) with an R^2 value of more than 0.99. The column configuration was loaded and unloaded on the top plate. Restraining forces described herein are relative to that position on the column.The resulting calibration records can be consulted in Figure 5.14b and Table 5.2. This allowed determination of the columns' true loading response.

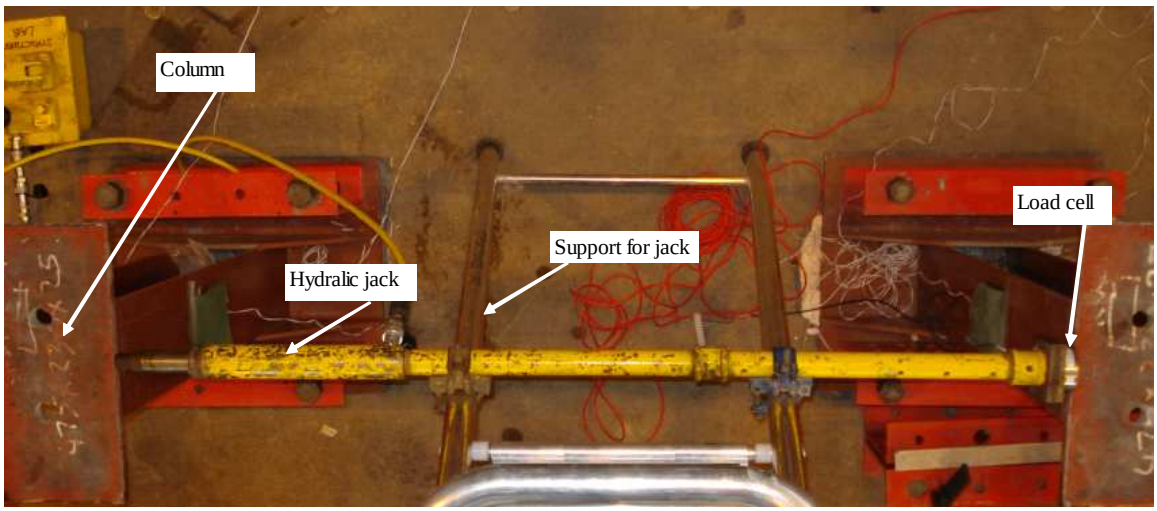

(a)

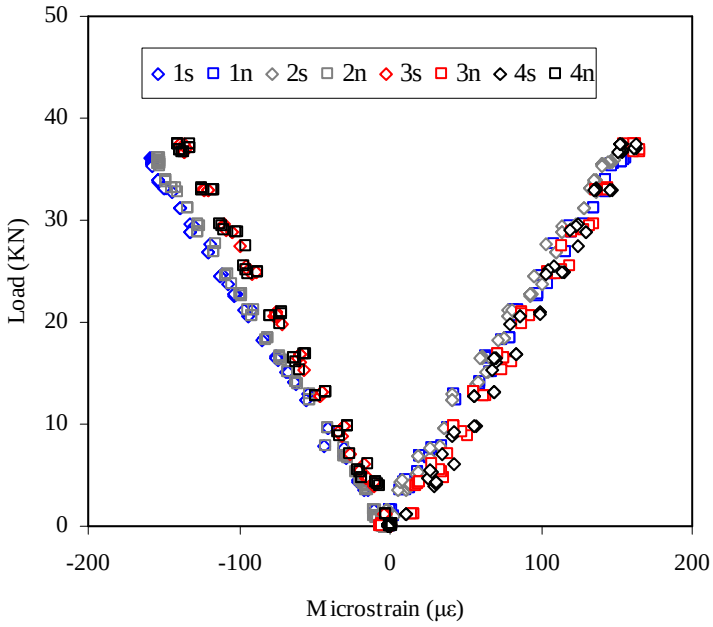

(b)

Figure 5.14: Column calibration (a) set up and (b) results.

Since the slabs were exposed to thermal gradients, there is no accurate way to determine the exact position of thrust against the supporting columns, and therefore axial forces in this chapter are estimated assuming thrust at the mid-depth of the column top plate. Strain gauges were placed within 2 mm of the location shown in Figure 5.2.

Table 5.2: Column calibration coefficients.

Column strain gauge	Strain (με) to load (kN) Coefficient
SG1S	0.23
SG1N	0.23
SG2S	0.24
SG2N	0.24
SG3S	0.27
SG3N	0.23
SG4S	0.24
SG4N	0.27

Notes: Column gauge locations can be referred to in Figure 5.2.

5.4.4 Slab deflections

A protected instrumentation frame was installed above each slab during testing. The frame was used to support five (string pot) position transducers to measure slab deflections as well as acting as a support for cables from all sensors (see Figure 5.2). The frame was protected from heating effects with one inch Ceraboard 100^{TM} fibre boards (Figure 5.11). One thermocouple was installed to monitor the temperature of the frame.

Five Celesco^{TM} string-pot position transducers with a measurement range of 127 mm were used to measure slab deflections. Figure 5.15 shows their attachment from the instrumentation frame and the top surface of the slab.

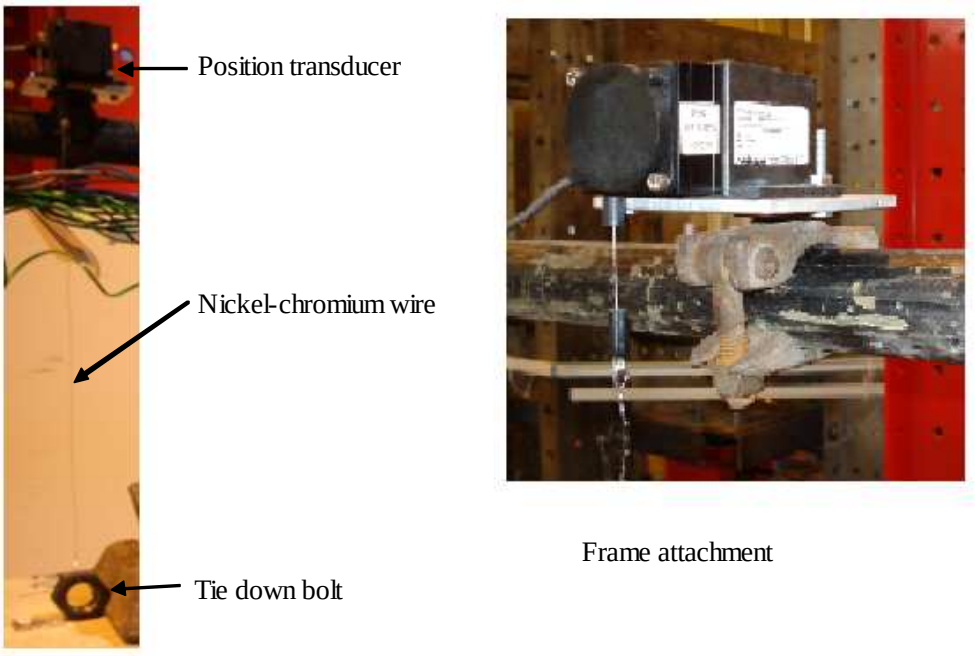

Figure 5.15: String pot position transducer configuration.

These were connected using heat resistant nickel-chromium wire attached to a bonded steel bolt at the slab surface, and placed at mid span and span quarter points

of the central bay (see Figure 5.2). The deflection at midspan of the outer bays was also monitored. Position transducers were placed within 1 cm of the locations specified.

5.5 Testing procedures

This section describes the procedures used, from casting of the slabs, through testing, to decommissioning. Selected measurements are given where they affect the test procedures used.

5.5.1 Casting and assembly

The as-constructed reinforcement diagram for Slab B is shown in Figure 5.16. These images were taken prior to casting the concrete. A levelled steel channel bed was constructed below the formwork to guarantee that when the slabs were cast they would have the specified thickness along their full length. Slabs A and C were constructed identically to Slab B; however without tendon ducting or grout vents as indicated in Figure 5.16.

To guarantee the as-designed tendon drape and concrete cover to the reinforcement, hand cut concrete chairs of variable size were installed below the reinforcement. A total of 15 blocks were used to support the prestressing steel and plastic ducting along the length of the slab. Twelve concrete chairs were used to support each non-prestressed reinforcement bar. Ten reinforcement links were added to support the negative moment tensile reinforcement. Steel wire (diameter 2 mm) was then used to guarantee fixity of the steel and chair to the film-faced formwork (Figure 5.17) and to prevent reinforcement from floating during concrete casting operations. Embedded thermocouples were fixed at the appropriate locations. Two vertical anchor tubes were cast at each column location. Lifting hooks were also installed at the slabs' quarter points. These were placed outside of the heated region.

Slab B, with bonded prestressing, had a small hole drilled in the top of the plastic prestressing duct near mid span, adjacent to the grouting vent. Two thermocouples were inserted into the duct to monitor temperatures within the duct during testing. The precise positioning of these thermocouples was therefore unknown; however they were verified by excavating after testing.

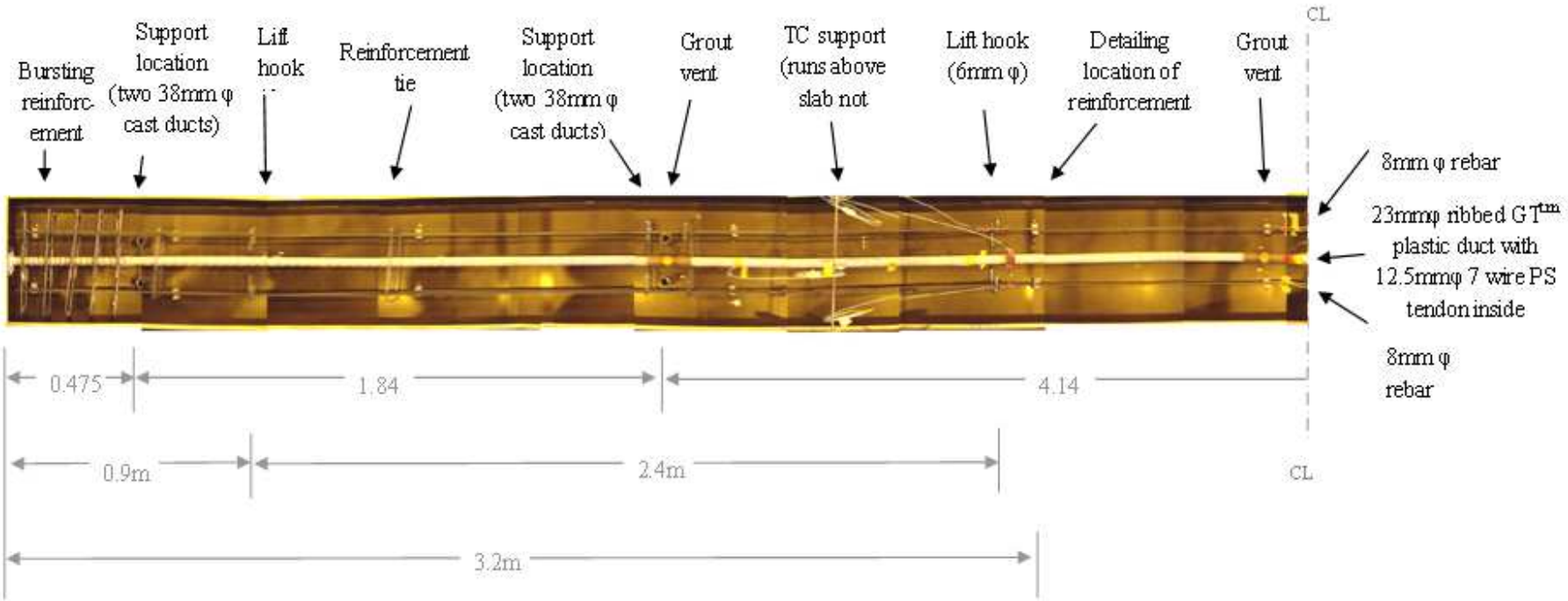

Notes: *Slab B is built symmetrical about the center line. Slabs A and C use one unbonded seven wire tendon rather than a cast plastic cast duct with tendon. All slabs are built identically within +/-5mm.*

Figure 5.16: Slab B panoramic photo take just before casting the concrete

Figure 5.17: Unbonded tendon on a concrete chair tied down to form work.

All three slabs were cast using ready mix RC40/50 concrete (see Figure 5.18). The specified maximum aggregate size was 10 mm. Additional cubes (100 mm × 100 mm) and cylinders (100 mm diameter × 200 mm tall) were cast concurrently and cured next to the test specimens. Three cubes and three cylinders were tested at 28 days in accordance to BS EN 12390 (2000) parts 1 to 8. The cubes had a compressive strength of 41 ± 2 MPa (average ± standard deviation), whereas the cylinders had a split cylinder tensile strength of 2.8 ± 0.5 MPa. The non-prestressed 8 mm diameter reinforcement tested to an ultimate strength of 658 ± 7 MPa (this is inline with similar reinforcement described in Elghazouli et al., (2009) tested to 624 MPa), and the prestressing tendon's centre wire was tested to 2033 ± 11 MPa ultimate strength. The slabs were left to cure for more than six months (being cast during November 2011 and tested beginning June 2012).

(a)

(b)

Figure 5.18: (a) Slabs before casting and (b) slabs after casting

5.5.2 Lifting

The slabs were lifted onto their supports according to lifting guidelines set out by the CPCI (2007) design manual using four hoist points made out of 6 mm diameter mild steel reinforcement (Figure 5.16). A layer of approximately 1 cm deep cementitious grout, consisting of one part Portland cement and three parts siliceous sand (with maximum diameter 0.5 mm) by mass with a water-to-cement ratio of 0.4, was placed on each column head prior to seating. The slab was then placed on this grout and enabled to settle naturally so that the slab would not crack during seating. For each column-slab connection, two 20M Grade 10.9 bolts were inserted into the precast column ducts which were cast into the slabs. These ducts were then also grouted to create a rigid connection between the slab, column, and bolt. A top layer of grout of

about 1 cm thickness was added, a rigid steel plate (identical to the column top plates) was placed on top of the grout, and the bolts were tightened (see Figure 5.6). This process was repeated for all four columns, creating four semi-rigid connections between the slab to be tested and the column supports; thus simulating as much as possible the conditions that would be found in a real multi-bay building.

5.5.3 Tendon stressing

Slab stressing operations are hazardous and as a result they were performed by an external contractor, ConForce UK, who performed this duty as an in-kind contribution to the project. The tendons in all slabs were stressed to approximately 1341 ± 7 MPa (about 125 kN). The slab was stressed in three ramps of approximately 450 MPa each during one hour. When the target load (near 70% of the tendons' ultimate tensile strength) was achieved the prestressing anchors were set and the jacks released and removed. The subsequent phase of testing did not commence until prestress loss differences during any consecutive 24 hour interval was less than 0.5 MPa. This was necessary so that short-term creep losses in the slabs would not influence the heating tests.

The unbonded slabs were then loaded, whereas the bonded slab was grouted prior to loading. The bonded PT slab was grouted with Parex^{tm} cable grout (65 MPa compressive strength after 28 days) inside the embedded plastic monostrand cable duct. This work was also performed with the assistance of ConForce UK. Loading commenced two weeks after grouting in this case. For all slabs, after seating and short term losses, average tendon stress stabilised near 1165 ± 13 MPa on the day of testing – this is a realistic in-service stress level for post-tensioned tendons in a real building.

5.5.4 Loading

Slabs were loaded with lead weights. Each lead weight was weighed, sequentially numbered, and placed identically for each slab. Placement of weights was as shown in Figure 5.1. The expected theoretical deflection from the lead weights at mid span for the continuous slab was predicted to be 2.1 mm. The actual short term deflection prior to testing was measured as 1.6 ± 0.5 mm. Less than 10 MPa of tendon stress

increase (due to tendon elongation from deflection) was observed in any test during or after loading. In all cases there was a minimum one week interval between loading and heating.

5.5.5 Heating

Slabs A and B were heated locally with the radiant heaters until it was assured that the presumed 'critical temperature' of the prestressing steel tendon was reached, according to EN 1992-1-2 (CEN, 2004) (i.e. until 350ºC was recorded at the tendon location). This resulted in total heating times of approximately 200 minutes and 215 minutes for Slabs A and B, respectively. Slab C was heated until the higher critical temperature used in North American guidance (IBC, 2012; Abrams and Cruz, 1961) was reached (i.e. until 426ºC was measured at the tendon). This resulted in a total heating time of 270 minutes for Slab C. After these criteria were achieved the propane supply was turned off and the radiant heaters were removed from beneath the slabs to allow them to cool to ambient temperature. Each slab was continuously monitored for 24 hours during both the heating and cooling phases.

After cooling, Slabs A and B were heated a second time until the tendon reached a temperature close to 426°C. This resulted in an additional heating time of approximately 190 minutes in both cases.

5.5.6 Post-test examination

Because the true ultimate capacities of the PT slabs at ambient condition were unknown, a residual capacity test to failure had little scientific value for comparison purposes. Therefore the slabs were not loaded to failure after heating. However the unloading behaviour of the slabs was of interest to study the residual deflections after the applied load was removed. After unloading, slabs A and C were de-tensioned. All parameters were monitored during de-stressing and the amount of post-test camber was compared to the original camber imposed during the prestressing operations. The tendons were then extracted and analysed for their residual properties. Finally the slabs were cut in two and removed from the laboratory. Thermocouple placements were then verified by excavating from the concrete. Four moisture content samples were extracted in the anchorage zones of both ends of the slab (the

unheated portions of the slab). The grout from Slab B was also tested for moisture content. All moisture contents were determined by dehydration mass loss following heating at 120°C for two days.

5.5.7 Safety considerations

Post-tensioning operations have inherent risks. A number of measures were taken during the experiments to ensure the safety of all involved personnel. The primary concern was the potential for tensile rupture of the stressed prestressing steel while testing. If the tendon broke during testing there was a concern for safety. An additional concern was the safety of individuals near the radiant heater system during testing. As such, and despite the best efforts to ensure proper instrumentation performance throughout the tests, no risks were taken to re-apply or modify instrumentation near the live tendons or radiant heaters during testing. This was an issue during testing of Slab C for which two strain gauges malfunctioned on Column 1 near the anchorage at the start of the test. No attempt was made to remedy this during the test. And hence the data were lost. Additionally, because of the risk of slab collapse during cooling, the radiant heaters were removed from underneath the slab during cooling, thereby blocking the thermal imaging camera.

5.6 Observations and discussion

The results of the slab tests in heating and in cooling are provided in this section. Where appropriate, further details of the experiments and procedures are given. Several important, interrelated structural responses are considered in sequence: (1) slab temperatures, (2) tendon stress and strength, (3) restraint development, and (4) deflection behaviour.

5.6.1 Slab temperatures

Exposed soffit temperature observations

The repeatability of heating exposure for the tests is crucial for making comparisons between the respective slab responses, and this is influenced primarily by the consistent performance of the radiant panel assembly (both spatial and temporal) between tests. Since on first heating the material properties of the slabs were

expected to be similar, a comparison of recorded exposed soffit temperatures in tests A, B and C is useful to compare the consistency of the heating provided. Tests A.1 and B.1 are not used for this comparison since material degradation would have affected heating behaviour.

Table 5.3 presents temperature-time data for the slab soffit at midspan from thermocouples up until three hours during tests A, B and C. Averages within the table are calculated from the exposed soffit thermocouples for each test. This represents three thermocouples for Slab A and C, and two thermocouples for Slab B. (one thermocouple in Slab B failed during testing). A full average of all eight thermocouples and the resulting standard deviation is also tabulated. Slab C was heated for a longer total duration, so Table 5.3 includes data only up to three hours of heating.

Table 5.3: Comparison of exposed soffit temperatures at mid span for Tests A-C.

Test time (mins)	Test A °C		Test B °C		Test C °C		Averaged results °C[C]
	Average	Standard deviation	Average	Standard deviation	Average	Standard deviation	
30	426	10	428	43	379	7	409+/-21
60	498	29	496	46	454	7	481+/-32
90	522	24	525	29	488	7	510+/-25
120	559	47	539	27	511	9	536+/-36
150	602	45	557	21	532	16	565+/-42
180	593[b]	-	571	17	564	48	-

[a] Data for Test B is based on 2 thermocouples due to an instrument malfunction
[b] Data is based on only 1 thermocouple so no deviation could be calculated
[c] Average and standard deviation data is based on 8 thermocouples for Tests A-C

In general there was reasonable consistency of heating between all three tests, confirming the repeatability of testing using the radiant heater assembly. The complete heating cycle of the exposed soffit thermocouple at mid span below the tendon for tests A, B, and C is shown in Figure 5.19. A dip in the measured temperature for Slab A (during Test A) was caused by the radiant heaters being turned off temporarily when a ‘blow-back’ occurred and the heaters had to be re-lit.

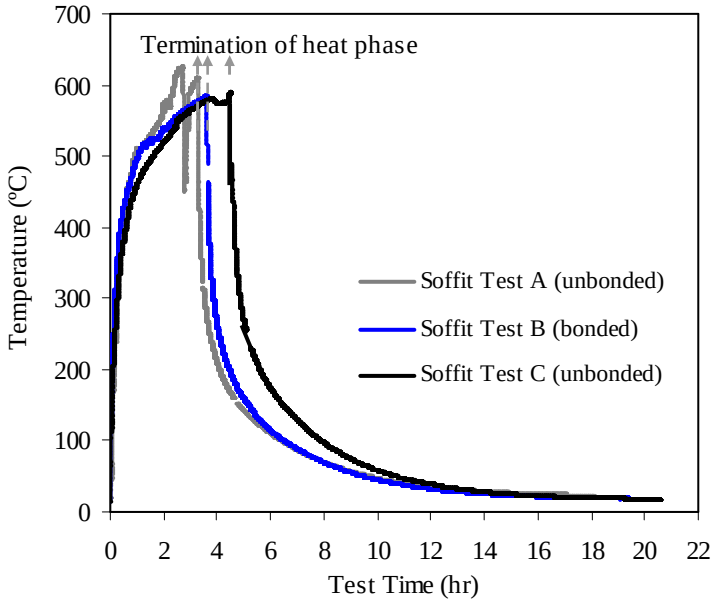

(a)

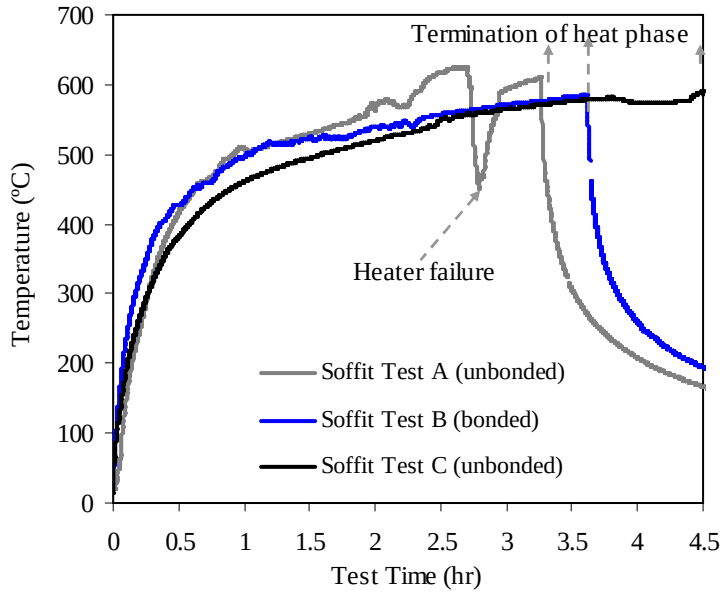

(b)

**Note that the average for slab A is from a single thermocouple beyond 3 hours due to instrumentation failure*

Figure 5.19: (a) Comparison of averaged exposed soffit temperatures of slab at mid span as measured by thermocouples and (b) with time scales adjusted.

To explore possible spatial distributions of temperatures along the exposed soffit a thermal imaging camera was used. The thermal imaging data were also compared to the thermocouple data for verification purposes. It was expected that

there might be some non-uniformity in heating; however the maximum standard deviation observed along the length of the prestressing steel tendon according to the thermal imaging data was never greater than 40°C during any test (see Table 5.4).

Table 5.4: Averaged exposed soffit temperatures using thermo camera at mid span for Tests A–C.

Test time (mins)	Test A °C		Test B °C		Test C °C	
	Average	Standard deviation	Average	Standard deviation	Average	Standard deviation
30	442	31	446	31	435	32
60	522	34	502	39	487	27
120	567	40	530	24	526	28
180	585	37	551	23	559	32

Notes: Values are representative of nine equally spread data points along the heated portion of the soffit.

Thus there was reasonable uniformity of heating over the entire heated region. Figure 5.20 gives a comparison between thermocouples in Test A with the thermal imaging data.

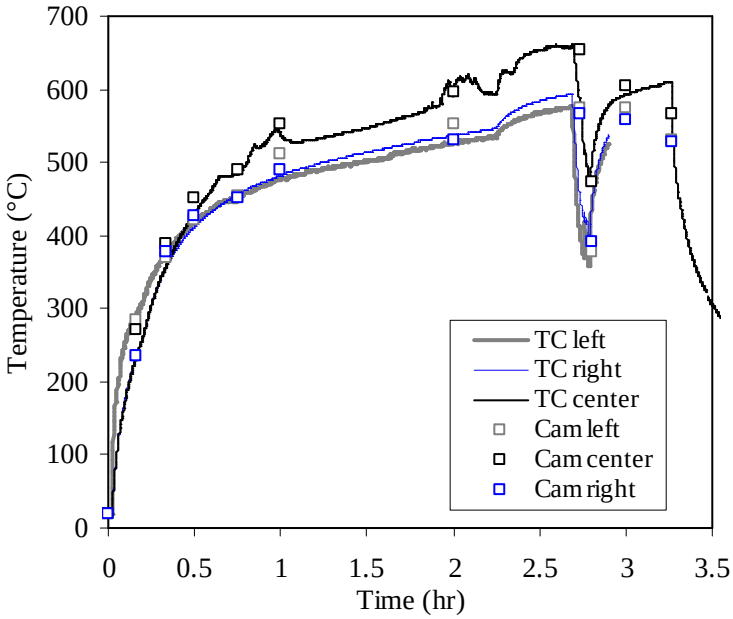

Figure 5.20: Comparison of exposed soffit temperatures of slab at midspan using thermocouples (TC) with thermal imaging camera (Cam) for Test A.

The same comparison is shown for Tests B and C in Figure 5.21. The data indicate good correlation between the thermal imaging camera and the thermocouples.

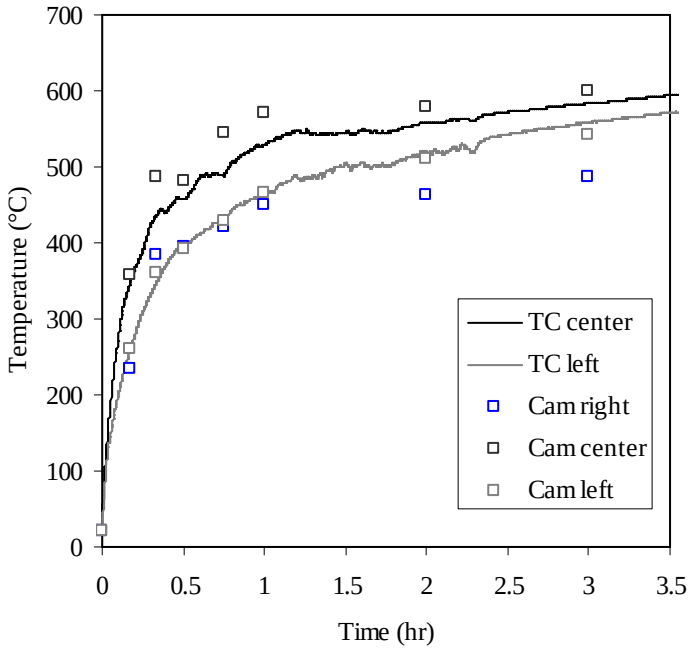

(a)

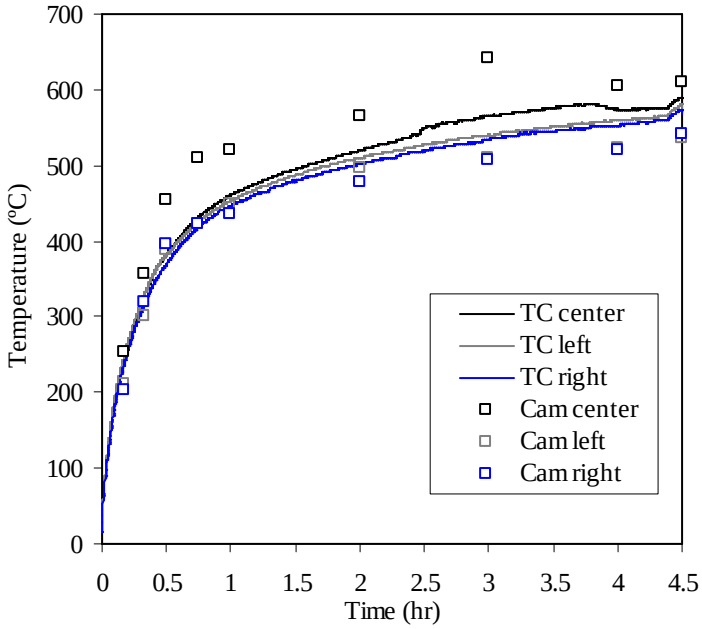

(b)

Figure 5.21: Comparison of exposed soffit temperatures of slab at midspan using thermocouples (TC) with thermal imaging camera (Cam) for (a) Test B and (b) Test C.

It is expected that changes in the concrete (predominantly from dehydration) will affect the slabs' thermal properties on second heating. Using the same heating

configurations slabs A and B were heated a second time. The second heating, and subsequent cooling of the slabs can enable deeper understanding of concrete behaviour at high temperatures. Figure 5.22 gives a comparison between the exposed soffit temperatures measured at midspan for Tests A, A.1, B and B.1 based on temperatures measured by the midspan thermocouple (centre of the soffit). A full comparison was impossible since in Test B.1 this thermocouple failed after 1 hour (in fact most exposed soffit thermocouples failed during second testing). However for the first hour it is apparent that the slabs heated more rapidly than during the first heating cycle under the same heating exposure, as expected.

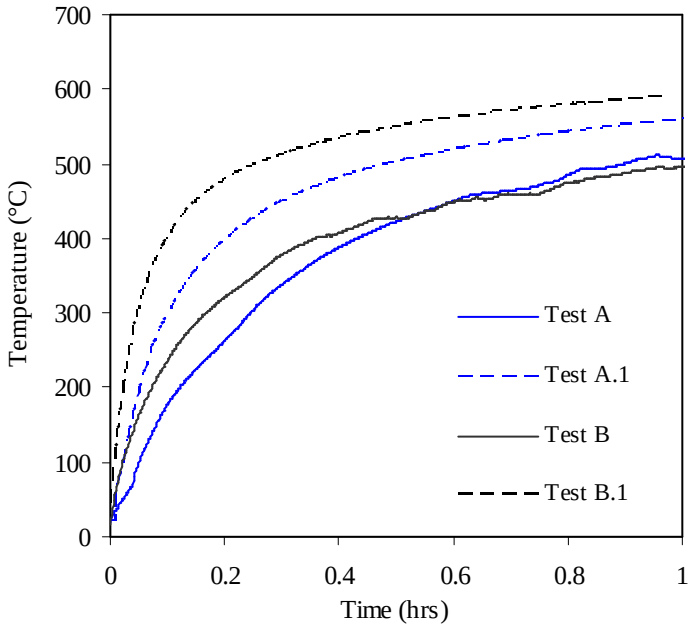

Figure 5.22: Comparison of first and second heating of the exposed soffit with respect to centremost thermocouple.

Unexposed surface temperatures

Unexposed surface temperatures at midspan for tests A, B and C are plotted in Figure 5.23 (these represent an average of two thermocouples installed on the unexposed surface of the concrete at midspan of the slab). These data can be used to highlight the thermal gradient through the slab, which would promote thermal bowing during heating.

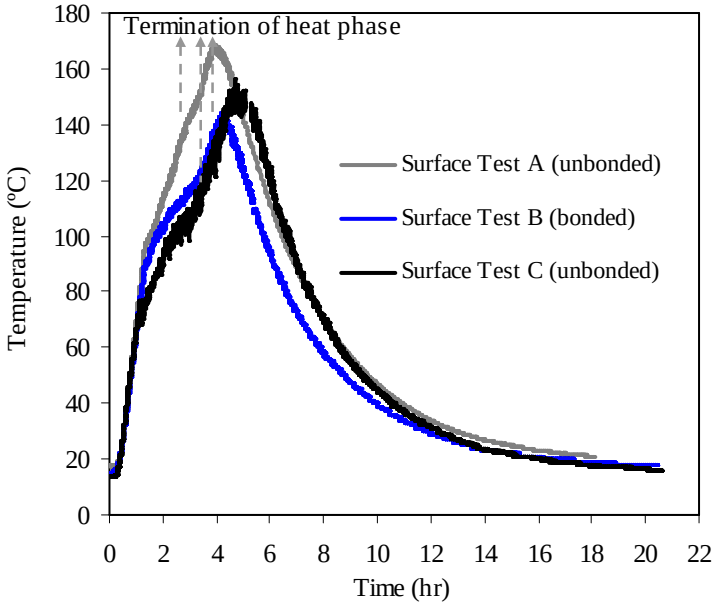

(a)

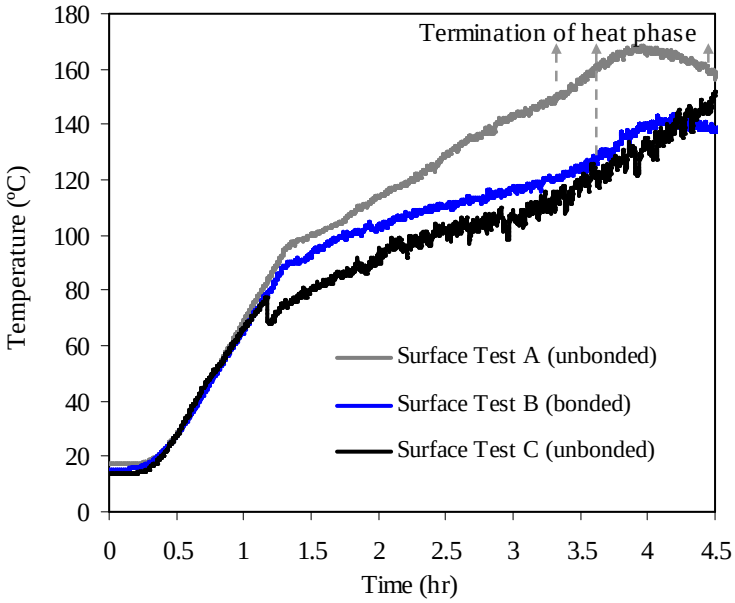

(b)

Figure 5.23: (a) Comparison of averaged unexposed surface temperatures of slab at mid span as measured by thermocouples and (b) with time scales adjusted.

With reference to the preceding discussion of exposed soffit temperatures, a temperature difference can be observed which increases in size as the tests progress, and for all tests eventually exceeds 450°C; thus considerable thermal bowing should be expected. Figure 5.24 illustrates this maximum thermal gradient in the slab as monitored from the start of the test to the end of cooling. This specific figure is constructed on the basis of the difference between the middle most thermocouple readings taken on the unexposed surface and the exposed surface at midspan.

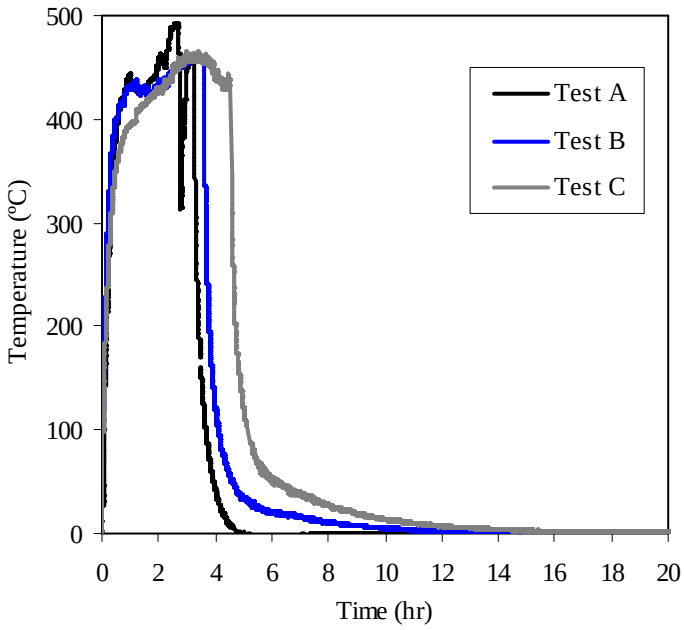

Figure 5.24: Difference in temperature between the unexposed and exposed surfaces of the slab as measured by centremost thermocouples.

Reinforcement temperatures

Figure 5.25 shows the average of the two prestressing steel tendon temperatures taken from thermocouples on the tendon at mid span for all three slabs during first heating; it is assumed that this would be the highest tendon temperature recorded anywhere, since this is where maximum tendon drape occurred and was the most heated location in terms of both radiative view factor and direct convective heating from the radiant panels. The deviation between the two tendon thermocouples in each slab never exceeded ±2.2°C (essentially the accuracy of a Type K thermocouple).

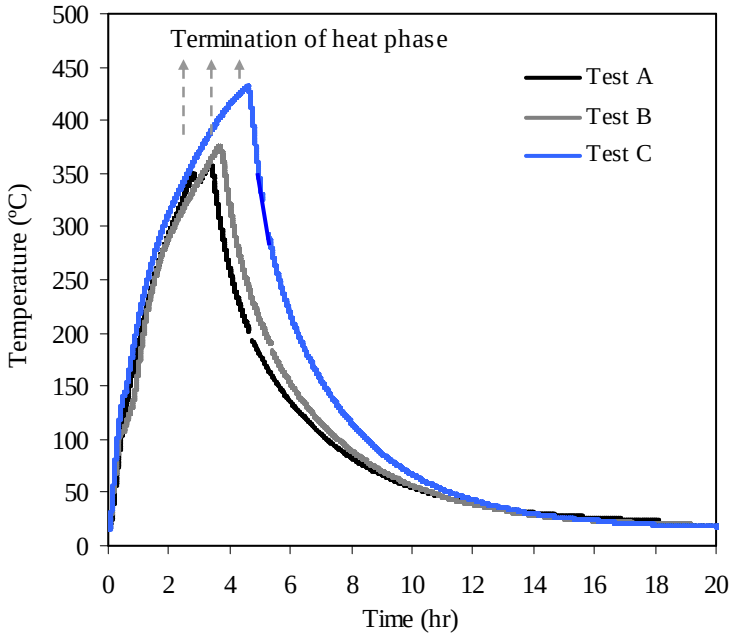

(a)

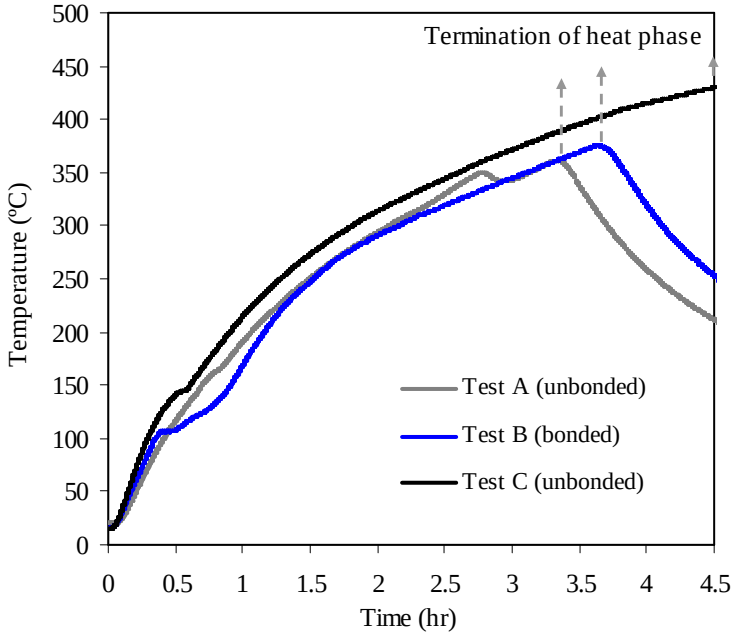

(b)

Figure 5.25: (a) Comparison of average prestressing steel temperatures in slab and (b) with time scales adjusted.

Test B demonstrated a reduction in heating rate in the temperature region near 100°C, which is thought to be due to the higher (measured) moisture content of the cementitious grout which was used to create a bonded PT situation within the plastic

post-tensioning duct; this was 6% moisture content (by mass) as compared with the surrounding concrete in which it was about 4%.

Maximum temperatures during the first heating for Tests A and B reached more than 350°C, the critical temperature given by EN 1992-1-2 (CEN, 2004). During second heating and in Test C, the prestressing tendons were heated to more than 426°C, which the critical temperature given by IBC (2012).

Reinforcement temperatures were slightly higher than those recorded at the tendons, although these temperatures never exceeded 500°C during any test. The slab design called for these bars to actually be 400 MPa in ultimate strength at ambient. The reinforcement was tested in ambient at 658 ± 7MPa. The strength behaviour is inline with the 8 mm diameter cold worked mild reinforcement tested by Elghazouli et al. (2009); using their reduction factors at 500°C there would have been more than 400 MPa in tensile strength remaining at high temperature.

5.6.2 Tendon stress levels

As clearly shown in the preceding chapters, the relationship between tendon stress and temperature is critical for unbonded PT structures, and under certain combinations of stress and temperature tendons may experience tensile rupture due to heating alone. The variation of tendon stress with the tendon temperature measured at midspan is plotted in Figure 5.26 for Tests A and C. Since Test B had a grouted and bonded tendon, this slab showed no measureable stress relaxation during heating as observed from the load cells installed at the tendon anchorages.

Figure 5.26 shows that considerable stress relaxation was observed for both slabs with unbonded tendons. Obviously this is due to a combination of thermal and structural actions, including thermal elongation of the tendon, thermal expansion of the concrete, thermal bowing of the slab, reductions in elastic modulus of the tendon at elevated temperature, and creep of the tendon. Reductions in tendon stress increase and accelerate with increasing temperature, and even continue once the heating is stopped due to the thermal inertia in the concrete. A minimal amount of stress recovery is evident during the cooling phase, indicating that considerable irrecoverable creep of the tendons had occurred.

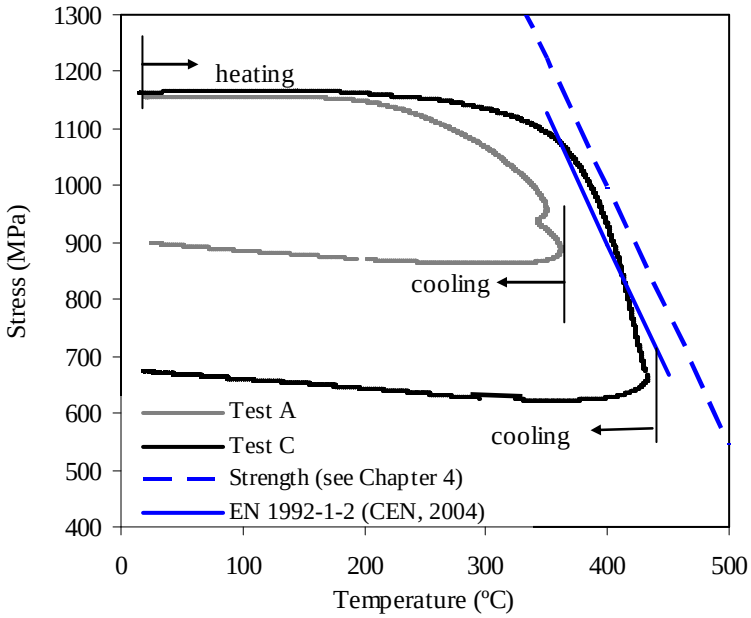

(a)

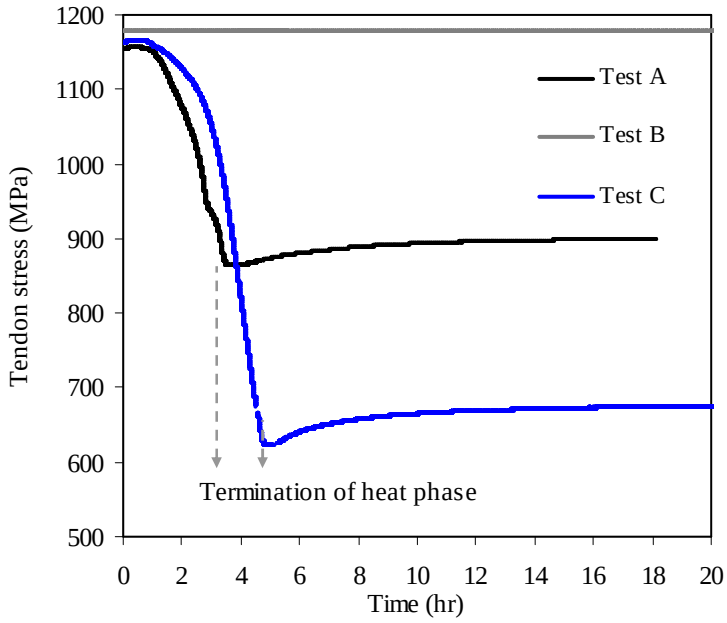

(b)

Figure 5.26: First heating (a) unbonded prestressing steel stress relaxation with respect to measured tendon temperature and (b) prestressing steel stress relaxation with respect to time for all slabs.

The potential for irrecoverable creep in unbonded tendons within concrete in fire has been postulated previously in Chapter 3, and the data in Figures 5.26(a) and 5.26(b) confirm that this is a reality. The observed stress relaxation (or lack of stress

relaxation) would have an impact on a structure's ability to balance the deflection and other inter-related consequences on the PT slabs. Relative restraining forces and deflection of the slab would be directly impacted by stress relaxation. This is because the prestressing steel tendon's pre-compressive action on the slab would diminish on heating, as well as its ability to balance applied loading. Whether such structural actions could be defensibly modelled using the best available finite element codes, even for this simple case with a very well defined thermal profile, remains an open question.

As already stated, one issue of concern in unbonded PT slabs during fire is that localised heating of the prestressing steel tendon could result in sudden tensile rupture. Strength reduction relationships with increasing temperature are available for cold-drawn prestressing steel wire in the literature, for example in EN 1992-1-2 (CEN, 2004), and this is also plotted in Figure 5.26a. Additionally a best fit ($R^2 > 0.99$) reduction line from strength test data (>200ºC) developed in Chapter 4 is included. It is evident that Slab A did not seriously risk tensile failure of the tendon at any point during testing.

Test C included the aforementioned disk-spring anchorage which simulated a longer tendon length and thus a shorter heated length ratio (~10% instead of 17%). Plotting the stress relaxation-temperature results for Test C in comparison of Test A confirms that for shorter heated length ratios less recoverable relaxation will occur. The data for Test C indicate an interception with the EN 1992-1-2 (CEN, 2004) strength reduction curve for prestressing steel at high temperature, however the tendon stress does not intercept the strength reductions extrapolated from the data presented in Chapter 4. Post fire evaluation of the slabs confirmed a discrete location of necking on the prestressing steel tendon representing 10% area reduction and indicating that the tendon was indeed on the verge of failure during this test. This gives some credibility to the EN 1992-1-2 (CEN, 2004) reduction factors as a conservative means by which to predict tendon failure under stress at high temperature. It must be noted that heated length ratios below 13% represent the more likely fire scenario in a real building, and these were not tested. This would be akin to a multi bay structure of 40 m in total length heated in a single bay (or compartment). For larger structural configurations (>40 m in total floor plate

dimension), smaller heated length ratios should be expected in practice. In the case of Test C, had the spring simulated an even greater length of unbonded tendon, such as to simulate just one additional structural bay, the tendon is likely to have ruptured.

The above discussion has not considered the possible effects of more rapid heating, which would result in less time-dependent prestress losses and possibly an earlier stress-strength interception resulting in tendon rupture.

5.6.3 Restraining forces

It is well known that restraining forces and secondary load carrying mechanisms may benefit the performance of structural systems during fire. However there are cases where high restraining forces can influence the formation of perimeter cracking, column shear loading (and even failure), and/or slab spalling due to induced compressive stresses. Restraining forces are generated based on the boundary conditions at the supports and the stiffness of the surrounding structure.

As already noted, each supporting column had two identically placed calibrated strain gauges which allowed the columns to be used effectively as load cells (see Figure 5.2). A number of assumptions were made to estimate the applied force on the column head from measured strain. First, it was assumed that the columns were at uniform temperature. Given that they were not directly exposed to heating this was considered to be reasonable. Second, it was assumed that the total strain measured on the column was the sum of the flexural and axial strain components. Through the aforementioned calibration exercise (see Section 5.4.3) the flexural strains were converted into an applied reaction force. However since fluctuations in temperature exist within the laboratory during testing (for every test these were monitored on Column 3) the axial strain is influenced by the temperature of the column. Therefore the normal reaction force applied vertically on the columns could not be accurately resolved. Figure 5.27 illustrates a comparison of interpreted axial strain compared to the theoretical thermal strain using the measured temperature at Column 3 for Test A (the theoretical value is calculated with known thermal expansion coefficients for structural steel, i.e. 12 $\mu\varepsilon/°C$ (Ghosh, 2009)). A lag can be observed between the strains which prohibits compensation of data, however it can be seen that the columns are indeed being affected by temperature

changes in the laboratory (even small temperature changes). The horizontal thrust/restraint measurement is assumed not to be influenced by temperature changes in the laboratory by assuming that temperature change is uniform in the supporting columns.

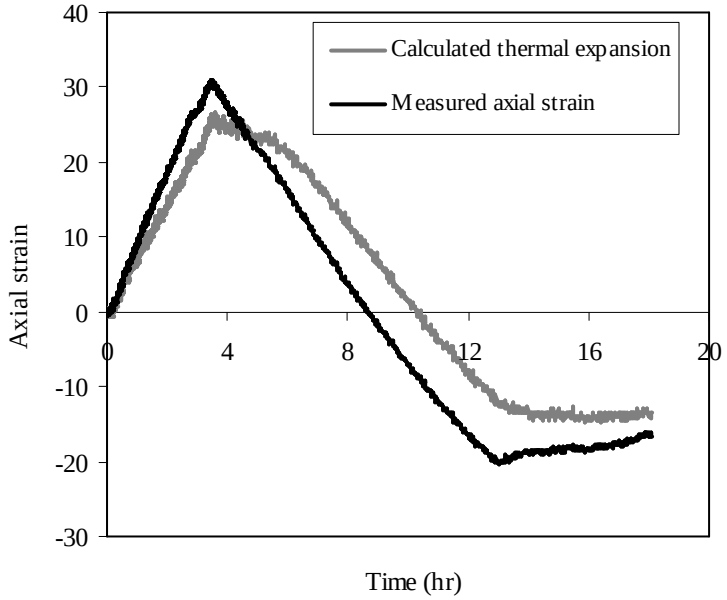

Figure 5.27: Comparison between axial measured strain on Column 3 in Test A and strain calculated assuming a measured temperature and a thermal expansion coefficient of 12 $\mu\varepsilon / °C$ for structural steel.

Table 5.5 gives the average thrust exerted by the slab on the columns during heating and thermal pull (contraction) after cooling for all columns (1 through 4) for all tests. The averages for Test C are compiled only on the basis of three columns (2-4), since Column 1's strain gauges failed during testing. The thrust is resolved into stress by considering the full cross-sectional area of the slab. These stresses were less than 0.5 MPa in all cases. A consistent response in most tests indicated that all columns experienced a similar thrust-contraction response.

Table 5.5: Maximum thrusts and pulls on columns.

Test #	Maximum thrust in heating (kN)	Relative compressive stress difference for maximum thrust (MPa)	Maximum pull in cooling (kN)
A	15.7+/-3.0	0.34+/-0.07	4.8+/-1.7
A.1	21.9+/-7.0	0.48+/-0.15	0.3+/-1.3
B	16.3+/-2.8	0.36+/-0.06	3.4+/-1.6
B.1	19.4+/-2.2	0.42+/-0.05	2.4+/-2.2
C	13.4+/-2.8	0.29+/-0.06	5.2+/-2.0

Figure 5.28 gives the change in longitudinal thrust during heating on each column during Test A. Figure 5.29 illustrates the averaged relative longitudinal thermal thrust generated for all tests (deviations are given in Table 5.5). Figure 5.29 also shows that thermal contraction on cooling induced tension for all tests.

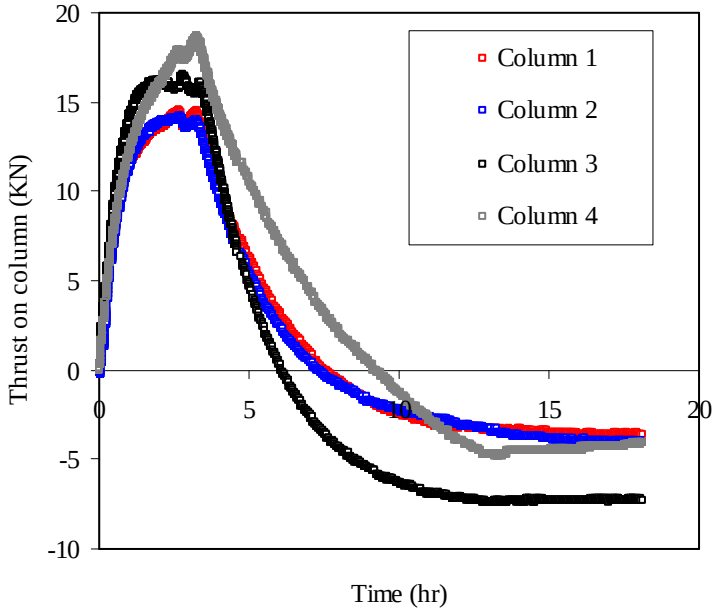

Figure 5.28: Restraint forces for each column in Test A.

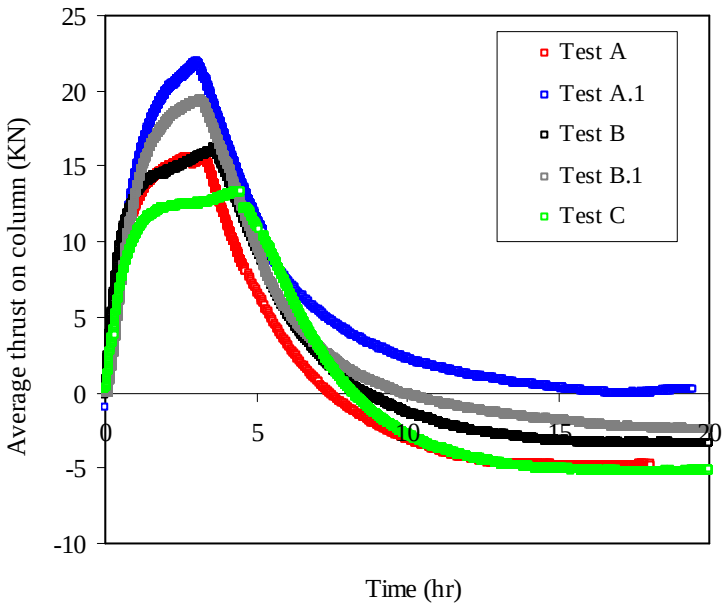

Figure 5.29: Average restraint forces for all tests.

It is important to note that the observed restraint forces apply for one boundary (heat and support) condition only. These forces (stress) were relatively small during the current tests; however they are representative only of a thin strip of slab as tested. When considered for a real slab which is two-way and placed on an arbitrary 4 m × 4 m grid (while still heated within a centre bay over half its area, assuming a exerted stress of 0.5MPa and the slab being the same thickness), a restraining force of 100 kN or more could easily be exerted on each column.

Had more of the slabs' soffit been heated or had the slabs been heated to a higher temperature it is possible that larger thermal thrusts would have been induced. This raises important questions about the shear capacity of supporting concrete columns and their ability to resist lateral and axial forces to prevent progressive collapse mechanisms. For rational design in a performance based environment, the likely fire scenario and likely end/intermediate support conditions must therefore be known.

5.6.4 Deflections

To date no experiments have carefully described the deflection behaviour of a restrained and continuous (one-way) PT slab during localised heating. The deflection response is crucial to identify and understand various interacting mechanisms occurring in the structural system during fire; and also for validating computational models of PT slabs during fire.

Figure 5.30 shows the respective vertical deflections at the mid points for tests A, B and C during first heating, with deflections zeroed at the onset of heating. The deflection behaviour of the second heating, tests A.1 and B.1, are present in Figure 5.31 (separated for clarity). In all cases quarter point deflections were approximately one half the midspan values. End spans (unheated) displayed negligible deflections.

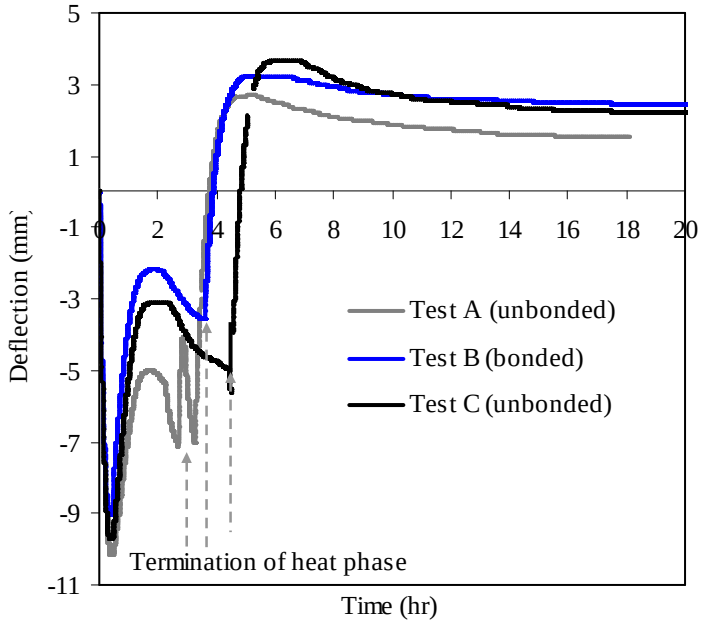

(a)

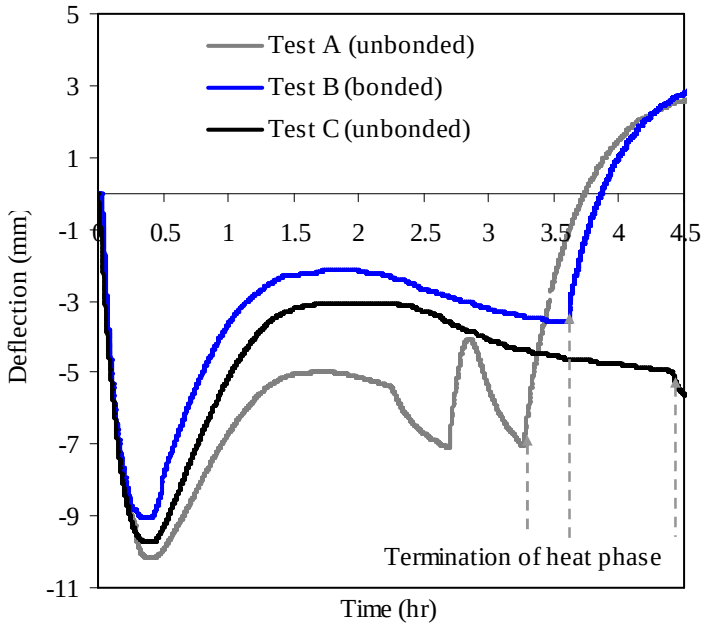

(b)

Figure 5.30: (a) Slab vertical deflections recorded at mid span during heating and cooling phases for first heating and (b) with time scale adjusted.

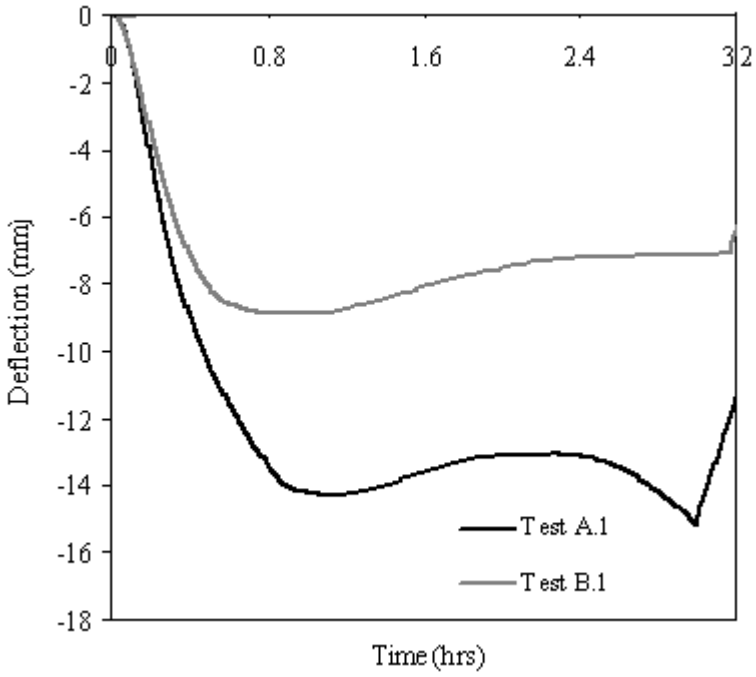

Figure 5.31: Slab vertical deflections recorded at mid span during heating and cooling phases for second heating with time scale adjusted.

All tests displayed four distinct deflection trends during heating:

(1) **Thermal bowing** – High thermal gradients developed during initial heating promoted thermal bowing early in the tests and caused a rapid downward deflection in all cases. This reached a peak of 9-10 mm within about 30 minutes of heating in all cases.This general behaviour was also observed on second heating.

(2) **Concrete stiffness degradation** – When the rate of heating on the exposed surface of the concrete began to slow and the soffit temperature exceeded 450ºC, the slabs' deflection reversed in direction and the slabs cambered upward. This response was likely due to transient (time and temperature dependant) creep damage and stiffness reduction of the concrete close to the heated face. A reduction in slab stiffness and sufficiently high tendon prestress (>1000MPa at this moment during testing, as confirmed by Figure 5.25(b)) promoted cambering of 5-7 mm within the heated region only. This increasing camber persisted until approximately two hours into the tests. During second heating this cambering response appeared however at a smaller magnitude. The small magnitude could be due to already induced permanent plastic deformation from the first heating,

since it is known that load induced thermal strain predominately occurs on first heating for concrete and is largely absent from repeated thermal cycles (Khoury, 2006). The behaviour may also be influenced by a steadily decreasing thermal gradient, though differences in exposed soffit and surface temperature indicated in Figure 5.24 suggest that the thermal gradient in the slab was still increasing during this stage.

(3) **Prestressing steel tendon creep** – After the prestressing steel tendons reached temperatures of about 300ºC, prestress relaxation of the tendons accelerated due to creep and thermal elongation. The resulting reduction in tendon stress caused global increases in deflection, thus cancelling out the cambering response of the locally heated region. On second heating, Test A.1 illustrated a linear increase in deflection in this region.

(4) **Cooling** – The deflection reversed on cooling due to thermal contraction and reductions of thermal bowing. Tests A and C experienced nearly the same recovery of deflection as occurred due to thermal bowing. When the exposed soffit of the slabs dropped below 100ºC, the slabs began to deflect once again. This suggests that the slabs may have been absorbing moisture from the atmosphere rehydrating the lime in the Portland cement causing an expansive (deflection) effect (Khoury, 2006). Interestingly all slabs exhibited a final upward (camber) after cooling. This is indicative of permanent plastic deformation of the concrete. On first heating, tests A and C exhibited more deflection as compared with Test B, this likely due to prestress relaxation in the tendons. The bonded slab (Slab B) maintained prestress and thus had the least overall deflection throughout. In second heating, since tests A.1 B.1 both experienced more thermal bowing during heating, they naturally exhibited more cambering during cooling than during their first heating cycle.

The deflection responses for the first heating cycle are illustrated in Figure 5.32. All position transducers for slabs at midspan are indicated. Note that one position transducer in Test C malfunctioned and is not reported in this figure. Outer span deflections were negligible, and were below 1 mm for the duration of all tests, and are therefore not discussed in detail.

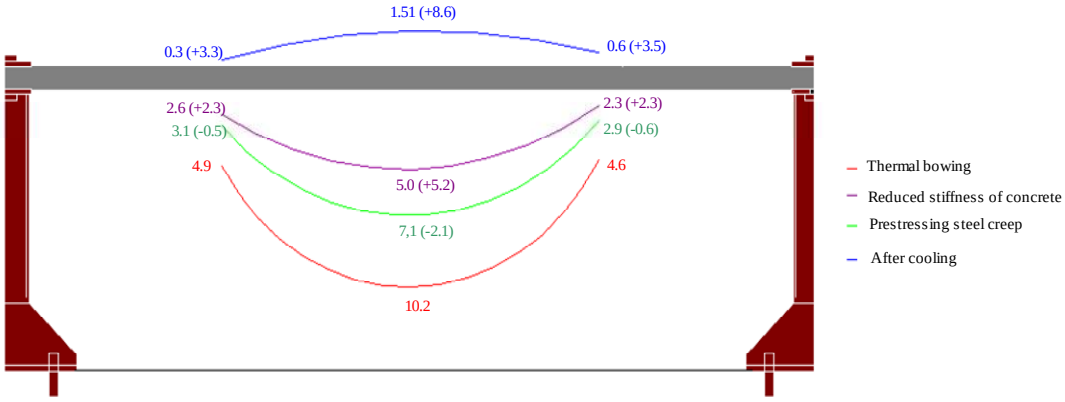

(a)

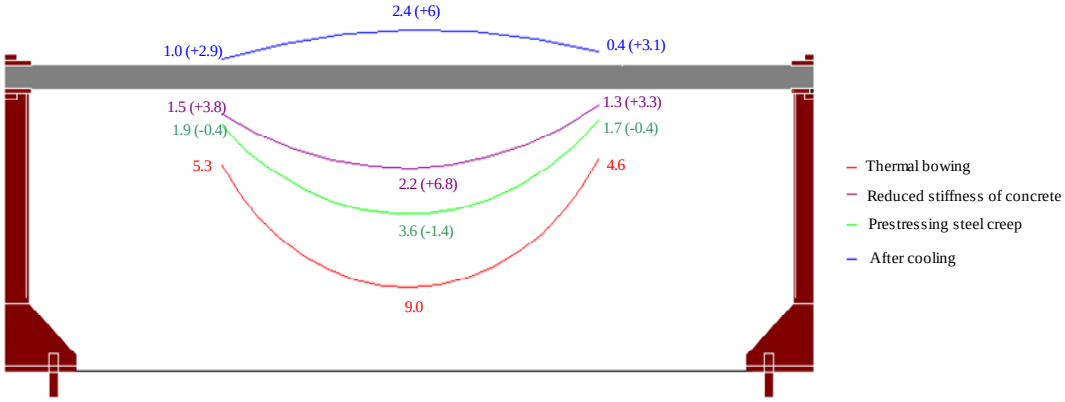

(b)

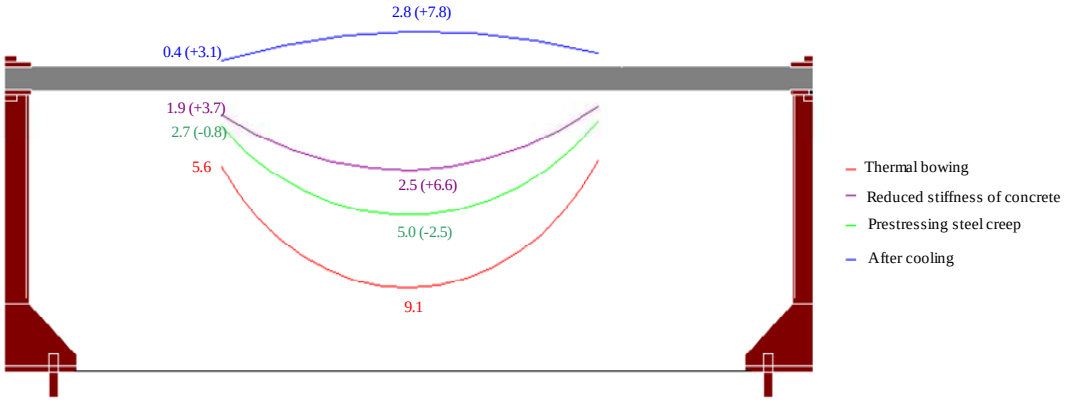

(c)

Notes: + denotes camber, - denotes deflection. Deflection profiles are interpolated between gauges. Profiles not to scale. One position transducer in Test C failed during testing, therefore these values are not shown.

Figure 5.32: Deflection profiles for centre span as measured by position transducers for first heating of PT slabs (a) Test A (b) Test B and (c) Test C.

5.7 Post-heating evaluation

A post-heating evaluation was conducted for each slab. Each slab was analyzed for cracking and spalling. The slabs were then unloaded and de-stressed to observe the changes in deflection. For slabs A and C the prestressing steel was analyzed after heating (Slab B's bonded prestressing steel could not be extracted safely). The final evaluation included excavating to determine thermocouple placement and concrete cover depth at critical locations, thereby confirming a satisfactory tendon drape. Selected observations for each slab are given in Table 5.1 and Table 5.6, discussed below.

Table 5.6: Post heating evaluation.

Slab	Change in deflection		Remaining prestress (MPa)	Peak tendon temperature (°C)	Remaining strength (tensile strength) (MPa)	Residual strength (hardness) (MPa)
	Deloading (mm)	Destressing (mm)				
A	-6.10	5.36	567	426	1666	1675
B	-3.27	-	1176	438	-	-
C	-2.51	3.17	670	430	1532	1584

Note: tendon could not be safely extracted from Slab B
, -ve deflection values indicate camber

Slab A

A transverse crack was present at each support (adjacent to Columns 2 and 3) of width less than 1 mm and extending to the depth of the upper layer of mild steel reinforcement (Figure 5.33).

Figure 5.33: Discrete transverse cracking at column location (Slab A, Test A.1 shown).

These cracks were present for all slabs and all tests (Figures 5.34 through 5.36 illustrate cracking patterns for all slabs).

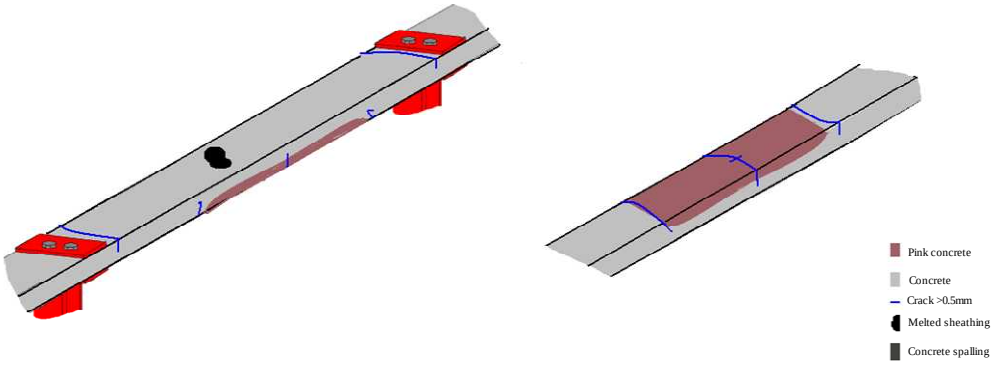

(a) (b)

Figure 5.34: Cracking and heating pattern of Slab A centre span (a) unexposed surface view and (b) exposed surface view (upturned).

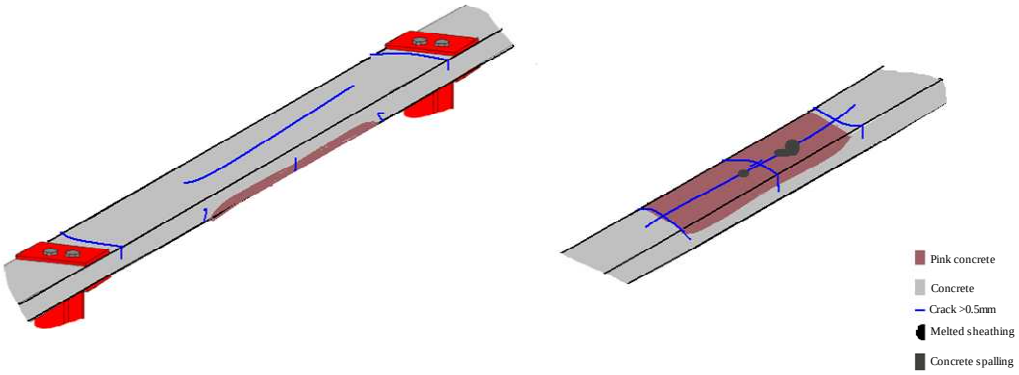

(a) (b)

(c)

Figure 5.35: Cracking and heating pattern of Slab B centre span (a) unexposed surface view (b) exposed surface view (upturned) and (c) actual longitudinal crack width.

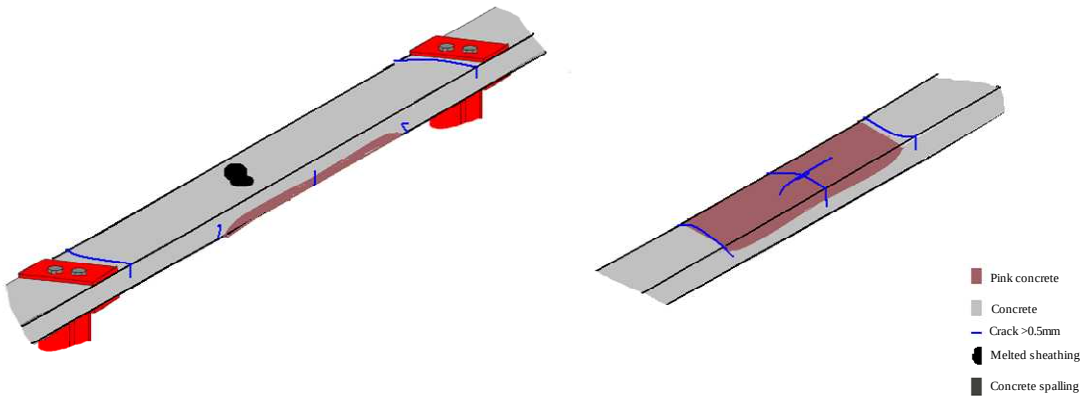

(a) (b)

Figure 5.36: Cracking and heating pattern of Slab C centre span (a) unexposed surface view (b) exposed surface view (upturned).

No spalling was present on the exposed soffit of Slab A. During both tests A and A.1, black smoke was observed at the top of Slab A; this was thought to be smoke from burning of the prestressing steel sheathing emerging through the embedded thermocouples wires. This was also observed for Slab C (Test C). Small transverse cracks were also seen along the exposed soffit of the slab within the heated region.

When unloading Slab A, a residual camber of 6.1 mm was measured at mid span, and a subsequent deflection of 5.4 mm was measured when de-stressing the tendon. These values, despite the prestress loss, were greater than the original camber (4.2 mm) and deflection on loading (2.13 mm). Similar increases were observed for slabs B and C and are thought to be a result of degradation of material properties and irreversible strains in the concrete during heating.

Once de-stressed, the prestressing tendon was extracted. A portion of the tendon was used to assess the diamond pyramid hardness (taken as an indicator of tensile strength). A diamond permit hardness value of 443 was measured, indicating a strength of 1584 MPa and agreeing with a measured peak temperature in the range of 400-450°C; this is from strength-hardness correlations given by Roberston et al. (2013) from the aforementioned associated MEng thesis project at Edinburgh (included as Appendix C). A portion of the tendon was also tested to failure in tension, giving an ultimate strength of 1545 MPa. This is in line with residual tensile

strength testing of prestressing steel presented previously by MacLean (2007), and is similar to the diamond permit hardness correlation made above.

After cutting the slab in two it was sectioned using a diamond saw and the concrete cover was confirmed within 2 mm of the design at all locations. A layer of approximately 10 mm of pink coloured concrete was identified at the exposed surface of the slab's soffit. Pink concrete is known to occur at temperatures as greater than 300ºC and is a key indicator of concrete which has lost strength Colour changes in concrete are known to be dependent on exposure temperature due to the oxidisable iron content in the cement (Ingham, 2009), so this can indicate damaged concrete by phase changes in the cement used. Slabs B and C also exhibited the same 'pink' zone depth. Slab C, which had only been heated once (but for a longer duration) had a similar pink layer of about 10 mm in depth.

Slab B

Very mild spalling (sloughing type at late stage, as opposed to the more damaging explosive concrete cover spalling which is often observed in fire tests of concrete members, and a discrete section of cover loss early in the test) was noted visually and with the use of the thermal imaging camera during testing. Figure 5.37 illustrates the time of first spalling of the concrete at 8 minutes into testing. This location below the tendon was examined post test, and a small (< 5 mm wide, by 5 mm deep) section of concrete was missing. A second spalling location was observed within the heated region. After the second heat and on examination the grouted duct coating of the prestressing steel could be observed at the spalling location, indicating that the presence of the duct (and burning polymer) may have exacerbated cover separation. Discrete cracks were observed near the location of the duct's corrugated ribs. These may have been caused by the removal of the duct by melting, and then the tendon's restrained movement in heating. Figure 5.38 illustrates these cracks.

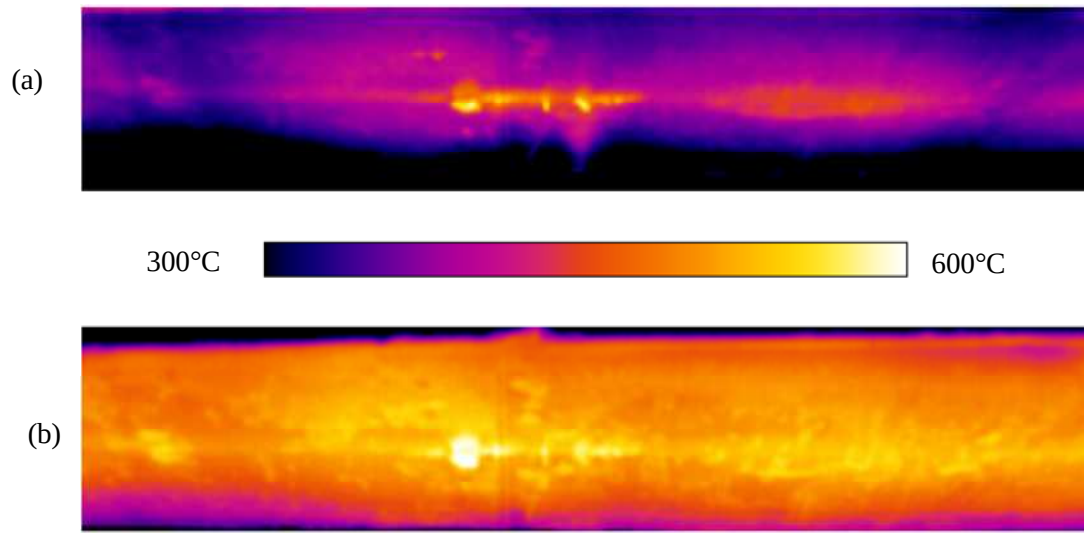

Figure 5.37: Two thermal imaging camera images taken during testing in Test B (a) at 8 minutes and (b) at 2 hours.

Figure 5.38: Exposed section of grouted duct after Test B.1 on exposed soffit.

Transverse and longitudinal cracking (<1 mm) were both observed, as shown in Figure 5.35(a through c). Longitudinal cracks are formed due to expansion of the tendon longitudinally which relives compressive forces on the concrete, the concrete is then subjected to tensile forces which can split weaker sections (near tendons). Such longitudinal cracks have been observed in many previous tests of post-tensioned concrete elements during fire. A longitudinal crack appeared on both the

exposed soffit and the top surface of the slab on first heat. The crack was only in the heated region (extending approximately 10 cm in the cold zone on both sides) and was coincident with the location of the prestressing tendon. This supports the hypothesis laid out in Section 2.5 that under a local fires, longitudinal cracking should arrest where the prestressing steel is no longer exposed to high temperature. This would be due to the relaxation of prestress in one location, and maintenance of the precompression outside the heated location. The larger duct size (23mm) may have contributed to forming a crack where it was visually absent in slabs A and C. This may be due to a smaller effective concrete section to resist tensile stresses. A camber of 3.3 mm was observed at midspan after unloading of Slab B. This value was greater than the original deflection (1.5 mm) from loading, excavation confirmed thermocouple placements were near the axis distance within the grout near center span. Full grouting of the post-tensioning duct was confirmed within the centre span.

Slab C

Discrete transverse cracking was present on the slab at mid span and at the supports as shown in Figure 5.36. Some discrete longitudinal cracks were confirmed along the exposed soffit of Slab C below the location of the tendon; however these were very fine and barely noticeable.

As for Slab A, no spalling or cover separation was identified for Slab C. Verification of the spring behaviour was made by noting the spring compression after stressing to approximately 125 kN (a compression of 55 mm) and after cooling with a tendon force of approximately 62 kN (a compression of 22 mm). This confirms the spring calibration given in Figure 5.9.

When unloading Slab C a camber of 2.5 mm was measured at midspan and a subsequent deflection of 3.2 mm was observed when de-stressing the tendon. Again, these values were greater than the original camber (1.8 mm) and deflection (1.2 mm).

During testing flaming was observed on the slab soffit parallel to the tendon. This flaming was likely caused by the tendon grease from inside the prestressing sheath igniting as it seeped through the surface of the slab. An excavated section of Slab C is shown in Figure 5.39 which shows residual sheathing traces through the

depth of the concrete. Also shown in Figure 5.39 is the aforementioned ‘pink’ concrete.

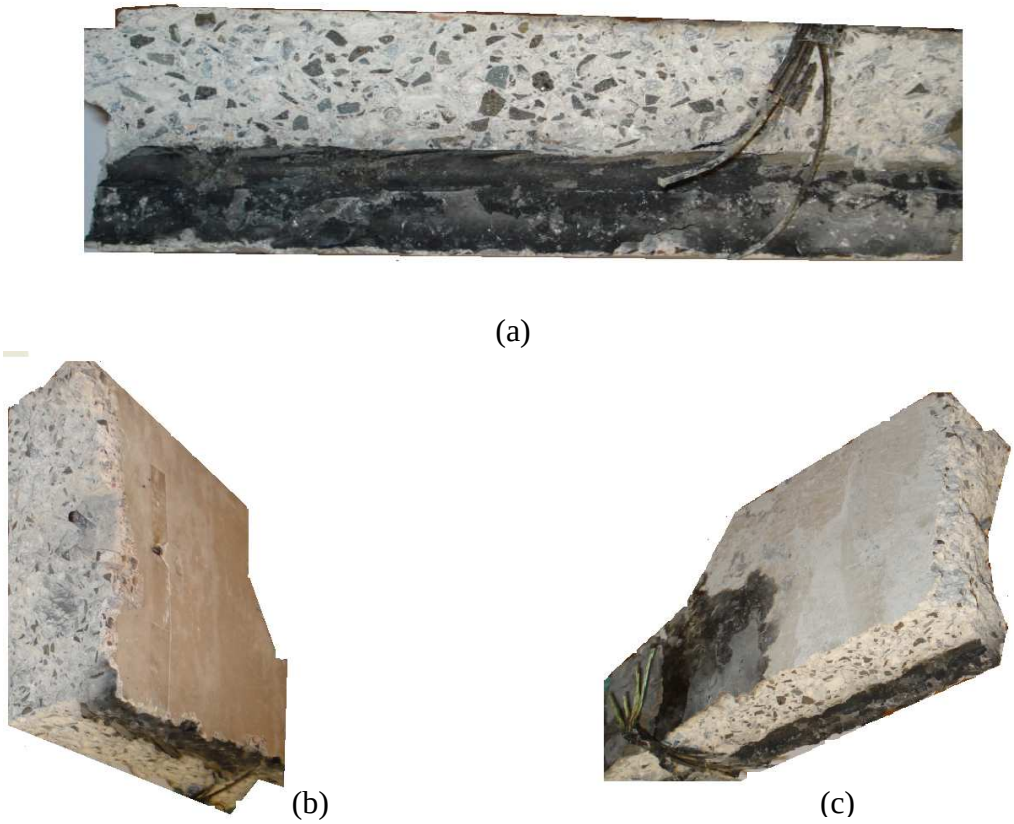

(a)

(b)

(c)

Figure 5.39: Excavated section of Slab C (a) profile (b) exposed soffit and (c) unexposed surface.

As for Slab A, the tendon was extracted and analysed. The diamond pyramid hardness was measured at 462, indicating strength of 1666 MPa and verifying a peak temperature in the range of 400-450°C. The remaining tendon was tested and gave an ultimate strength of 1685 MPa. This is in line with residual tensile strength testing of prestressing steel presented previously by MacLean (2007).

5.8 Implications for computational modelling

An *a posterori* modelling exercise was performed using the experimental data; (1) to further validate the tendon deformation parameters developed in Chapter 4; and (2) to help steer future research activities which may help in performing advanced computational modelling of unbonded PT concrete slabs.

Thermal boundary conditions

Prior to performing modelling the thermal boundary condition representative of heating conditions experienced during testing needed to be established. As described in Section 5.6.1, there was some minor variation in heating along the slab. A representative equation was therefore developed which adequately describes the temperature-time exposure to the slab induced in Tests A, B and C:

$$T_{surface} = T_{ambient} + 775.74(1 - e^{-1.15\sqrt{t}}) - 72.63(\sqrt{t}) \qquad [5.2]$$

Where $T_{surface}$ is the temperature of the exposed surface, $T_{ambient}$ is the ambient room temperature, and t is time in hours. The curve represents a best fit least squares approximation of the average of eight thermocouples used over from the exposed soffit in Tests A, B, and C (see Table 5.3). The curve was defined on the first two and a half hours of heating and extrapolated beyond this point. Using this initial heating curve and the heat transfer analysis program (Bisby 2005) from Chapter 3, through thickness slab temperatures were estimated for tests A, B and C and used to determine tendon temperatures based on the experimental heating. The input thermal model parameters considered a 95 mm thick slab with 4% moisture content. Equation 5.2 is only valid for use only with the current tests.

The resulting temperatures from the thermal modelling were compared to the experimental thermocouple temperature observations of the average surface temperature of the exposed soffit, tendon temperature, and the top of the slab at mid span. These comparisons are given in Figures 5.40 through 5.42. The figures indicate some difficulties in heat transfer modelling with the moisture in concrete at the early stages. This is especially exaggerated with the results of the bonded slab which had a measured grout moisture content near 6% (note the obvious plateau in moisture in Figure 5.41). Since the heat transfer model does indicate good agreement at temperatures known to be important for creep of prestressing steel (i.e. in the range of 300°C) the data is satisfactory for predicting temperatures which prestressing steel embedded in concrete will experience.

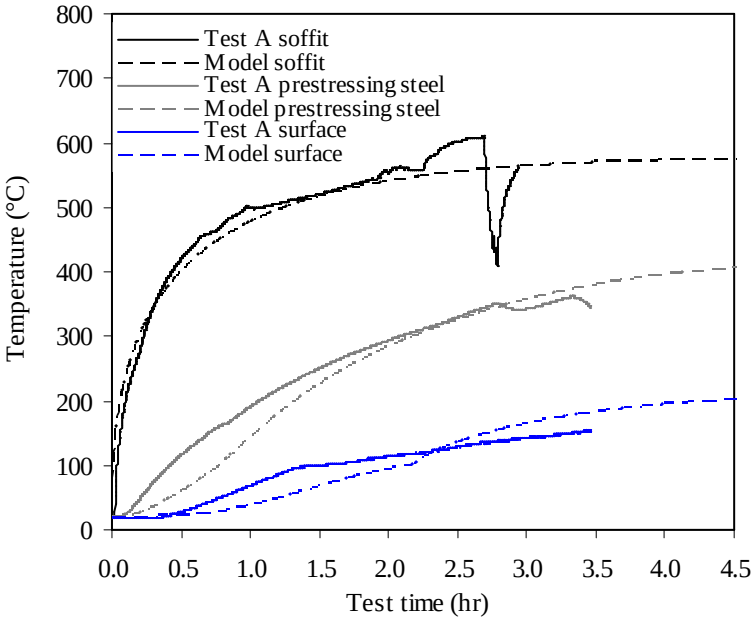

Figure 5.40: Test A thermal profile at mid span with modelled and measured temperatures.

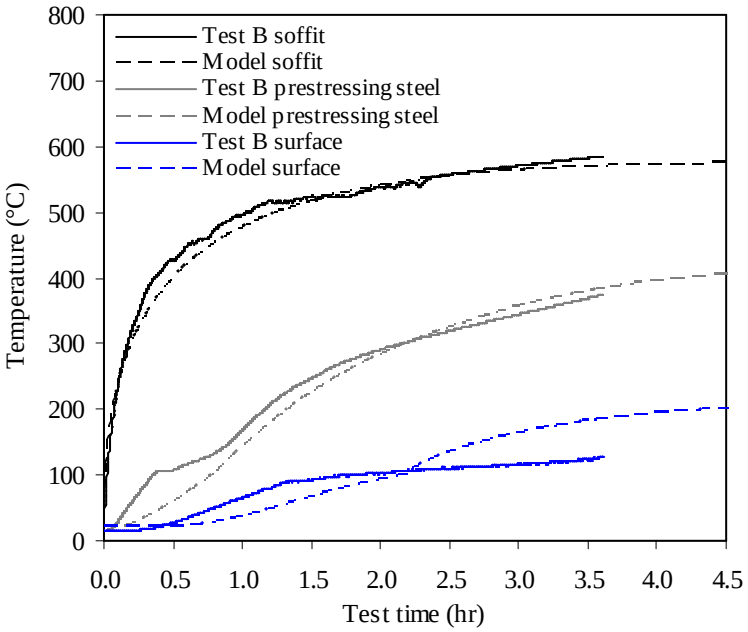

Figure 5.41: Test B thermal profile at mid span with modelled and measured temperatures.

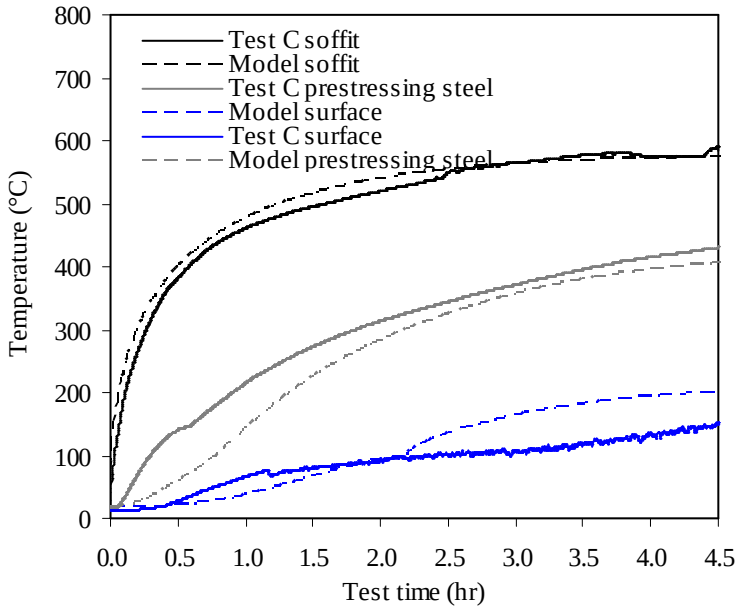

Figure 5.42: Test C thermal profile at mid span with modelled and measured temperatures.

Modelling tendon stress relaxation

The heat transfer analysis used above was coded to run alongside the prestress relaxation model presented previously in Chapter 3, using the improved creep parameters developed in Chapter 4 for BS 5896-12 (BSi, 2012) prestressing steel. The model input parameters assumed that the length of the slab was 17.3 m for Test C to account for the presence of the spring anchorage.The stress relaxation results for Tests A and C are shown in Figure 5.43.

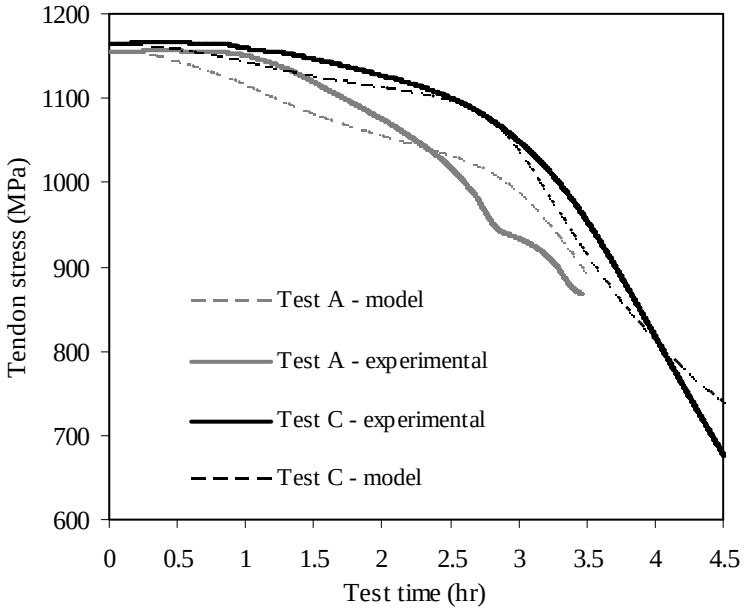

Figure 5.43: Observed prestressing steel stress relaxation versus modelled values (temperature effects only modelled)

Test A showed a maximum difference of 47 MPa (5% error), while Test C showed a maximum difference of 27 MPA (3% error) during the first three hours of testing. The accuracy in modelling appears in line with that shown in Chapter 4 (less than 6% error).

The experimental data from Tests A and C show little stress relaxation at the start of the tests, whereas the modelling predicts clear relaxation during this period of the tests. This could be due to tendon elongation caused by thermal bowing at the start of the test, which would counteract stress relaxation induced by heating and is not accounted for in the modelling. As shown in Section 5.6.4, deflection (12 mm maximum) was relatively small considering the spanning length (4140 mm length), and thus the resulting elongation from deflection alone of the tendon would be small. The comparison between Tests A and C however supports Chapter 4's new creep parameters and the overall modelling approach suggested herein.

Advanced modelling of the tests presented herein

Future work is likely to expand the modelling exercises presented above for other heating scenarios and to model the full structural response of the tested slabs, accounting for the applied load, deformations of the concrete, and support

movements. Issues which would need additional attention in order to defensibly develop a more advanced computational model include:

- **Mechanical re-stressing of unbonded tendons** – Many inter-related structural mechanisms will influence the deformation response of the PT slabs (and unbonded tendons) during a fire. Future modelling should attempt to consider the roles of thermal bowing, loss of precompression, discrete cracking, and restraint on the stress level of unbonded tendons.
- **Consequences of tendon rupture** – None of the tests were able to examine the effect of prestressing steel rupture on load carrying capacity of the structure. Future research must be conducted that can understand the effect of immediate load shedding to mild bonded reinforcement and if the structure can maintain the applied load after tendon rupture.
- **Concrete behaviour in fire** – This thesis focuses on the unbonded tendon characterization; quantifying it satisfactorily. The thesis only begins to investigate concrete material behaviour in fire. Concrete's spalling risks, cracking, thermal strain under load, material parameters etc all need continued research in fire to accurately model structural interactions.
- **Additional testing** – Future tests must be conducted that can rationally compare the differences in structural reactions between different fire sizes and severities. It is true with respect to the tendon that localised heating may induce premature rupture of the unbonded prestressing steel; but more uniform heating may induce higher restraining forces which could cause significant deformations of the slab and cause failures elsewhere in the structure.

Once a satisfactory model can be built and rationally validated against these tests it will be possible to move towards a rational performance based assessment of full structural response to fire for unbonded PT concrete construction.

5.9 Summary

The main objective of the experiments described in this chapter was to investigate the thermal and structural response of multiple span continuous, restrained one-way PT concrete slabs exposed to localised heating. Despite the comparatively simple layout of these tests and the well defined uniform heating applied to the slabs'

exposed soffits, the resulting global response is extremely complex and demonstrates numerous thermal and mechanical actions which would need to be carefully considered to rationally model even these extremely simple PT concrete structures. However, the tests will enable future efforts to build rational models which account for the requisite complexities. In the meantime, several conclusions can be formulated on the basis of the test results presented herein:

- Considerable prestress losses occurred during heating. The magnitude of the prestress relaxation was primarily influenced by the heated length ratio, as well as time, temperature, and loading conditions.
- Premature tendon rupture is a realistic and likely scenario for smaller heated length ratios in unbonded PT concrete slabs. This helps to validate experimentation and modelling described in Chapters 3 and 4.
- Restraining forces will be generated when a PT slab is exposed to localised heating; these may be of sufficient magnitude to cause distress to supporting columns. More severe heating will increase the magnitude of these forces.
- The continuous and restrained, one-way spanning PT slabs tested herein exhibited four distinct phases of deflection, as described previously. These trends are influenced by a complex interplay between stiffness degradation of concrete and prestressing steel tendons, plastic and creep deformation, and thermal expansion/contraction. Any attempt to numerically model such systems in fire must defensibly account for this complexity to be considered credible.

Chapter 6

Conclusions and Recommendations

"An ignorant person may make many mistakes without being aware that he has done so, and the slightest failure is probably fatal to everyone…"
- James Braidwood
1st Firemaster of Edinburgh and founder of the London Fire Brigade
(Braidwood, 1849)

6.1 Summary

Most jurisdictions are currently moving toward the adoption of performance-based structural fire design codes, and it is thus becoming crucial that the behaviour of all structures, including unbonded PT concrete structural systems in high temperature and fire, be scientifically and rationally understood. Post-tensioned concrete slabs are widely believed to benefit from 'inherent fire endurance.' This belief is based on results from standard fire tests performed on simply supported specimens more than five decades ago. Such tests are of debatable credibility; they do not capture the true structural behaviour of real buildings in real fires, and they do not reflect modern PT concrete construction materials. The objective of this thesis has been to develop a better understanding of the structural and thermal response of PT concrete slabs, particularly as related to the performance of the unbonded prestressing tendons, at high temperature. The thesis has made the case that before defensible computational modelling of unbonded PT structures in fire can be performed, a much better understanding of, and ability to model, the specific performance of the unbonded prestressing tendons is required; it has set out to develop and validate the required modelling capabilities and material input parameters.

A review of previous experiments and real case studies on fire exposed PT concrete structures was provided in Chapter 2 to determine whether current code guidance for the fire-safe design of modern PT concrete slabs is adequate. Both bonded and unbonded post-tensioning configurations were considered. Research gaps were identified, in particular highlighting the risk of tendon rupture due to localised heating. The review indicated that for unbonded prestressing tendons during a localised fire the interaction between thermal relaxation and plastic deformation (which is dominated by creep) could result in failure considerably

earlier than expected (or predicted) based on available design guidance, especially in cases where concrete cover is reduced as restraining mechanisms and load redistribution are thought to provide additional structural capacity in a fire. Since unbonded prestressing tendons run continuously in unbonded PT slabs, local damage to tendon will affect the integrity of adjacent bays in a building. In the event that no bonded steel reinforcement is provided (as permitted by some design codes) a PT concrete slab could lose tensile reinforcement across multiple bays of the structure, even those remote from fire, as highlighted in real building case studies in Chapter 2.

Using the existing literature and available design guidance, modelling was presented in Chapter 3 which illustrated the stress-temperature-time interactions for stressed prestressing steel under increasing temperatures, thereby developing an understanding of tendon response to high temperature. Chapter 3 clearly demonstrated that most existing design guidance is unable to rationally describe the behaviour of contemporary prestressing steel, thus necessitating a revisiting of input parameters for analysis of prestressing steel at high temperature in Chapter 4.

The high temperature material behaviour of modern prestressing steels was considered in Chapter 4, both experimentally and analytically. Uniaxial tensile tests were performed on prestressing steel specimens from various regions around the world to induce constant axial stress at high temperature. The observed deformation was monitored, using a high resolution digital image correlation (DIC) technique. The measurement technique was validated and shown to be practical for such applications by assessment at ambient and at high temperature. A new analytical model of the temperature- and time-dependent deformation of prestressing steel was developed and validated based on the observed behaviour from tests under various heating scenarios. The new model can be used under any heating scenario (corresponding to uniform or localised heating). The behaviour of modern prestressing steel was compared against historical prestressing steel, showing that there were clear high temperature behavioural differences. For the first time for prestressing steel, cross-sectional area reductions were monitored with the DIC technique during tertiary creep indicating that failure was a manifestation of localised necking.

With the behaviour of modern unbonded prestressing tendons in variable heating accurately defined, other structural actions within a real PT concrete structure (thermal bowing, restraint, concrete stiffness loss, continuity, spalling, slab splitting etc.) which may also play significant roles influencing the slab's response in fire were considered experimentally in Chapter 5. Three non-standard structural fire experiments were performed on continuous and restrained PT concrete slabs. This was done in an effort to better understand the response of PT concrete structures to localised high temperature exposure, and to validate the use of the computational stress relaxation model for a tendon located inside a real concrete structure during heating. This was the first time a continuous PT slab which included axial, vertical and rotational restraint has been studied at high temperature. Unbonded PT slabs were heated locally in the centre span using a radiant panel array until the embedded prestressing steel in concrete reached a critical temperature. The structural response during all tests indicated a four phase deflection response which differs from the response of a simply supported slab during a standard fire test. Deflection trends in the continuous slab tests were due to a complex combination of thermal expansion and plastic damage. These test results will enable future efforts to build and validate rational computational modelling capability which can account for the requisite complexities of even this relatively simple structural system; however performing this analysis was initially beyond the scope of the current PhD project.

6.2 Conclusions

The following key conclusions can be drawn on the basis of the computational modelling and experimental testing presented in this thesis:

- For unbonded prestressing tendons during a localised fire the interaction between thermal relaxation and plastic deformation could result in failure considerably earlier than expected based on available design guidance that is in the form of critical temperature.
- Modern prestressing steel sourced from three different mills around the world show clear sensitivity to behavioural changes at elevated temperature (i.e. creep model input parameter variations), in part due to manufacture and metallurgy of the specimens.

- New material input parameters to approximate creep strain in prestressing steel in high temperature have been developed and presented. These parameters have been validated against previous testing by the author, as well as against new testing using dedicated stress relaxation tests at elevated temperature. In all cases the maximum error observed was less than 6%.
- Design guidance and test procedures available prior to this thesis were incapable of assessing tendon rupture due to high temperature creep for modern prestressing steels. Chapters 3 and 4 have provided experimentation and modelling to address this need. These efforts have identified that premature tendon rupture is a likely scenario in real buildings and that this is likely to occur before the required fire resistance is met. The PT concrete slabs tested in this thesis validated this behaviour.
- The new material input parameters for use within available creep models have been shown to be capable of modelling stress relaxation in continuous unbonded post tensioned slabs.
- Realistic but as simplified as possible (while incorporating the necessary factors) post-tensioned concrete elements were tested under localised heating and demonstrated highly complex structural response. Thermal bowing at test commencement was observed with cambering from slab stiffness degradation following when concrete reached a temperature of about 450ºC. This was then followed by deflection when the prestessing steel experienced creep initiating at a tendon temperature greater than about 300ºC. During cooling cambering from contraction of concrete was observed. Any attempt to numerically model post tensioned concrete systems in fire will need to defensibly account for these complexities and others noted above. The tests presented herein provide badly needed test data which can be used to develop and validate future computational modelling for performance based fire design.

Several additional secondary conclusions can be drawn from the research presented herein, including:

- DIC was shown to be a reliable method to measure longitudinal (and lateral) deformation of prestressing steel at high temperatures; it is not hampered by some of the limitations that prevent traditional strain measurement techniques

from being used at high temperatures or for measuring high strains up until the instant of failure.

- Using DIC for cross-sectional area reduction analysis during elevated temperature uniaxial tensile testing (i.e. for monitoring necking an calculating true stress and strain) has allowed initial assessment of high temperature creep behaviour in the Tertiary (failure) phase, indicating that this appears as a manifestation of localised necking in prestressing steel.
- Material analysis of three prestressing steels indicated that the microstructure at temperatures below 500ºC appeared stable. Since changes in microstructure appear negligible below this temperature, the transient creep test can therefore be used for any prestressing steel in lieu of time consuming steady state tensile creep testing.
- Considerable time dependent tendon prestress losses occurred during heating of the continuous and unbonded PT concrete slabs. The magnitude of this stress relaxation was influenced by the degree of heated length ratio.
- The distinction between creep strain and mechanical plastic strain (i.e. yielding) breaks down at elevated temperature. As the temperature of the steel increases and its yield strength and elastic modulus decrease, yielding and creep deformation become intertwined and the classical definitions of these strains can lose meaning.
- Available mechanical property reduction models for prestressing steel, which 'implicitly' account for high temperature creep, cannot possibly capture the time-dependency of creep deformation under transient heating conditions as would occur in a real fire.
- Cracking and spalling patterns differed between the bonded and unbonded PT concrete slabs. The results suggest that the maintained compression from lack of stress relaxation in the bonded slab promoted more damage to the concrete upon heating.
- While the EN 1992-1-2 (CEN, 2004) prestressing tendon rupture predictions (proposed strength versus temperature reductions) appear defensible on the basis of the experiments presented in Chapter 5, North American guidance with a

higher critical temperature appears not to be defensible for realistic heated length ratios.

- Considerable restraining forces will be generated when a PT slab is exposed to localised heating; these could be of sufficient magnitude to cause distress to supporting columns.

6.3 Design Recommendations

Overall, the research presented herein shows that some of the current design guidance for modern unbonded PT concrete slabs is inadequate as it cannot prevent sudden rupture of unbonded prestressing tendons in either standard or localised fires in real unbonded PT buildings in real fires. The broader structural consequences of the loss of prestressing reinforcement remain largely unknown, and it is difficult to conclusively state whether other relevant structural interactions (such as membrane actions, moment redistribution, etc) may prevent a given PT slab from collapsing during or after a fire. Such questions will likely need to be asked, and answered, using validated computational modelling in the future (validated using the tests presented herein, and others). However, on the basis of the research presented herein the following design recommendations are considered prudent to update existing guidance.

Parameters used to predict creep deformation

Three distinct sets of creep parameters were developed in Chapter 4 which can be used to accurately estimate creep deformation, and in turn stress relaxation, of a stressed unbonded prestressing tendon at elevated temperature. These creep parameters are recommended to be used conjunction with the Harmathy (1967) equation (repeated as Equation 6.1) to estimate the total creep strains (and therefore stress relaxation):

$$\varepsilon_{cr} = \frac{\varepsilon_{cr,0}}{\ln 2} \cosh^{-1}\left(2^{\frac{Z\theta}{\varepsilon_{cr,0}}}\right) \qquad [6.1]$$

There are two main reasons that an engineer may need to estimate creep of a prestressing tendon at elevated temperature: (1) to evaluate the potential for prestress

relaxation and the possible consequences for overall structural performance or failure modes (where maximum credible tendon stress losses are desired), and (2) to conservatively predict tendon rupture (where minimum tendon stress losses are desired). In the event that an estimate of stress relaxation of prestressing steel is needed to consider fire degraded flexural or shear capacities of a post tensioned concrete slab (which rely on the in service stress level for estimation of capacity), the Creep parameters derived for the BS 5896-12 (2012) prestressing steel (from Chapter 4 and repeated below in Equation 6.2) should be used.

$$Z = ae^{b\sigma} = 1.02x10^{16} e^{0.019\sigma} \qquad 687 \text{ MPa} < \sigma < 1300 \text{ MPa} \qquad [6.2]$$

$$Z = 0.7x10^{8} \sigma^{5.0} \qquad 200 \text{ MPa} < \sigma < 687 \text{ MPa}$$

$$\varepsilon_{cr,0} = c\sigma^{d} = 1.072x10^{-7} \sigma^{1.64}$$

These parameters can be used for the full service stress range, and will predict more relaxation than the parameters derived to the AS/NZS 4672-07 (2007) prestressing steel; and hence more conservative flexural and shear performance predictions in the event that the prestressing tendons do not rupture during fire.

If, however, a designer wants to predict the earliest stress-strength interception which is an indicator of premature tendon rupture, the following creep parameters (which are based on those derived for AS/NZS 4672-07 (2007) prestressing steel herein) should be used with Equation 6.1 to predict creep damage.

$$Z = ae^{b\sigma} = 4.37x10^{14} e^{0.015\sigma} \quad 700 \text{ MPa} < \sigma < 1200 \text{ MPa} \qquad [6.3]$$

$$\varepsilon_{cr,0} = c\sigma^{d} = 1.15x10^{-11} \sigma^{2.72}$$

However, while these creep parameters will estimate less stress loss than those presented in Equation 6.2, they are based on a limited stress range therefore they may not be practical in the event that a designer needs to determine stress relaxation below 700 MPa for tendon rupture.

Developing new creep parameters for additional specific prestressing steels

If a designer needs (or wants) to develop their own creep parameters for alternative prestressing steels at elevated temperatures, rather than using those derived and

presented herein; an appropriate suite of a limited number creep tests may be used to determine new material input parameters. To do this, the minimum number of necessary tests, in the opinion of the author, is five. These are:

- Two steady state tests are needed at the same stress level but different temperatures to derive an activation energy which can relate time and temperature effects. The author recommends that the chosen stress level should be performed between the upper end stress level of the expected in-service stress amount (ie. 1200MPa) and a lower end stress level that the designer will tolerate in the event of high temperature exposure. This lower bound value may represent the stress loss needed to cause a failure mode. The temperatures of these tests must follow three criterion: they must be below 500ºC for prestressing steel; two temperatures should be chosen which are different; and the temperatures in conjunction with the stress level must not cause mechanical yielding before the constant load level is achieved. The last point is so to produce a θ-ε_{cr} creep curves with minimal influences from mechanical damages at the start of the test. EN 1992-1-2 could be used as guidance in the absence of new tensile strength tests for these yield values.
- A minimum of three transient tests at different service stress levels (within the aforementioned stress range of interest) including one stress level equal to one of the two steady state tests noted above is needed.

It would be preferable to conduct as many transient tests as possible, at different loads, to accurately characterise the behaviour of the steel at all relevant stress levels. A repeat transient test at the same sustained stress level as the steady state test could also be conducted to provide verification of the definition of activation energy. Additional repeat tests would further instil confidence in the new creep parameters.

Cover requirements for unbonded PT concrete slabs

As far as the prescriptive axis distance requirements stated by EN 1992-1-2 (CEN, 2004) are concerned, the assumed critical temperature of 350ºC appears to be defensible for simply supported slabs, although for shorter heated length ratios it may to be insufficient to prevent tendon rupture before the fire resistance period is

achieved. Increasing the EN 1992-1-2 prescribed covers by about 5 mm could adequately address the issue of tendon rupture under localised heating for the simply supported case. For North American design guidance in particular (IBC, 2012) the assumed critical temperature of 426°C is difficult to rationalise and in need of revision. In all modelling cases in Chapter 3, the IBC (2012) covers were considerably less than required to prevent tendon rupture before the prescribed fire resistance time was achieved. For example, for 120 minutes fire resistance an additional 18 mm of concrete cover is required to prevent tendon rupture for smaller heated length ratios for the simply supported case. In both EN 1992-1-2 (CEN, 2004) and the IBC (2012) the required concrete covers (or axis distances) for restrained slabs are further reduced even from the unrestrained case, since collapse prevention during fire is assumed to be aided by restraint and continuity (redistribution of moments). While this approach may be defensible on the basis of available standard furnace test data, it virtually guarantees that tendon rupture will occur in restrained slabs well before the prescribed fire resistance time is met. At the very least the EN 1992-1-2 (CEN, 2004) cover requirements should be universally adopted in North American codes, assuming the premature tendon rupture is to be avoided during fire.

Minimum bonded reinforcement in unbonded PT concrete slabs

It is currently difficult to justify in many cases that slab failure would not occur during or after a fire in the event of tendon rupture, particularly for structures without minimum amounts of bonded reinforcement. Designers should thus be required to supply a minimum amount of bonded reinforcement in all unbonded PT slabs to enable load shedding to the bonded reinforcement in the event of tendon rupture (rather than no bonded reinforcement as is permitted in certain regions of a slab in some codes). The recommended bonded reinforcement ratios of 0.2% as prescribed by Van Herberghan and Van Damme (1983) should be sufficient for the time being. Future research is needed to defensibly suggest the minimum amount needed. Additionally, a series of transverse ties may help prevent longitudinal cracking along the tendon in unbonded PT slabs (if this is presumed to be problematic).

6.4 Research recommendations

Despite the comparatively simple layout of the slab tests and the well defined uniform heating applied to the slabs' exposed soffits, the resulting global response is highly complex and demonstrated numerous thermal and mechanical actions which would need to be carefully considered to rationally model even these extremely simple PT concrete structures. This thesis repreasents a starting point in our understanding of PT concrete structures in fire and the following is a list of research recommendations which should be considered as the structural community moves towards performance based structural fire design for unbonded post tensioned concrete structures. Undoubtably as these topics are pursued, additional research needs will also be identified.

- **Attempt to model the tests presented in Chapter 5** – The most obvious future research objective is to attempt to computationally model the observed response of the slab tests presented in Chapter 5 of this thesis. This thesis has focused on characterization and quantification of the high temperature response of prestressing steel. The work presented only begins to investigate concrete material and structural behaviour in fire. A detailed study into the thermal and mechanical behaviour of concrete and concrete structures may aid modelling efforts in the future to evaluate the responses observed during these tests.
- **Consequences of tendon rupture** – The consequences of tendon rupture on the capacity of UPT slabs and whole buildings must be researched in the future. None of the slab tests were able to examine the effect of prestressing steel rupture on the global structure and the subsequent load shedding response. Future research must be conducted that can highlight the effects of load shedding to mild bonded reinforcement (if present) and if the structure can support the applied load after tendon rupture. This will help identify the minimum passive (bonded) reinforcement that is required for fire-safe design. Additionally, the assessment of likely and or possible failure modes of whole concrete structures should be considered in the future as this is an issue for all concrete structures in fire.
- **Mechanical re-stressing of unbonded prestressing steel** – There are many inter-related structural actions which will influence the deformation response of

the prestressing steel in a fire. Future research needs to consider the roles that thermal bowing, loss of precompression, loss of load balancing ability, perimeter cracking, and restraint on the concrete have on the stress level of unbonded prestressing steel.

- **Improvement of the DIC technique** – Refinement of the DIC algorithm may decrease the scatter present in measurement and allow the failure behaviour of the prestressing steel to be studied more closely in the Tertiary phase.
- **Understanding the impacts of manufacturing of prestressing steel** – Additional investigation should be undertaken to characterize the manufacturing process of prestressing steel at different mills internationally to identify the impacts of different metallurgy and manufacturing procedures on the creep properties of prestressing steels at high temperature.
- **Further investigation into Tertiary creep mechanisms** – Further studies into the controlling mechanisms (cracking, necking etc.) of tertiary creep behaviour are necessary to help our understanding and improve our capabilities to model this behaviour.
- **Additional testing** – With reference to the quote provided at the start of Chapter 5, future tests must be conducted that can rationally compare the differences in structural reactions between different fire sizes and severities. It is true with respect to the tendon that localised heating may induce premature rupture of the unbonded prestressing steel; however more uniform heating may induce higher restraining forces which could cause significant deformations of the slab and cause other types of failures.
- **Spalling** – Despite considerable dedicated research efforts over the past twenty years or so, the phenomenon of fire-induced spalling of concrete cover concrete remains poorly understood and difficult to predict and/or control. Future research should develop an ability to guarantee that no spalling occurs in a concrete structure exposed to fire. Without this ability modelling concrete structures to predict their real behaviour in fire is essentially impossible.

References

A

Aalami, BO. (2007). “Critical Milestones in Development of Post-Tensioned Buildings.” *Concrete International*, October, 52-56.

Abrams, MS. and Cruz, C. (1961). “The Behaviour at High Temperature of Steel Strand for Prestressed Concrete.” *Journal of PCA Research and Development Laboratories*, September, 3(3), 8-19.

ACI. 318. (1983). “Building Code Requirements for Reinforced Concrete.” *Rep. No. ACI 318-83,* American Concrete Institute, Detroit, 1983.

Aimin, Y., Yuli, D., and Litang, G. (2013). “Behaviour of Unbonded Prestressed Continuous Concrete Slabs with the Middle Span and Edge Span Subjected to Fire In Order.” *Fire Safety Journal*, 56, 20-29.

ACI. 318 (2008). "Building Code Requirements for Structural Concrete." *Rep. No. ACI 318-08,* American Concrete Institute, Farmington Hills, MI.

ACI. 423. (2005). “Recommendations for Concrete Members Prestressed with Unbonded Tendons”. *Rep. No. ACI 423.3-05,* American Concrete Institute, Farmington Hills, MI.

Anderberg, Y. (1983). "Properties of Materials at High Temperatures: Steel." *Rep. No. TVBB-3008,* Division of Building Fire Safety and Technology, Lund Institute of Technology, Lund University, Sweden.

Allouche, E. N., Campbell, T. I., Green, M. F., and Soudki, K. A. (1998). "Tendon Stress in Continuous Unbonded Prestressed Concrete Members - Part 1: Review of Literature." *PCI Journal*, 43(6), 86-93.

Allouche, E. N., Campbell, T. I., Green, M. F., and Soudki, K. A. (1999). "Tendon Stress in Continuous Unbonded Prestressed Concrete Members - Part 2: Parametric Study." *PCI Journal*, 44(1), 60-73.

ASTM. (2001). “Test Method E119-01: Standard Methods of Fire Test of Building Construction and Materials” *Rep. No. E119-01,* American Society for Testing and Materials, West Conshohocken, PA.

ASTM.(1965). "A421-65 Standard Specification for Uncoated Stress- Relieved Steel Wire for Prestressed Concrete." *Rep. No. A421 / A421M-01,* American Society for Testing and Materials, West Conshohocken, PA.

ASTM. (2003). "A416-03 Standard Specification for Steel Strand, Uncoated Seven-Wire for Prestressed Concrete." *Rep. No. A416 / A416M-01,* American Society for Testing and Materials, West Conshohocken, PA.

Ashton, L., and Bate, S. (1961). “Discussion on the Fire-resistance of Prestressed Concrete Beams- paper 6444.” *ICE Proceedings*, 20(2), 305-320.

B

Background documents EC2. (2004). “Background Documents to EN 1992-1-2 Eurocode 2: Design of Concrete Structures –Part 1-2: General rules – Structural fire design.” European Committee for standardization, Brussels, July.

Bailey, CG., and Ellobody, E. (2009a). “Comparison of Unbonded and Bonded Post-Tensioned Concrete Slabs under Fire Conditions.” *The Structural Engineer*, October, 87 (19), 23-31.

Bailey, CG., and Ellobody, E. (2009b). “Fire Tests on Unbonded Post-Tensioned One-way Concrete Slabs.” *Magazine of Concrete Research*, 61 (1), 67-76.

Bailey, CG., and Ellobody, E. (2009c). “Whole-Building Behaviour of Bonded Post-Tensioned Concrete Floor Plates Exposed to Fire.” *Engineering Structures*, 31, 1800-1810.

Bailey, CG. (2002). “Holistic Behaviour of Concrete Buildings in Fire.” *Proceedings of the Institution of Civil Engineers, Structures and Buildings*, August, Issue 3, 199-212.

Bailey, CG., White, D., and Moore D. (2000). “The Tensile Membrane Action of Unrestrained Composite Slabs Simulated Under Fire Conditions.” *Engineering Structures*, 22, 1583–1595.

Barth, F., and Aalami, B. (1992). “Controlled Demolition of an Unbonded Post-Tensioned Concrete Slab.” *PTI special report*, 34 pp.

Babrauskas, V., and Williamson RB. (1978a). “The Historical Basis of Fire Resistance Testing- Part 1.” *Fire Technology*. 304-315.

Babrauskas, V., and Williamson RB. (1978b). “The Historical Basis of Fire Resistance Testing- Part II.” *Fire Technology*. 184-194, 205.

Bisby, L., Gales, J., and Maluk, C. (2013). “A Contemporary Review of Large-scale Non Standard Structural Fire Testing (circa 1980-present).” *Fire Science Reviews*, 2(1).

Bisby, LA., and Take, WA. (2009). “Strain Localisations in FRP-confined Concrete: New Insights.” *Proceedings of the Institution of Civil Engineers Structures and Buildings*, 162: 301-209.

Bisby, L., and Kodur, V. (2005). “Evaluation of Fire Endurance of Concrete Slabs Reinforced with Fiber Reinforced Polymer Bars.” *ASCE Journal of Structural Engineering*, 131(1), 34-43.

Bletzacker, RW. (1967). “Fire Resistance of Protected Steel Beam Floor and Roof Assemblies as Affected by Structural Restraint.” *Symposium on Fire test methods. American Society of Testing Materials*, p 63-90.

Braidwood, J. (1849). “On Fire Proof Buildings.” *Proceedings of the Institution of Civil Engineers.* 141-163.

Brannigan, F., and Corbett, G. (2009). “Building Construction for the Fire Service.” fourth ed., Jones and Bartlett, Sudbury MA.

BSi. (1997). “Structural use of concrete. BS 8110-1” British Standards Institution, London.

BSi. (2000). “Testing hardened concrete. BS 12390-1-8” British Standards Institution, London.

BSi. (2002). “Eurocode 1, Actions on Structures, General Actions, Actions on Structures Exposed to Fire.” British Standards Institution, London.

BSi. (2002). “Eurocode 2, Design of Concrete Structures -Part 1-1: General Rules and Rules for Buildings.” British Standards Institution, London.

BSi. (2012). “Specification for High Tensile Steel Wire and Strands for the Prestressing of Concrete, BS 5896-12.” British Standards Institution, London.

Buchanan, AH. (2001). “Structural Design for Fire Safety.” Wiley, New York, NY.

Burns, NH., and Hemakom, R. (1977). “Test Scale Model of Post- tensioned Flat Plate.” *Journal of the Structural Division*, June, 1237-1255.

C

CSTR. (2005). “Post Tensioned Concrete Floors Design Handbook.” *CSTR 43*, Concrete Society, Camberley Surrey.

Canadian Standards Association. (2004). “CAN/CSA A23.3-04: Design of Concrete Structures.” CSA, Ottawa, ON.

CCAA. (2010). “Fire Safety of Concrete Buildings.” *Cement Concrete & Aggregates Australia - CCAA T61*, 37 pp.

CEN. (2004). “Eurocode 2: Design of Concrete Structures, Parts 1-2: General rules-Structural fire design, EN 1992-1-2.” European Committee for standardization, Brussels.

CEN. (2005). “Eurocode 3: Steel design, Parts 1-8: Joints and welds, EN 1993-1-8.” European Committee for standardization, Brussels.

Collins, M. P., and Mitchell, D. (1987). “Prestressed Concrete Basics.” Canadian Prestressed Concrete Institute, Ottawa, ON.

Clark, N., and Walley, T (1953). “Creep of High Tensile Steel Wire.” *ICE Proceedings*, 2(2). 107-154.

CPCI. (2007). “Design Manual: Precast and Prestressed Concrete.” Canadian Prestressed Concrete Institute. Ottawa Canada.

D

Davis, J. (2004). “Tensile Testing.”, ASM International, 2nd ed. 278 pp.

Dwaikat, MB., and Kodur, V. (2008). “Approach for Modelling the Fire Induced Restraint Effects in Reinforced Concrete Beams.” *Fire Safety Journal*, 43: 291-307.

Dwaikat, MB., and Kodur, V. (2009). “Hydrothermal Model for Predicting Fire-Induced Spalling in Concrete Structural Systems.” *Fire Safety Journal*. April. 425-434.

Dorn, JE. (1955). “Some Fundamental Experiments on High Temperature Creep.” *J.Mech.Phys.Solids*, 3(2), 105-116.

E

Ellobody, E., and Bailey, CG. (2008). “Testing and Modelling of Bonded and Unbonded Post-Tensioned Concrete Slabs in Fire.” *Proceedings from the Fifth International Conference on Structures in Fire*, Singapore, 392-405.

Ellobody, E., and Bailey, CG. (2009). “Modelling of Unbonded Post-Tensioned Concrete Slabs under Fire Conditions.” *Fire Safety Journal*, 44, 159-167.

F

Franssen, JM. and Bruls. (1997). “Design and Tests of Prestressed Concrete Beams.” *Fire Safety Science*, 5, 1081–1092.

G

Gales, J. (2009) “Transient High-temperature Prestress Relaxation of Unbonded Prestressing Tendons for Use in Concrete Slabs.” *M.Sc. Thesis*, Department of Civil Engineering, Queen’s University, Kingston, On, Canada. 197 pp.

Gales, J., Bisby, L., MacDougall, C., and MacLean, K. (2009). “Transient High-Temperature Stress Relaxation of Prestressing Tendons in Unbonded Construction.” *Fire Safety Journal*, 44, 570-579.

Gales, J., Bisby, L., and Maluk, C. (2012). “Structural Fire Testing – Where are We, How Did We Get Here, and Where are We Going?” *Proceedings of the 15th International Conference on Experimental Mechanics*, Porto, Portugal. 22 pp.

Ghalleb, A. (2013). “Calculating ultimate tendon stress in externally prestressed continous concrete beams using simplified formulas.” *Engineering Structures*, 46, 417-430.

Ghosh, K. (2009). “Analysis and Design Practice of Steel Structures. PHI, New Dehli.

Giroux, PF., Dalle, F., Sauzay, M., Mapaplate, J., Fournier, B., and Gourgues-Lorenzon, A. (2010). “Mechanical and Microstructural Stability of P92 Steel Under Uniaxial Tension at High Temperature.” *Materials Science and Engineering A*, 527, 3984-3993.

Gillie, M. (2009). “Analysis of Heated Structures: Nature and Modelling Bench Marks.” *Fire Safety Journal*, 44, 673–680.

Grant, B., Stone, H., Withers, P., and Preuss, M. (2009). “High- temperature Strain Field Measurement Using Digital Image Correlation.” *Journal of Strain Analysis*, 44, 263-271.

Gustaferro, AH., Abrams, M., and Salse, E. (1971). “Fire Resistance of Prestressed Concrete Beams Study C: Structural Behaviour During Fire Tests.” *PCA Research and Development Bulletin*. 29 pp.

Gustaferro, AH. (1973). “Fire Resistance of Post-Tensioned Structures.” *PCI Journal*, March-April, 18(2), 38-62.

H

Harmathy, TZ. (1967). “Comprehensive Creep Model.” *Transactions of the ASME Journal of Basic Engineering*, 89(3): 496-502.

Harmathy, T., and Lie, TT. (1970). “Fire Test Standard in the Light of Fire Research” *ASTM STP 464*, pg 85-97.

Harmathy, TZ., and Stanzak, W. (1970). “Elevated-Temperature Tensile and Creep Properties of Some Structural and Prestressing Steels.” *Fire Test Performance ASTM Special Technical Publication 464*, ASTM, Philadelphia Pa, 186-207.

Hill, A. W., and Ashton, L. A. (1957). "Fire Resistance of Prestressed Concrete." *Civil Engineering (London)*, 52(617), 1249-1253.

Himmelwright, A. (1899). “Tests.” Roebling company, New York. 200pp.

Holdsworth, S. (2010). “Advances in Assessment of Creep Data During the Past 100 years.” *Transactions of the Indian Institute of Metals*, 63 (2-3), 93-99.

Holmes, M., Anchor, R. D., Cook, G. M. E., and Crook, R. N. (1982). "Effects of Elevated Temperatures on the Strength Properties of Reinforcing and Prestressing Steels." *Structural Engineer, Part B: R&D Quarterly*, 60B(1), 7-13.

Hertz, KD. (2003) “Limits of Spalling of Fire-exposed Concrete.” *Fire Safety Journal*, 38, 103–116.

I

Iwankiw, N., Beyler, C., and Beitel, J. (2008). “Testing Needs for Advancement of Structural Fire Engineering.” *Fifth International Conference on Structures in Fire*, Singapore, 334-343.

Ingham, J. (2009). “Forensic Engineering of Fire-damaged Structures.” *Proceedings of the Institution of Civil Engineers: Civil Engineering*, 12-17.

IBC. (2012). “International Building Code.” International Code Council, USA.

IStructE. (2006). “Manual for the Design of Concrete Building Structures to Eurocode 2.” The Institution of Structural Engineers and British Cement Association.

ISO 834. (1999). “Fire Resistance Test – Elements of Building Construction.” International Organization for Standardization, Geneva.

J

Jeschke, J., Ostermann, D., Krieg, R. (2011). “Critical Strains and Necking Phenomena for Different Steel Sheet Specimens Under Uniaxial Loading.” *Nuclear Engineering and Design*, 241, 2045-2052.

Jimenez, GA. (2009) “Assessment and Restoration of Post-Tensioned Buildings – Parking Ramp Structures.” *Proceedings of the 2009 Structures Congress ASCE*, pp. 1954-1963.

K

Kelly, F., and Purkiss, J. (2008). “Reinforced Concrete Structures in Fire: A Review of Current Rules.” *The Structural Engineer*, 86(19), 33-39.

Khan, S., and Williams, M. (1995). “Post-Tensioned Concrete Floors.” Butterworth-Heinemann, London.

Khoury, GA., and Anderberg, Y. (2000). “Concrete Spalling Review, Fire Safety design.” Report submitted to Swedish National Road Administration.

Khoury, GA. (2006). “Strain of Heated Concrete During Two Thermal Cycles. Part 2: Strain During First Cooling and Subsequent Thermal Cycle” *Magazine of Concrete Ressearch*, 58, 387-400.

Kodur, V., and Phan, L. (2007). “Critical Factors Governing the Fire Performance of High Strength Concrete Systems.” *Fire Safety Journal*, 42, 482–488.

Kodur, V., and McGrath, R. (2003). “Fire Endurance of High Strength Concrete Columns.” *Fire Technology*, 39, 73–87.

L

Law, M., and Beever, P. (1995). “Magic Numbers and Golden Rules.” *Fire Technology*, 77-83.

Lee, D., and Bailey, CG. (2006). “The Behaviour of Post-tensioned Floor Slabs in Fire Conditions.” *International Congress on Fire Safety in Tall Buildings*, Santander, Spain, pp. 183-201.

Lewinsohn, CA., Bakis, CE., Tressler, RE. (1996). “Methods of Determining the Temperature Dependence of Primary Creep.” *Fiber, Matrix, and Interface properties, ASTM STP 1290*, pp 9-18.

Lie, TT. (1992). “Structural Fire Protection.” ASCE, New York, NY, 1992.

Lin, T.Y. (1963). “Load-Balancing Method for Design and Analysis of Prestressed Concrete Structures.” *ACI Journal, Proceedings*, 60 (6), June, pp. 719-742.

Ling, Y. “Uniaxial True Stress-strain After Necking.” *AMP Journal of Technology*, 5, 37-48.

Litang, G., Dong, Y., Aimin, Y. (2004). “Experimental Investigation of the Behaviour of Continous Slabs of Unbonded Prestressed Concrete with End Span Under Fire.” *Journal of Building Structures*, 25(2), 118-123. (in Chinese).

Lukkunaprasit, P. (1990). “Unbonded Post-Tensioned Concrete Flat Plates Under 5-hours of fire.”*11th FIP congress in Hamburg Germany*, S61-S64.

M

MacDougall, C., and Bartlett, FM., (2003). “Tests of Unbonded Seven-Wire Tendon with Broken Outer Wires.” *ACI Structural Journal*, 100(5), 581-588.

MacLean K. (2007). “Post-fire Assessment of Unbonded Post-tensioned Concrete slabs: Strand Deterioration and Prestress Loss.” *M.Sc Thesis*, Department of Civil Engineering, Queen’s University, Kingston, ON, Canada.

MacLean, K., Bisby, LA., and MacDougall, CC. (2008). “Post-fire Assessment of Unbonded Post-tensioned Slabs: Strand Deterioration and Prestress Loss.” *ACI-SP 255: Designing Concrete Structures for Fire Safety*, American Concrete Institute, 10 pp.

Martin, L., and Purkiss, J. (2006) “Concrete Design to EN 1992.” Butterworth-Heinemann, 2nd Ed.

Morovat, M., Lee, J., Engelhardt, M., Taleff, T., Helwig, T., and Segrest V. (2012). “Creep Properties of ASTM A 992 Steel at Elevated Temperatures.” *Advanced Materials Research*, Vol 446-449 786-792.

N

Nawy, E. (2008). “Concrete Construction Handbook”, 2nd ed., CRC Press, Boca Raton.

NZS 3101. (2006). “The Design of Concrete Structures.” Standards New Zealand, Wellington, NZ.

NZS 4672. (2007). “Prestressing Strand Standard.” Standards Australia New Zealand, Wellington, NZ.

NIST. (2008). “NCSTAR 1A: Final Report on the Collapse of World Trade Center Building 7” National Institute of Standards and Technology, Gaithersburg, USA, 130pp.

NBCC. (2005). “National Building Code of Canada 2005” National Research Council of Canada, Ottawa, ON.

P

Pan, B., Wu, D., Wang, Z., and Xia, Y. (2001). “High-temperature Digital Image Correlation Method for Full Field Deformation Measurement at 1200ºC.” *Measurement Science and Technology*, 22,1-10.

PCI. (1972). “Prestressed Concrete Institute Post Tensioning Handbook.” Chicago Illinois, 1972.

PCA. (2005). “Portland Cement Association Design Notes: Time saving Design Aids: Two way Post-Tensioned Design.” Portland Cement Association..

Post, N., and Korman, R. (2000). “Implosion Spares Foundations.” *Engineering News Record*, June 12, 12-13.

Poston, R., and Dolan, C. (2008). “Re-organizing ACI 318.” *Concrete International*, July, 43-47.

PTI. (2006). “Post-Tensioning Manual-Sixth Edition.” Post-Tensioning Institute, Phoenix, AZ.

Purkiss, JA. (2008). “Fire Safety Engineering: Design of Structures.” BH, London, UK.

R

Roberston, L., Dudorova, Z., Gales, J., Vega, E., Stratford, T., Blackford, J., and Bisby, L. (2013). “Micro-structural and Mechanical Characterization of Post-tensioning Tendons Following Elevated Temperature Exposure.” *Applications of Structural Engineering Conference*, Prague, CZ, 474-479.

S

Sarasota Herald (1955). “Prestressed Concrete is Fire Resistant.” Feb 27, pg 58.

Sarkkinen, D. (2006). “Fire Damaged Post-tensioned Slabs.” *Structure Magazine*, June, 32-34.

Selvaggio, SL., and Carlson, CC. (1967). “Restraint in Fire Tests of Concrete Floors and Roofs.” *Symposium on Fire Test Methods American Society of Testing Materials*, p 63-90.

Shipp, M., Fraser-Mitchell, J., Chitty, R., Cullinan, R., Crowder, D., and Clark, P. (2009). “Fire Spread in Car Parks; a summary of the CLG/BRE Research programme findings.” BRE Global Limited, Bucknails Lane, Watford, Hertfordshire, UK, 15 pp.

Schneider, R., and Lange, J. (2010). “Constitutive Equations and Empirical Creep Law of Structural Steel S460 at High Temperatures.” *Proceedings from the Sixth International Conference on Structures in Fire*. 727–734.

Scheider, I., Brocks, W., and Cornec, A. (2004). “Procedure for Determination of True Stress-strain Curves From Tensile Tests with Rectangular Cross-Section Specimens.” *Transactions of the ASME*. 126: 70-76.

Smith, W. (1996). “Principals of Material Science and Engineering.” McGraw Hill, NY.

Spyrou, S. and Davison, J. (2001). “Displacement Measurement in Studies of Steel T-stub Connections.” Journal of Constructional Steel Research. 57. 647-659.

Stern, I. (2009) “Restoration of Long Span Plate Post-Tensioned with Unbonded Tendons - after fire.” Lecture given at the 2002 fib Congress, Osaka, Japan.[online] Available at <http://www.yde.co.il/> [Accessed December 22nd 2009].

Stern-Gottfried, J., Rein, G., and Torero, J. (2009). “Travel Guide: A Newly Developed Methodology, Based on Concept of ‘Travelling Fires’ in Large

Enclosures, Will Assist With Structural Fire Analysis." *Fire Risk Management*, November, 12-16.

Stern-Gottfried, J., Rein, G., Bisby, L., and Torero, J. (2010). "Experimental Review of Homogeneous Temperature Assumption in Post-Flashover Compartment Fires." *Fire Safety Journal*, 45(4), 249-261.

T

Taranath, BS. (2010). "Reinforced Concrete Design of Tall Buildings." CRC Press, Taylor and Francis.

Troxell, GE. (1959a). "Fire Resistance of a Prestressed Concrete Floor Panel." *Journal of the American Concrete Institute*, August, 97-105.

Troxell, GE. (1959b). "Fire Test of Six inch Deep Prestressed Concrete Flat Slabs." Fire Prevention Research Institute, Gardena, Calif., December.

Troxell, GE. (1962). "Fire Resistance of Prestressed Concrete." *ACI Special publication No. 5*, Detroit, MI, 59-85.

Troxell, GE. (1965). "Prestressed Lift Slabs Withstand Fire." *ASCE Civil Engineer*, September, 64-66.

U

Underwriters Laboratories. (1966). "Report on Prestressed Pre-tensioned Concrete Inverted Tee Beams and Report on Prestressed Concrete Inverted Tee Beams Post-Tensioned." *R4123-12A*, Underwriters' Laboratories Inc, USA.

Underwriters Laboratories. (1968). "Report on Unbonded Post-Tensioned Prestressed Reinforced Concrete Flat Plate Floor with Expanded Shale Aggregate." *PCI Journal*, 45-56.

V

VanHeberghen, P., and VanDamme, M. (1983). "Fire Resistance of Post-Tensioned Continuous Flat Floor Slabs with Unbonded Tendons." *FIP notes*, 3-11.

W

Williams-Leir, G. (1983). "Creep of Structural Steel in Fire: Analytical Expressions." *Fire and Materials*. 7(2), 73-78.

Wilshire, B., and Burt, H. (2008). "Damage Evolution During Creep of Steels." *International Journal of Pressure Vessels*, 85, 47-54.

Williams, SJ., Bache, MR., and Wilshire, B. (2010). “Recent Developments in Analysis of High Temperature Creep and Creep Fracture Behaviour.” *Materials Science and technology,* 26 (11), 1332-1337.

White, DJ., Take, WA., Bolton, MD. (2003). “Soil Deformation Measurement Using Particle Image Velocimetry (PIV) and Photogrammetry.” *Geotechnique*, 53(7), 619-631.

Y

Yao, H., Xuan, F., Wang, Z., and Tu, S. (2007). “A Review of Creep Analysis and Design under Multi-axial Stress States.” *Nuclear Engineering and Design*, 237, 1969-1986.

Z

Zener, C., and Hollomon J. (1944). “Effect of Strain Rate Upon Plastic Flow of Steel.” *Journal of Applied Physics*, 15-22.

Zhao, Y., Guo, Y., Wei, Q., Topping, T., Dangelewicz, A., Zhu, Y., Langdon, T., Lavernia, E. (2009). “Influence of Specimen Dimensions and Strain Measurement Methods on Tensile Stress-Strain Curves.” *Materials Science and Engineering A*, 525, 68-77.

Zhang, H., Davie, CT., Pearce, CJ., and Bicani, N. (2009). “A Numerical Model for Prediction of Spalling of Concrete Exposed to Elevated Temperatures.” *Proceedings of the International Conference Applications of Structural Engineering*. 301-306.

Zheng, W. and Hou, X. (2008). “Experiment and Analysis on the Mechanical Behaviour of PC Simply Supported Slabs Subjected to Fire.” *Advances in Structural Engineering*, 11(1), 71-89.

Zheng, W., Hou, X., and Xu, M. (2007). “Experiment and Analysis on Fire Resistance of Two-span Unbonded Prestressed Concrete Continuous Slabs.” *Journal of Building Structures*, 28(5), pp 13 (in Chinese).

Zheng, W., Hou, XM., Shi, DS., and Xu, MX. (2010). “Experimental Study on Concrete Spalling in Prestressed Slabs subjected to Fire.” *Fire Safety Journal*, 45, 283–297.

Zollman, C., Garavaglia, M., Rubin, A. (1960). “Prestressed Concrete Resists Fire Damage.” *ASCE Civil Engineer*, December, 36-41.

Appendix A:

Large Scale Structural fire testing – where are we, how did we get here, and where are we going?

From:

Gales, J., Bisby, L., and Maluk, C. (22–27 July 2012) Structural fire testing – where are we, how did we get here, and where are we going? Proceedings of the 15th International Conference on Experimental Mechanics. Porto, Portugal. 22 pp.

LARGE-SCALE STRUCTURAL FIRE TESTING – HOW DID WE GET HERE, WHERE ARE WE, AND WHERE ARE WE GOING?

John Gales[1], Cristián Maluk[2], and Luke Bisby[3]
[1, 2, 3] BRE Centre for Fire Safety Engineering, The University of Edinburgh, UK
Emails: j.gales@ed.ac.uk, c.maluk@ed.ac.uk, luke.bisby@ed.ac.uk

ABSTRACT

Structural fire testing is experiencing a renaissance. Both the research and regulatory communities are currently confronting the inherent problems associated with using simplified, single element tests on isolated structural members subjected to standard temperature-time curves to demonstrate adequate structural performance of buildings in fires. Indeed, this international symposium on "Fire Testing and Experimental Validation" is an indication of renewed interest in this area. This involves a shift in testing philosophy from prescriptive standard fire testing to large-scale non-standard fire testing using real fires. This follows more than a century during which the standard fire resistance test has been the predominant means of characterizing the response of structural elements and materials in fires. Large-scale non-standard tests performed around the world during the past three decades have identified numerous shortcomings in our understanding of real building behaviour in real fires; these could not have been observed through standard tests. However, while identifying many of these shortcomings appears as novel insight, many such insights have been well known for decades but have remained largely unaddressed due to the pervasive use of the standard fire test. Only now, with a keen interest in understanding and a willingness to change our testing, design, and regulatory approaches, can these shortcomings be addressed. This paper briefly reviews the available data and knowledge from large scale non-standard fire tests conducted in the past thirty years, and defines current gaps in knowledge and research needs for rational and holistic fire-safe structural design of buildings.

Keywords: real fire tests, standard fire tests, structural fire design, research gaps

1. BACKGROUND AND OBJECTIVES

Structural engineering design of buildings requires attention to many different load types and combinations (i.e., wind, earthquake, etc); however a structure's complex behaviour in fire is currently overly simplified during design. Fire is not typically considered as a load during the structural design of a building. This simplification is justified on the basis of results from standard fire tests of simple building elements or isolated structural assemblies in testing furnaces which subject the loaded elements to a *standard* temperature-time curve. The result of such tests is a time to failure subject to the standard fire; this is termed a fire resistance rating. The current system of fire rating building elements has been in existence since the turn of the last century and remains (largely) unchanged since its initial development, despite major advances in both fire safety science and structural fire modelling. This paper discusses the origins of the standard fire resistance test, some of the limitations in using this for fire testing or design, some of the complexities of the response of real buildings in fire, and the resulting research gaps that currently exist.

The origins of the standard fire test stem from early attempts to make a fire resistive comparison of different building materials and systems to assess claims of "fire proof" construction in the late 19th century (Woolson, 1916). The fire resistive principal, originally studied by Ira Woolson, was not meant to be a final 'solution' to the structural fire design and regulatory problems that were being encountered at the turn of the 20th century; rather it was meant to serve as a practice correction at that time, specifically in the wake of the Baltimore and San Francisco conflagrations (Fitzpatrick and

Condron, 1914). At that time, the building construction industry was being flooded with various 'fireproof' building system patents which had either never actually been tested or which failed to provide appropriate levels of protection in real fires (Fitzpatrick and Condron, 1914). The standard fire test thus emerged as a test for comparative performance in the most severe possible fire. The earliest references to standard fire resistance tests are found from New York, a city which was undergoing rapid innovation in construction during the late 1800s, brought on by novel lightweight structural designs (e.g. the emergence of corrugated iron and concrete composite floor systems). Structural configurations and materials were quickly changing in efforts to save space and build higher.

The city's building fire codes initially began with the restrictions on certain structural materials known to be problematic in fire (New York Building Code, see Smith, 1905), but subsequently called for comparative performance of materials in floors and partitions for strength in fire *and after cooling*. Walls and floors were crucial for *stopping fire spread* and *preventing conflagrations* in dense urban centres. The original test for a floor (though not a national standard at the time) called for a sustained 'average' gas phase temperature equivalent to 927ºC (1700ºF) for 4 hours (with peaks to 1093 ºC (2000ºF)), hose stream cooling, and finally residual testing to higher loads (4 times the sustained fire service load) for a further 24 hours. If after this test the floor's deflection did not exceed 1.4% of its span, the element was assumed to have 'passed' (Stewart and Woolson, 1902). See Figure 1. The thermal scenario was *intended* to be more severe than a real fire – according to popular opinion "*no ordinary room would have enough inflammable material in it to maintain a 1700ºF fire for more than 30 minutes*". The basis for this heating regime was fire fighters' qualitative experience in New York. Ira Woolson stated regarding his test method, "*when fearful consequences may result from a failure of a structure due to fire, no test is too severe which reasonable care and expense in construction can resist*". Similar work was also underway in the UK at this time led by Edwin Sachs (Sachs, 1902).

Fig. 1 Early 'furnace' test circa 1902 (Stewart and Woolson, 1902)

Changes to the *standard* time temperature curve were made through the years in various iterations of ASTM standards (though with increasingly less emphasis on residual capacity of the elements after a fire), and by the late 1920s the fire test had been extended to include columns and other various structural elements (Hull and Ingberg, 1925); evolving into the various similar standard fire test(s) currently used internationally. Even in the late 1920s however, it was widely known that the standard fire was by no means representative of reality, and efforts principally by Simon Ingberg (1928a) began to correlate a fire *severity* – using measurements from real burn out compartment tests – to the standard fire curve based on the Equal Area Concept. Other researchers continued with the development of new concepts of equivalent fire severity based other severity metrics (Maximum Temperature Concept, Minimum Load Capacity Concept, and Time-Equivalent Formulae). Buildings could then be re-classified, not only by fire activation risk, but also by functions of fuel load, and building elements which had 'equivalent' standard fire resistance times could then be specified. Today, fire safe structural design still relies predominantly on the concepts of equivalent fire severity,

and is based on a considerable oversimplification of real fire (and structural) behaviour by assuming unrealistic standard fires for design and comparative fire testing.

By the early 1980s, over-reliance on standard fire testing was widely recognized as limiting innovation in architecture and construction, and technical papers began to appear which openly questioned the rationality and applicability of standard fire tests. For example, pioneering fire engineer Margaret Law noted that (Law, 1981);

1. the standard temperature-time curve is not representative of a real fire in a real building – indeed it is physically unrealistic and actually contradicts knowledge from fire dynamics;
2. the required duration of fire exposure in the standard test (or the time equivalent exposure) is open to criticism on a number of grounds and should be revisited; and
3. the loading and end conditions are not well defined – and clearly cannot represent the continuity, restraint, redistribution of loads, and membrane actions in real buildings.

Fire engineering researcher David Jeanes (Jeanes, 1982) also commented in 1982 that "*although the traditional approach of assigning time for a given structural element or assembly allowed for a comparative measure between different types of construction; it is hard pressed to represent actual structural performance in a real fire due factors of restraint, redistribution of loads, moment resistance, as these are difficult to quantify and duplicate in tests.*"

While admittedly structures fail only very rarely in fires, when they do fail it is almost always for reasons that would not be expected on the basis of standard fire resistance testing (Beital and Iwankiw, 2008). The complexities of a real fire and real buildings are not captured in standard tests (Figure 2, discussed later). Efforts made in testing and design for other extreme loads such as earthquake and wind design have advanced tremendously over the past century, however the fire community still uses (essentially) the same (oversimplified) principals developed more than a century ago to 'demonstrate' or 'certify' fire safety in buildings.

The structural fire engineering community is now waking up to the pitfalls of using standard fire testing and the opportunities that a more rational approach might present. A gradual shift in testing philosophy to large scale non-standard fire testing using real fires, rather than standard temperature-time curves, seems now to be underway, and a fire testing renaissance is occurring aimed at not merely capturing the comparative structural performance of isolated materials, but at rationally defining the full suite of interactions to be expected in real buildings in real fires. A survey of the literature (e.g. Almand, 2012) shows that more than thirty such tests have been performed internationally during the last 30 years. Much like the boom in early structural fire testing following the conflagrations of the early 20th century, which led eventually to the standard fire test (and which has apparently 'largely' resolved the conflagration issue in the developed world), the majority of these large scale structure fire tests occurred after tragic events such as September 11th 2001 and have demonstrated unique structural fire failures which are not captured by current standard fire test practices.

Given the goal of the current symposium within this conference on experimental mechanics, this paper discusses non-standard large scale structural fire testing, giving several examples or exemplar tests available in the literature and identifies knowledge gaps and research needs identified in these tests – specifically with respect to fire exposure (dynamics), measurement methods, structural optimization issues, and failure modes and definitions. Through a review of the literature in this area it is clearly shown that many needs have been identified in the past 30 years through large scale non-standard fire tests but remain unaddressed.

Fire Model \ Structural Model		Materials & Partial Elements	Single Elements	Sub-Frame Assemblies	Transiently Simulated Restrained Assemblies	Full-Scale Structures
		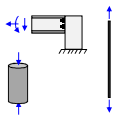	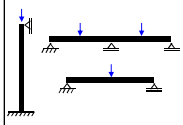	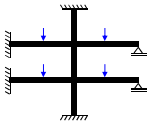	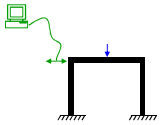	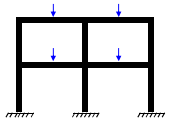
Elevated Temperature Exposures (transient or steady-state)	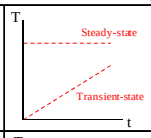	Generate design/model input data	O/R [T]	M/C	M/C	M/C [E.1-2]
Standard Fires	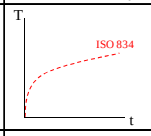	Generate design input data	**Obtain fire resistance ratings (STANDARD) [T]**	O/R [O]	M/C [W]	M/C [A]
Equivalent Fire Severity to a Standard Fire	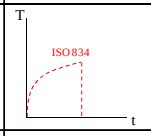	Validation of fire severity concept	Obtain fire resistance ratings (using alternative metric for fire severety) [Q]	O/R	O/R	M/C [B];[G];[N]
Parametrically Defined Model Fires	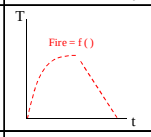	Generate design input data (highly dependant time-temperature phemnomenon)	O/R	O/R [K];[M];[R];[S]	O/R	O/R [E.3-5]; [H];[J];[L];[U];[V]
Localised Model Fires	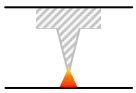	Generate design input data (highly dependant time-temperature phemnomenon)	O/R	O/R	O/R	O/R
Zone Model Fires	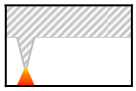	Research (highly dependant time-temperature phemnomenon)	M/C	O/R	O/R	O/R [I]
Field Model Fires	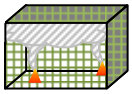	Research (highly dependant time-temperature phemnomenon)	M/C	M/C	O/R	O/R
Real Fires	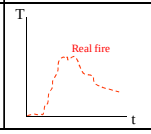	Research (highly dependant time-temperature phemnomenon) [P]	M/C	M/C [C];[D];[F]	O/R	**Research REAL behaviour in a REAL fire [E.6]**

M/C− of Marginal Credibility; O/R− used for Occasional Research

* Reference Table 1

Fig. 2 Objective of structural fire testing based on the structural assembly and the time-temperature exposure

Table 1 Non-standard large scale tests

Test*	Year	Name of the test and/or main institution involved	Reference
[A]	1982	AISI / NBS, USA	Jeanes, 1982
[B]	1985	Stuttgart-Vaihingen University, Germany	British Steel, 1999
[C]	1992	BHP - William's Street, Australia	British Steel, 1999
[D]	1994	BHP - Collins Street, Australia	British Steel, 1999
[E]	1996	British Steel and BRE Cardington (six tests)	British Steel, 1999
[F]	1998	CTICM, France	Vassart and Zhao, 2011
[G]	1999	BRE Cardington, United Kingdom	Lennon et al., 2000
[H]	2001	BRE Cardington, United Kingdom	Bailey, 2002
[I]	2003	BRE Cardington, United Kingdom	Wald et al., 2006
[J]	2003	CTU, Cardington, United Kingdom	Wald et al., 2006
[K]	2006	CTU, Ostrava, Czech Republic	Chlouba et al., 2009
[L]	2007	Harbin Institute of Technology, China	Dong and Prasad, 2009a
[M]	2007	BRE, United Kingdom	Bailey and Lennon, 2008
[N]	2008	CTU, Mokrsko, Czech Republic	Chlouba and Wald, 2009; Wald, 2010; Wald, 2011
[O]	2008	FRACOF, Metz, France	Vassart and Zhao, 2011
[P]	2008	COSSFIRE, Metz, France	Vassart and Zhao, 2011
[Q]	2010	Hong Kong Polytechnic University, China	Wong and Ng, 2011
[R]	2010	CCAA-CESARE, Australia	CCAA, 2010
[S]	2010	University of Ulster, United Kingdom	Nadjai et al., 2011
[T]	2011	TU, Munich, Germany	Stadler et al., 2011
[U]	2011	TU, Vienna, Austria	Ring et al., 2011
[V]	2011	University of Edinburgh / Indian Inst. of Tech., Roorkie, India	Sharma et al., 2012
[W]	2011	NRC, Ottawa, Canada	Mostafaei, 2011a; Mostafaei, 2011b
[X]	2011	CTU, Veseli, Czech Republic	Wald et al., 2011
[Y]	Planned	University of Victoria / CESARE, Melbourne, Australia	Proe and Thomas, 2010

* Reference Table 2 and Figure 2

2. REPRESENTATIVE NON-STANDARD LARGE SCALE STRUCTURAL FIRE TESTS

Many large scale non-standard fire tests are reported in the literature (refer to Table 1), however it is beyond the scope of the current paper to describe all of these. Table 2, which runs throughout this paper at the bottom each page, provides a timeline of the various large scale non-standard tests which have been performed around the world since 1982, along with a brief description of the test performed and a reference to the original testing report or research publication. No significant discussion of Table 2 is included in the current paper, but the interested reader is encouraged to consult the source references provided.

The renaissance of large-scale structural fire testing started with tests performed by the American Iron and Steel Institute (AISI) and the National Building Standards (NBS) in the early 1980s with the objective of assessing the *global* behaviour of steel-concrete composite frame structures and validating a computer model, FASBUS II, for structural response to fire (Jeanes, 1982). A large scale non-standard structural fire test was executed circa 1982, on a two story, four bay (4.9 m × 6.1 m each in plan), composite steel-framed building. The test structure as meant to represent a corner section of a typical mid-rise office building.

A fire compartment was built into the corner bay of the structure. A fire load was supplied by propane burners which 'reproduced' 100 minutes of the ASTM E119 (ASTM, 1980) standard time temperature curve.

Water tanks were used to simulate the design live loads. This test demonstrated 'full structure' response to a fire, and highlighted a number of differences in response between the performance of a real structure and the performance of an isolated structural element, albeit in both cases under a standard fire heating scenario. Despite the compelling evidence provided by this early test that standard fire testing is not representative of reality, it was more than 10 years before the next major test programme was performed, this time in the United Kingdom but again supported by the steel industry.

During 1996 a number of exemplary large-scale non-standard structural and non-structural (fire dynamics) fire tests were performed in an eight story composite steel-framed test building constructed at the Cardington test site of the UK Building Research Establishment (British Steel, 1999). This test program surely represents the most comprehensive and realistic test series that has ever been performed, and is a key reason why the steel industry has been able to aggressively promote performance-based structural fire design in the subsequent decades, with significant economic and sustainability benefits in steel-framed buildings. The 21 m × 45 m building was three bays by five bays, and had a total height of 33 m. All beams were designed as simply supported, acting compositely with a floor slab on steel decking. Beam-to-beam connections were made using fin-plate connections and beam-to-column connections using flexible end plates. Sandbags were used to simulate gravity loads for typical office occupancy in the tests.

Table 2(a) Non-standard large scale tests time line (1982-1992)

1982	1985	1992
AISI/NBS, USA Two storey, four bay steel frame with concrete slab (9.75 × 12.2 m), fire exposure using a ASTM E119 furnace curve. Validated the computer modelling program, FASBUS. [A]	**Stuttgart-Vaihingen Univ., Germany** Water and concrete-filled columns with composite steel concrete construction, fire exposure using timber cribs. Demonstrated the performance-based refurbishment of building post fire. [B]	**BHP - William's Street, Australia** Steel concrete composite frame (4 × 4 m compartment), fire exposure using office furniture. Demonstrated use of sprinkler system to prevent collapse, suggested fire protection was not necessary for underside of composite slab. [C]

In particular, Test #6 of Cardington's 1996 tests series was meant to assess the global structural behaviour of a large rectangular corner-compartment. The fire load was given by representative office furniture, which, based on previous fuel surveys, resulted in more fuel than the 80% fractile fire load recommended by the European standards. In this test, as with most compartment fire tests performed during the Cardington test program, the columns were protected to avoid local buckling as was experienced in one of the early tests. A subsequent Cardington test was performed in 2003 (Wald et. al, 2006). All of the compartment fire tests executed during the Cardington tests series were done exposing the structure to both a heating and cooling phase; in some occasions this resulted in failures (local buckling near the connections and cracking of the composite slabs) during the cooling phase. This behaviour has also been seen in real fires and in other non-standard large scale structural fire tests (e.g. Harbin, China in Dong and Prasad, 2009b) reviewed for this paper. Taken together, the seven Cardington tests demonstrated many important aspects of the full-structure response of composite steel-framed buildings during fire. In particular, they shed light on the secondary load carrying mechanisms which can be activated during fire to prevent collapse, the potential importance of restraint to thermal expansion on heating (and thermal contraction on cooling) on localized buckling and/or connection failures, and the fact that full-structure response in fire is markedly different than that observed in standard fire resistance tests performed in furnaces.

In the case of regular grid plan composite steel-framed buildings such as the one tested at Cardington, the fire resistance appears to be far greater than is normally assumed on the basis of standard furnace tests.

In 2001, as part of the European Concrete Building Project (Bailey, 2002), a test on a seven storey reinforced concrete building was performed, also at the Cardington UK test site. The full-scale building represented a typical commercial office building. The three bays by four bays building had total dimensions of 22.5 × 30 m, with two core areas, which included steel cross-bracing to resist lateral loads. The test took place inside a 15 m × 15 m ground floor compartment. The main purpose of the test was study the global behaviour of the reinforced concrete building, with special attention in assessing the influence of restraint from the surrounding cold structure. Also, the impact of spalling on the structure's load-bearing capacity was a focus of the analysis. Vertical loads were applied, throughout the whole building, by means of evenly distributed sand bags, replicating design imposed loads, partitions, raised floor, ceiling and service loads. The fire load was given by timber cribs evenly distributed (40 kg/m^2) to simulate one of Eurocode's parametric fire (CEN, 2004). 40 kg/m^2 is known as a representative fuel loading of an office structure (see Lennon and Moore, 2003). Structural stability was maintained during testing. However, significant deformation of perimeter columns was observed. This was attributed to lateral thermal expansion of the slab undergoing compressive membrane action. Severe spalling of the underside of the floor slab was also observed, starting six minutes from the start of the test. This was attributed to the high in-plane compressive stresses within the slab undergoing compressive membrane action. This test again demonstrated that the performance of real structures in real fires is markedly different than the response of isolated elements tested in standard furnaces, both in terms of structural response and potential failure modes.

Table 2(b): Non-standard large scale tests time line (1994-1996)

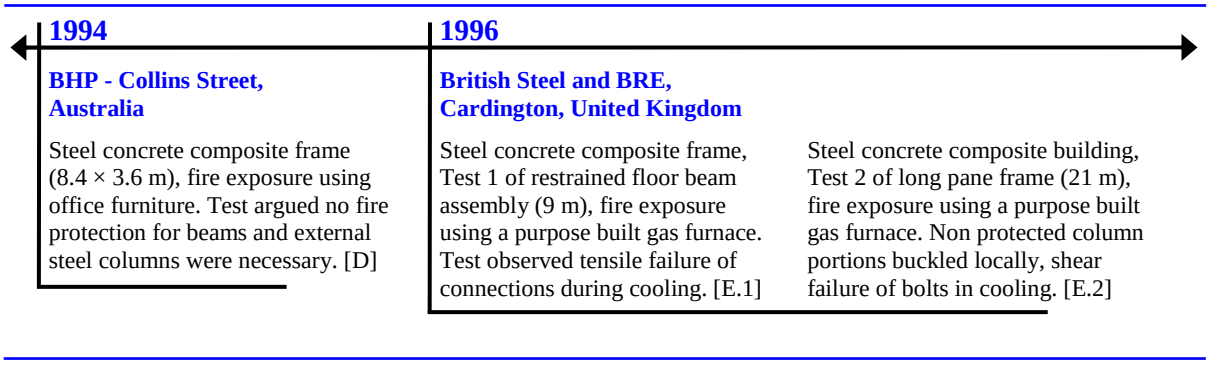

In 2010, Cement Concrete & Aggregates Australia in collaboration with the Centre for Environmental Safety and Risk Engineering, executed a large scale non-standard fire test inside a 30 m^2 purpose built fire test enclosure (CCAA, 2010). In this test, post-tensioned concrete slabs and high strength concrete columns were tested. The fire load was given by timber cribs evenly distributed at 124 kg/m^2 within the enclosure, in order to replicate the AS 1530.4 (AS, 2005) standard time-temperature curve (similar to ISO 834 (1999) used in Europe). A number of variables were studied to assess the behaviour of the post-tensioned members exposed to fire with a particular focus on propensity for explosive concrete cover spalling – e.g. concrete compressive strength, aggregate type, addition of polypropylene fibres, and spacing of reinforcement ties. The assessment of multiple variables in large scale structural fire is common practice due to the high costs and time involved in the execution of these types of tests.

No realistic mechanical restraint was provided during testing, and members were tested as single elements, despite the fact that all of these issues are known to be crucial in real structures during fire. The analysis of the test results only confirmed that the addition of polypropylene fibres reduced propensity for spalling.

The above paragraphs highlight a handful of the large scale non-standard tests available in the literature. Due to the costs and uniqueness of non-standard large scale structural fire tests, such tests are typically densely instrumented with the objective of gleaning as much useful information as possible. Thermocouples (measuring gas and structural elements' temperatures, at the surface or embedded inside elements), plate thermometers, heat flux metres, pressure gauges, displacement gauges (mechanical and laser based), load cells, inclinometers, GPS based monitoring displacement system (Ring et. al, 2011), video cameras, thermal imaging cameras, and other means of visual and acoustic (particularly for assessing the occurrence of fire induced spalling) sensors have all been used in many of the tests reviewed for this paper.

3. THE STANDARD FIRE TEST VERSUS REALITY

The full suite of non-standard large scale structural fire tests reviewed for this paper (see Table 2) present an opportunity to identify real structural responses (and failure modes) when subjected to real fires, and then to use this knowledge to predict the behaviour of coupled building systems in fire. Unfortunately, in many cases, the tests failed to address the importance of using a realistic fire exposure by explicitly choosing to replicate a *standard* time-temperature curve by the burning of a fire load (e.g. timber cribs, gas burners, pool fire, etc.) under a pre-calculated ventilation condition. In only a few occasions has the aim been to replicate a realistic, dynamic fire with the spatially and temporally variable thermal conditions which this implies (non-homogeneity, high increase of temperature during flashover, and cooling phase). It is the authors' view that this clearly exposes a lack of understanding of fire dynamics and heat transfer from the structural fire testing community. In many cases, researchers have chosen to increase the complexity (realism) of the tests by scaling up the realism of the structural assembly or system tested, without similarly scaling up the complexity (realism) of the fire scenario.

Table 2(c): Non-standard large scale tests time line (1996)

1996 (continued)		
British Steel and BRE, Cardington, United Kingdom		
Steel concrete composite building, Test 3 of floor compartment (9 × 6 m), fire exposure using timber cribs. Test observed membrane actions and load path changes, structure behaved 'well'. [E.3]	Steel concrete composite building, Test 4 of floor compartment (9 × 6 m), fire exposure using timber cribs. Test observed interaction between exposed and non-exposed structure. [E.4]	Steel concrete composite building, Test 5 of large compartment (18 × 21 m), fire exposure using timber cribs, though not as severe as tests 3 and 4. Test observed connection failures in cooling. [E.5]

In developing and performing a large scale non-standard fire test, researchers should apply the principle of 'consistent crudeness' (Buchanan, 2001). This principle was originally coined by Platt et al. (1994) in describing a defensible approach to computational modelling of structural response to fire, in that modellers must use similar degrees of crudeness in performing a structural analysis for fire as they do in modelling the thermal insult to the structure.

It is not defensible to perform a detailed computational fluid mechanics analysis of a fire scenario and then impose this on an isolated concrete beam, nor is it defensible to apply the standard fire exposure to a detailed multi-storey finite element model of a building – the same principle applies to large scale non-standard structural fire testing. An attempt to partly address these issues has been carried out at the National Research Council Canada–NRC (Mostafaei, 2011a; Mostafaei, 2011b), by implementing a system (Hybrid Fire Testing) in which single elements are tested and mechanical boundary conditions are transiently modified in a loop feedback system, in order to replicate those in a real building in fire (see entry 2:4 in Figure 2). To the knowledge of the authors, this system has only been executed using a standard fire test, and even though, many of the assumptions, both in the thermal and mechanical domain haven't been fully resolved, this approach represents one of the few efforts in realistically replicating the mechanical boundary conditions in fire.

The implications of the principle of consistent crudeness with respect to structural fire testing are shown schematically in Figure 2, where possible options for treatment of both experimental fire exposure and structural test assembly/configuration are shown in a matrix format. The vertical axis shows the levels of complexity with which the 'fire' can be treated (from simple, steady-state or transient heating all the way up to a real fire), and the horizontal axis shows the complexity of the 'structure' from material and component testing all the way up to a real, three-dimensional structure. Selected cells in the matrix show what the objective of using a particular combination of fire and structural model might be. For instance, entry 2:2 in the matrix shows the combination of a standard fire curve with a single structural element – this is the standard fire test from which all prescriptive structural fire resistance ratings are obtained.

In order to ensure consistent crudeness in structural fire testing, diagonal movements should be followed in the table, with increasing complexity in both the vertical and horizontal directions; this leads naturally to the 8:5 entry, which represents real building response to a real fire. It is noteworthy that while most structural engineers will understand the important differences between material or member testing and full structure testing in terms of structural response, very few are sufficiently competent in fire science to understand the important differences between uniform heating, the standard fires, a zone fire model, a field fire model, or a real fire. One consequence of this is that most large scale structural fire tests which have been performed over the years have sought to reproduce the standard fire, rather than to simulate a real fire. Paradoxically, it is the authors' belief that most of the true opportunities in structural fire engineering will be found by taking more rational account of the fire, rather than by increasing the complexity of our structural test assemblies.

Table 2(d): Non-standard large scale tests time line (1996-1999)

1996	1998	1999
British Steel and BRE, Cardington, United Kingdom Steel concrete composite building, Test 6 of floor compartment (162 m^2 not square), fire exposure using office furniture. Steel mesh lap error during construction, cracking around columns developed during cooling. [E.6]	**CTICM, France** Car park building, unprotected composite steel concrete frame (16 × 32 m), fire exposure using 3 cars, beams reached a temperature of 700ºC with no collapse. Tests highlighted beneficial membrane actions. [F]	**BRE, Cardington, United Kingdom** Timber frame building, compartment fire (24.1 × 12.4 m). fire exposure using timber cribs, global behaviour assessed as well. Some worries over potential for fire spread in adjoining compartments and vertically through the windows. [G]

Also given in Figure 2 are assessments of whether certain combinations of fire and structural simplification are used for occasional research (O/C) or are of marginal credibility (M/C) in the opinion of the authors. It is clear from the matrix that the structural fire engineering community takes far more account of realistically treating the structure than realistically treating the fire, and in doing so we head closer toward the areas of the matrix with marginal credibility.

4. KNOWLEDGE GAPS AND RESEARCH NEEDS IN STRUCTURAL FIRE TESTING

Considering the complexities of real fires in real buildings shown in Figure 2, structural fire testing is a difficult and complicated endeavour. The last 30 years of non-standard large scale fire testing (refer again to Table 2 and Figure 2) have demonstrated renewed scientific interest in the various issues involved, however considerable research is still needed to safely define the true behaviour of real structures in real fires.

4.1 Fire Behaviour

As noted by authors going back to (at least) 1981, the standard temperature-time curve is not representative of a real fire in a real building. In order to truly understand the response of real buildings in real fires, tests of structures and structural elements are required under credible worst case natural fire exposures. Depending on the type of structure and the occupancy under consideration, this may require experimental consideration of localized, compartmentalized, horizontally and/or vertically travelling, smouldering, or hydrocarbon fires, all of which have the potential to introduce structural actions or interactions which are not captured by the standard fires.

Investigations into combustion and the affects of ventilation on real fires had begun in the late 1700s (Richardson, 2003). At this time it was well known that ventilation, fuel load, and other factors could affect the behaviour of a fire in a building (Holland, 1793). However no rational method of fire prediction was available during this time. Real fire behaviour was not really considered in any meaningful way until Simon Ingberg's 1928 paper on the severity of building fires. Ingberg's contribution was to relate the standard fire to an 'equivalent' real fire on the basis of a 'time-temperature-energy' comparison. Ingberg simplified real fire behaviour using a prescriptive approach of relating fuel load to the standard fire time by 'implicitly' including most other effects known to govern fire behaviour; *"shutters in the walls were regulated to give what was deemed to be the proper amount of air for maximum fire conditions within the room"* (Ingberg, 1928a). This method proved popular, largely because it enabled the fire testing community to continue to use the standard fire despite the acknowledged (even in 1928) unrealism. Ingberg's work still serves as a fundamental basis for contemporary standard fire resistance rating requirements.

Table 2(e): Non-standard large scale tests time line (2001-2003)

2001	2003	2003
BRE, Cardington, United Kingdom Concrete frame building, Compartment floor fire (2 × 2 bays, 225 m^2), fire exposure using timber cribs. Compartment failed and most instrumentation lost, beneficial membrane action demonstrated in building, spalling observed. [H]	**BRE, Cardington, United Kingdom** Eight hollow core concrete frame building tests (12 × 12 m), fire exposure using timber/plastic cribs. Tests studied fire dynamics of growth, burning, and cooling stages of fire studying effect of Insulation, openings, and fuel load. [I]	**Czech Technical University (CTU), Cardington, United Kingdom** Steel concrete composite building, of large compartment (11 × 7 m), fire exposure using timber cribs, loaded to 56% of its ambient temperature capacity. Cracking occurred at column heads, sustained greater deflections than earlier tests. [J]

The simplification of complex real fire behaviour continues in current practice. The Eurocode's parametric fires (CEN, 2004), for example, seek to empirically account for various factors such as fuel load, type, ventilation conditions, thermal properties of the boundaries, radiant heating from walls, compartment size, etc. These fires represent the most 'advanced' fire models which would typically be used for structural fire analysis is most building structures. However, as recently as 2003 compartment tests performed in the UK (Lennon and Moore, 2003), relating parametric fires to real fire behaviour showed problems with this approach. The Parametric fires were developed on the basis of fires in small compartments which are not representative of many modern 'open' structures. It is well known that a fire does not behave homogenously within a compartment (even in Ingberg's time (1928)) and that temperatures exceed those considered 'average' (Stern-Gottfried et al. 2009). To date, no modern non-standard large scale fire test has considered the global structural effect (loss of stiffness to the frame to maintain beneficial membrane actions etc.) of a travelling vertical fire.

In the absence of additional test data to verify new fire behaviour models for various types of modern structural configurations, we are forced to extend empirical fitted relations which may not hold, making our predictions and structural design for safety in fire sometimes difficult to justify. To hold true to the original intention that a structure is to be designed for the credible worst case fire, we must better understand (and implement in design) true fire behaviour and its effects on different building materials and configurations.

4.2 Measurement Methods

Some large scale non standard fire tests had been conducted prior to 1980 (e.g. Ingberg, 1928b). Most of these tests considered wooden structures, which were mostly functions of easily observable qualitative charring analysis (Holland, 1793). Qualitative analysis can be limited; subsequently with improved technology around 1900, quantitative measurement of structures in fire emerged that considered deflection and temperature measurement (see Stewart and Woolson, 1902). Today, non-standard large scale structural fire tests are densely instrumented, further increasing the costs and time to setup, as well as adding a degree of practical complexity to the actual execution of the test.

Most SFE authors agree that more complete data are required from both standard and non-standard structural fire tests. Better information on strains and displacements during testing would allow a more accurate understanding of response, and would provide additional data which are essential for high quality computational model development and validation.

The need for new types of sensors, such as wireless sensors to be used during fire tests, has been noted previously (Kodur et. al, 2011). However, the authors of the current paper feel that what is really needed is a better understanding of what is being measured; i.e. *What should be measured in order to truly understand the global performance of the element of the structure being tested?*

Table 2(f): Non-standard large scale tests time line (2006-2007)

2006	**2007**	**2007**
CTU, Ostrava, Czech Republic	**Harbin Institute of Technology, China**	**BRE, United Kingdom**
Steel concrete composite building (3.8 × 6 m), fire exposure using timber cribs, only gas and steel temperature measured. No structural implications discussed. [K]	Steel concrete composite frame (2, 3.6 × 3.6 m bays), fire exposure using four oil fired burners. Beam to column connections failed in cooling, tensile cracking of slabs observed near ends. [L]	Hollow core prestressed concrete slab building (18 × 7 m), fire exposure using timber cribs. Test demonstrated that properly designed and detailed buildings would behave well in a fire, with some cooling phase fractures though. [M]

4.3 Structural Optimization

Modern structures are highly optimized, increasingly by the use of sophisticated computer analysis, in an attempt to reduce the mass, cost, environmental impact, carbon emissions, and embodied energy in buildings (Terrasi, 2007). Modern structures also increasingly make use of innovative materials, such as high strength, self-consolidating concrete, fibre reinforced polymers (FRPs), structural adhesives, stainless steel, etc, and innovative structural systems such as unbonded post-tensioned flat plate concrete slabs, the responses of which during fire are not well known in many cases (Gales et al. 2011). New materials and structural systems must be rationally understood before they should be applied with confidence in buildings; such an understanding demands large-scale non-standard fire testing, in particular because the standard furnace tests that were developed for conventional construction materials and systems are based on structural response and failure definitions which often are not applicable to the innovative ones (e.g. Bisby and Kodur, 2007).

4.4 Structural Interactions and Asymmetry

The available test data from large-scale non-standard fire tests, while extensive, still cover only a tiny fraction of the possible structural configurations that are represented within the current global building stock, let alone the highly optimized and sustainable buildings of the future. With a few notable exceptions, the majority of structural fire tests conducted to date, whether standard or non-standard, have studied regular, symmetrical, highly idealized structures. Modern structures increasingly make use of irregular floor plates with varying span lengths, bay sizes, construction types, etc. The possible influence of irregular floor plans and complex building forms needs to be investigated, both experimentally and numerically, if performance-based structural fire engineering of both conventional and modern buildings is to be credibly performed with confidence. Indeed the importance of irregular building layouts, the position of service cores, and lateral restraint to thermal expansion are already known (through computational modelling studies of real highrise buildings) to be potentially important for full-structure response to fire.

4.5 Compartmentation and Fire Spread

To date, most large-scale structural fire testing has focused on prevention of structural collapse during fire, and relatively little attention has been paid to preservation of compartmentation under large deformations in real structures during fire; this is particularly of concern given the large floorplate deflections and wide discrete cracking which have been widely observed in large-scale fire tests on steel-concrete composite slabs (refer to the Cardington tests). The impacts of vertical and lateral deformations of structural frames on fire stopping and both horizontal and vertical compartmentation should be studied in order to preserve life safety in buildings which are now becoming ever more reliant on defend-in-place life-safety strategies (for instance in highrise buildings where fire safety strategies are often fundamentally based on the assumption that a fire will be confined to the floor (and even room) of origin and phased evacuation is put in place).

Table 2(g): Non-standard large scale tests time line (2008)

2008	2008	2008
CTU, Mokrsko, Czech Republic	**FRACOF, Metz, France**	**COSSFIRE, Metz, France**
Steel concrete composite building (12 × 18 m), mix of different components and structural systems. fire exposure using timber cribs. Various localized failure modes were observed using a variation of instrumentation. [N]	Steel concrete composite sub frame (8.8 × 6.7 m), corner compartment fire, fire exposure using gas furnace. Insulation integrity failure due to improper mesh lapping, though system behaved well in heating and cooling. [O]	Steel concrete composite sub frame (6.7 × 9 m), corner compartment fire, fire exposure using gas furnace. No global collapse despite flexural failure of secondary beam, rated building achieved its standard fire rating time. [P]

Furthermore, given that many structural fire engineers already have serious concerns about the quality of installed fire stopping between floors in multi-storey buildings, large-scale non-standard fire tests should perhaps be considered in which vertical fire spread is explicitly simulated using natural fires to evaluate the structural impacts of credible worst case fires burning simultaneously on more than one floor of a structure.

4.6 Detailing and Construction Errors

Taken together, the large-scale non-standard fire tests reported in the literature highlight a number of important construction details and potential construction errors which may appear inconsequential to a building contractor, but which may have a profound impact on the structural fire response and integrity of a building during fire. Examples of this include integrity of fire stopping during large deformations (refer to above), lapping of steel reinforcing mesh, anchorage of steel reinforcing mesh over shear studs on protected perimeter beams, use of deformed versus smooth bars for reinforcement (potentially leading to strain localization and tensile failure of deformed steel bars during fire), proper anchorage and grouting of hollowcore slabs, use of specific types of bolted steel connections to promote connection ductility and rotational capacity during fire, quality, uniformity, and robustness of structural fire protection materials (either passive or intumescent), and so on. Serious unknowns continue to surround many, if not all, of these issues, and there is a need for testing to support the development of best practice guidance which can be used to provide quality assurance programs on construction sites of so-called 'fire engineered' buildings.

4.7 Cooling Phase Behaviour and Residual Capacity

A number of localized structural failures or adverse structural responses of steel connections, concrete flat plate slabs, and hollowcore slabs have been observed during the cooling phase of both real fires in real buildings (e.g. Firehouse.com, 2004; Bamonte et. al, 2009) and non-standard heating regimes in large-scale structural fire experiments (e.g. Bailey and Lennon, 2008; British Steel, 1999). Structural actions resulting from creep, localised and/or global plastic deformation, local buckling, and thermal contraction and restraint, all need to be better understood for all types of structures if designers are to realistically be expected to design for burnout of a fire compartment without structural collapse (which was the explicit intent of current SFE requirements when originally envisioned and developed during the 1920s).

Furthermore, the residual structural capacity of fire damaged structures which have undergone large deformations is not well known, meaning that many fire-damaged structures will need to be demolished after a fire (e.g. New York Times, 1997). This is particularly true for so-called fire-engineered composite steel frames, which explicitly *rely* on large deformation behaviours to mobilize the tensile membrane actions in fire which are necessary to support gravity loads (British Steel, 1999).

Table 2(h): Non-standard large scale tests time line (2010)

2010	2010	2010
Hong Kong Polytechnic University, China	**CCAA-CESARE, Australia**	**University of Ulster, United Kingdom**
Reinforced concrete (7.8 × 4.8 m),. fire exposure using ethanol pool fire, spalling and associated protection of concrete columns emphasized from tests. [Q]	Multi strand post tensioned slabs on high strength columns (6 × 5 m), fire exposure using timber cribs, spalling primarily observed with some remedial design suggestions regarding polypropylene fibres. [R]	Composite steel (cellular)-concrete building (15 × 9 m), fire exposure using timber cribs, unprotected cellular beams demonstrated beneficial membrane action. [S]

4.8 Data for Model Calibration, Validation and Verification

Experimental data are essential for calibration, validation, and verification of both existing and emerging computational modelling techniques to simulate the response of structures and structural elements in fire. This requirement holds both at the material level and at the structural (i.e. system) level. As noted by Kodur et al. (2011), high-temperature constitutive material models are needed to generate reliable input data for models and to better understand system response to fire and possible failure modes. Such data must be developed using an appropriate framework for understanding the stress-temperature-time-strain interrelationships at play in most engineering materials. An excellent framework for materials characterization at elevated temperature has been presented more than two decades ago by Anderberg (1986), but the complexities shown in this framework are rarely explicitly acknowledged in SFE analysis or design.

4.9 Connections

As noted previously, a range of studies have already been performed on connection performance in fire (largely for steel structures) (e.g. Ding and Wang, 2007; Yu et. al, 2009; 2011; Yuan et. al, 2011). However, given the range of possible connection types, full-structure responses to fire, and failure modes, additional research is needed to better understand the full range of possible connections, to develop and validate computational modelling capabilities to predict connection response, and to suggest best practice guidance to steel fabricators on the types of connections which should be applied in practice to ensure structural robustness in fire.

Proper details for the connection of precast concrete elements in buildings to ensure robust performance in fire is also required (Bailey and Lennon, 2008). Important lessons can be learned on these issues by studying the literature and available design provisions on the seismic design of structural connections (FEMA, 2000a; FEMA 2000b; AISC, 2005); it may be appropriate to develop similar provisions for structural robustness against fire.

Table 2(i): Non-standard large scale tests time line (2010-2011)

2011	**2011**	**2011**
TU, Munich, Germany Steel-concrete composite (5 × 12.5 m), fire exposure using timber cribs, information is currently sparse on these tests. [T]	**TU, Vienna, Austria** Reinforced concrete frame abutment, fire exposure gas burners, demonstrated benefits of polypropylene fibres to prevent spalling and give unusual structural shape data for model development. [U]	**University of Edinburgh / Indian Inst. of Tech., Roorkie, India** Reinforced concrete building (9 × 12 m), fire exposure using kerosene pool fire, frame was pre damaged to simulate fire after a earthquake without collapse, no spalling observed. [V]

4.10 Failure Modes

As already noted, when real structures fail in fires it is rarely for the reasons that might be expected on the basis of standard fire resistance testing. In many cases, global failure is precipitated by some form of localised failure or structural distress, such as discrete cracking in concrete, rupture of tensile steel reinforcement, failure of a connection, local buckling of structural steelwork, shear (punching) failure of a concrete slab, rupture of an unbonded prestressing tendon, etc. Unfortunately, the only way to observe and understand such failure localizations, which depend in virtually all cases on the three dimensional interactions between elements of structure during both heating *and* cooling, is to perform large-scale non-standard structural fire tests on real buildings. Only once the possible failure modes are *known* can they be rationally incorporated into computational models for full structure response.

5. CONCLUSION: WHERE DO WE GO FROM HERE?

This paper has briefly reviewed the historical basis of the standard furnace test, summarized (Table 1 and 2) more than 24 large-scale non-standard structural fire tests performed during the last three decades, and highlighted research gaps in structural fire engineering – many of which have actually been known since the early years of standard fire resistance testing – which remain with respect to our understanding of the real structural performance of buildings when subjected to real fires.

The original intent of the standard fire test was to provide a worst case comparative test for competing building materials and systems, and is based on an extremely limited knowledge of fire dynamics. The initial intent was to address a specific concern at the time the test was developed, rather than to develop a compliance test which would be used, unchanged, for more than a century. However, once the standard fire test was set out in codified form, the inertia of the compliance industry has made it difficult and painful to change or to take more rational approaches, despite the many economic and sustainability benefits that might be realized.

As a result, the structural fire engineering community finds itself in a difficult situation; we feel able to perform detailed, optimized, performance-based structural design for fire, yet we have neither the industry wide motivation to do this nor the validation tests required to show that our computational analysis tools and methods are truly defensible for the full range of possible building types and geometries. Structural fire testing is typically restricted to being performed in standard furnaces, and are evaluated based on meeting the criteria of this test – this is the *de facto* performance metric. Even when performance-based design is permitted and undertaken, the performance metric is often taken as ‘equivalent to the standard fire.’ The standard fire has thus inadvertently become the performance objective, rather than a proper performance objective taking into account the range of fire risks and failure consequences for the specific building being designed.

Table 2(j): Non-standard large scale tests time line (2011-)

2011	**2011**	**Planned**
NRC, Ottawa, Canada Single reinforced concrete column, fire exposure using gas furnace, realistic transient support conditions were replicated using the Hybrid Fire Testing (HTF) approach. Test demonstrated the successful implementation of HTF. [W]	**CTU, Veseli, Czech Republic** Steel-concrete composite (10.4 × 13.4 m), fire exposure using timber cribs, information and insight is currently sparse on these tests. [X]	**University of Victoria / CESARE, Melbourne, Australia** Planned steel concrete composite test which data is not available. [Y]

The current lack of dedicated research efforts or funding to investigate real structural performance in fire means that the few large-scale non-standard tests which are occasionally performed tend to be 'demonstration' fire tests – they rarely use credible real fire loads, and as noted they invariably attempt to link performance back to the 'assumed' performance objectives of the 'equivalent' standard fire exposure. As a result, most such tests have limited scientific value and typically yield only a small fraction of the useful information that they could; in each case a research opportunity is lost.

The result of the above approaches is a continuing and genuine lack of understanding of all the research gaps noted in the previous section. As a community, we remain in a situation that when structural failures are observed in real fires they are rarely for the reasons that would expected on the basis of standard furnace testing. The obvious rhetorical question seems to be: *Are we 'pretending' to engineer structures for fire and simply getting 'lucky' because fires are statistically rare events, and because our structures are so rarely challenged to the levels we assume in the standard fire test?*

In the future, structural fire testing must surely move away from the standard fire resistance test. In particular, the continuing development of computational analysis tools, both for fire modelling and for modelling structural response during heating are advancing on a weekly basis. Rather than focus on standard fire tests, the structural fire engineering community might better focus efforts on developing better material inputs for computational models; for instance on developing a true ability to predict, model, and prevent spalling, or an ability to model discrete cracking and fracture during fire. We might also better focus on large scale non-standard fire resistance tests which genuinely build an understanding of, and ability to predict, full structure response to fire. This will necessitate real fire tests in real buildings (e.g. Rein et. al, 2007) with sufficient instrumentation to rationally understand both the fire *and* the structural response. Alternatively, tests are needed such as those envisioned for the new structural fire testing facility which is (encouragingly) currently under construction at NIST, USA (NIST, 2011). In both of the above cases, *a priori* round robin modelling studies are needed to defensibly demonstrate the ability to model full structural response to fire. Only with the above steps taken will the structural fire engineering community be certain that our full structure analysis and design (for structures other than regular steel-concrete composite frames) are true engineering rather than fortuitous pretence.

ACKNOWLEDGMENTS

The authors would like to acknowledge the support of the School of Engineering at the University of Edinburgh, which is part of the Edinburgh Research Partnership in Engineering and Mathematics, The Natural Science Engineering Research Council of Canada, The Ove Arup Foundation, and The Royal Academy of Engineering.

REFERENCES

AISC, 2005. ANSI/AISC 341-05 – Seismic Provisions for Structural Steel Buildings. *American Institute of Steel Construction (AISC)*, Chicago, 334pp.

Almand K, Phan L, McAllister T, Starnes M, and Gross J, 2004. SFPE Workshop for Development of a National R&D Roadmap for Structural Fire Safety Design and Retrofit of Structures. *NISTIR 7133, National Institute of Standards and Technology*, Gaithersburg, MD, 188pp.

Almand K, 2012. Structural Fire Resistance Experimental Research Priority – Needs of U.S. Industry, final report. *The Fire Protection Research Foundation (FPRF)*, 55pp.

Anderberg Y, 1986. Modelling steel behaviour. *Presented at the International Conference on Design of Structures Against Fire*, Aston University, Birmingham, UK, April 15-16, 5pp.

Anon T, 1986. *Brand Verhalten von Stahl und Stahlverbund Konstructionen (Fire Behaviour of Steel and Composite Construction)*, Verlag TUV Rheinland.

Arup Fire, 2005. Fire resistance of concrete enclosure – Work Package 2: Spalling categories. *Elaborated for the Nuclear Safety Directorate of the Health and Safety Executive (HSE)*, London, UK, 36pp.

AS, 2005. AS 1530.4-2005 – Methods for fire tests on building materials, components and structures - Fire-resistance test of elements of construction. *Australian Standards*, 151pp.

ASTM, 1980. ASTM E119. Fire testing of building construction materials. Standard E-119. *American Society of Testing Materials*, PA, 1980.

ASTM, 2011. ASTM E119-11a: Standard methods of fire test of building construction and materials. *American Society for Testing and Materials*. West Conshohocken, PA, 34pp.

Bamonte P, Felicetti R, and Gambarova PG, 2009. Punching Shear in Fire-Damaged Reinforced Concrete Slabs. *ACI Special Publication 265, American Concrete Institute*, Farmington Hills, USA, pp. 345-366.

Bailey CG. Lennon T, and Moore D, 1999. The behaviour of full-scale steel framed buildings subjected to compartment fires. *The Structural Engineer*, 77 (8) pp. 15-21.

Bailey CG, 2002. Holistic behaviour of concrete buildings in fire. *Proceedings of the Institution of Civil Engineers, Structures and Buildings*, 152 (3), pp. 199-212.

Bailey CG and Lennon T, 2008. Full scale fire tests on hollowcore slabs. *The Structural Engineer*, 86 (6), pp. 33-39.

Bailey CG and Khoury GA, 2011. *Performance of Concrete Structures in Fire – An in-depth publication on the behaviour of concrete in fire*. Ruscombe Printing Ltd, Reading, UK, 203pp.

Beitel J and Iwankiw N, 2008 Analysis of Needs and Existing Capabilities for Full-Scale Fire Resistance Testing. *NIST GCR 02-843-1 (Revision), National Institutes for Standards and Technology*, 98pp.

Bisby L and Kodur V, 2007. Evaluating the fire endurance of concrete slabs reinforced with FRP bars: Considerations for a holistic approach. *Composites Part B: Engineering*, 38 (5-6), pp. 547-558.

British Steel, 1999. *The behaviour of multi-storey steel frame buildings in fire*. British Steel, Rotherham, United Kingdom, 82pp.

Buchanan A, 2001. *Structural design for fire safety*. Wiley, 444pp.

CCAA, 2010. Fire Safety of Concrete Buildings. *Cement Concrete & Aggregates Australia - CCAA T61*, 37pp.

CEN, 2004. BS EN 1992-1-2:2004 – Eurocode 2: Design of concrete structures — Part 1.2: General rules — Structural fire design. *European Committee for Standardization*, Brussels, 100pp.

Chlouba J and Wald F, 2009. Connection Temperatures during the Mokrsko Fire Test. *Acta Polytechnica*, 49 (1), pp. 76-81.

Chlouba J, Wald F, and Sokol Z, 2009. Temperature of Connections during Fire on Steel Framed Building. *International Journal of Steel Structures*, 9 (1), pp. 47-55.

Ding J and Wang YC, 2007. Experimental study of structural fire behaviour of steel beam to concrete filled tubular column assemblies with different types of joints. *Engineering Structures*, 29 (12), pp. 3485-3502.

Dong Y and Prasad K, 2009a. Experimental Study on the Behavior of Full-Scale Composite Steel Frames under Furnace Loading. *Journal of Structural Engineering*, 135 (10), pp. 1278-1289.

Dong Y and Prasad K, 2009b. Thermal and structural response of a two-story, two bay composite steel frame under fire loading. *Proceedings of the Combustion Institute*, 32 (2), pp. 2543-2550.

FEMA, 2000a. FEMA-350 – Recommended Seismic Design Criteria for New Steel Moment-Frame Buildings. *Federal Emergency Management Agency (FEMA)*, 224pp.

FEMA, 2000b. FEMA-3555D – State of the Art Report on Connection Performance," prepared for the SAC Joint Venture Partnership, *Federal Emergency Management Agency (FEMA)*, 305pp.

Firehouse.com, 2004. Seven Swiss fire fighters die in collapsed parking garage. Available at http://www.firehouse.com/news/lodd/seven-swiss-firefighters-die-collapsed-parking-garage, created November 27 2004, accessed on 31st March 2011.

Fitzpatrick F and Condron T, 1914. Fire proof construction. *American School of Correspondenc*e, Chicago, 337pp.

Gales J, Bisby LA, and Gillie M, 2011. Unbonded Post Tensioned Concrete in Fire: A Review of Data from Furnace Tests and Real Fires. *Fire Safety Journal*. 46, 151-163.

Holland H, 1973. Resolutions of the Associated Architects. *Associated Architects (defunct)*, 81pp.

Huang S, Burgess I, and Davidson B, 2011. A structural fire engineering prediction for the Veselí fire tests. *Proceedings of the International Conference on Applications of Structural fire Engineering*, Prague, Czech Republic, pp. 411-416.

Hull WA and Ingberg SH, 1925. Fire resistance of concrete columns. *Notes from US bureau of standards. Tech paper 272*, pp. 379-381.

Ingberg S, 1928a. Tests of the Severity of Building Fires. *NFPA Quarterly*, 22, pp. 43-61.

Ingberg S, 1928b. Fire Test of Brick Joisted Buildings. *NFPA Quarterly*, 22, pp. 62-68.

ISO, 1999. ISO 834-1:1999: Fire Resistance Tests - Elements of Building Construction -Part 1: General Requirements. *International Organization for Standardization*, Geneva, Switzerland, 25pp.

Jeanes D, 1982. Predicting Fire Endurance of Steel Structures. *American Society of Civil Engineers (ASCE) National Convention*, Las Vegas, Nevada, April 26-30, 1982. Preprint 82-033.

Joyeux D, Kruppa J, Cajot LG, Schleich JB, Van de Leur P, and Twilt L, 2001. Demonstration of real fire tests in car parks and high buildings, CEC Agreement 7215– PP/025. CTICM, France – Profil-Arbed Receherches, Luxembourg – TNO, The Netherlands.

Kelly F and Purkiss J, 2008. Reinforced concrete structures in fire: a review of current rules. *The Structural Engineer*, 86 (19), pp. 33-39.

Kodur V, Garlock M, and Iwankiw N, 2011. Structures in fire: State of the art, research and training needs. *Fire technology* (in press).

Law M, 1981. Designing fire safety for steel – recent work. *Proceedings of the ASCE Spring Convention, American Society of Civil Engineers*, New York, 16pp.

Lennon T, Bullock M, and Enjily V, 2000. The fire resistance of medium-rise timber frame buildings. *World Conference on Timber Engineering*, Whistler Resort, British Columbia, Canada. July 31 - August 3 2000, 10pp.

Lennon T, 2003. The Natural fire safety concept- full scale tests at Cardington. *Fire Safety Journal*, 38. 623-643.

Mostafaei H, 2011a. Hybrid Fire Testing for Performance Evaluation of Structures in Fire – Part 1: Methodology, *Research Report No. RR-316, NRC Institute for Research in Construction*, August 26th, 20pp.

Mostafaei H, 2011b. Hybrid Fire Testing for Performance Evaluation of Structures in Fire – Part 2: Application, *Research Report No. RR-317, NRC Institute for Research in Construction*, September 28th, 34pp.

Nadjai A, Bailey C, Vassart O, Han S, Zhao B, Franssem J, and Simmsm I, 2011. Full-scale fire test on a composite floor slab incorporating long span cellular steel beams. *The Structural Engineer*, 89 (21), pp. 18-25.

New York Times, 1997 Philadelphia to Raze Site of High-Rise Fire. Available at http://www.nytimes.com/1997/11/14/us/philadelphia-to-raze-site-of-high-rise-fire.html, created November 14 1997, accessed 31st March 2012.

NIST, 2011. National Institute of Standards and Technology, National Fire Research Laboratory (NFLR). Available at http://www.nist.gov/el/fire_research/nfrl.cfm, created 27th April 2011, accessed 31st March 2012.

Platt DG, Elms DG, and Buchanan AH, 1994. A probabilistic model of fire spread with time effects. *Fire Safety Journal*, 22 (4), pp. 367-398.

Proe D and Thomas I, 2010. Planning for a Large-Scale Fire Test on a Composite Steel-Frame Floor System. *Proceedings of the 6th International Conference on Structures in Fire (SiF'10)*, June 2-4, Michigan State University, East Lansing, Michigan, USA, pp. 390-397.

Proe D and Bennetts I, 1994. Real Fire Test in 380 Collins Street Office Enclosure, *BHP Research Report No. BHPR/PPA/R/051/SG021A*. September 1994, 79 pp.

Richardson K, 2003. History of Fire Protection Engineering, *National Fire Protection Association*, Quincy, MA.

Rein G, Abecassis C, and Carvel, RO (editors), 2007. The Dalmarnock Fire Tests: Experiments and Modelling. *Published by the School of Engineering and Electronics, University of Edinburgh*, 211pp.

Ring T, Zeiml M, and Lackner R, 2011. Large scale fire tests on concrete design and results. *Presented at the 18th Inter-Institute Seminar for Young Researchers (IIS18)*, Budapest, Hungary, September 23-25 2011.

Sachs EO, 1902. Facts on Fire Prevention, Vol. 1 and 2, Batsford publisher, London.

Sharma U, Bhargava P, Singh B, Singh Y, Kumar V, Kamath P, Usmani A, Torero J, Gillie M, Pankaj, P, May I, and Zhang J, 2012. Full Scale Testing of a Damaged RC Frame in Fire. *Proceedings of The Institution of Civil Engineers, Structures and Buildings, Special issue on "Structures in Fire"* (in press).

Smith C, 1905. Building code recommended by the National Board of Fire Underwriters New York. James Kempster printing. 1st edition. 275 pp.

Stadler M, Mensinger M, Schaumann P, and Sothmann J, 2011. Munich Fire Tests on Membrane Action of Composite Slabs in Fire – Test Results and Recent Findings. *Proceedings of the International Conference on Applications of Structural fire Engineering*, April 29th 2011, Prague, Czech Republic, pp. 177-182.

Stewart P and Woolson IH, 1902. Making Buildings safe: Fire Proof Materials and methods of construction. *New York Tribune*, October 19 1902.

Terrasi GP, 2007. Prefabricated Thin-walled Structural Elements made from HPC Prestressed with Pultruded Carbon Wires," *Proceedings of the 8th International Symposium on Fiber Reinforced Polymer Reinforcement for Concrete Structures (FRPRCS-8)*, University of Patras, Greece, July 16-18 2007, 10pp.

Thomas IR, Bennetts ID, Dayawansa PH, Proe DJ, and Lewins RR, 1992. Fire Tests of the 140 William St Office Building. *BHP Research – Melbourne Laboratories Rep No. BHPR/ENG/R/92/043/SG2C*, February 1992.

Thomas IR, Bennetts ID, Poon SL, and Sims J, 1992. The Effect of Fire in the Building at 140 William St, *BHP Research – Melbourne Laboratories Rep No. BHPR/ENG/R/92/044/SG2C*, February 1992.

Vassart O, and Zhao B, 2011. FRACOF Engineering Background. *Report developed for the project Leonardo Da Vinci: Fire Resistance Assessment of Partially Protected Composite Floors (FRACOF)*. 132pp.

Wald F, Simões da Silva L, Moore D, Lennon T, Chaldna M, Santiago M, Beneš M, and Borges L, 2006. Experimental behaviour of a steel structure under natural fire. *Fire Safety Journal*, 41 (7), pp. 509–522.

Wald F, 2010. Fire Test on an Administrative Building in Mokrsko. *Printing house Česká Technika, Czech Technical University in Prague*. 152pp.

Wald F, 2011. Large Scale Fire Tests. *COST Action TU0904: Integrated Fire Engineering and Response Working Group*, Prague, Czech Republic, April 30 2011, 5pp.

Wald F. Jána T, and Horová K, 2011. Design of joints to composite columns for improved fire robustness – To demonstration fire tests. *Printing house Česká Technika, Czech Technical University in Prague*, 26pp.

Woolson I, 1916. Dwelling Houses: A code of Suggestions for constructions and fire protection recommended by the National Board of Fire Underwriters, *American Institute of Architects*. New York, 137 pp.

Wong YL and Ng YW, 2011. Technical Seminar - Effects of Water Quenching on Reinforced Concrete Structures under Fire, *presented at The Institution of Fire Engineers (Hong Kong Branch)*, August 23rd 2011, Kowloon Tong Fire Station, Kowloon Ton, Hong Kong.

Yu H, Burgess IW, Davison JB, and Plank RJ, 2009. Experimental investigation of the behaviour of fin plate connections in fire. *Journal of Construction Steel Research*, 65 (3), pp. 723-736.

Yuan Z, Tan KH, and Ting SK, 2011. Testing of composite steel top-and-seat-and-web angle joints at ambient and elevated temperatures: Part 2 – Elevated-temperature tests. *Engineering Structures*, 31 (9), pp. 2093-2109.

Appendix B:
A contemporary review of large-scale non standard structural fire testing (circa 1980–present)

From:

Bisby, L., Gales, J., and Maluk, C. (2013) A contemporary review of large-scale non standard structural fire testing (circa 1980–present). Fire Science Reviews. *2(1).*

A CONTEMPORARY REVIEW OF LARGE-SCALE NON-STANDARD STRUCTURAL FIRE TESTING

Luke Bisby[1*]
[*] Corresponding author
Email: luke.bisby@ed.ac.uk
John Gales[2]
Email: j.gales@ed.ac.uk
Cristián Maluk[2]
Email: c.maluk@ed.ac.uk
[1] Reader and Arup/RAEng Senior Research Fellow in Structures in Fire, BRE Centre for Fire Safety Engineering, The University of Edinburgh, Scotland EH9 3JL, UK
[2] BRE Centre for Fire Safety Engineering, The University of Edinburgh, Scotland EH9 3JL, UK

Abstract

In recent years, large-scale structural fire testing has experienced something of a renaissance. After about a century with the standard fire resistance test being the predominant means to characterize the response of structural elements in fires, both research and regulatory communities are confronting the many inherent problems associated with using simplified single element tests, on isolated structural members subjected to unrealistic temperature-time curves, to *demonstrate* adequate structural *performance* in fires. As a consequence, a shift in testing philosophy to large-scale non-standard fire testing, using *real* rather than *standard* fires, is growing in momentum. A number of custom made, non-standard testing facilities have recently been constructed or are nearing completion. Non-standard fire tests performed around the world during the past three decades have identified numerous shortcomings in our understanding of real building behavior during real fires; in most cases these shortcomings could not have been observed through standard furnace tests. Supported by a grant from the Fire Protection Research Foundation, this paper presents a review of relevant non-standard structural fire engineering research done at the large-scale around the world during the past few decades. It identifies gaps and research needs based both on the conclusions of previous researchers and also on the authors' own assessment of the information presented. A review of similar research needs assessments carried out or presented during the past ten years is included. The overarching objective is to highlight gaps in knowledge and to help steer future research in structural fire engineering, particularly experimental research at the large-scale.

Keywords
Fire resistance, Standard fire testing, Large-scale, Non-standard fires, Natural fires

1. Introduction and objectives

In 1981, pioneering fire engineer Margaret Law presented a paper at the ASCE Spring Convention in New York entitled "Designing fire safety for steel – recent work" (Law 1981). This paper presented a summary of work that she and colleagues at Arup Fire had completed to performance-engineer the structural fire safety of innovative and architecturally exciting buildings, for instance the Pompidou Centre in Paris. Among the topics covered in this paper, Law stated a number of criticisms of the standard fire resistance test and proposed a way forward using knowledge-based analytical approaches. Paraphrasing, Law's key criticisms (in the context of fire resistance testing of protected steel elements) were that:

1. the standard temperature-time curve is not representative of a real fire in a real building – indeed it is physically unrealistic and contradicts available knowledge of fire dynamics;
2. the required duration of fire exposure in the standard test (or the time-equivalent exposure) is open to criticism on a number of grounds and should be revisited;
3. the loading and end conditions in the standard test are not well defined – and clearly cannot represent the continuity, restraint, redistribution, and membrane actions in real buildings; and
4. The structural properties of the test specimen at room temperature are not well defined.

Many within the fire testing community will argue that standard furnace testing has advantages in terms of control and reproducibility, and that it is therefore useful for comparative testing and benchmarking. The authors agree with this view up to a point. However in the current paper we prefer the stance taken by Harmathy and Lie (1970), who rightly noted that "it always must be borne in mind that in a strict sense standard fire endurance (testing) is not a measure of the actual performance of an element in fire, and, furthermore, that it is not even a perfect measure for comparison." This key point appears to have been largely forgotten by the testing community, and a central purpose of the current paper is to show that the latter view is the more correct. A secondary purpose of the current paper is to show that a move away from standard furnace testing as the means to certify (and design) buildings to resist the effects of fires offers potential opportunities for improved efficiencies and enhanced sustainability in building construction, while it also offers a genuine hope of preventing unforeseen failures as the building construction industry implements additional optimization and innovation.

Now more than three decades after Law's paper was published, the Structural Fire Engineering (SFE) community continues to base the vast majority of its guidance and regulatory compliance requirements on standard fires and the standard fire resistance test (e.g. ASTM 2011, ISO 1999). A notable exception to this is in the use of so-called *natural fires* and performance-based objectives in the design and analysis of steel-framed buildings in Europe (Corus 2006). The fact remains, however, that the SFE community is only just beginning to truly wrestle with the true response of *real* structures (other than composite steel frames) in *real* fires. This is perhaps a consequence of the events of September 11, 2001, along with several other notable structural failures during fires (see Beitel and Iwankiw 2008). It has also been repeatedly noted in recent years that when structures do (rarely) fail in fires it is usually for reasons that would not (or could not) have been expected on the basis of standard furnace testing.

Structural fire testing is thus experiencing something of a renaissance. After more than a century with the standard fire resistance test being the predominant means to characterize the response of structural elements in fires, both the research and regulatory communities are now confronting the many inherent problems associated with using simplified single element tests, on isolated structural members subjected to unrealistic temperature-time curves, to demonstrate adequate structural performance in real fires. A gradual shift in testing philosophy to large-scale non-standard fire testing, using real rather than standard fires, is underway and a number of custom made non-standard testing facilities have recently come on line or are nearing completion (e.g. NIST 2011).

It is also noteworthy that all modern structural fire design uses detailed computer analysis for both fire and structural modelling during fire. One important purpose of large scale tests is to allow the calibration of these computer models, which can then be used to explore a wide range of other possible scenarios; this applies to both fire modelling and structural modelling.

With the above points in mind, the objectives of the current paper are:

- to provide an awareness of the numerous shortcomings of historical structural fire testing procedures which currently dominate the structural fire engineering community;
- to review SFE research needs assessments carried out or presented in the in the past ten years;
- to review the several dozen large-scale, non-standard fire tests conducted globally during the past three decades, to show what issues have been studied and what general conclusions can be drawn;
- to offer critical analysis of available experimental data and knowledge on large-scale non-standard fire resistance tests, and available structural testing facilities and capabilities; and
- to provide recommendations for future structural fire resistance testing and research.

2. Previous reviews and research needs assessments

Before presenting a review of available information on large-scale, non-standard fire, it is worthwhile to review previously published reviews, focused on this or similar issues, during recent years. A number of such reviews are available in the literature, and these are presented chronologically below.

2.1 British Steel (1999)

A comprehensive research report entitled “The Behaviour of Multi-Storey Steel Framed Buildings in Fire” was published by British Steel (1999). While the central purpose of the report is to summarize the results of six large-scale fire tests carried out at Cardington during 1995–1996 (described in detail below), the report also provides descriptions of the impacts of two real fires in real steel framed buildings;theBroadgate Fire of 1990 and the Churchill Plaza Fire of 1991 (British Steel 1999). The report also gives short summaries of prior large-scale non-standard structural fire tests performed on steel framed buildings, including the Australian BHP William Street and Collins Street Fire Tests (circa 1990), and a large structural fire test performed at Stuttgart-Vaihingen University, Germany in 1985 (discussed below).

The main conclusion was that, in steel framed buildings with steel-concrete composite slabs, the composite floor and supporting steelwork have a profound influence on the stability of the structure and that diaphragm and membrane actions, which are impossible to properly evaluate using single span furnace tests, should be considered and may considerably improve the fire resistance. These conclusions apparently formed the basis for the subsequent design and construction of the Cardington test building discussed in Section 3 of this paper.

2.2 Grosshandler (2002) – NISTIR 6890

In February 2002 the US National Institute of Standards and Technology's (NIST) Building and Fire Research Laboratory (BFRL) held a meeting of engineering and scientific experts in materials, fire protection, and structural design with the purpose of identifying the research required to underpin meaningful tests and predictive methods for use in evaluating the performance of structures subject to real fires. The specific objectives of the workshop were (Grosshandler 2002): to review current practices for achieving fire resistance; to explore the promise of fire dynamics simulations and structural behavior predictions at elevated temperatures; to identify new fire resistance options coming from materials science; to identify opportunities and needs in advanced computational methods; and to identify applications and needs for emerging measurement, instrumentation and test methods. The resulting recommendations which are directly relevant to large-scale structural fire testing, and which speak to some of the shortcomings of standard furnace testing, include (Grosshandler 2002):

- developing new experimental methods for measuring high temperature thermal and mechanical properties of structural and insulating materials, which are not well known for many newer construction materials;
- developing experimental facilities and capabilities for measuring the behavior of real-scale connections and assemblies under controlled fires that permit extrapolation to total building frame behavior up to the point of failure, which cannot be done using standard fire testing furnaces; and
- establishing as a goal the need to predict the performance of coupled building *systems* at elevated temperatures to the point of impending failure, rather than simply assessing the performance of isolated structural elements in testing furnaces up to some pre-defined failure criterion which may or may not represent impending failure.

2.3 Grosshandler (2003)

The International FORUM of Fire Research Directors published a position paper (Grosshandler 2003) on the evaluation of structural fire resistance in 2003. This paper was written in the wake of the September 11, 2001 collapses of WTC buildings 1, 2, and 7, and it focused on needs for designing structures for total burnout of the fuel load while considering full structure response to fire (as opposed to considering isolated elements). The paper discusses some of the inherent problems with a prescriptive approach to structural fire safety design and is critical of current standard test methods for characterization of structural response to fire. It also suggests that future research is necessary in support of the development of rational,

performance-based structural fire design codes. The main points expressed can be summarized as follows (after Grosshandler 2003):

- Current structural fire resistance *test methods must be revised* to address: (1) the response of structural elements up to ultimate failure rather than simply up to same pre-imposed fire resistance time; (2) the variability, and hence statistical uncertainty, of the various failure modes to be expected; and (3) an alternative fire rating system in units other than time.
- The *capabilities and limitations* of standard fire resistance test methods and computational tools must become more apparent to *all* members of the fire safety design, regulation, and fire and rescue communities.
- The prediction of the performance of coupled building *systems* to the point of impending failure in a fire should be established as a goal for the building industry.
- An international research effort is needed to move towards performance-based structural fire resistance design and to develop: (1) a comprehensive, high temperature database of the thermal and mechanical properties of building materials; and (2) facilities beyond the current state-of-the-art for experimental methods and protocols for measuring the response of structural connections when exposed to fire, as well as entire building frames.

2.4 Almand et al. (2004) - NlSTlR 7133

Almand et al. (2004) present a report entitled "NIST-SFPE Workshop for Development of a National R&D Roadmap for Structural Fire Safety Design and Retrofit of Structures: Proceedings," which was also developed in the wake of the September 11, 2001 collapses. The report represents the views of more than sixty leading thinkers in the structural fire safety engineering community and contains numerous recommendations for improvements to structural fire safety engineering design and practice. In particular, the report identifies five noteworthy deficiencies of building fire safety design practice (these still apply to current practice in 2013, and echo the deficiencies noted by Law (1981)):

1. Standard fire resistance methods stipulate a prescribed time-temperature exposure and are adequate to compare relative performance of structural *components;* however they do not provide information on the *actual performance* of a component in a *real* fire.
2. The role of connections, diaphragms, and multiple load paths in maintaining overall structural integrity during fire is *ignored* in structural fire design. Structural fire protection design methods are (generally) based on fire endurance tests of single elements and do not (typically) account for the behavior of connections or of the entire structure as a whole.
3. Analytical tools are currently *inadequate* to evaluate the effectiveness of alternative design and fire protection strategies to enhance structural fire endurance. *No practical tools exist* that couple fire dynamics to the structural system response.
4. Fire hazards to structures need to be better modelled and predicted to develop design criteria for both internal and external fires. This includes: (1) deterministic and probabilistic models for specifying the magnitude, location, and spatial distribution of fire hazards on structures; (2) determination of reliability-based load factors for combined dead, live, and fire loads and resistance factors for loss in structural strength and stiffness; and (3) methods for load and resistance factor design (LRFD) under fire conditions.
5. There is a lack of knowledge about the fire behavior of structures built with innovative structural or fire protection materials (application of innovative structural techniques and systems but making use of conventional materials should probably also be added here).

The key conclusions from this workshop relevant to the current discussion can be summarized as follows (after Almand et al. 2004):

- Research-quality laboratory and real building data are badly needed. This requires construction and

use of large-scale structural fire test facilities and better knowledge of engineering material properties at elevated temperature and performance of structural components under load during fire.

- Performance goals, criteria and methodologies are required for implementation in codes and standards, including *quantification of safety* provided by current prescriptive and performance-based methods, practice guidelines for the enforcement and engineering communities, development of a risk-based methodology for design fires, benchmark problems for validation of analysis tools (e.g. Gillie 2009), standardized test methods, and limit states and failure criteria.

2.5 Beyler et al. (2007) - NIST GCR 07–910

Beyler et al. (2007) present a report entitled "Fire Resistance Testing for Performance-based Fire Design of Buildings." This report seeks to identify the needed capabilities of a *standard fire resistance test* to support performance-based structural fire engineering in the United States, and to move SFE toward rational engineering of fire protection rather than relying on prescriptive requirements. It is noteworthy that this report was apparently written with an explicit intent to modify or enhance single element structural fire resistance testing using standard testing furnaces by improving the level of information and understanding that they might yield. Recommendations are made with respect to:

1. *furnace instrumentation*, for instance a transition to plate thermometers for furnace control, as has already been implemented in Europe (note that the use of plate thermometers improves consistency between test furnaces but does not totally address this issue);
2. *furnace operation*, for instance a new temperature time curve (which rises rapidly to 1200 °C and thereafter remains constant) is proposed as an upper bound to available data from compartment tests (whether an upper bound to the available compartment test data makes sense as a credible worst case design fire is doubtful);
3. *structural instrumentation*, for instance the true restraining force imposed during tests should be measured using load cells, and strain gauges should be used at critical locations; however it should be noted that strain gauges are notoriously unreliable during fire tests, a factor which the authors of the report seem unaware, and measuring restraining forces is far from straightforward in practice; and
4. *structural operations*, for instance it is proposed that all structural elements should be tested until failure, rather than to an arbitrary end-point based on temperature, fire rating, deflection, or deflection rate, so that the actual failure times, loads, and (most importantly) *mechanisms* can be properly observed.

2.6 Kodur et al. (2007) - NIST GCR 07–915

Kodur et al. (2007) present the outcomes of a "National Workshop on Structures in Fire: State-of-the-Art, Research and Training Needs," held at Michigan State University in June 2007. The report has also been slightly modified and presented as a journal publication (Kodur et al. 2011). The key objective of the workshop upon which the report is based was apparently "to enhance the research and training activities in the fire safety area by identifying the needs for research and for state-of-the-art improvement" (Kodur et al. 2007). The specific objectives were: to review the state-of-the-art in structural fire safety, to identify and prioritize research needs, to improve education and training in the US, and to develop plans to improve

provisions in codes and standards. Only the issues directly relevant to structural fire experiments are discussed herein.

In discussing the state-of-the-art in fire experiments, Kodur et al. (2007) note the serious drawbacks of standard furnace tests which are limited to tests on isolated structural elements. The resulting paucity of good experimental data and lack of properly validated models capable of predicting the real fire response of a structural system through the *entire range* of relevant behaviors are noted. Also it is claimed that, within the area of fire science and engineering, structural fire safety is the *least* developed area.

Kodur et al. (2007, 2011) comment on a lack of high temperature material properties and constitutive relationships (with a particular emphasis on high strength concrete and fire insulating materials) and on the drawbacks of standard fire test procedures stated by Law (1981); i.e. the fires have no decay phase and are physically unrealistic, structural interactions with adjacent framing are ignored, unknown and perhaps unrealistic load levels and restraint conditions are imposed. They note that current test methods and acceptance criteria give insufficient consideration to various limit states (i.e. limit states other than collapse) and that fire resistance tests on isolated elements generally consider only a limited number of parameters.

With respect to available information from large-scale non-standard structural fire tests, Kodur et al. (2007, 2011) note that a small number of tests on portal frames were conducted in the 1980's and 90's, however references to the resulting test reports are not provided. The Cardington tests by the Building Research Establishment (BRE) in the UK during the 1990s (British Steel 1999) are also briefly noted.

Research needs for structural fire experiments noted by Kodur et al. (2007) are (previously stated by Beyler et al. (2007) in most cases):

- Development of high-temperature constitutive material models and reliable input data for computational models to understand system response to fire and possible failure modes.
- Development of new and more reliable sensor technology (e.g. strain gauges, heat flux gauges, deflection gauges) to measure thermal and structural response parameters during fire tests.
- Collection and generation of test data for model verification and validation, particularly for modeling full structure response to fire and adequately predicting failure modes.
- Undertaking full-scale fire tests on decommissioned buildings to provide real data for model validation.
- Characterizing connection behavior in fire, since connections are noted as ‘significantly influencing’ the response of structural systems during fire.
- Improving procedures and specifications to modify standard fire tests including installation of additional instrumentation to capture detailed structural response, testing up to a failure limit state rather than a predefined end point, consideration of all failure limit states, and specifications on pre-test property measurements.

2.7 Beitel and Iwankiw (2008) - NIST GCR 02-843-1 (Revision)

A report by Beitel and Iwankiw (2008) was commissioned by NIST and completed in 2002 but was republished in 2008 with minor revisions. The purpose of the report was to analyze the needs and existing capabilities for full-scale fire resistance testing of structural connections, and consists of a survey of historical information on occurrences of fire in multi-story buildings which resulted in structural collapse. It also includes a survey of facilities capable of structural testing of building elements under fire (furnace) conditions, and an assessment of the needs for additional testing and/or experimental facilities to allow the *performance* of structural assemblies and fire resistance materials to be *predicted* under extreme fire conditions within actual buildings (Beitel and Iwankiw 2008).

The report contains descriptions of 22 cases where multi-storey buildings experienced fire-induced collapses between 1970 and 2002, with approximately equal distribution between steel, concrete, and masonry buildings, and with the majority of fires in office or commercial buildings. Specific details of the various collapses are omitted here. However, the following statements can be made on the basis of the information presented:

1. in most cases the critical failure modes observed in real buildings could not have been predicted on the basis of standard fire resistance (furnace) testing;
2. structural interactions and connection response played important roles in *all* cases; and
3. in several cases the collapses occurred *during the cooling phase* of the fire.

The report notes that "connections are generally recognized as the critical link in the collapse vulnerability of all structural framing systems, whether or not fire is involved." Also presented is a review of high-rise building fires without collapses, but with major structural damage, which leads to the suggestion that further work on the structural fire response of entire building frames should be conducted for both steel and concrete construction.

The final contribution of this report is to present a global survey of structural fire resistance testing capability, essentially by surveying fire research and testing laboratories around the world as to their capabilities with respect to both vertical and horizontal structural elements. The focus appears to be on structural fire testing capabilities involving *furnace testing*, as opposed to tests using *real* fires. Based on the responses, the authors conclude that many laboratories are able to perform standard furnace fire resistance tests of various sizes, types of fire exposure (heating but not necessarily controlled cooling), loading, and measurements. They note that several unusually large furnaces exist and that these could be used to evaluate structural connections or combinations of building elements, however they also note that *no single laboratory is currently able to test large-scale structural assemblies under the full range of applicable loading and fire exposure conditions*.

Beitel and Iwankiw (2008) also provide a needs assessment for structural fire testing, which they begin by highlighting the limitations of standard fire resistance testing, all of which have already been noted above and widely acknowledged since the late

1970s. The major research needs noted include (paraphrasing and with considerable repetition from reports already presented):

- developing a better understanding of the interactions between structural elements and the thermally-induced loadings in a building during fire;
- understanding opportunities for load redistribution and alternative load paths in buildings to prevent global failure;
- demonstrating the performance and robustness of connections in fire;
- investigating the impacts of multiple floor fires and heating of elements from both sides;
- performing fire tests on elements of realistic scale, particularly large members with long spans;
- developing better instrumentation for use during fire tests;
- understanding and demonstrating the reliability of structural fire protection materials; and
- development of a *unique testing facility* to accommodate the required size, appropriate loading and the fire exposures needed for longer, wider or taller members.

2.8 Other reviews

As part of the European Cooperation in Science and Technology (COST) Action TU0904: Integrated Fire Engineering and Response Working Group, a summary of available large-scale structural fire tests conducted globally was presented by Frantisek Wald at a COST Action TU0904 Working Group meeting in April 2011 (Wald 2011). This paper presents a summary, with source references and brief descriptions, of a number of large-scale non-standard furnace tests, all of which are described in the following sections. However, the report provides little insight into the key conclusions from the fire tests, nor does it discuss knowledge gaps or research needs.

Vassart and Zhao (2011) produced an 'Engineering Background Document' as part of an EU Commission-funded Leonardo Da Vinci project on "Fire Resistance Assessment of Partially Protected Composite Floors (FRACOF)." The document includes detailed summaries of a number of large-scale non-standard structural fire resistance tests performed in Europe, including the Cardington tests (see below) and tests on open, steel-framed car parks performed in France (also discussed below). It also includes evidence from real fires at Broadgate and Churchill Plaza, and from small-scale fire resistance tests performed at the University of Manchester (Bailey and Toh 2007). Few insights are presented however.

3. Large-scale Non-standard tests

The current review is interested in modern era large-scale, non-standard structural fire resistance testing, with a particular emphasis on experiments aimed at better understanding the full-structure response of *real* buildings in *real* fires. In general, the review is focused on tests which have used real fires rather than testing furnaces to provide the thermal insult to the tested assembly. However, in some cases furnaces have been used to perform structural fire resistance tests which clearly fall outside the scope of typical standard fire testing procedures, and some of these have been included. In performing this review, more than 30 individual large-scale tests have

been identified since the early 1980s, although in some cases (as in the case of the Cardington steel frame tests) multiple tests were performed and reported over a period of months or years in a single test structure. The following sections present overviews of the available test reports and common themes are identified wherever possible. The tests are categorized chronologically and based on the primary materials of construction.

In an effort to provide a coherent framework within which to consider the various tests presented in the following sections, Table 1 provides a ‘crudeness framework’ which categorizes possible structural fire testing with respect to both the level of complexity of the ‘fire model’ and the level of complexity of the ‘structural model’ used in testing. This figure has been created following the lead of Buchanan (2001) who has previously presented a similar table to show that researchers must strive to achieve ‘consistent crudeness’ during testing in terms of how they treat the fire and the structure.

Table 1 'Crudeness framework' which categorizes possible structural fire testing methodologies with respect to both the level of complexity of the 'fire model' and the level of complexity of the 'structural model' used in testing

Fire Model \ Structural Model		Materials & Partial Elements	Single Elements	Sub-Frame Assemblies	Transiently Simulated Restrained Assemblies	Real Structures
		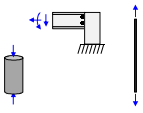	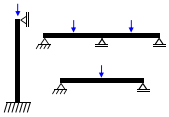	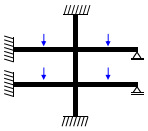	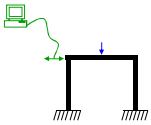	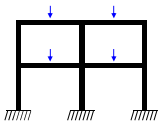
Elevated Temperature Exposures (transient or steady-state)	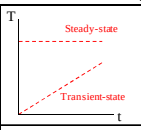	**38** Generate design/model input data	**5**	**5**		**9a - 9b**
Standard Fires	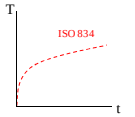	Generate design input data	**23 - 24 - 26 27 - 41** Standard fire resistance tests	**1 - 3 - 10 18 - 21 - 22 28 - 29 - 39**	**36 - 39 - 40**	**2 - 14**
Equivalent Fire Severity to a Standard Fire	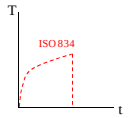	Validation of fire severity concept	**41** Fire resistance ratings (using alternative severety metrics)	**34 - 39 - 43**	**39 - 40**	**4 - 12**
Parametrically Defined Model Fires	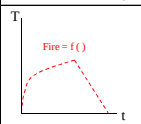	Generate design input data	**25**	**19 - 39**	**39**	**9c - 9d - 9e 15**
Localised Fires		Generate design input data				**13**
Zone Model Defined	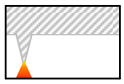	Research		**35**		
Field Model Defined	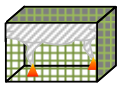	Research				
Real Fires		**22** Research	**30 - 31**	**6 - 7 - 8 - 11 17 - 20 - 32 33 - 37 - 42**		**9f - 16 - 42** REAL behaviour in a REAL fire

(Instructions for use of the digital version – Click on any of the cells, row titles or column titles to highlight the corresponding test or tests in Table 2).

Table 2 Large-scale non-standard structural fire tests listed in chronological order

Test*	Year (approx.)	Name of test and/ or research institute	Reference
1	1959	Unbonded post-tensioned beam and slab assembly, USA	Troxell, 1959
2	1982	AISI and NBS, USA	Jeanes, 1982
3	1983	Multi-span continousunbonded post-tensioned slabs, Belgium	Van Herberghen and Van Damme, 1983
4	1985	Stuttgart-Vaihingen University Germany	British Steel, 1999
5	1986	Steel beams and portal frames with uniform heating, Germany	Rubert and Schaumann, 1986
6	1987	Steel portal frame with fire load of wooden cribs, BRE, UK	Cooke and Latham, 1987
7	1992	BHP-William Street, Australia	British Steel, 1999
8	1994	BHP-Collins Street, Australia	British Steel, 1999
9a	1996	BRE Cardington Steel Building (Test 1), UK	British Steel, 1999
9b	1996	BRE Cardington Steel Building (Test 2), UK	British Steel, 1999
9c	1996	BRE Cardington Steel Building (Test 3), UK	British Steel, 1999
9d	1996	BRE Cardington Steel Building (Test 4), UK	British Steel, 1999
9e	1996	BRE Cardington Steel Building (Test 5), UK	British Steel, 1999
9f	1996	BRE Cardington Steel Building (Test 6), UK	British Steel, 1999
10	1997	Punching shear test in standard testing furnaces Germany	Kordina, 1997
11	1998	Car Park Fire Tests, CTICM, France	Vassart and Zhao, 2011
12	1999	BRE Cardington Timber Frame, UK	Lennon et al., 2000
13	1999	Tests on steel portal frames with pool fires, UK	Wong et al., 1999
14	1999	Tests on steel portal frames with furnace with furnace exposure, China	Zhao and Shen, 1999
15	2001	BRE Cardington Concrete Building, UK	Bailey, 2002
16	2003	BRE Carington Steel Building (Test 7), UK	Wald et al., 2006

17	2006	Ostrava Fire Test, Czech Technical University, Czech Republic	Chlouba et al., 2009
18	2007	Harbin Institute of Technology, China	Dong and Prasad, 2009a
19	2007	BRE Hollow-Core Slab Fire Test, UK	Bailey and Lennon, 2008
20	2008	Mokrsko Fire Test, Czech Technical University, Czech Republic	Chlouba and Wald, 2009; Wald, 2010; Wald, 2011
21	2008	FRACOF Fire Test, Metz, France	Vassart and Zhao, 2011
22	2008	COSSFIRE Fire Test, Metz, France	Vassart and Zhao, 2011
23	2008	Long span post-tensioned slab tested in a large furnace, UK	Kelly and Purkiss, 2008
24	2008	Model continuous post-tensioned concrete slab standard fire, China	Li-Tang et al., 2008
25	2008	Steel frames tested under 'natural' fires, Portugal	Santiago et al., 2008
26	2009	Two-dimensional steel frames in custom furnace, China	Dong and Prasad, 2009b
27	2010	Continuous post-tensioned concrete slabs in furnace, China	Zheng et al., 2010
28	2010	Planar portal frames in standard fire exposures, China	Han et al., 2010
29	2010	Hong Kong Fire Test, Hong Kong Polytechnic University, China	Wong and Ng, 2011
30	2010	CCAA-CESARE Test, Australia	CCAA, 2010
31	2010	University of Ulster, UK	Nadjai et al., 2011
32	2011	Punching shear tests in standard testing furnaces, Belgium	Annerel et al., 2011
33	2011	TU Munich Fire Tests, Germany	Stadler et al., 2011
34	2011	TU Vienna Fire Tests, Austria	Ring et al., 2011
35	2011	University of Edinburgh and IIE Roorkie Test, India	Sharma et al., 2012
36	2011	NRC, Ottawa, Canada	Mostafaei, 2011
37	2011	Veseli Fire Test, Czech Technical University, Czech Republic	Wald et al., 2011

38	N/A	University of Sheffield's connection testing furnace, UK	Yu et al., 2011
39	N/A	CERIB Promethee Facility, France	Robert et al., 2009
40	N/A	BAM Column Test Facility, Germany	Korzen et al., 2010
41	N/A	CSTB Vulcain Test Facility, France	CSTB, 2011
42	N/A	NIST NFRL Extension Test Facility, USA	NIST, 2011
43	Planned?	University of Victoria CESARE Fire Test, Melbourne, Australia	Proe and Thomas, 2010

* Reference Table 1.

It is obvious in Table 1 that standard furnace testing falls near the top left corner of the table, where both the fire and the structure are treated in a very crude fashion. The bottom right corner of the table represents 'reality', and so tests which lie close to the diagonal are most defensible from a consistent crudeness perspective.
Each of the testing programs discussed below has been placed within a cell of this table on the basis of an assessment by the authors of the current paper, allowing readers to gain an intuitive sense of which studies push the community towards the most realistic and defensible outcomes.In Table 2, testing programs discussed are listed in chronological order.

3.1 Steel-concrete composite construction

American iron and steel institute and national building standards test (1982)

The renaissance of large-scale structural fire testing probably started with tests performed by the American Iron and Steel Institute (AISI) and the National Building Standards (NBS) with the objective of assessing the *global* behavior of steel-concrete composite frame structures and validating an early computer modeling package, called FASBUS II, for structural response to fire (Jeanes 1982). A large-scale non-standard structural fire test was executed on a two-story, four-bay (9.8 m × 12.2 m in plan) composite steel-framed building. The test structure was intended to represent a corner section of a typical mid-rise office building. A fire compartment was built into one corner bay of the structure, and a fire load was supplied by propane burners which 'reproduced' 100 minutes of the ASTM E119 (ASTM 1980) standard fire. Water tanks were used to impose the design live loads during the test.

While few details of the test are available in the literature, the test clearly demonstrated that 'full structure' response to a fire was markedly different to that which would be expected on the basis of furnace testing. It highlighted a number of differences in response between the performance of a real structure and the performance of an isolated structural element, albeit in both cases under a standard fire heating scenario. Most importantly, secondary load paths, structural interactions, membrane actions, and discrete cracking in the concrete slabs, none of which would

have been identified by furnace tests, were all identified as playing roles in the structure's response.

Stuttgart-Vaihingen University Fire Test (1985)

Another early large-scale non-standard fire test was performed at Stuttgart-Vaihingen University, Germany, in 1985 (Anon 1986). Little information on this test is available in the English literature; only a brief description is available in the British Steel (1999) report on the Cardington fire tests (see below).

The Stuttgart-Vaihingen University test was performed on the third floor of a four-storey steel framed office building in which many different forms of steel and concrete composite elements had been used. The building incorporated water filled columns, partially encased columns, concrete filled columns, steel-composite beams, and various types of composite floor systems. The imposed fire load consisted of wooden cribs over about one third of its floor area. The structure was loaded by water-filled barrels.

Despite gas phase temperatures in excess of 1000 °C, the building maintained its structural integrity and experienced maximum beam deflections of only about 60 mm. The building was refurbished after the fire and subsequently occupied as an office and laboratory space. Little other information is available.

William Street Tests (circa 1992)

In the early 1990s a series of four fire tests was performed by steel company BHP to investigate the structural fire performance of a specific steel-framed office building in Melbourne, Australia. The existing 41 storey building (140 William Street) was undergoing renovation and refurbishment after an extensive asbestos removal program. The test was intended to show that with the installation of a light hazard sprinkler system and a non-fire rated suspended ceiling, that the passive fire protection could be removed from the structural steelwork of the beams and the underside of the steel deck floors (British Steel 1999, Thomas et al. 1992a).

A test building was constructed to simulate a typical single storey corner bay of the Willam Street building; i.e. an isolated 12 m × 12 m bay. The fuel load consisted of typical office furnishings amounting to a fuel load of about 53.5 kg/m^2. Gravity loads were applied using water tanks.

The first two tests were concerned primarily with the effectiveness of the proposed sprinkler system, and as such the fires were not significant for the structure. The third test examined the structural and thermal performance of the composite slab. In this test the beams had 'partial fire protection' and the entire floor assembly was protected (to unknown extent) by a suspended ceiling system which 'remained largely in place' during the fire exposure. Peak gas phase temperatures were about 1254 °C, but the (protected?) composite slab supported the imposed service load.

The fourth test used unprotected steel beams and composite slab, although still with a suspended ceiling, and had a peak gas phase temperature of 1228 °C. The maximum beam temperatures in this test were 632 °C, and the maximum beam deflection was 120 mm (with no 'obvious signs' of impending collapse). 'Most' of the beam deflection was recovered on cooling.

Taken together, the four William Street tests were used to demonstrate, with minimal analysis, that the light hazard sprinkler system was adequate to prevent deformation and collapse and that fire protection was not required on the beams or underside of the composite slab in this building (British Steel 1999).

Collins Street Test (circa 1994)

Shortly after the William Street tests, BHP performed a fire test in a steel-framed test building which was intended to simulate a section of a proposed multi-storey building in Collins Street, Melbourne (British Steel 1999, Proe and Bennetts 1994). The test was concerned primarily with the fire dynamics and measured temperatures in the steel, and is not particularly enlightening in terms of structural response.

An 8.4 m × 3.6 m compartment was loaded with 44–49 kg/m^2 of 'typical' office furniture. Peak gas phase temperatures of 1163°C were recorded, although the maximum steel beam temperature was only 470 °C. It is noteworthy that this test also included a suspended ceiling, which considerably reduced the temperatures measured in the structural elements, and that the structure had no imposed loading other than self-weight.

On the basis of this test, BHP successfully argued that no fire protection was required to the beams and the external steel columns. It has recently been noted (Vassart and Zhao 2011) that the Williams and Collins Street Fire tests have enabled – in conjunction with risk assessments and the use of sprinkler systems with a 'sufficient' level of reliability – the use of unprotected beams in six multi-storey office buildings between 12 and 41 storeys in Australia (up to 1999). However, exactly what level of 'reliability' is required of the sprinkler systems is not stated. The reliance of these conclusions on the performance of the non fire rated suspended ceilings is also highly problematic in practice (British Steel 1999) and thus difficult to justify.

BRE Cardington Steel Building Tests (1996)

In 1996 a number of large-scale non-standard structural fire tests were performed in an eight storey composite steel-framed test building constructed at the Cardington site of the UK Building Research Establishment (BRE). In total, seven fire tests on this structure are reported in the literature, with the definitive reference for the first six of these being a research report by British Steel (1999). The building was 21 m × 45 m and three bays by five bays in plan, and had a total height of 33 m. All beams were designed as simply supported acting compositely with a 130 mm thick concrete slab on steel decking. Beam-to-beam connections were made using fin-plate

connections and beam-to-column connections using flexible end plates. Sandbags were used to simulate gravity loads for a typical office occupancy. A plan view of the test structure is given in Figure 1; this also shows the approximate locations and compartment sizes for the various fire tests performed.

Figure 1Plan view of the Cardington Test Frame and locations of the seven fire tests performed in this structure (reproduced after Vassart and Zhao (2011)).

Test 1 studied the behavior of a single 9 m long internal, restrained secondary beam (along with the surrounding floor slab) in an edge bay of the building. The beam was heated inside a custom built 8 m × 3 m gas-fired furnace. The connections were kept outside the furnace and were thus not directly heated. The beam was heated relatively slowly (at between 3 and 10 °C per minute) to a peak temperature close to 900 °C, while the temperatures and deflections of the structure were monitored. This test was intended to examine the effects of restraint on a heated beam from the surrounding cooler structure. The peak steel temperature was 887 °C measured on the bottom flange, while the peak gas temperature was 913 °C. The most notable observations were that:

- the 'runaway' displacement which is typically observed in standard furnace tests of simply supported steel beams was not observed, despite maximum temperatures of 875 °C being observed in the beam's bottom flange;
- local buckling (and hinging) occurred at both ends of the beam just inside the furnace where the beam transitioned from cool to hot; and
- tensile failure of the beam-to-column end-plate connections occurred during the cooling phase of the fire due to contraction of the steel on cooling.

Test 2 was used to study the behavior of a single storey plane frame across the entire profile of the building. This included four columns and three primary beams (see Figure 1). The test was again performed inside a custom built gas fired furnace, in this case 21 m × 2.5 m in plan. The top 800 mm of the columns and all beams and the underside of the composite slab were left unprotected, including the beam-column connections. The heating regime was similar to Test 1. The peak steel temperature was 800 °C while the peak gas temperature was 820 °C. Notable observations were that:

- the exposed (top) portions of the columns buckled locally and squashed by about 180 mm when their temperatures reached 670 °C;
- this column deformation caused a permanent deformation of 180 mm over all floors above the fire compartment (indicating that fire protection of columns is of paramount importance); and
- many bolts in the fin-plate connections between the primary and secondary beams (which had been heated over a length of only 1 m adjacent to the primary beams) sheared due to thermal contraction of the secondary beams on cooling.

Test 3 was concerned with the behavior of the complete floor system, with a particular interest in membrane actions and alternative load paths. The test was performed on the 1st floor of the building in a 9 m × 6 m corner-compartment (see Figure 1), using a fire load of 45 kg/m^2 of timber cribs. This resulted in a peak measured gas phase temperature of 1071 °C. All columns, beam-to-column connections, and edge beams were protected. The key observations were that:

- a maximum vertical displacement of less than span/20 occurred at the centre of the secondary beam at a peak temperature of 954 ºC (less than half of this deflection was recovered on cooling and the

structure was left with considerable irreversible deformations);

- the structure showed no signs of collapse; and
- buckling occurred near some of the beam-to-column connections in both the web and the lower flange, although in this test there was no shear failure of the bolted connections.

Test 4 was also concerned with the behavior of the complete floor system, but also studied issues in compartmentation using steel stud partition walls. This test was performed in a 54 m^2 corner compartment of the second floor of the building (refer to Figure 1) using timber cribs with a fire load of 40 kg/m^2. All columns and connections were fire protected. The maximum recorded gas phase temperature was 1051 °C, whereas the peak steel temperature was 903 °C measured at the bottom flange of the central beam. Conclusions were that:

- a large slab displacement of 269 mm occurred at the centre of the compartment, which remained 160 mm after cooling;
- interactions between the fire exposed floor framing and the non fire exposed wind bracing above the test compartment were observed, reducing beam displacements and demonstrating the potential importance of capturing full-structure interactions during fire tests; and
- No local buckling was observed and the connections showed no signs of fracture on cooling.

Test 5 was a large compartment test intended to study the global behavior of the structure in a 21 m × 18 m, side-compartment between the second and third floors of the building (Figure 1). The compartment area was 340 m^2 and was uniformly fire loaded with wooden cribs at 40 kg/m^2. All of the steel beams, including the edge beams, were left unprotected; columns and connections were protected. The maximum recorded gas phase temperature was only 746 °C, and the maximum steel temperature was 691 °C at the centre of the compartment. Despite these relatively low temperatures a number of interesting observations were made, including that:

- a maximum slab displacement of 557 mm was recorded which only recovered to 481 mm on cooling;
- local buckling was observed near the beam-to-beam connections; and
- several of the end-plate connections fractured down one side on cooling, and in one case the web detached from the end-plate resulting in a total loss of shear capacity, which caused large cracks in the composite slab above the connection but did not lead to collapse.

Test 6 was a demonstration test using a fire load of real office furniture, again to study the global behavior of the structure in a large (18 m × 9 m), open plan corner-compartment of the building. In addition to office furniture, wood and plastic cribs were added to give a fire load of 45 kg/m^2. Primary and secondary beams, including beam-to-beam connections, were exposed to the fire, while columns and beam-to-column connections were protected. A maximum gas phase temperature of 1213 °C was recorded, with maximum temperatures of the unprotected steel in the range of 1150 °C. The main observations were that:

- maximum vertical deflections of 640 mm were observed and recovered only to 540 mm on cooling;
- the structure showed no signs of impending collapse, although the wind bracing in the floors above the test compartment probably offered alternative load paths (and the structure was able to rest on the blockwork walls forming the fire compartment at least one location during the test); and
- the composite steel-concrete floor slab showed considerable cracking around one of the columns during cooling; investigation revealed that the steel mesh reinforcement in the concrete slab had not been lapped correctly but simply butted together (this is clearly undesirable).

Test 7 is reported in detail by Wald et al. (2006) and studied the global behavior of the structure in an 11 m × 7 m, side-compartment of the building. This test was concerned primarily with issues around tensile membrane action and the robustness of steel connections during fire. Two primary beams (unprotected), two columns (protected), and three secondary beams (unprotected) were exposed to fire (Figure 1) with a fire load consisting of 40 kg/m^2 of wood cribs. The maximum recorded gas phase temperature was 1108 °C, with a maximum steel temperature of 1088 °C. Key observations were that:

- no collapse was observed despite maximum deflections up to 1200 mm which recovered by about 925 mm on cooling;
- buckling of the beams occurred adjacent to the joints during the heating phase resulting from restraint to thermal expansion provided by the surrounding structure; and
- as in Test 6, cracking of the concrete slab occurred at the column heads due to non-lapped steel mesh in the concrete slab.

Taken together, these seven tests demonstrated many important aspects of the full-structure response of composite steel-framed buildings during fire. In particular, they shed light on the secondary load carrying mechanisms which can be activated during fire to prevent collapse, the potential importance of restraint to thermal expansion on heating (and thermal contraction on cooling) on localized buckling and/or connection failures, and the fact that full-structure response in fire is markedly different than that observed in standard fire resistance tests performed in furnaces. In the case of regular grid plan composite steel-framed buildings such as the one tested at Cardington, the fire resistance appears to be far greater than is normally assumed on the basis of furnace tests. This conclusion has been used to great advantage in recent years by the Steel Construction Industry (in particular in Europe) to justify removal of passive fire protection from secondary steel beams and steel decking in composite framed steel buildings, with considerable aesthetic, economic, sustainability, and constructability benefits.

Car Park Fire Tests (1998–2001)

A series of fire tests was conducted by the European Coal and Steel Council on an open-sided composite steel-framed car park structure circa 2002 (see Joyeux 2002). The objective of these tests was to show ‘satisfactory’ structural fire performance without requiring any fire protection to the structure. A single story structure 16 m × 32 m in plan, with a height of 3 m, was constructed from unprotected steel columns, steel-concrete composite beams, and a steel-concrete composite slab with a depth of 120 mm. The structure was loaded with real cars, and the fuel (in the most severe of the three tests) consisted of three real cars burning simultaneously and exposing a ‘significant area’ of the floor to the flames of the fire in a localised manner (Vassart and Zhao 2011). This resulted in the steel beams above the fire being heated to more than 700°C.

No collapse of the structure was observed during the tests, and maximum vertical deflections of only 150 mm were observed in the composite deck. These tests again highlighted the positive influence of full structure response (particularly membrane actions) for composite steel structures during fire. These tests have subsequently

been used to develop 3D modeling tools and design tables for the structural fire design of composite car parks which have been used in a number of fire safety engineering projects in France (Vassart and Zhao 2011).

Ostrava Fire Tests (2006)

Chlouba et al. (2009) briefly describe two fire tests on an unprotected steel floor carried out in a three-storey office building in Ostrava, Czech Republic, in 2003. The fire compartment was 3.8 m × 6.0 m in plan with a height of 2.8 m. Mechanical load was applied and wooden cribs were used to give a fire load density of 1039 MJ/m^2. The first test used a localised fire to measure the temperature of a steel column and beams close to the centre of the localised fire. The second test was a compartment test and was designed to obtain the gas temperatures in the fire compartment and the temperatures of the steel beams. However, the reported results did not address structural performance.

Harbin Institute of Technology Tests (circa 2007 & 2010)

Dong and Prasad (2009a) present the details of a large-scale experimental study to 'understand the performance of structural frames under fire loading' and to 'to serve as a database with which to check and validate numerical models.' To do this, they constructed a planar two-storey, two-bay composite steel sway portal frame with fixed column base connections and subjected it to thermal loading by placing it inside a custom made testing furnace under sustained gravity loading.

Each bay of the frame spanned 3.6 m and each storey was 2.8 m in height. The frame consisted of three vertical steel columns, linked together by four steel-concrete composite beams with composite action assured using shear studs. The depth of the reinforced concrete slab was 100 mm and the width of slab was 1000 mm. Beam-to-column connections were bolted end-plate connections which were designed to transfer both moments and shear forces. Beams were unprotected, but columns and beam-to-column connections were insulated. A unique testing furnace was designed to accommodate the frame while applying vertical loading with hydraulic jacks and allowing the large displacements expected during testing. Full details of the rather unusual test facility are given by Dong and Prasad (2009a).

Three individual tests were conducted; these differed in the number of 'compartments' that were heated by the furnace and in the relative location of the heated compartments. Tests included both heating and cooling phases using non-standard fires with peak gas phase temperatures in the range of 900°C occurring after between 60 and 115 minutes. Keeping in mind that this (two-dimensional) frame structure cannot be considered representative of a real (three-dimensional) structure, the key conclusions resulting from this study were that (Dong and Prasad 2009a):

- none of the columns in any of the tests displayed local buckling or plastic hinge formation;
- structural failure was observed in the beam-to-column connections, the composite beam and the concrete slab. This was caused by contraction of the steel beams on cooling resulting in tensile connection failure (note that this occurred in tests when the beam was exposed to the fire but the

connections were insulated, thus minimizing the heating of the connection.);

- local buckling of the steel beams near the end of their heated spans was observed (again this has been seen in prior tests by others);
- tensile cracking of the concrete slabs was observed near the span ends (as expected); and
- unsurprisingly, the deformation process and time to failure of the structure depended on the number and relative location of compartments that were heated (it should be noted that it is not clear how the authors define 'failure').

Mokrsko Fire Test (2008)

A large-scale fire experiment was conducted in a purpose-built test structure by the Czech Technical University during September 2008. The test was performed in Mokrsko, Czech Republic, and was designed to study the overall behavior of a test structure as well as its individual elements (Wald 2010, Chlouba and Wald 2009). A problem in interpreting the results of this test is that six different wall structures and three types of flooring systems were all tested simultaneously, so the impacts of localized failures of individual components are difficult to separate from the global response of the structure.

Wald (2011) states that the main objective this test was to observe the temperatures of header plate connections which were partially encased in the concrete slab, the behavior of castellated composite beams with sinusoidal openings (called 'Angelina' beams), and the behavior of unusual beams with thin corrugated steel webs. The test structure was intended to represent one floor of an office building 12 m × 18 m in plan with a height of 4 m. Wooden cribs totalling 35.5 kg/m^2 were used for the fire load and plastic bags filled by 'road-metal' were used to apply gravity loads representing a typical office occupancy.

Some interesting behaviors were observed during this test, because the structure was a mix of different components and systems it cannot be considered representative of any real structure, a number of interesting localized failure modes were observed. The interested reader is encouraged to consult (Wald 2010) for a full description of the test and its outcomes.

FRACOF Fire Test (circa 2008)

Vassart and Zhao (2011) present the results of two fire tests performed as part of an EU Commission-funded Leonardo Da Vinci project on "Fire Resistance Assessment of Partially Protected Composite Floors (FRACOF)." The first of these tests was called the FRACOF test and was intended to investigate the applicability of the Cardington test conclusions for standard fires of longer duration (up to 120 minutes as opposed to 90 minutes), for different construction details, and for the effect of higher gravity loading applied during the fire. To investigate these issues, a single bay (intended to represent a corner bay of a larger structure) of a composite steel framed building was constructed. The building was one storey high and 8.74 m × 6.66 m in plan, with columns at the four corners, two primary beams spanning 6.6 m between the columns and four secondary beams spanning 8.74 m between primary

beams. The 155 mm deep composite slab spanned 2.2 m between secondary beams. All four columns and the perimeter beams were fire protected, whereas the internal secondary beams and composite slab were left unprotected. Care was taken around the perimeter of the structure to ensure good connection between the composite slab and the perimeter beams.

Loading was applied to the structure using sand bags equally distributed over the floor plate, and the entire bay was exposed to the ISO 834 (ISO 1999) standard fire for 120 minutes using a furnace (with response monitored also during the cooling phase). Full details of the results are not reported here, but the main observations were that (Vassart and Zhao 2011):

- no collapse was observed for more than 120 minutes of fire exposure despite tensile failure of steel mesh reinforcement in the concrete slab;
- failure of the integrity and insulation criteria were observed due to the formation of a central crack across the slab resulting from premature failure of the reinforcing steel mesh in the composite slab (however what is meant by 'premature' is not clear);
- 'proper' overlapping of reinforcing steel mesh in the composite slab is essential to activate tensile membrane action and to ensure continuity of load transfer, particularly around columns;
- concrete cracking at the edge of the floor was limited and had no influence on the integrity and insulation performance of the floor (although it should be noted that the rotational restraint of the floor slab at the perimeter was probably marginal as continuity of the floor plate was not assured); and
- the floor behaved 'satisfactorily' during the heating and cooling phases of the fire, as did all protected joints between steel members.

COSSFIRE Full Scale Fire Test (circa 2008)

The second test described by Vassart and Zhao (2011) was called the COSSFIRE test and was similar to the FRACOF test in scale but with minor modifications which allowed investigation of six different slab edge connections during a single standard fire exposure. Details of the test structure are omitted here, but it was essentially a composite steel framed structure of the same size as the FRACOF structure, with protected perimeter beams and columns but unprotected secondary beams and a 135mm deep steel-concrete composite slab. It is noteworthy that this test structure incorporated an unprotected secondary edge beam. The structure was loaded using sandbags and subjected to 120 minutes of the ISO 834 (ISO 1999) standard fire with response being monitored during the cooling phase. It was observed that:

- the deflection of the floor was more than 500 mm after 120 minutes, although it behaved 'very well' and there was no sign of failure 'in the central part' of the floor;
- the test was stopped due to large deflection and flexural failure of the unprotected secondary edge beam, however this failure did not lead to global collapse due to load redistribution from membrane effects;
- local buckling was observed in unprotected secondary beam connections, near to the joints and in the lower flange and web, although all connections performed well during both heating and cooling phases;

- no failure of the edge connections between concrete slab and steel members (via shear studs) was observed;
- cracking of concrete around columns, could have a negative impact on integrity criteria;
- no significant cracking of the concrete slab was observed in the central part of the floor, meaning that the reinforcing steel mesh behaved in membrane action up to 500 °C; and
- an edge detail of lapping steel reinforcing mesh in the concrete slab over shear studs on the edge beams was effective and should be applied in practice for this type of structure.

University of Ulster Fire Test (2010)

Nadjai et al. (2011) present the results of a full-scale non-standard structural fire test performed by the University of Ulster (and collaborators) in Northern Ireland in February 2010. The fire test was on an unrestrained composite floor system supported on long-span cellular steel beams, and was apparently aimed at studying the development of tensile membrane action when the unprotected steel beams in the central part of a structural bay are cellular, rather than solid web, beams.

The structure was single bay, 15 m × 9 m in plan, and with a height of 3 m. The surrounding infill walls were not fixed to the composite floor at the top to allow vertical movement of the floor. All of the columns and perimeter beams were fire protected. The composite deck slab had a total depth of 120 mm and was fixed to edge beams by lapping the steel reinforcing mesh over shear studs welded to the perimeter beams (as in the case of the COSSFIRE test). A natural fire was imposed using wooden cribs at a load of 587 MJ/m^2, resulting in a gas phase temperature 500 mm below the ceiling at 75 minutes which peaked at 1055 °C.

The main conclusions from this study demonstrated that using cellular secondary beams to support a composite slab does not jeopardise the tensile membrane action that develops in such a slab in a fire situation. Maximum steel reinforcing mesh temperatures in the slab were less than 375 °C, suggesting less than 5% strength loss. As an aside, it is noteworthy that despite using various tools (e.g. the Ozone program (Cadorin et al. 2001) and the predicted parametric fire curve specified in BS EN1991-1-2 (CEN 2002)) to predict anticipated compartment temperatures, the actual fire was more severe than predicted.

TU Munich Fire Tests (2010)

Stadler et al. (2011) reported large-scale non-standard tests on a steel-concrete composite slab intended to enable structural fire designers in Germany to take account of membrane action for SFE design of composite beam-slab systems. The main objective of the project was to understand the behavior of intermediate beams between two composite slab panels. To do this, two fire tests were performed on composite slab panels 5 m × 12.5 m in plan with unprotected secondary beams in different directions and configurations. Rather unusually, all edge beams were protected with an intumescent coating. The orientation of the secondary beams, the flooring system and the intumescent coating system were all varied. The first test

used a ‘lattice girder precast concrete slab’ while the second used a profiled steel sheeting composite slab. The structure was exposed to a natural fire using wooden cribs to obtain gas temperatures which exceeded 900 °C during both tests. Very little other information is currently available on the test results.

Veseli Fire Tests (2011)

Wald et al. (2011) have presented results from two fire tests performed by the Czech Technical University in Veseli, Czech Republic, during 2011 to investigate the ‘design of joints to composite columns for improved fire robustness.’ The tests were performed in a rather unusual purpose-built test structure designed to represent a section of an office building. The two storey building was 10.4 m × 13.4 m in plan with a height of 9 m, and incorporated a number of innovative construction techniques, including steel fiber reinforced concrete slabs, concrete-filled structural hollow section columns, several different external cladding systems, partial fire protection in various parts of the structure, and a number of different beam to column connection details. A natural fire exposure was imposed, consisting of non-uniformly placed timber cribs with a fuel load of 174 MJ/m^2 in the central region of the structure. The applicability of the results of these tests to real structures is not clear since the many factors investigated confound the results of individual features. In any case, detailed experimental observations and conclusions from these tests are not yet available.

University of Victoria CESARE Fire Test (Planned?)

Proe and Thomas (2010) present plans for a large-scale fire test on a steel-frame composite concrete floor system suspended 3 m above the floor of a test building in Melbourne, Australia ‘in late in 2010.’ The authors stated that ‘the test will facilitate investigation of the fire behavior of one storey of a typical office building structure as used in Australia for a particular configuration of unprotected steel beams.’ Essentially the test is meant to study membrane action in composite steel framed buildings in a manner similar to the Cardington, FRACOF, and COSSFIRE tests described previously, however using a natural pool fire in this case. Apparently the test structure had plan dimensions of 20 m × 16 m, incorporating nine columns and divided into two bays in each orthogonal direction. The test was designed to shed light on (Proe and Thomas 2010):

- the ability of protected beams to support load being shed from unprotected beams;
- the effect of beam deflection at the slab perimeter on tensile membrane action;
- the effect of reinforcement ductility and strain localisation on slab failure and deflection; and
- the effect of perimeter horizontal displacement and forces on column capacity.

However, on the basis of information available in the literature it is not clear exactly how these issues were addressed by this specific test (in comparison to previous tests on steel-concrete composite slabs) and no publications appear to be available which describes the test outcome. It is therefore not clear if this test has actually been (or will be) conducted.

3.2 Fire tests on portal frames and Sub-frame assemblies

A number of medium and large-scale non-standard fire tests on steel or steel-concrete composite portal frame structures are available in the literature. These are not directly relevant to the current review since they fail to simulate most of the requisite interactions that might play roles in real structures. However, it is instructive to be aware of the work that has been performed in this area.

Rubert and Schaumann (1986) present a series of tests on 1:4 to 1:6 scale steel beam and portal frame structures heated under non-standard exposures using a series of electrical resistance heaters. Structures tested included a simple elbow frame, a portal, and a double portal. The results were used to develop a basic method for assessment of the fire resistance steel framed assemblies under bending stress.

Cooke and Latham (1987) performed a single test on a full-scale loaded steel portal frame subjected to fire from a compartment containing wooden cribs (which reached a maximum temperature of only 830°C). This test demonstrated the deflection behaviour of the portal in a natural fire.

Zhao and Shen (1999) experimentally studied the deformation behavior of unprotected two-dimensional, single-storey, single span steel portal frames exposed to fire. Three tests were performed on steel frames with welded beam-to-column moment connections under different load levels and heating regimes within a custom built gas furnace. Loads were applied only to the column heads, with no applied loads on the top beams of the portal frames.

Wong et al. (1999) performed an experimental study, apparently the only one of its kind, investigating the fire performance of steel portal frame buildings. These tests involved a scaled portal frame building constructed from four portal frames with a span of 6 m at 1.5 m centres and with a rafter pitch of 15°. The building was clad with profiled steel sheeting. The base connection condition of the columns was varied (pinned or fixed) amongst three separate tests. Pool fires were used to expose single portals to localized heating, with the columns remaining relatively cool, and the response and failure modes of the structure were observed.

Santiago et al. (2008) present details of a unique testing facility and a series of tests on six steel ‘sub-frames’ under a ‘natural fire’ at the University of Coimbra, Portugal, using a custom designed array of gas burners. These tests were intended to provide insight into the influence of various connection types on the behavior of steel sub-structures in fire. The test structures consisted of two thermally insulated columns and an unprotected steel beam with a 5.70 m span supporting a lightweight composite concrete slab. Pinned supports were imposed at the top and bottom of the columns. Six tests were performed, varying the beam-to-column connection configuration. These tests demonstrated the already well-known appearance of large tensile forces and reversal of bending moments during the cooling phase of a fire, as well as the fact that these forces may result in failure of the joint.

In addition to the work discussed previously on two-storey, two-bay composite steel portal frames, Dong and Prasad (2009b) have also presented result from furnace tests on two full-scale composite steel frames with a height of 2.8 m and a span of 3.6 m. In one frame both the beam-to-column connections and the columns themselves were protected, while in the other test only the beam-to-column connections were protected. The frames were subjected to both heating and cooling phases using a specially designed furnace.

Han et al. (2010) have recently presented results from a testing program on six planar portal frame structures with a span of 2.4 m and a height of 1.46 m in which the columns consisted of concrete-filled steel hollow structural sections and the beams consisted of reinforced concrete T-sections. These tests were intended to reproduce multi-storey composite construction systems used in China. Test parameters included the shape of the columns (circular or square), the level of axial load in the columns, the load level in the beams, and the beam-column stiffness ratio. Only the beams were directly heated during these tests, following the ISO 834 standard fire. While omitting the details of the study and its conclusions, the test showed – rather importantly – that two failure modes were observed: column failure, or beam failure. The fire resistances of the frame were generally *lower* than those of individual concrete-filled columns tested in isolation but higher than those of isolated reinforced concrete beams. This is a clear indication that in some situations the performance of a structural element in a real building may be *not as good* as its performance would be in a furnace test; it thus contradicts *the fundamental assumption* which is widely used to justify furnace testing of isolated structural elements as a credible worst case scenario for comparison.

3.3 Testing on steel connections in fire

In addition to the large-scale non-standard fire tests presented above, a number of testing programs have been undertaken in the past two decades to investigate the performance of connections in steel structures subject to both standard and non-standard heating scenarios. Full details of these are not included here, but the interested reader could refer to Yu et al. (2009, 2011) for information on fire testing of steel bolted connections, Ding and Wang (2007) for information on fire testing of connections between steel beams and concrete-filled hollow structural sections, Chung et al. (2010) for tests on steel beam-to-column moment resisting connections, and Yuan et al. (2011) for information on fire testing of connections involving steel-concrete composite beams, including the influence of the concrete deck slab. The important conclusion from this body of work is simply that, as already noted, the performance of structural connections in fire is of fundamental importance to the response of real structures in real fires, and that the relevant failure modes are impossible to observe or predict using standard furnace testing of isolated structural elements.

3.4 Reinforced and prestressed concrete

Comparatively fewer large-scale, non-standard structural fire tests have been performed on reinforced or prestressed concrete structures; mostly because in the absence of explosive cover spalling there is a prevailing view that concrete structural elements tend to perform very well in standard furnace tests when compared against unprotected steel elements. Hence, there the concrete industry appears to see relatively little economic benefit arising from support of detailed and costly testing programs to investigate and/or demonstrate the possible benefits of rationally accounting for full structure interactions and alternative load carrying mechanisms (such as membrane action) in reinforced or prestressed concrete structures during fire. Conversely, the steel construction industry has aggressively supported large-scale non-standard structural fire testing largely because of the obvious and considerable economic benefits (and hence competitive edge) that such testing often enables. Nevertheless, a small amount of relevant testing on concrete structures is available in the literature and is described in the following sections. In general the available testing of concrete structures shows that their behaviour in fire is considerably more complicated than would be assumed on the basis of the available prescriptive guidance; this may present both possible benefits and possible risks for concrete structures in fire.

'Non-Standard' testing in furnaces

Despite the fact that concrete structural elements tend to perform well in isolation during standard furnace tests, it is worth noting that the concrete industry originally led the structural fire resistance community in performing what would now be considered as 'unusual' non-standard furnace tests on concrete structural 'assemblies' rather than focusing on standardized tests. For instance, early testing on two-way post-tensioned concrete slabs and beam-slab assemblies performed in the United States during the 1950s used combinations of beams and slabs to study the two-dimensional response of these types of structures (Troxell 1959). A wealth of furnace test data are available from these early tests, however the focus in the current paper is on more recent efforts so these 'historical' tests are not discussed in detail.

In recent years several authors have presented the results of fire tests on concrete elements or assemblies using custom made or modified standard furnaces to study specific structural response issues or specific types of concrete structures which cannot be easily investigated using a standard 'component' approach. Notable examples include:

- Van Herberghen and Van Damme (1983), who used a modified standard floor furnace to study the fire resistance of post-tensioned continuous but unrestrained flat floor slabs with unbondedprestressing tendons in standard fire conditions;
- Kordina (1997), who used a modified floor furnace to investigate the punching shear behavior of reinforced concrete flat slabs in standard fire conditions;
- Kelly and Purkiss (2008), who used an oversized floor furnace to study the fire resistance of simply-supported, partly-restrained, long-span post-tensioned concrete slabs under standard fire exposure;

- Li-Tang et al. (2008), who studied the structural fire behavior of model-scale, three-span continuous unbonded post-tensioned concrete slab strips in a custom built furnace subject to a standard fire;
- Zheng et al. (2010), who performed a series of standard fire tests on two-span, continuous post-tensioned concrete slabs in a furnace with a central support built inside the heating chamber; and
- Annerel et al. (2011), who used a modified standard floor furnace to perform punching shear tests on concrete slabs subjected to a standard fire.

Many other examples are available in the literature, but these are peripheral to the current paper, which is concerned predominantly with *real* fire exposures which include a cooling phase.

Cardington Concrete Building Test (2001)

To the knowledge of the authors, only a single large-scale natural fire test of a 'real' multi-storey concrete building has ever been performed. Bailey (2002) presents the results of a natural fire test on a full-scale, seven-storey cast in-place concrete building performed at BRE's Cardington test site. The building was constructed as a demonstration building to develop best practice guidance for modern concrete construction technologies, and it therefore incorporated several different concrete mixes and construction techniques. It was three bays by four bays and 22.5 m × 30 m in plan. It had two cores which incorporated cross bracing for lateral load support. The concrete slab was 250 mm thick and the columns were either 400 mm square (internal columns) or 400 mm × 250 mm (perimeter columns). A number of different reinforcing layouts were used throughout the building, however the reinforcement in the first and second floor slabs was traditional loose bar with 'hook-and-bob links' for shear resistance around the columns (Bailey 2002).

The main aim of the fire test was to investigate the behavior of a full-scale concrete framed building subjected to a realistic compartment fire and applied static design load. This entailed (after Bailey 2002):

- investigating how the building in its entirety resisted or accommodated large thermal expansions from the heated parts of the structure (lateral thermal expansion of the floor slab in particular);
- identifying beneficial and detrimental modes of whole building behavior that cannot be observed through standard fire tests on isolated structural elements;
- investigating the overall effects of concrete cover spalling and determining its possible significance on the behavior of the whole building; and
- comparing test results and observations from large-scale fire tests with current methods of SFE design.

The fire exposure was within a fire compartment at an edge bay of the building with an area of 225 m^2 between the ground and first floor, with a height of 4.25 m. The compartment walls were structurally isolated from the concrete slab and columns to prevent them from influencing the structural response to the fire. One internal column was exposed to the fire and eight additional columns were partially exposed to the fire. The columns were made from high strength concrete (103 MPa compressive cube strength), so 2.7 kg/m^3 of polypropylene fibers were added to the concrete mix to prevent explosive spalling of the columns. The cover to all internal

steel reinforcement was specified as 20 mm. The structure was loaded during testing using sand bags, and the fire consisted of timber cribs with a load of 40 kg/m^2.

Full details of the test and its results are not provided here; however the following key observations and conclusions were made (after Bailey 2002):

- A maximum gas phase temperature of 950°C was recorded 25 minutes after ignition, after which point the instrumentation was lost (the temperature was considered 'likely' to have continued rising).
- Gas temperatures were reduced between 12 and 13 minutes due to explosive spalling of the soffit of the floor slab. The spalling of the slab's soffit was extensive and reduced the severity of the fire throughout the test and exposed the bottom reinforcing bars. Spalling was explosive and likely exacerbated by high in-plane compressive stresses in the slab caused by restraint to thermal expansion.
- Vertical displacements towards the edge of the building were larger than the displacements near the centre and showed no signs of a stabilizing plateau.
- The slab remained stable and supported the load 'by compressive membrane action at small slab vertical displacement'. It should be noted however that compressive membrane action can only occur at small displacements, and thus if the slab's vertical displacements were greater or lateral restraint surrounding the heated slab were less then, as noted by Bailey (2002), 'it is difficult to see how the slab could have supported the static load.'
- Lateral thermal expansion of the slab resulted in considerable lateral displacement of the external columns; as has been identified as the cause of previous failures of concrete structures during fires.

BRE Hollow-Core Slab Fire Test (2007)

Two large-scale non-standard structural fire tests were performed by BRE at Middlesbrough, UK, to study the performance of hollowcore concrete slabs on steel beam flooring systems (Bailey and Lennon 2008). These tests were performed in the wake of worrying results from tests (Van Acker 2003) and incidences of failures of hollowcore slabs during real building fires in Europe (De Feijter and Breunese 2007). The BRE tests were intended to understand whether tying together and grouting of hollowcore slabs in a floor plate is sufficient to prevent premature shear failure which has been witnessed in small scale tests on hollowcore elements, and therefore to provide practical design guidance without the need for expensive and unnecessary tying.

Both tests had hollowcore floor plates supported on protected steelwork and they were identical except for the connection details between the hollowcore units and the supporting steel beams; the second test had a more robust detail to tie the hollowcore units and beams together. The fire compartment was 7.0 m × 17.8 m in plan and had a height of 3.6 m. Fifteen 1200 mm wide × 200 mm deep standard hollowcore slabs with a concrete compressive strength of 85 MPa, and a relatively low moisture content of 2.8% by mass at the time of testing, were placed in a single row to form the roof of the fire compartment.

In Test 1 the hollowcore slabs sat directly on the supporting steel beams and the joints between the units and the gaps around the columns and units were grouted. In Test 2, U-shaped steel bars were placed in the cores and looped around shear studs

fixed to perimeter beams. The cores were then grouted, as were the ends of the slab, the gaps between the slabs, and the gaps between the units and the columns. The slabs were uniformly loaded with sandbags and exposed to a natural fire using 32.5 kg/m^2 of evenly distributed wooden cribs. The intent was to follow the ISO 834 curve for the first 60 minutes of fire exposure.

The primary observations and conclusions were that (after Bailey and Lennon 2008):

- properly designed and detailed hollowcore floor systems have inherent fire resistance and behave very well when subjected to severe fire scenarios (i.e. more 'severe' than a standard fire);
- the maximum average gas phase temperature was greater than 1000 °C in both tests;
- the hollowcore floor performed well during the cooling phase of the fire, and the applied load was supported for the full duration;
- the edge units fractured locally during the cooling phase of the fire but this did not lead to loss of overall load bearing capacity;
- there was no significant spalling of the units;
- different end restraint conditions did not affect the measured vertical displacement, however restraint conditions in Test 2 kept the outer proportion of the edge slab in place when it fractured along its length; and
- there was evidence of a lateral compressive strip forming at the ends of the units caused by restraint to thermal expansion which would have enhanced the flexural, and possibly shear, capacity of the units.

Hong Kong Fire Test (2010)

A large-scale non-standard fire test on unloaded concrete columns was performed in a real building in Hong Kong in August 2010 (Wong and Ng 2011). The purpose of this test was apparently to study the effects of water quenching on the fire performance of high strength concrete in a building fire. The tests were interested specifically in various grades of high strength concrete local to Hong Kong, in the effects of spalling of various grades of concrete with or without polypropylene fibers or wire mesh reinforcement, and in the effects of passive protective coatings on enhancing the fire resistance of concrete structures.

Forty unloaded concrete columns of various types were placed inside a 'converted concrete pump house' structure which had been converted into a fire testing chamber, and were subjected to a very severe pool fire. The key conclusion of the research project was that in order to prevent spalling in high strength concrete columns, insulating or fire-resisting coating materials should be used to restrict the heat transferred into the concrete or polypropylene fibers or wire mesh should be provided in column members. These tests are inapplicable to real fires in real buildings. The testing methods employed in this study are unorthodox, even for non-standard structural fire testing.

CCAA-CESARE Fire Test (2010)

Cement, Concrete and Aggregates Australia (CCAA 2010) have reported a single large-scale non-standard fire test on high strength concrete columns and post-

tensioned concrete slabs. The purpose of the test was to understand the fire performance of post-tensioned slabs and high strength concrete columns made from concrete using common Australian aggregates (with aggregate type being a known risk factor for explosive spalling). As such, the tests aimed to assess the magnitude and extent of spalling in a 'real' fire and to provide guidance on possible measures to limit its effects.

Twelve columns and three post-tensioned slabs were tested in a single fire enclosure. The columns differed in terms of concrete compressive strength, aggregate type, and the use of polypropylene fibers in the concrete mix. Columns were pre-compressed using a tensioned internal steel bar which was anchored at the column ends to simulate the compressive loading to be expected in a real multi-storey concrete building (although it is the opinion of the authors of the current paper that this is a fairly poor representation of such a scenario). The three post-tensioned slabs tested in this study differed only in terms of aggregate type.

The fire test was accomplished by placing the columns inside a plasterboard enclosure with internal dimensions of 4.25 m × 5.4 m in plan × 3.3 m high. The post-tensioned slabs were placed to form the roof of the enclosure. The fire load consisted of 124 kg/m^2 of wooden cribs, resulting in gas phase temperatures which exceeded 1000°C after about 45 minutes. From this test, the authors concluded that (CCAA 2010):

- the addition of fibers to the high strength mix has a dramatic effect in reducing the level of spalling (suggesting that a comparatively low dosage rate of 1.2 kg/m^3 is appropriate);
- the placement of column ties at closer spacing does not reduce the level of spalling (which contradicts prior research in this area);
- the post-tensioned slab containing one particular aggregate type spalled badly and hence consideration should be given to incorporating polypropylene fibers for this type of construction; and
- one of the post-tensioned slabs exhibited no spalling whatsoever whereas an identical slab spalled at both ends; no explanation was provided.

TU Vienna Fire Tests (2011)

Ring et al. (2011) present limited results of four large-scale non-standard fire tests on 'frame-like' concrete structures performed to investigate the redistribution of loading within reinforced concrete structures subjected to fire (with a stated interest in tunnels). The tests were explicitly designed to provide data for the development, assessment, and validation of numerical tools for predicting the structural fire response of concrete tunnel structures.

The frames were triangular and tubular in shape and were constructed on an exterior soil slope (refer to the source publication for figures of the unusual test structures) and was loaded during testing to simulate a soil overburden. Two of the frames were made from concrete incorporating polypropylene fibers and two were constructed without fibers. The fire load was supplied to the inside of the triangular tubes, with the bottom of the tubes insulated, using oil-burners following a pre-specified

temperature history that rose to 1200 °C in nine minutes and remained at 1200 °C for three hours.

The results of these tests are not particularly helpful in terms of fire resistance of buildings, although they do provide data for validation of computational models and they again demonstrate the well known benefits of incorporating polypropylene fibers to prevent explosive spalling in fire.

3.5 Timber-framed buildings

It appears that only one large-scale non-standard structural fire test of a timber structure has ever been presented in the literature, and even this is of limited interest from a structural load bearing point of view. Lennon et al. (2000) present results from a large-scale compartment fire test conducted within a full-scale six-storey timber frame building, again at BRE's Cardington test site, in September 1999. The purpose of the test was to evaluate and demonstrate the performance of medium-rise timber frame buildings subject to real fires.

The fire was provided by uniformly distributed timber cribs and was imposed within a single apartment on the third storey of the building. Flame spread was uninhibited and ventilation was arranged so as give the worst case fire severity. A key test objective was to evaluate the effectiveness of fire compartmentation in preventing fire spread from the compartment of origin to adjoining compartments and in maintaining the integrity of the evacuation routes and structural stability (Lennon et al. 2000). Full details of the test are omitted here, but the following general conclusions were drawn:

- The performance of the complete timber frame building subject to a real fire was at least equivalent to that which would have been obtained from standard fire tests on its individual elements.
- Timber frame construction can meet the functional requirements of the UK Building Regulations in terms of limiting internal fire spread and maintaining structural integrity.
- The *standard of workmanship is of crucial importance* in providing the necessary fire resistance performance especially nailing of plasterboards, and in ensuring the correct location of cavity barriers and fire stopping.

A series fire tests on a single-storey timber building has also been presented by Peng et al. (2011), although these did not result in any conclusions of significance for structural fire engineering.

4. Large-scale Non-standard fire testing facilities

A number of dedicated fire testing facilities are available globally that can be used to conducted large-scale non-standard fire tests, and a number of new facilities have recently been completed, are under construction, or are in the planning stages; these can be divided into (1) real fire test facilities, (2) unusual, custom made, or modified fire testing furnaces, and (3) facilities under construction or in the planning stages.

4.1 Real fire test facilities

A number of 'real fire' testing facilities are available globally. In addition to the numerous outdoor test sites which have been used to perform large-scale non-standard structural fire tests in recent years (e.g. British Steel 1999, Chlouba et al. 2009, Wald 2010, Vassart and Zhao 2011, Stadler et al. 2011, Wald et al. 2011, Ring et al. 2011, Sharma et al. 2012, described previously), many government and private sector fire testing laboratories have large burn halls which can be used to perform custom made fire tests on real structures (or parts of structures) using natural fires. Examples include (in no particular order):

- the University of Victoria's CESARE fire testing facility in Australia, which houses a 15MW oxygen calorimeter for measurement of combustion products during large experimental fires (Victoria University 2011);
- the Building Research Establishment's large burn hall, which has smoke management used for determining heat release rates, in the United Kingdom (BRE 2011);
- the National Research Council of Canada's (NRCC) burn hall in Almont, Canada, which is 55 m × 30 m in plan with a ceiling height of 12.5m (NRCC 2011);
- the FM Global Fire Technology Laboratory, USA, which houses a large burn hall with a footprint of 3120 m^2 and includes a 20 MW fire products collector (FM Global 2009);
- Southwest Research Institute (SwRI), USA, which houses a 'state-of-the-art full-scale furnace facility and a full-scale indoor test facility' (SwRI 2011);
- the Tianjin Fire Research Institute, which apparently has a very large burn hall at its South River Test Site, China, although very few details regarding this facility and its capabilities are currently available in English (TFRI 2011); and
- the SINTEF research laboratory, Norway, which has a 590 m^2 (36 m × 16.5 m) burn hall with a ceiling height between 22 m and 28 m designed for all types of large-scale fire tests and able to withstand the heat and smoke load of a 12 m^2 gasoline pool fire with 18 m high flames (SINTEF 2011).

These real fire testing facilities typically do not have the capability of performing tests with variable or lateral structural loading, and most do not offer calorimetry or smoke management to determine heat release rates or smoke analysis for density and toxicity. The Building Research Establishment's Cardington Test Hall (British Steel 1999) is no longer available.

In addition to these real fire research facilities, many national and private sector fire research organizations have one or more standard structural testing furnaces which can be (and in many cases have been) modified to perform non-standard tests of structural elements. Furnaces of various types, sizes, and configurations are available at most of the laboratories listed above.

4.2 Unusual, custom made, or modified furnaces

A number of custom-designed furnace testing facilities are available globally which can be used to study various aspects of the response of structures and structural components to fire in a variety of non-standard ways. These may be based on existing standard fire testing furnaces or may be custom-designed from scratch and based either on gas-fired burners or on electrical heating. A few notable examples are given below.

The Fire Safety Engineering Research and Technology Centre at the University of Ulster, Northern Ireland (FireSERT), has a reconfigurable standard floor furnace which has been modified to permit testing of specimens larger than would be typical. The furnace can also test assemblies or vertical and horizontal elements.

The University Coimbra, Portugal, has a unique 'natural fire' testing rig which is capable of testing steel sub-frame assemblies under exposure to gas burners with the ability to spatially and temporally vary the thermal insult to loaded test assemblies (Santiago et al. 2008). Tests performed using this facility are briefly described above in Section 3.2.

An example of a system which is based on a pre-existing standard testing furnace is the column testing facility at the Federal Institute for Materials Research and Testing (BAM), in Berlin, Germany. The BAM column testing facility is based on a standard column furnace, but rather than simply applying a constant axial testing load during fire, it can use a 'hybrid' sub-structuring system where the entire column is tested inside the furnace and measured forces are read and target displacements are controlled via simulated modeling into the substructure in real time (Korzen et al. 2010). The BAM furnace is capable of producing an ISO 834 (ISO 1999) fire on columns of up to 3.55 m in height. The furnace is fired by six oil burners. Six electro-hydraulic control channels are used to actively control mechanical boundary conditions (two bending rotations each at top and bottom, axial displacement at the bottom, and horizontal displacement at the top). This testing methodology allows single elements to be tested in isolation while the rest of the structure is 'simulated' by actively controlling the boundary conditions in real time during the test. A similar approach has recently been taken at the National Research Council of Canada, Ottawa, Canada, where an existing standard column testing furnace has been upgraded to permit 'hybrid' testing of isolated structural elements by active control of applied loads during testing, again using coupled numerical analysis of the full structure in real time (Mostafaei 2011).

An example of a unique fire testing furnace based on electrical heating is the University of Sheffield's connection testing furnace (Yu et al. 2011). This relatively small-scale facility was custom designed to allow testing of bolted steel connections at elevated temperature under the appropriate combinations of moment, shear, thrust, and rotation that would be expected in a real building in a fire. Heating is accomplished using electrical resistance heaters, and loading is applied by a relatively complicated mechanism of restraining frames and loading jacks. This allows detailed, rational studies of the response of bolted steel connections under a wide range of possible structural and thermal actions.

Probably the best example of a custom made structural testing facility which is currently available for large-scale non-standard structural fire testing is the CERIB-Promethée testing facility in Epernon, France. This facility has been operational since 2008 (Robert et al. 2009), and was developed to expand existing standard fire tests, to incorporate boundary conditions which would occur due to restraint and interaction between hot and cold zones in a real fire in a real building, and to provide

validation data for thermo-mechanical simulations of real structures during fire. The facility essentially consists of a gas-fired furnace with integrated mechanical loading frames that can reproduce interactions between the parts of the structure under testing and those that are unexposed. The furnace measures 6 m × 4 m × 2.5 m (adjustable to 4.1 m), although a specimen length of 10 m can be installed due to the modular furnace construction. Restraint and structural interactions are simulated via multi directional loading using an array of 29 hydraulic jacks with loading capacities up to 3 MN. These jacks can be actively controlled by coupling to numerical analysis of the full structure in real time (although it is not clear if this has yet been accomplished in practice). The furnace is heated by 16 gas burners and is capable of simulating various standard fires including ISO 834 (ISO 1999) and hydrocarbon curves (CEN 2002). Despite the capabilities of this furnace, it appears that relatively few of these capabilities have yet been used to produce publishable scientific outputs, likely because the current prescriptive SFE regulatory framework effectively discourages investment in rational testing.

4.3 Facilities under construction

In addition to the facilities noted above, a number of unique fire testing facilities are currently under construction. Notable examples are the construction of a new 9 m tall testing furnace at the Centre Scientifiqueet Technique du Bâtiment (CSTB), Paris, France, and the current large-scale extension to the National Fire Research Laboratory (NFRL) at NIST, USA.

The CSTB facility under construction, called ‘Vulcain’, is a particularly large, modularized and reconfigurable standard testing furnace which will be able to test walls of 3 m width and 9 m height, long span floors with a weight of up to 30 tonnes, and various combinations of walls, columns, beams, and slabs in two and three dimensions (CSTB 2011).

NIST’s extension to the NFRL will create a unique ‘real fire’ testing facility which will combine most of the best aspects of available testing facilities elsewhere (NIST 2011). The facility will combine the capability to test large-scale multiple bay, multi-storey structures, subject to real fires with real fuel loads, while applying controlled loads both vertically and laterally and providing data on heat release rates and gas analysis. The test area will consist of an 18.3 m × 27.4 m strong floor with an adjacent 9.1 m high × 18.3 m wide concrete strong wall. The strong wall will act to stabilize a test specimen to prevent uncontrolled failure, to provide lateral restraint, or to laterally load a structure to simulate earthquake damage. A 13.7 m × 15.2 m overhead hood will provide heat release rate calorimetry data up to fires 20 MW in size (NIST 2011). It is not currently clear what specific testing is planned for this facility once operational.

5. Knowledge gaps and research needs

It is clear from the preceding sections that a considerable volume of large-scale non-standard structural fire testing has been performed in recent decades. A range of

custom made structural fire engineering testing facilities have been commissioned or are currently under construction, and the SFE community appears to be actively engaging with the identified gaps in knowledge. Given the considerable research effort which has been undertaken thus far, it is worthwhile to ask where future research in structural fire engineering should be directed, particularly in light of the novel testing facilities which are soon to be available.

The following is a non-exhaustive list of knowledge gaps and research needs suggested either by previous authors or which have been identified during the preceding discussion.

5.1 Fire exposure

As noted by authors going back to (at least) 1970, the standard temperature-time curve is not representative of a real fire in a real building. In order to truly understand the response of real buildings in real fires, tests of structures and structural elements are required under credible worst case natural fire exposures. Depending on the type and geometry of structure and the occupancy under consideration, this may require experimental consideration of localized, compartmentalized, horizontally and/or vertically travelling, smouldering, or hydrocarbon fires, all of which have the potential to introduce structural actions or interactions which are not captured by standard fires. In particular, the true dynamics of travelling or spreading fires in large compartments has received only limited attention within the research literature (e.g. Stern-Gottfried and Rein 2012), and essentially zero attention in large scale structural fire tests. There appears to be no facility in the world which is capable of producing (or reproducing) truly natural fire exposures on structures of realistic scale and construction, although the new NIST facility (Section 4.3) will go some way towards making this a reality.

5.2 Structural interactions and asymmetry

The available test data from large-scale non-standard fire tests, while extensive, still cover only a tiny fraction of the possible structural configurations that are represented within the current global building stock, let alone the highly optimized and sustainable buildings of the future. With a few notable exceptions, the majority of structural fire tests conducted to date, whether standard or non-standard, have studied regular, symmetrical, highly idealized structures. Modern structures increasingly make use of irregular floor plates with varying span lengths, bay sizes, construction types, etc. The possible influence of irregular floor plans and complex building forms needs to be investigated, both experimentally and numerically, if performance-based structural fire engineering of both conventional and modern buildings is to be credibly performed with confidence. Indeed the importance of irregular building layouts, the position of service cores, and lateral restraint to thermal expansion are already known (through computational modeling studies of real high rise buildings) to be potentially important for full-structure response to fire (e.g. Usmani et al. 2006, Flint et al. 2007, McAllister et al. 2012, Flint et al. 2013).

5.3 Failure localizations

When real structures fail in fires it is rarely for the reasons that would be expected on the basis of standard fire resistance testing. In many cases, global failure is precipitated by some form of localised failure or structural distress, such as discrete cracking in concrete, rupture of tensile steel reinforcement, failure of a connection, local buckling of structural steelwork, shear (punching) failure of a concrete slab, rupture of an unbondedprestressing tendon, etc. Unfortunately, the only way to observe and understand such failure localizations, which depend in virtually all cases on the three dimensional interactions between elements of structure during both heating *and* cooling, is to perform large-scale non-standard structural fire tests on real buildings. Only once all of the possible failure modes are *known* can they possibly be rationally incorporated into computational models for full structure response to fire.

5.4 Compartmentation and fire spread

To date, most large-scale structural fire testing has focused on prevention of structural collapse during fire, and relatively little attention has been paid to preservation of compartmentation under large deformations in real structures during fire; this is particularly of concern given the large floorplate deflections and wide discrete cracking which have been widely observed in large-scale fire tests on steel-concrete composite slabs (see Section 3.1). The impacts of vertical and lateral deformations of structural frames on fire stopping and on both horizontal and vertical compartmentation should be studied to preserve life safety in buildings which are now becoming ever more reliant on defend-in-place life-safety strategies (for instance in highrise buildings where fire safety strategies are typically based on the assumption that a fire will be confined to the floor of origin).

Furthermore, given that many structural fire engineers already have serious concerns about the quality of installed fire stopping between floors in multi-storey buildings, large-scale non-standard fire tests should perhaps be considered in which vertical fire spread is explicitly simulated using natural fires to evaluate the structural impacts of credible worst case fires burning simultaneously on more than one floor of a structure.

5.5 Detailing and construction errors

Taken together, the tests described in this report highlight a number of important construction details and potential construction errors which may appear inconsequential to a building contractor, but which may have a profound impact on the structural fire response and integrity of a building during fire. Examples of this include integrity of fire stopping during large deformations, lapping of steel reinforcing mesh, anchorage of steel reinforcing mesh over shear studs on protected perimeter beams, use of deformed versus smooth bars for reinforcement (potentially

leading to strain localization and tensile failure of deformed steel bars during fire), proper anchorage and grouting of hollowcore slabs, use of specific types of bolted steel connections to promote connection ductility and rotational capacity during fire, quality, uniformity, and robustness of structural fire protection materials (either passive or intumescent), and so on. Serious unknowns continue to surround many, if not all, of these issues, and there is a need for testing to support the development of best practice guidance which can be used to provide quality assurance programs on construction sites of so-called 'fire engineered' buildings.

5.6 Cooling phase behavior and residual capacity

A number of localized structural failures or adverse structural responses of steel connections, concrete flat plate slabs, and hollowcore slabs have been observed during the cooling phase of both real fires in real buildings (e.g. Firehouse.com 2004, Bamonte et al. 2009) and non-standard heating regimes in large-scale structural fire experiments (e.g. Bailey and Lennon 2008, British Steel 1999). Structural actions resulting from creep, localised and/or global plastic deformation, local buckling, and thermal contraction and restraint, all need to be better understood for all types of structures if designers are to realistically be expected to design for full burnout of a fire compartment without structural collapse.

Furthermore, the residual structural capacity of fire damaged structures which have undergone large deformations is not well known, meaning that many fire-damaged structures will need to be demolished after a fire (e.g. New York Times 1997). This is particularly true for so-called fire-engineered composite steel frames, which explicitly rely on large deformation behavior to mobilize the tensile membrane actions which are necessary to support gravity loads and prevent collapse during fire (British Steel 1999).

5.7 Instrumentation and measurement

Most SFE authors agree that more complete data are required from both standard and non-standard structural fire tests. Better information on strains and displacements during testing would allow a more accurate understanding of response, and would provide additional data which are essential for high quality computational model development and validation. The need for new types of sensors, such as wireless sensors to be used during fire tests, has been noted previously (Kodur et al. 2011). However, the authors of the current review feel that what is really needed is a better understanding of what is being measured; i.e. *What should be measured in order to truly understand the global performance of the element of the structure being tested?*

5.8 Data for model calibration, validation and verification

Experimental data are essential for calibration, validation, and verification of both existing and emerging computational modeling techniques to simulate the response of structures and structural elements in fire. This requirement holds both at the

material level and at the structural (i.e. system) level. As noted by Kodur et al. (2011), high-temperature constitutive material models are needed to generate reliable input data for models and to better understand system response to fire and possible failure modes. Such data must be developed using an appropriate framework for understanding the stress-temperature-time-strain interrelationships at play in most engineering materials. An excellent framework for materials characterization at elevated temperature was presented more than two decades ago by Anderberg (1986), however the complexities shown in this framework are rarely explicitly acknowledged in SFE analysis or design.

5.9 Structural optimization and the Use of New materials and systems

Modern structures are highly optimized, increasingly by the use of sophisticated computer analysis, in an attempt to reduce the mass, cost, environmental impact, carbon emissions, and embodied energy in buildings (Terrasi 2007). Modern structures also increasingly make use of innovative materials, such as high strength, self consolidating concrete, fiber reinforced polymers (FRPs), structural adhesives, stainless steel, etc., and innovative structural systems such as unbonded post-tensioned flat plate concrete slabs; the responses of which during fire are not well known in many cases. New materials and structural systems must be rationally understood before they should be applied with confidence in buildings. Such an understanding demands large-scale non-standard fire testing, in particular because the standard furnace tests that were developed for conventional construction materials and systems are based on structural response and failure definitions which often are not applicable to newer innovative ones (e.g. Bisby and Kodur 2007).

5.10 Connections

As noted previously, a range of studies have already been performed on connection performance in fire (largely for steel structures) (e.g. Ding and Wang 2007, Yu et al. 2009, 2011, Yuan et al. 2011). However, given the range of possible connection types, full-structure responses to fire, and failure modes, additional research is needed to better understand the full range of possible connections, to develop and validate computational modeling capabilities to predict connection response, and to suggest best practice guidance (in particular to steel fabricators) on the types of connections which should be applied in practice to ensure structural robustness in fire. Proper details for the connection of precast concrete elements in buildings to ensure robust performance in fire is also required (Bailey and Lennon 2008). Important lessons can be learned on these issues by studying the literature and available design provisions on the seismic design of structural connections (FEMA 2000a, FEMA 2000b, AISC 2005); it may be appropriate to develop similar provisions for structural robustness in fire.

5.11 Explosive spalling of concrete

Structural fire design of modern reinforced and prestressed concrete structures relies on the assumption that the concrete will not spall during fire. This assumption is

based largely on data from large-scale standard fire tests of concrete elements tested in isolation in furnaces during the past 60 to 70 years. However, there is legitimate concern (Kelly and Purkiss 2008) that modern concrete structures, which incorporate concrete mixes with considerably higher concrete strengths, are more susceptible to spalling than was historically the case. Whilst preliminary guidance on the means by which spalling can be addressed by designers is available in the structural Eurocodes (CEN 2004), research is badly needed to understand the respective roles of the various factors which are known to increase a concrete's propensity for spalling during fire (e.g. high strength, high stress, high moisture, low permeability, small amounts of bonded reinforcement, use of silica fume, rapid heating, etc.) (ArupFire 2005, Bailey and Khoury 2011), such that defensible preventative actions can be taken. For instance, more specific and defensible guidance is needed on the requirement to add a certain amount of polypropylene fibers to the concrete mix to prevent spalling. Interactions in real structures have the potential to significantly influence development of spalling in a fire, so large-scale tests under natural fires are needed to truly understand the propensity for, and the structural consequences of, spalling in real concrete structures.

5.12 Timber structures

A critical issue for the structural fire protection of timber structures appears to be the integrity of fire proofing materials such as gypsum plasterboard (Lennon et al. 2000). Additional research is required to better understand the factors leading to 'fall-off' of plasterboard and other fire stopping materials and systems during fire. It is important to recognise the difference between light timber frame buildings (where the fire resistance of wood must be protected by gypsum lining materials) and heavy timber buildings which rely on the predictable charring rate of large timber members.

Another critical issue for timber structures is the performance after the fire has gone out. Designers are often concerned that charred timber will continue to char after all flaming has ceased, which makes it difficult or impossible to design for a complete burnout as is done for concrete or steel structures. More research is needed in this area, and this can only be done with large scale structural fire testing.

6. Conclusion

This paper has presented a review of structural fire engineering research done at the large-scale around the world during the past four decades. It has identified gaps and further research needs based both on the conclusions of previous studies and also on the authors' own assessments of the information presented. Areas where particular research attention is needed include:

- non-standard fire exposures;
- structural interactions and asymmetry;
- failure modes and failure localizations;
- the effects of structural deformation on compartmentation and fire spread;
- detailing best practice and the influence of construction details on overall structural fire

performance;

- cooling phase behavior and residual capacity after fire;
- functional and meaningful instrumentation and measurement during fire testing;
- development of data which are useful for model calibration, validation and verification;
- the influence of structural optimization and novel structural materials on structural fire performance;
- the performance of various types of connections during fire, particularly during the cooling phase;
- causes, prevention, and impacts of explosive concrete cover spalling; and
- the performance of both light-frame and solid timber buildings both during and after real fires.

It is hoped that the information presented in this review might help steer future research in structural fire engineering, particularly in the case of non-standard experimental research at the large-scale.

Acknowledgments

The authors would like to acknowledge the generous support of Kathleen Almand and the Fire Protection Research Foundation. We would also like to thank the School of Engineering at the University of Edinburgh, which is part of the Edinburgh Research Partnership in Engineering and Mathematics, The Ove Arup Foundation, The Natural Science Engineering Research Council of Canada, The UK Royal Academy of Engineering and The Lloyd's Register Educational Trust.

Competing Interests

The authors declare that they have no competing interests.

Authors' Contributions

This paper represents a true joint effort between the three listed authors. Doctoral candidates Gales and Maluk performed the bulk of the literature search, informed through discussion with their supervisor, Bisby. Gales and Maluk each created first drafts of various sections of the paper, each on an approximately 50% basis, while Bisby structured the paper, added insight, and performed final editing etc. The order of authorship is therefore somwhat arbitrary, and the authors consider that all three contributed equally. All authors read and approved the final manuscript.

References

Anon (1986) brandverhalten von stahl und stahlverbund construction (Fire behaviour of steel and composite construction).Verlag, TUV, Rheinland

AISC (2005) ANSI/AISC 341–05 – Seismic Provisions for Structural Steel Buildings. American Institute of Steel Construction (AISC), Chicago

Almand K, Phan L, McAllister T, Starnes M, Gross J (2004) NISTIR 7133: SFPE Workshop for Development of a National R&D Roadmap for Structural Fire Safety Design and Retrofit of Structures. National Institute of Standards and. Technology, Gaithersburg

Anderberg Y (1986) Modelling steel behaviour. Paper presented at the International Conference on Design of Structures Against Fire. Aston University, Birmingham, pp 15–16, 15–16 April 1986

Annerel E, Lu L, Taerwe L (2011) Punching shear tests on flat concrete slabs at high temperatures.Proceedings of the 2nd International RILEM Workshop on Concrete Spalling due to Fire Exposure.RILEM Publications S.A.R.L., Delft, pp 125–131, 5–7 October 2011

ArupFire (2005) Fire resistance of concrete enclosure – Work package 2: Spalling categories. Authored for the Nuclear Safety Directorate of the Health and Safety Executive (HSE). Arup Group Ltd, London

ASTM (1980) ASTM E119: Fire Tests of Building Construction and Materials. American Society for Testing and Materials, Philadelphia, PA

ASTM (2011) ASTM E119-11a: Standard methods of fire test of building construction and materials. American Society for Testing and Materials, West Conshohocken

Bailey CG (2002) Holistic behaviour of concrete buildings in fire.Struct Build 152(3):199–212

Bailey CG, Toh WS (2007) Behaviour of concrete floor slabs at ambient and elevated temperature. Fire Safety Journal 42(6–7):425–436

Bailey CG, Lennon T (2008) Full scale fire tests on hollowcore slabs. The Structural Engineer 86(6):33–39

Bailey CG, Khoury GA (2011) Performance of Concrete Structures in Fire – An in-depth publication on the behaviour of concrete in fire.Ruscombe Printing Ltd, Reading, Surrey, UK

Bamonte P, Felicetti R, Gambarova PG (2009) Punching Shear in Fire-Damaged Reinforced Concrete Slabs. ACI Special Publication 265. American Concrete Institute, Farmington Hills, pp 345–366

Beitel J, Iwankiw N (2008) NIST GCR 02-843-1 (Revision) – Analysis of Needs and Existing Capabilities for Full-Scale Fire Resistance Testing. National Institutes for Standards and Technology, Gaithersburg

Beyler C, Beitel J, Iwankiw N, Lattimer B (2007) NIST GCR 07–910 – Fire resistance testing for performance-based fire design of buildings. National Institute of Standards and Technology, Gaithersburg

Bisby LA, Kodur VKR (2007) Evaluating the fire endurance of concrete slabs reinforced with FRP bars: Considerations for a holistic approach. Composites Part B: Engineering 38(5–6):547–558

BRE (2011) Fire Test Facilities., Available via http://www.bre.co.uk/page.jsp?id=417. Accessed 7 December 2011

British Steel (1999) The behaviour of multi-storey steel frame buildings in fire. British Steel, Rotherham

Buchanan A (2001) Structural design for fire safety. Wiley, West Sussex, UK

Cadorin JF, Pintea D, Franssen JM (2001) The Design Fire Tool OZone V2.0 - Theoretical Description and Validation On Experimental Fire Tests. University of Liege, Belgium

CCAA (2010) Fire Safety of Concrete Buildings. Cement Concrete & Aggregates Australia, St Leonards, Australia

CEN (2002) BS EN 1991-1-2:2002 – Eurocode 1: Actions on structures — Part 1–2: General actions — Actions on structures exposed to fire. European Committee for Standardization, Brussels

CEN (2004) BS EN 1992-1-2:2004 – Eurocode 2: Design of concrete structures — Part 1.2: General rules — Structural fire design. European Committee for Standardization, Brussels

Chlouba J, Wald F (2009) Connection temperatures during the mokrsko fire test. ActaPolytechnica 49(1):76–81

Chlouba J, Wald F, Sokol Z (2009) Temperature of connections during fire on steel framed building. International Journal of Steel Structures 9(1):47–55

Chung H-Y, Lee C-H, Su W-J, Lin R-Z (2010) Application of fire-resistant steel to beam-to-column moment connections at elevated temperatures. Journal of Constructional Steel Research 66:289–303

Cooke GME, Latham DJ (1987) The inherent fire resistance of a loaded steel framework. Steel Construction Today 1:49–58

Corus (2006) Fire resistance of steel-framed buildings. Corus Construction and Industrial, Scunthorpe

CSTB (2011) Vulcain., Available via http://www.cstb.fr/le-cstb/equipements/feu/vulcain.html. Accessed 1 December 2011

De Feijter MP, Breunese MP (2007) 2007-Efectis-R0894(E) – Investigation of Fire in the Lloydstraat Car Park, Rotterdam. Effectis Nederland BV, The Netherlands

Ding J, Wang YC (2007) Experimental study of structural fire behaviour of steel beam to concrete filled tubular column assemblies with different types of joints. EngStruct 29(12):3485–3502

Dong Y, Prasad K (2009a) Thermal and structural response of a two-story, two bay composite steel frame under fire loading. Proc Combust Inst 33:2543–2550

Dong Y, Prasad K (2009b) Experimental study on the behavior of full-scale composite steel frames under furnace loading. J StructEng 135(10):1278–1289

FEMA (2000a) FEMA-350 – Recommended Seismis Design Criteria for New Steel Moment-Frame Buildings. Federal Emergency Management Agency, Hyattsville, USA

FEMA (2000b) FEMA-3555D – State of the Art Report on Connection Performance. Prepared for the SAC Joint Venture Partnership. Federal Emergency Management Agency, Hyattsville, USA

Firehouse.com (2004) Seven Swiss firefighters die in collapsed parking garage., Available via http://www.firehouse.com/news/lodd/seven-swiss-firefighters-die-collapsed-parking-garage. Accessed 6 December 2011

Flint G, Lamont S, Lane B, Sarrazin H, Lim L, Rini D, Roben C (2013) Recent lessons learned in structural fire engineering for composite steel structures. Fire Technology, published online ahead of print. doi:10.1007/s10694-012-0291-8

Flint G, Usmani A, Lamont S, Lane B, Torero J (2007) Structural response of tall buildings to multiple floor fires. J StructEng 133(12):1719–1732

FM Global (2009) The FM Global Research Campus. FM Global, USA

Gillie M (2009) Analysis of heated structures: nature and modelling bench marks. Fire Safety Journal 44(5):673–680

Grosshandler WL (2002) NISTIR 6890 – Fire Resistance Determination and Performance Prediction Research Needs Workshop. National Institute of Standards and Technology, Gaithersburg

Grosshandler WL (2003) The international FORUM of fire research directors: A position paper on evaluation of structural fire resistance. Fire Safety Journal 38:645–650

Han L-H, Wang W-H, Yu H-X (2010) Performance of RC Beam to Concrete Filled Steel Tubular (CFST) Column Frames Subjected to Fire.Proceedings of the 6th International Conference on Structures in Fire. Michigan State University, East Lansing, 2–4 June 2010, 358–365

Harmathy TZ, Lie TT (1970) Fire Test Standard in the Light of Fire Research, Fire Test Performance – ASTM STP 464, American Society for Testing and Materials, Philadelphia, 85-97

ISO (1999) ISO 834–1:1999: Fire Resistance Tests – Elements of Building Construction – Part 1: General Requirements. International Organization for Standardization, Geneva

Jeanes D (1982) Predicting fire endurance of steel structures. National ASCE Convention, Las Vegas, pp 82–033, April 26–30. Preprint pgs

Joyeux D, Kruppa J, Cajot LG, Schleich JB, Van de Leur P, Twilt L (2001). Demonstration of real fire tests in car parks and high buildings, CEC Agreement 7215–PP/025. CTICM, France – Profil-ArbedReceherches, Luxembourg – TNO, The Netherlands

Kelly F, Purkiss J (2008) Reinforced concrete structures in fire: a review of current rules. The Structural Engineer 86(19):33–39

Kodur VKR, Garlock MEM, Iwankiw N (2007) NISTGCR 07–915 – Structures in fire: state of the art, research and training needs. National Institute of Standards and Technology, Gaithersburg

Kodur VKR, Garlock MEM, Iwankiw N (2011) Structures in fire: State of the art, research and training needs. Fire Technol 48(4):825–839

Kordina K (1997) Ueber das brandverhaltempunkthestuetzterstahlbetonplatten (Investigations on the behaviour of flat slabs under fire).DAfsib H 479:106S

Korzen M, Rodrigues J, Correia A (2010) Composite columns made of partially encased steel sections subjected to fire. Proceedings of the 6th International Conference on Structures in Fire. Michigan State University, East Lansing, pp p 341–348, 2–4 June 2010

Law M (1981) Designing fire safety for steel – recent work. Proceedings of the ASCE Spring Convention. American Society of Civil Engineers, New York, 11–15 May 1981

Lennon T, Bullock MJ, Enjily V (2000) The fire resistance of medium-rise timber frame buildings. World Conference on Timber Engineering, Whistler, Canada, 31 July-3 August 2000

Li-tang G, Li X, Chen L, Yuan A (2008) Experimental investigation of the behaviours of unbondedprestressed concrete continuous slabs after fire. Concrete (in Chinese), 2008–02

McAllister TP, Gross JL, Sadek IH, Kirkpatrick SW, MacNeill RS, Zarghamee MS, Erbay OO, Sarawit AT (2012) Structural Response of World Trade Center Buildings 1, 2 and 7 to Impact and Fire Damage. National Institute of Standards and Technology, Gaithersburg, 18 October 2012

Mostafaei H (2011) RR-316 – Hybrid Fire Testing for Performance Evaluation of Structures in Fire - Part 1: Methodology. National Research Council of Canada, Ottawa, 26 August 2011

Nadjai A, Bailey CG, Vassart O, Han S, Zhao B, Franssen JM, Simms I (2011) Full-scale fire test on a composite floor slab incorporating long span cellular steel beams. The Structural Engineer 89(21):18–25

New York Times (1997) Philadelphia to Raze Site of High-Rise Fire., Available via http://www.nytimes.com/1997/11/14/us/philadelphia-to-raze-site-of-high-rise-fire.html. Accessed 7 December 2011

NIST (2011) Project: National Fire Research Laboratory Commissioning and Operations., Available via http://www.nist.gov/el/fire_research/nfrl/project_nfrl.cfm. Accessed 5 December 2011

NRCC (2011) Burn Hall – Three Storey Exterior Wall Test Facility., Available via http://www.nrc-cnrc.gc.ca/eng/facilities/irc/burn-hall.html. Accessed 9 December 2011

Proe D, Bennetts I (1994) Real Fire Test in 380 Collins Street Office Enclosure. BHP Research Report No.BHPR/PPA/R/051/SG021A. BHP Billiton Limited, Melbourne

Proe D, Thomas I (2010) Planning for a Large-Scale Fire Test on a Composite Steel-Frame Floor System.Proceedings of the 6th International Conference on Structures in Fire. Michigan State University, East Lansing, pp p 390–397, 2–4 June

Peng W, Hu L-H, Yang R-X, Lv Q-F, Tang F, Xu Y, Wang L-Y (2011) Full scale test on fire spread and control of wooden buildings.Procedia Engineering (in Chinese) 11:355–359

Ring T, Zeiml M, Lackner R (2011) Large scale fire tests on concrete design and results. Poster presented at the 18th Inter-Institute Seminar for Young Researchers, Budapest, Hungary, pp 23–25, September 2011

Robert F, Rimlinger S, Collet E, Collignon C (2009) PROMETHEE, The innovative fire resistance testing centre for structures. International Conference on Applications of Structural Fire Engineering, Prague, Czech Republic, pp 19–21, February 2009, Annex 14

Rubert A, Schaumann P (1986) Structural steel and plane frame assemblies under fire action. Fire Safety Journal 10(3):173–184

Santiago A, da Silva LS, Vaz G, Vila Real P, Lopez AG (2008) Experimental investigation of the behaviour of a steel sub-frame under a natural fire. Steel and Composite Structures 8(3):243–264

Sharma UK, Bhargava P, Singh B, Singh Y, Kumar V, Kamath P, Usmani A, Torero J, Gillie M, Pankaj P, May I, Zhang J (2012) Full scale testing of a damaged RC frame in fire. Struct Build 165(7):335–346

SINTEF (2011) Large test hall., Available via http://www.sintef.no/home/Building-and-Infrastructure/SINTEF-NBL-as/About-SINTEF-NBL/Laboratories/Large-test-hall/. Accessed 9 December 2011

Stern-Gottfried J, Rein G (2012) Travelling fires for structural design. Part II: design methodology. Fire Safety Journal 54:96–112

SwRI (2011) Fire Testing Services.Available via http://www.swri.org/4org/d01/fire/fireres/home.htm. Accessed 5 December 2011

Stadler M, Mensinger M, Schaumann P, Sothmann J (2011) Munich fire tests on membrane action of composite slabs in fire – test results and recent findings. Proceedings of the international conference on applications of structural fire engineering, Prague. Czech Republic 29:177–182, April 2011

Terrasi GP (2007) Prefabricated Thin-walled Structural Elements made from HPC Prestressed with Pultruded Carbon Wires. Proceedings of the 8th International Symposium on Fiber Reinforced Polymer Reinforcement for Concrete Structures. University of Patras, Greece, 16–18 July 2007

TFRI (2011) I hold China-US fire protection technology and fire codes academic exchange activities., Available via http://www.tfri.com.cn/manage/html/1356.html. Accessed 9 December 2011

Thomas IR, Bennetts ID, Dayawansa PH, Proe DJ, Lewins RR (1992a) Fire Tests of the 140 William Street Office Building, BHP Research Report No. BHPR/ENG/R/92/043/SG2C. BHP Billiton Limited, Melbourne

Troxell GE (1959) Fire resistance of a prestressed concrete floor panel. Journal of the American Concrete Institute 56(8):97–105

Usmani A, Roben C, Johstone L, Flint G (2006) Tall building collapse mechanisms initiated by fire. SiF'06. Proceedings of the 4th International Workshop Structures in Fire, East Lansing, Michigan, 2–4 June 2010

Van Acker A (2003) Shear resistance of prestressed hollow core floors exposed to fire. StructConcr 4(2):65–74

Van Herberghen P, Van Damme M (1983) Fire resistance of post-tensioned continuous flat floor slabs with unbonded tendons (U.T.). FIP Notes 1983/4:3–11

Vassart O, Zhao B (2011) FRACOF Engineering Background. Report developed for theLeonardo Da VinciProgramme: Fire Resistance Assessment of Partially Protected Composite Floors (FRACOF). European Commission, Education and Culture DG, Bordeaux, France

Victoria University (2011) Fire test facilities.Available via http://www.vu.edu.au/centre-for-environmental-safety-and-risk-engineering-cesare/fire-test-facilities. Accessed 7 December 2011

Wald F, Simões da Silva L, Moore DB, Lennon T, Chaldna M, Santiago M, Beneš M, Borges L (2006) Experimental behaviour of a steel structure under natural fire. Fire Safety Journal 41(7):509–522

Wald F (2010) Fire Test on an Administrative Building in Mokrsko. Czech Technical University, Printing house Českátechnika, Prague, Czech Republic

Wald F (2011) Large Scale Fire Tests. COST Action TU0904. Integrated Fire Engineering and Response Working Group, Prague, Czech Republic, April 30

Wald F, Jána T, Horová K (2011) Design of joints to composite columns for improved fire robustness – To demonstration fire tests. Czech Technical University, Printing house Českátechnika, Prague, Czech Republic

Wong YL, Ng YW (2011) Technical Seminar – Effects of Water Quenching on Reinforced Concrete Structures under Fire. Presented to The Institution of Fire Engineers (Hong Kong Branch). Kowloon Tong Fire Station,Kowloon, 23 August 2011

Wong SY, Burgess IW, Plank RJ, Atkinson GA (1999) The response of industrial portal frames to fires. ActaPolytechnica 39(5):169–182

Yu H, Burgess I, Davison J, Plank R (2011) Experimental and numerical investigations of the behavior of flush End plate connections at elevated temperatures. J StructEng 137(80):80–87

Yu H, Burgess IW, Davison JB, Plank RJ (2009) Experimental investigation of the behaviour of fin plate connections in fire. Journal of Constructional Steel Research 65(3):723–736

Yuan Z, Tan KH, Ting SK (2011) Testing of composite steel top-and-seat-and-web angle joints at ambient and elevated temperatures: Part 2 — Elevated-temperature tests. EngStruct 31(9):2093–2109

Zhao JC, Shen ZY (1999) Experimental studies of the behaviour of unprotected steel frames in fire. Journal of Constructional Steel Research 50:137–150

Zheng WZ, Hou XM, Shi DS, Xu MX (2010) Experimental study on concrete spalling in prestressed slabs subjected to fire. Fire Safety Journal 45:283–297

Appendix C:
Micro-structural and mechanical characterization of post-tensioning tendons following elevated temperature exposure

From:

Roberston, L., Dudorova, Z., Gales, J., Vega, E., Smith, H., Stratford, T., Blackford, J., Bisby, L. (19–20 April 2013) Micro-structural and mechanical characterization of post-tensioning tendons following elevated temperature exposure. Applications of Structural Engineering Conference. Prague, CZ. 474-479.

MICROSTRUCTURAL AND MECHANICAL CHARACTERISATION OF POST-TENTIONING STRANDS FOLLOWING ELEVATED TEMPERATURE EXPOSURE

Lucie Robertson[a], Zuzana Dudorova[a], John Gales[a], Esther Vega[a], Holly Smith[a], Tim Stratford[a]*, Jane R. Blackford[b], Luke Bisby[a]

[a] BRE Centre for Fire Safety Engineering, School of Engineering, Univ. of Edinburgh, Edinburgh, EH9 3JL, UK
[b] Institute for Materials and Processes, School of Engineering, Univ. of Edinburgh, Edinburgh, EH9 3JL, UK

Abstract

Prestressing strands lose strength and become more susceptible to creep deformation when they are heated during a fire. The consequent loss in prestressing force could under certain conditions result in structural collapse, potentially outwith the heated region of the structure. This paper describes a test programme characterising the changes in microstructure of steel prestressing tendons exposed to elevated temperatures. The residual strength tests, hardness testing, and elevated temperature mechanical test were performed to demonstrate how recovery and recrystallisation of the initially work-hardened steel produce changes in its mechanical properties at elevated temperatures. The research results of this paper are beneficial not only in the fire design of post-tensioned structures using modern prestressing steel, but also in the assessment of the tendons' residual strength after being affected by fire.

Keywords: Prestressing steel, microstructure, hardness, residual strength, creep.

1 Introduction

The prestressing tendons used in pre-tensioned and post-tensioned concrete construction can be greatly affected by elevated temperature, potentially resulting in catastrophic collapse of a structure. Even if collapse does not occur, heating can reduce both the strength of the tendon at elevated temperature, and the residual strength after it has cooled down, and the tendon can undergo creep deformation. The extent of damage is often not visually quantifiable and another means of assessment must therefore be sought.

This paper reports a study of the changes in physical and mechanical properties of a modern prestressing steel at high temperatures. It examines how the microstructure, hardness and residual tensile strength of the steel is affected by temperature. The aims are to (a) provide fundamental information on the behaviour of prestressing steel subjected to fire temperatures, and to (b) allow the post-fire condition of a tendon to be assessed by means of a simple, cheap, and non-destructive hardness test.

1.1 Previous Work Characterising the Effect of Temperature upon Prestressing Steel

The tendons in pre- or post-tensioned concrete are embedded in concrete that provides good insulation; however it is possible for the tendon to reach temperatures over 400°C, and well above this temperature if the tendon or the tendon duct are exposed directly to fire following spalling or cracking of the cover concrete (Gales *et al.*, 2011).

The strength of prestressing steel decreases significantly when exposed to temperatures above 300°C (Holmes *et al.* 1982; Neves *et al.*, 1996; Maclean, 2007), and can loose 50% of its strength at high temperatures. Preloading the strands prior to testing makes little difference to its behaviour. There is a slight increase in strength, however, for temperatures above 700°C (Abram & Erlin, 1967; Holmes *et al.*, 1982).

The mechanical performance of prestressing steel follows from the changes in microstructure that occur as it is heated. Prestressing steel is a cold-drawn, pearlitic steel (a eutectoid mixture of iron carbide and ferrite). At ambient temperature its microstructure consists of thin, elongated pearlite grains. Between 400°C and 700°C, spheroidisation occurs (in which the iron carbide in the pearlite forms globules), accompanied by recovery (in which the dislocations present due to cold working are annihilated). Upon heating to temperatures above 700°C, the matrix recrystallises completely and forms new grains, which then grow over time (Abrams & Erlin, 1967).

A correlation between hardness, tensile strength, microstructure and temperature was established for prestressing steel in the 1960s by Abrams & Erlin (1967). Modern steel, however, has a different chemical composition; the composition of the prestressing steel studied in this paper is compared to those used in previous studies in Tab. 1. The current BS 5896 steel has a higher carbon content and a lower phosphorus and sulphur content than the steel tested by Abrams & Erlin. Gales *et al.* (2012) have identified that existing design guidance may overestimate creep deformation, as a result of the changes in the steel used for prestressing tendons. Consequently, the design guidance may be non-conservative for predicting tendon rupture during a fire, and it is important to re-examine the performance of prestressing steels at high temperatures.

Tab. 1 - Carbon and main alloy content in the steels used in previous and current studies.

	C (%)	Mn (%)	P (%)	S (%)	Si (%)
Abrams & Erlin (1967)	0.794	0.498	0.0118	0.0376	0.288
Neves *et al.* (1996)	0.824	0.712	0.02	0.013	0.235
MacLean (2007)	0.80	0.868	0.023	0.012	0.45
Current Tests (BS 5896, 2000)	0.90	0.66	0.007	0.014	0.25

2 PROCEDURE

The tests were performed on prestressing steel strands and core wires made to British Standard BS 5896 (2000). The hardness, residual strength and microstructure of the steel were studied after cooling.

2.1 Heat Treatment

Unloaded and unrestrained strands were heated to temperatures of 200, 400, 500, 600, 700 and 800°C. Two samples were tested for each exposure temperature. The samples were placed in a furnace and heated from room temperature to the target temperature at 10°C/min, using four thermocouples to monitor the furnace and sample temperatures. The specimens were then held at the target temperature for 1.5 hours, followed by air-cooling to simulate natural cooling following a fire. This heating regime matched previous tests by MacLean (2007).

An additional four samples were heated to 400°C and held for periods of 4 and 8 hours (corresponding to the study by Abrams & Erlin, 1967). These samples allowed the effect of soak time upon microstructure and hardness to be studied at 400°C, for which significant changes in mechanical properties start to occur (Neves *et al.*, 1996; MacLean, 2007; Myers & Bailey, 2009).

2.2 Hardness

Vickers hardness tests were performed on all the heated core wires. 30 mm long samples were ground using P400 silicon carbide paper to produce a flat, clean surface at least 2 mm wide. The samples were mounted in a special stand, tested under the equivalent of a 30kg mass, and the appropriate conversion used to obtain the Diamond Pyramid Hardness (DPH) value. Four hardness tests were performed in the centre of each sample (to eliminate the influence of the sample edges) and the results were averaged.

2.3 Microstructure

Microstructural observation of both transverse and longitudinal sections of the samples were conducted through a Zeiss Axioscope light microscope. Two 10 mm long sections were cut from each sample and mounted in EpoxiCure resin. These were ground using gradually finer grit paper and then polished with cloths and diamond paste, to obtain a flat, scratch-free surface. The samples were etched with 2% Nital to expose the grain structure.

2.4 Residual Tensile Strength

Residual tensile strength tests were performed on the core wires after cooling using an Instron 600LX universal testing machine. The samples were tested using a free length of 50mm, at a strain rate of 2 mm/min (to avoid creep effects). Digital Image Correlation (DIC) was used to measure the steel strains during the tests (see Gales *et al.* (2012) for details).

2.5 Tension Test

The core wire from a prestressing strand was heated at 10°C/min to a temperature of 500°C and held for 15 mins. The sample was loaded at 1mm/min whilst maintaining the temperature at 500°C. The test was stopped before failure to observe necking, which occurred in two distinct places. The necked sections were tested for hardness and prepared for microscopy as described above.

3 RESULTS AND DISCUSSION

The results obtained during this study are compared with prior research by Abrams & Erlin (1967), Holmes (1982), Neves (1996), MacLean (2007), and Myers & Bailey (2009). These authors studied the change in residual mechanical and material properties of loaded and/or unloaded prestressing steel samples with temperature.

3.1 Microstructure

Fig. 1 shows the microstructure of the longitudinal sections at different temperatures and soak times. The elongated pearlite grains are clearly shown in the non-heated prestressing steel (Fig. 1a). The extensive cold-drawing during manufacture of the steel wire results in very fine grains that cannot be distinguished in the transverse direction.

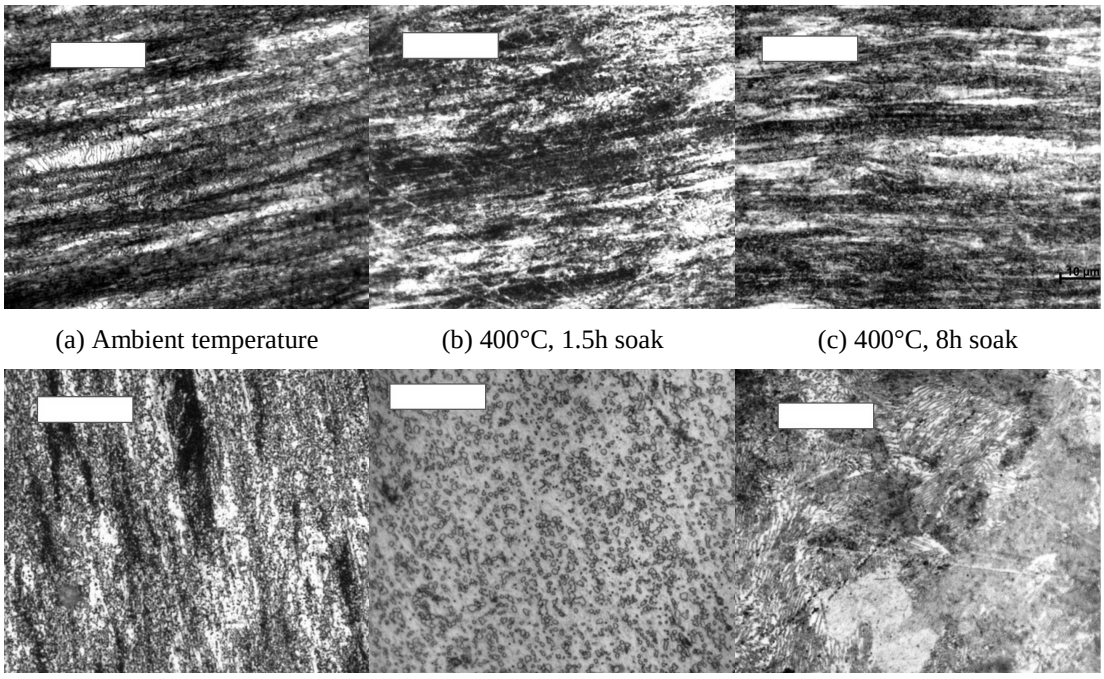

(a) Ambient temperature (b) 400°C, 1.5h soak (c) 400°C, 8h soak

(d) 600°C, 1.5h soak (e) 700°C, 1.5h soak (f) 800°C, 1.5h soak

Fig. 1 – Longitudinal sections for different exposure temperatures and times.
The length bar is 20 □m long.

A similar microstructure with long, fine grains is evident for samples that have been heated up to 500°C (Figs. 1b and 1c), and it is not possible resolve the individual grains in the transverse view. However, the pearlitic banding is less clear in the 400°C samples. Whilst (even at 1000× magnification) it was difficult to discern this banding, it is possible to see that the proportion of pearlitic banding was lower. For the 8h soak time, the original structure is still visible, but the clear pearlitic structure has disappeared and slightly grainier dark and light bands are visible. This suggests that the effect of this temperature upon the steel is time dependent.

For temperatures above 500°C pearlite starts to dissociate into ferrite and globular iron carbide, and the microstructure is a mixture of the pearlite grain structure and the new globular structure. This is evident at 600°C in both longitudinal (Fig. 1d) and transverse directions.

At temperatures above 700°C the directionality of the original grain structure is lost. Above the eutectoid temperature (≈727°C), the steel transforms to austenite, but re-forms into coarse pearlite colonies upon cooling (Figs 1e and 1f). Decarburisation is also observed for these temperatures; after heating, the samples were coated in a carbon layer and the proportions of ferrite in the microstructure near the surface were higher.

Similar trends were observed by Abrams & Erlin, Neves *et al.* and MacLean, despite the different compositions of the steels that they tested (Tab. 1).

3.2 Hardness vs. Temperature

The results from the Vickers hardness tests are shown in Fig. 2, which plots the reduction in hardness with exposure temperature.

There is no significant change in hardness for temperatures up to 300°C, with a marked decrease in hardness above 400°C. A minimum hardness (equal to 40% of the un-heated hardness) occurs for steel heated to 700°C. At 800°C, the hardness increases slightly (to 60%) due to recrystallization. These results correlate with those obtained by Abrams & Erlin (1967).

The multiple points at 400°C in Fig. 2 are due to the soak times of 1.5, 4 and 8h. The longest exposure resulted in the lowest hardness value, with a difference of not more than 8% (55 DPH) between the longest and shortest exposure times.

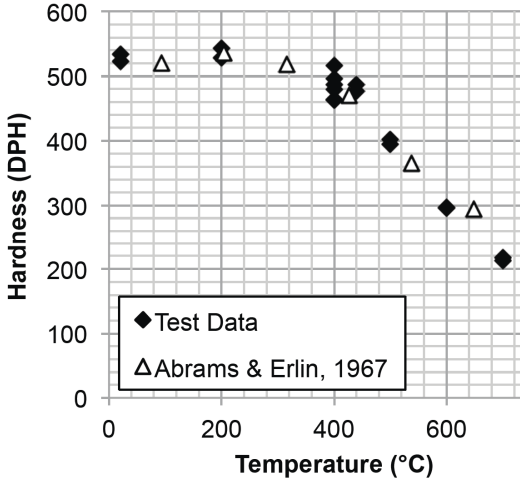

Fig. 2 - Hardness variation with temperature.

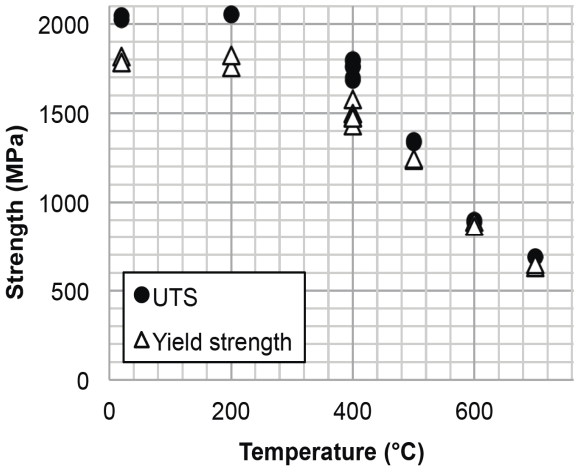

Fig. 3 - Strength variation with temperature.

3.3 Residual Strength vs. Temperature

Fig. 3 shows how the residual yield tensile strength and ultimate tensile strength (UTS) varied with exposure temperature. The yield strength was the stress at which the prestressing steel samples ceased to behave linearly. There is very strong similarity between Figs 2 and 3, confirming the correlation between strength and hardness.

As with hardness, significant change in tensile strength occurs for temperatures below 300°C. The strength is reduced at 400°C, but neither the yield or ultimate tensile strengths are significantly affected by the exposure times at this temperature (the results are within 120MPa of each other). The minimum strength occurs at 700°C, where the UTS has reduced by nearly 70%, and the yield strength by around 60%. The strength recovers slightly at 800°C, with a residual UTS around 50% of the unheated strength.

Stress-strain curves were plotted using the DIC measurements of strain (but are not included here). The elastic portion of the response gave a Young's modulus (E) close to 210GPa, which is in the range defined by the manufacturer. The residual value of E did not vary significantly with exposure temperature. The stress-strain curves for the majority of the specimens had clear elastic-plastic regions with very little hardening. Those exposed to 800°C, however, were similar to those for mild steel, with hardening, a consequence of the un-worked microstructure of the steel following heating to 800°C (Fig. 1f).

Fig. 4 compares the UTS results from the present study (from Fig. 3) to the results from previous studies, normalised with respect to the unheated strength. The trend is the same as for previous work. A recovery of residual UTS is also observed for 800 °C by Neves *et al.* and Abrams & Erlin.

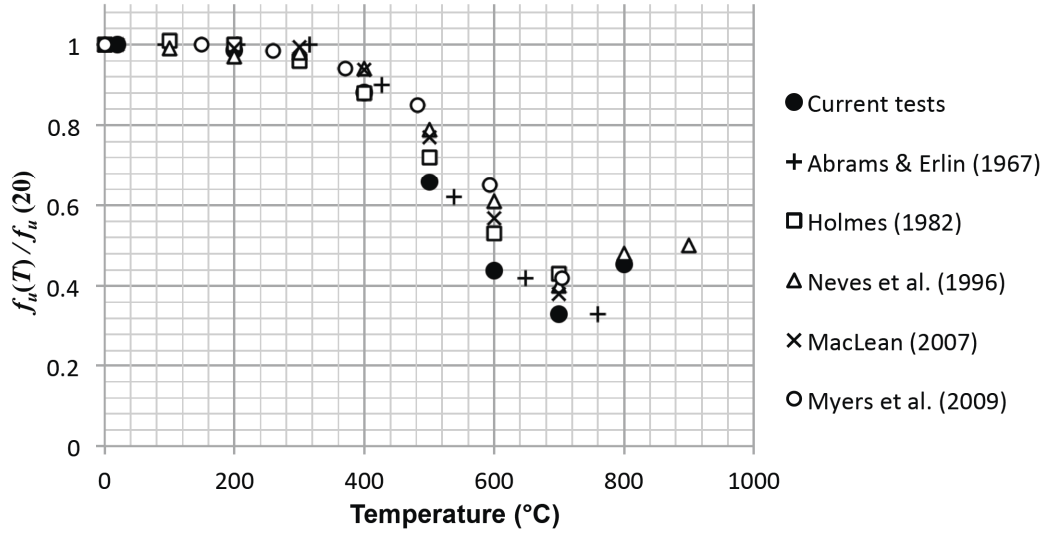

Fig. 4 - Comparison of UTS test data with previous studies

3.4 Heated Tension Test at 500°C

The strength test conducted at 500°C was used to determine whether loading at elevated temperature affects the hardness or microstructure of the steel (after it has been cooled). There was a small decrease in hardness of 8.3% compared to the unloaded sample. The loaded tests by Abrams & Erlin (1967) gave a similar result, which they deemed to be neglible, but it should be noted that the difference in hardness is similar in magnitude to that resulting from the different exposure times at 400°C.

The microstructure of samples taken from the necked region was similar to that of unloaded test, although the plastic deformation would have caused the formation of microcavities in the necked region.

3.4 Hardness as an Assessment of Residual Strength

The results demonstrate that the hardness of the modern prestressing steel (to BS 5896) correlates very well with the residual UTS, in a similar manner to historic prestressing steel (Abrams & Erlin, 1967).

Portable hardness testing may allow the residual tensile strength of a post-tensioning tendon to be assessed following a fire without needing to recourse to destructive test methods that require samples of steel to be removed from the structure.

Care is required, due to the non-unique values of hardness that occur between 600°C and 800°C, because hardness testing cannot distinguish steel exposed to these two temperatures. The ductility of the 800°C exposed steel will be higher, but this would require microstructural examination or mechanical testing. It is unlikely, however, that prestressing tendons exposed to any temperature in the 600°C to 800°C could be retained because of the consequent large reduction in strength.

4 SUMMARY

This study has examined how exposure to elevated temperatures up to 800°C affects the microstructure, hardness, and residual tensile strength of a modern prestressing steel.

Whilst the chemical composition of the British Standard steel examined here differs from the prestressing steels examined in previous studies (from the 1960s onwards), its elevated temperature performance is similar. Residual strength loss occurs from 400°C., with a maximum ultimate tensile strength of 70% at 700°C. The exposure time does not greatly affect its residual properties.

The residual strength loss is accompanied by a reduction in the steel's hardness, and this may allow hardness testing as a non-destructive method to establish the residual strength of a prestressing tendon following fire.

REFERENCES

Abrams M. S. & Erlin B. (1967). *Estimating Post-Fire Strength and Exposure Temperature of Prestressing Steel Using Metallographic Method.* Portland Cement Association, Skokie, USA.

BS 5896 (2012). *Specification for High Tensile Steel Wire and Strands for the Prestressing of Concrete,* BSi, London.

Gales J., Bisby L. A. & Gillie M. (2011). *Unbonded Post-Tensioned Concrete in Fire: A Review of Data from Furnace Tests and Real Fires.* Fire Safety Journal, 46(4), 151-163

Gales, J. Bisby L. A. & Stratford T. (2012). *New Parameters to Describe High-Temperature Deformation of Prestressing Steel Determined Using Digital Image Correlation.* Structural Engineering International, 22(4), 476-486

Holmes M. E., Anchor, R., Cook, G., & Crook, R. (1982). *The Effects of Elevated Temperatures on the Strength Properties of Reinforcing and Prestressing Steels.* The Structural Engineer, 60(13), 7-13

MacLean K. J. (2007). *Post-Fire Assessment of Unbonded Post-Tensioned Concrete Slabs: Strand Detorioration and Prestress Loss.* Master's Thesis, Queen`s Univ., Kingston, Ontario, Canada.

Myers J. J., & Bailey W. L. (2009). *Residual Properties of Seven-wire Low Relaxation PrestressingTendon Subjected to Extreme Temperatures.* PCI National Bridge Conference, San Antonio.

Neves C. I., Rodrigues, J. & de Padua Loureiro, A. (1996). *Mechanical Properties of Reinforcing and Prestressing Steels after Heating.* Journal of Materials in Civil Engineering, 8(4), 189-19

Appendix D:
Slab Capacity

D.1 Applied Loading

Dead load = 24.5 kN/m3* (0.475m*0.1m)
= 1.16 kNn/m

Live load = 2.05 kN/m

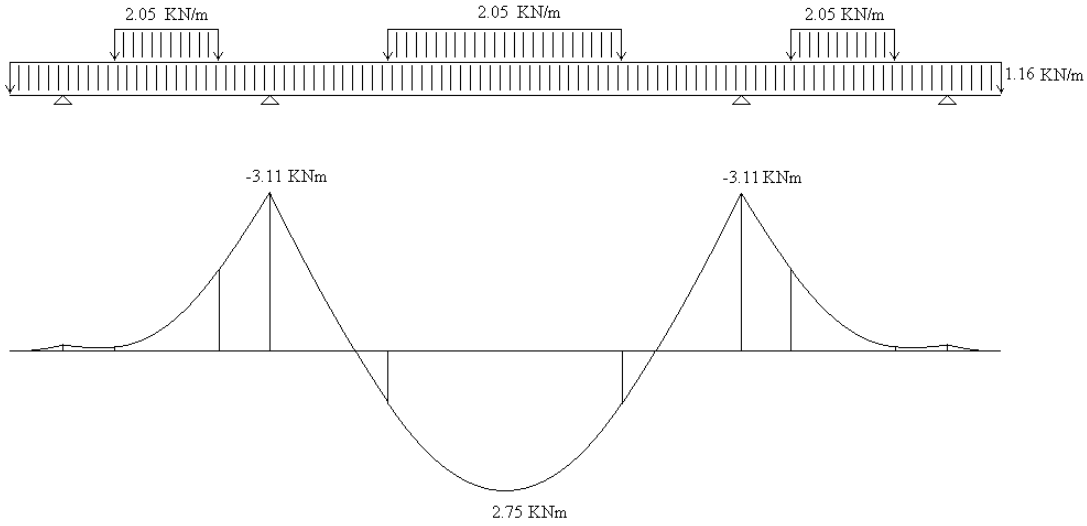

*****Note that the applied moment used for the load ratio does not include secondary effects from prestressing. These effects would act to increase the flexural moment at midspan.

Applied moment: 2.75 kNm (+ve flexure) 3.11 kNm (-ve flexure)
Factored applied moment: 3.9 kNm (assuming 1.3 DL and 1.5 LL)

D.2 Approximate Resistance

CAN/CSA A23.3-04 (CSA, 2004) code equations were used to approximate the flexural capacity of the UPT slab in both positive (midspan) and negative bending (support). This code was chosen as it represents distinct endeavours to understand the unbonded PT behaviour (Allouche, 1998,1999). Bonded behaviour due to compatibility of the concrete with the prestressing steel will be of higher strength and therefore lower load ratio.

The neutral axis depth at assumed plastic hinges, c_y, is found from Equation D.1.

$$c_y = \frac{\phi_s A_s f_y + \phi_p A_p f_{py} - \phi_s A_s' f_y'}{\alpha_1 \beta_1 \phi_c f'_c b_c} \quad [D.1]$$

where *A* is the area of reinforcement provided, the subscript *s* denotes mild reinforcement, the subscript *p* denotes prestressed reinforcement, the subscript *c* denotes concrete, ϕ is a code specific resistance factor (factors of 0.65 for concrete, 0.85 for mild steel, and 0.9 for prestressing steel may be assumed, given that load ratio is the likely capacity these values are taken as unity), *b* is the width of the slab (475 mm), α_1 is the ratio of average stress in a rectangular compression block to the specified room temperature concrete strength f'_c (assumed as 30 MPa), the subscript ' represents compressive properties where applicable, and f_y, f_{py} represent the yield strength of mild and prestressed reinforcement respectively (chosen as 400 MPa for mild steel reinforcement, and 1674 MPa for prestressing steel).

The resulting c_y values for each plastic hinge are subsequently used to calculate the stress in the prestressed reinforcement at ultimate limit state, f_{pr}, according to Equation D.2, which is adapted from Clause 18.6.2(b) of CSA A23.3-04 (CSA, 2004):

$$f_{pr} = f_{pe} + \Delta f_{pr}$$
$$f_{pr} = f_{pe} + \frac{8000}{l_o} \sum_n (d_p - c_y) \leq f_{py} \quad [D.2]$$

where f_{pe} represents the prestress in the tendons after all short and long term losses (conservatively chosen as 1000MPa), d_p is the extreme compression fibre to the centroid of the prestressing steel at the location of the plastic hinge, l_o is the tendon length between anchors, and *n* is the number of plastic hinges required to form a failure mechanism (three for an interior span). Eurocode requirements allow this calculation to be simplified with a straight value of Δf_{pr} equal to 100 MPa (see Ghalleb 2013).

The compressive stress block depth, a_c, is given by Equation D.3:

$$a_c = \frac{\phi_s A_s f_y + \phi_p A_p f_{pr} - \phi_s A_s' f_y'}{\alpha_1 \phi_c f'_c b_c} \quad [D.3]$$

Using f_{pr} and considering the contributions from the flexural steel and the concrete the moment resistance, M_r, can be estimated using Equation D.4:

$$M_r = \phi_p A_p f_{pr} (d_p - \frac{a_c}{2}) + \phi_s A_s f_y (d_s - \frac{a_c}{2}) - \phi_s A_s' f_y' (d_s' - \frac{a_c}{2}) \quad [D.4]$$

The resulting moment for negative flexure (the lowest moment) is 7.35KNm with a representative load ratio of 0.42. This factor is assuming resistance factors taken as unity. If resistance factors are used the load ratio increases to 0.48 as the moment decreases to 6.40Knm.